The Kyushu Institute of Technology
Kyutech

Study on Modular-Wall-Solid-State-Battery, A Feasible Solution for Nanosatellites Design Challenges and Reliability Improvements

超小型衛星の設計課題解決と信頼性向上のための実現可能な一解決である Modular-Wall-Solid-State-Battery に関する研究

By
Mr LIMAM LAKHDAR

Department of Applied Sciences for Integrated System Engineering
Kyushu Institute of Technology, Kyutech, Kitakyushu, Japan

This dissertation is submitted for the degree of
Ph.D

09/2018 ~ 09/2021

Doctoral committee

• Prof. Kenichi Asami	(Supervisor)	Kyushu Institute of Technology, Kyutech
• Prof. Okuyama Kei-ichi	(Supervisor)	College of Science and Technology, Nihon University
• Prof. HIRAKI Koju	(Jury‘s member)	Kyushu Institute of Technology, Kyutech
• Prof. Cho Mengu	(Jury‘s member)	Kyushu Institute of Technology, Kyutech
• Prof. KOMORI Mochimitsu	(Jury‘s member)	Kyushu Institute of Technology, Kyutech
• Prof, TOYODA Kazuhiro	(Jury‘s member)	Kyushu Institute of Technology, Kyutech

Reference to any specific commercial product, process, or service by trade name, trademark, manufacturer, or otherwise, does not constitute or imply its endorsement by the author.

“Difficult roads lead to beautiful destinations…”

To my parents, my sisters, all my family, & friends…
any words cannot express my gratitude for their
encouragements and supports during all this period…

Thank you…

LIMAM Lakhdar

Acknowledgements

Firstly, I would like to express my sincere gratitude to my supervisor Prof. OKUYAMA Kei-Ichi at The *College of Science and Technology*, *Nihon University* for all the support during my PhD and related research, for his motivation, and advice. His consulting helped me in my researches and writing the thesis.

Also, Prof. Kenichi Asami as my administrative supervisor at the *Kyushu Institute of Technology*, for his support during the preparation of my graduation and the preparation for all phases related to the dissertation defence.

Besides my advisors, I would like to thank the rest of my thesis committee: Prof. HIRAKI Koju, Prof. CHO Mengu, Prof KOMORI Mochimitsu, and Prof. TOYODA Kazuhiro, for consecrated their precious time for considering reviewing this work, and their insightful comments and encouragement, but also for the hard question which incented me to widen my research from various perspectives.

I want to acknowledge the Ministry of Education, Culture, Sports, Science and Technology of Japan (*MEXT*) in collaboration with the United Nations of Outer Space Affaire (*UNOOSA*) to provide all kinds of support and for the scholarship.

Also, the company "*Prologium*", which gives accessibility to work on their solid-state batteries, and for the trust to carry several tests and evaluation for scientific purposes.

My sincere thanks also go to Mr. Yoshio Sato and all members of Toa Denki and *ARTRON TECH INC*. for their coordination and being the mediator between *Prologium* company and *Okuyama* laboratory.

As well as *Mechanical Electronics Laboratory Fukuoka Industrial Technology Center*, and Mr Kazuki Watanabe from *Well Research Company*.

I would like to thank my lab mates for the rich discussions, and for the hard work. Also, I thank all staff and my friends in the following institutions: the *Kyushu Institute of Technology* and The *College of Science and Technology*, *Nihon University*.

NASA and *JAXA* should be acknowledged too as the source of some open-source material that makes the research and study more fluent and accessible to all, as well as all scientific journals that regroup and share valuable information for all researches community.

Last but not the least, I would like to thank my parents, my sisters and my family for being present spiritually throughout all my PhD and my life in general.

Abstract

Restricted budgets and high requirements push engineers to think for smaller satellites, simpler design, with fast delivery but good enough to accomplish all the missions onboard the satellite. The recent progress in miniaturized space system technologies may make it possible for small satellite and microsatellites, with high reliability and less costly platforms that greatly reduce development costs. The desired capabilities of Nanosatellites to enable their applications in communication, earth observation, and new scientific instruments require advanced technology to face the design's challenges with the constraints of volume and mass. The power subsystem as one of the main subsystems in a satellite should be capable to assure enough power to accomplish the mission in good conditions for the payload and others subsystems.

The study of the state of the art of different energy storage used in space lead to focus on a new kind of battery with an advanced technology, which is the Solid-State-Battery, mainly knows as *Polymer* battery, however, it may not be limited to the *Polymer*, the *Ceramic* battery which belongs to the same family may be proposed. However, it has not the same popularity as the *Polymer* for the different ground applications as well as space, so far never been tested or used in space.

The present work has started first with the determination of the Nanosatellite challenges that are facing, then summarized them into four categories: *Development, Launch, Operation, and Design*. Finally, some solution may be adopted, especially for the non-space or emerging faring nations, as:

- *Development: Cooperation, Collaboration, Renting facility for testing …*
- *Launch: Contracting for launcher …*
- *Operation: Cooperation, Collaboration, …*
- *Design: Cooperation, Supervision, Heritages, …*

While the three challenges (in red, ***Fig 1***) may vary according to each institution with their capabilities and resources, the most common challenge that could be found is more about the design, from the mechanical constraints to the thermal and power management, until the safety, while high demands for several missions are requested in such as small size.

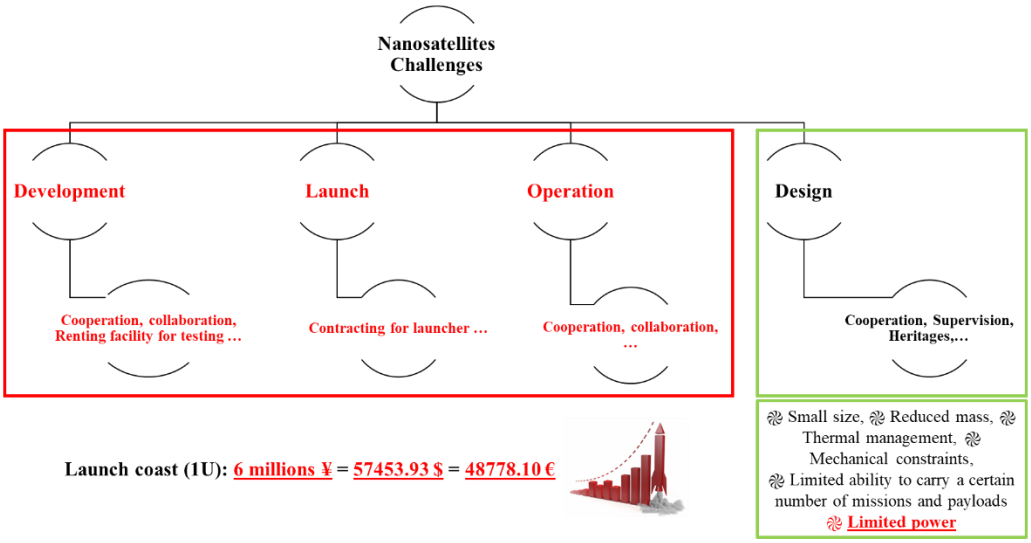

(Launch cost estimated in 2021 for 1U CubeSat, the cost increased three times then the last 3 years)

Fig 1 Nanosatellite challenges categories

The main contribution of the present work is to study the Nanosatellites Design Challenges related to the lack of power and size as well as the Reliability Improvement, in order to propose a solution. The main outcomes have been summarized into three axes as presented in ***Fig 2***:

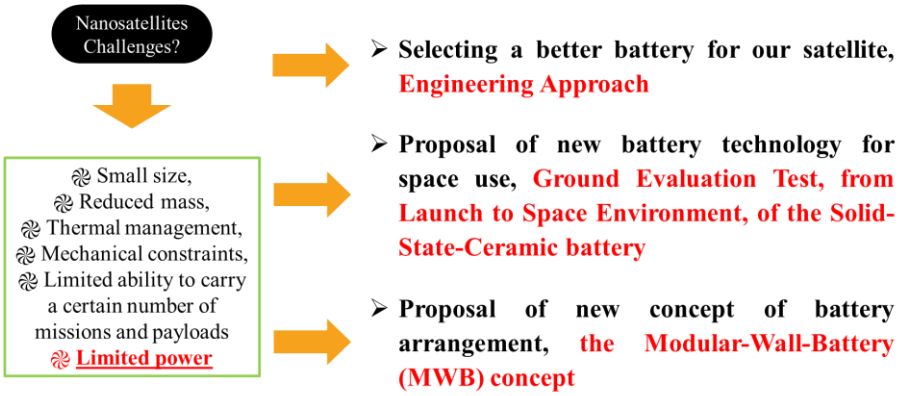

Fig 2 Outcomes of the study

1. Small satellite Battery Selection Engineering Approach, & Feasibility Study of the Solid-State Lithium-Ceramic-Battery' Application

The selection of the battery for any satellite project may depend on the mission requirements, much power with high electrical performances and safety issues are the most influential, especially while the development of small satellites is constantly increasing with the low-cost and fast development process. The need for more reliable and high-performance batteries to carry several missions became

necessary. However, the other requirements such as the volume and weight could have an effect on the final decision. Small batteries with high energy density may be the solution. The Lithium-Ion battery technologies are improved in order to meet these requirements by bringing higher energy density and a wide operating temperature range than the commercially available ones as well as a lower risk of explosion and firing.

In this work, an engineering approach for studying the compromise of capacity, weight, and volume between different kinds of batteries' technologies, additionally with their different design as cylindrical and pouch has been presented.

It is focusing on the application of the Solid-State Lithium-Ceramic-Battery, that have never been in flight in orbit, as well as never been tested on the ground for space application purpose, no research or publication has been published until now.

The work has started first with the comparison of this battery to the other technologies, and the study of the application feasibility on a real case: Ten-Koh satellite, with the effect on the design and in-orbit operation.

The Solid-State Lithium-Ceramic-Battery have been able to get a good ranking, especially with the wide operating temperature range that may reduce significantly the complexity of the design for the battery's arrangement, and decrease the use of heaters with reducing the power consumption during the eclipse. The approach can be also considered as a proposed procedure for the optimization of the battery's selection for small satellite projects.

2. Solid-State-Ceramic Battery, based *Oxide*, the First Evaluation & Application's Study for Nanosatellites.

Since the satellite is launched to space via a rocket, they must endure the hostile launch and space environment; therefore, they should be exposed to the real conditions within the ground testing, including all subsystems and components which should be carefully tested. Batteries have been exposed to shock, then tested under vibration within different frequencies' levels with sinewave, sine burst, and random. The ability of the Solid-State Lithium-Ceramic-Battery to withstand the vacuum and thermal vacuum for Low-Earth-Orbit applications has been demonstrated, with a minimum safety issue.

The work focuses on the physical degradation, the electrical performances and the internal resistance of the batteries based on the discharge capacity, the open-circuit voltage, and charge/discharge modes. Before and after each test, the physical properties of all batteries have been checked, several cycles of discharge and charge have been performed to check their performances and survivability after the evaluation test.

With 95% of capacity, batteries could demonstrate their ability to withstand the launch conditions successfully, they could be able to operate during several cycles after the test, so far, showing no degradation in their performances within the limits. Batteries have shown promising results regarding their survivability to thermal vacuum. After several cycles, they have kept almost the same performances, with the same internal resistance and 98% of capacity.

Also, a guideline for the battery evaluation test where the main lines for requirements and criteria for *launch* and *space environment* ground testing for the small satellite project has been provided.

3. Modular-Wall-Battery (MWB) Concept Proposal: Design, Requirements, and Simulation.

After getting promising results from the ground evaluation test, a proposed design concept of the battery arrangement onboard Nanosatellites, as well as small satellites, has been presented, the *Modular-Wall-Battery* combined to the selected *Ceramic* battery type in order to face the Nanosatellite challenges related to the small size and especially lack of power while improving the reliability with the proposed laminated pack, modularity of the concept as well as the redundancy.

The proposed concept aims to be applicable to all Nanosatellites as well as small satellites, keeping the design simpler without affecting the initial design of the satellite. The battery pack is more flexible for sizing according to the satellite power requirement with its customized battery pack based on the Flexible-Solid-State-Ceramic battery-based *Oxide*, the same battery technology that has been evaluated within the ground evaluation test. Finally, the *Modular-Wall-Battery* (*MWB*) is defined to be applicable to any kind of battery that fulfils the requirements related to the satellite power requirement as well as the *MWB* concept requirement.

The proposal includes a full definition of the design and a list of requirements that can be used for the design and also selecting the battery.

As the selected battery has been evaluated with showing so far good results. The concept has been included a feasibility application on Nanosatellites, an orbit interpretation and total power and capacity estimation provided to different Nanosatellite sizes. The results of the simulation of the concept on ground are planned to be published later in subsequent publication until the real test will be done onboard a Nanosatellite, this one for further analysis, as well as for comparison reasons.

However, the *Modular-Wall-Battery* concept could be able to save up to 99% in volume and provide enough power and capacity to the Nanosatellite, moreover, it may be considered as a good solution for the mass distribution which may have a

positive effect on the center of gravity. With the *Ceramic* battery, the battery arrangement becomes simpler due to the large temperature range of the battery and the material property, it is not necessary to have an Aluminum box or using too much heater during cold temperature (-20°C to -40°C).

Finally, the selected battery and customized pack have been proposed for the first space engineering demonstrative mission in order to analyze more in detail the performances of the battery within the proposed concept (*MWB*). The results from the mission may help to integrate the two proposals within the bus system of the next generation of small satellites as well as the Nanosatellites.

Articles

1. “Launch Environment Ground Test Evaluation with Multi-axis Vibration and Shock for Pouch Solid-State-Ceramic Battery Advanced Energy Storage”, International Review of Aerospace Engineering (IREASE), 13 (4), pp. 126-134, 2020 [***24***]. **(*Chapter IV*)**
https://doi.org/10.15866/irease.v13i4.18949

2. “Space Environment Evaluation Test of Solid- State-Ceramic Battery Advanced Energy Storage Under Vacuum and Thermal Vacuum”, International Review of Aerospace Engineering (IREASE), 13 (2), pp. 68-79, 2020 [***13***]. **(*Chapter IV*)**
https://doi.org/10.15866/irease.v13i2.18582

Conferences

1. “One Step Away from The Reliable Batteries for Small Spacecrafts with Solid-State-Ceramic Batteries”, the 71st International Astronautical Congress (IAC) – The CyberSpace Edition, 12-14 October 2020 by the International Astronautical Federation (IAF) [***132***]**.**
https://dl.iafastro.directory/event/IAC-2020/paper/55598/

Contents

List of Figures

List of Tables

Nomenclature

3D	Three dimensional
A	
ADCS	Attitude and Orbit Control and Determination
B	
BAT	Battery
C	
CF	Carbon Fiber
CFRP	Carbon Fiber
CFRTP	Carbon fiber reinforced thermoplastic
CDH	Command and Data Handling
CNES	
COMM	Communication
COTS	Commercial off-the-shelf
CTE	Coefficient of Thermal Expansion
D	
E	
EEPROM	Electrically Erasable Programmable Read-Only Memory
EM	Engineering Model
EPS	Electrical Power Supply
F	
FM	Flight Model
G	
GNSS	Global Navigation Satellite System
H	
HTV	Transfer Vehicle
H2B/H3B	Launch Vehicle
I	
J	
JAXA	Japan Aerospace Exploration Agency
K	
Kyutech	Kyushu Institute of Technology
L	
LATS	Lightweight Ablator Series for Transfer Vehicle Systems
LEO	Low-Earth-Orbit
M	
MLI	Multi-Layer-Insulator
N	
NASA	National Aeronautics and Space Administration
O	
OBC	On Board Computer
P	
PIC	Programmable Interrupt Controller
PEEK	Polyether Ether Ketone
PWM	Pulse Wide Modulation
PMU	Power Management Unit
PDU	Power Distribution Unit

Q
R
RAM Digital memory hardware
S
SAFT French batteries' company
S/C Spacecraft
SMIC Solar Module Integrated Converters
STM Structural and Thermal Model
SSB Solid State Battery
SSLCB Solid-State Lithium-Ceramic Battery
SoC System on Chip
SSTL Surrey Satellite Technology Limited
T
TVAC Thermal Vacuum Chamber
U
UART Universal Asynchronous Receiver-Transmitter
UDLC Ultra-Double Layer Capacitance
V
W
X
Y
Z

Chapter I

Introduction

I. Introduction

Since the space race has been restricted to only a few countries, nowadays, with the new space policy, the opportunities to design, develop, and launch a satellite to space have been reachable for almost any country. Emerging space nations are developing satellites by partnerships or beginning their own space program. Mastering and acquiring the space technology for these countries may help for developing sciences, monitoring the environment, also may be a part of national security. Additionally, it may be considered as a sign of power and sovereignty or a way for economic growth.

Due to the long time and high cost for satellite development and launch, several space actors have been interested in the development of small satellites, while these ones, especially the Nanosatellites, has been limited to only universities and institutes for educational purposes, nowadays all the space developers including the new startup companies even the space agencies have shown interest too. As represented in the work done by *Martin. N*, with the comparative growth in launches of small satellites done by *SSTL*, the total number of Mini/Micro/Nano-satellites in 2017 has exceeded more than three times the number of satellites with more than 500Kg [***1***]. The work has done by *Dong-Hyun. C et al.* is one example of the development of a low-cost CubeSat platform, which has represented the evolution of the Nanosatellites' development since 1998, while almost all the Nanosatellites have been developed by the universities, institutes, and schools. It is predicted to reach over 3000 Nanosatellites to be launched within the next six years [***2***]. Almost all the Nanosatellites have been listed in ***Fig. I-1*** and launched from 2008 to 2019, as well as for the ones scheduled until 2023, belong to the 1U and 3U CubeSat categories.

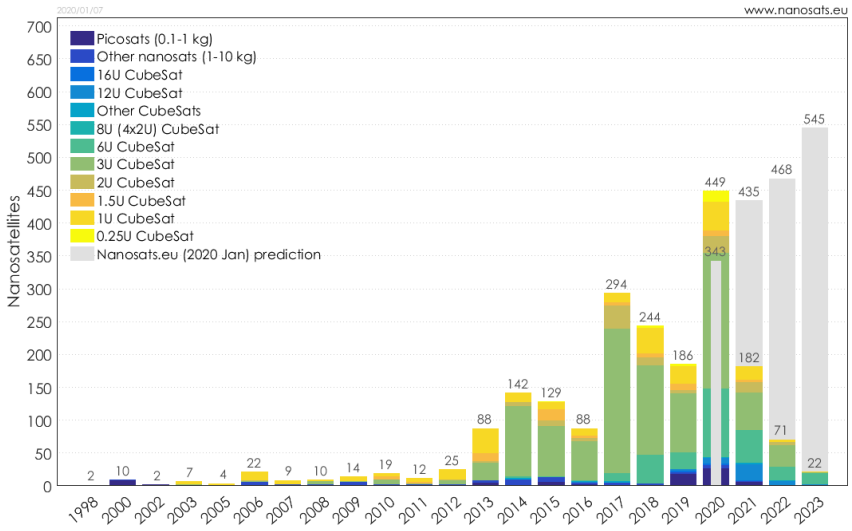

Fig I-1 Launched Nanosatellites by types since 1998
(*Data source https://www.nanosats.eu/*) [***3***]

Additionally, with the lean satellites, introduced in the work done by *CHO.M et al.*, the satellite development sector has been boosted with the low-cost satellites using COTS components and fast development for fast delivery with a small team [*4*]. Using the advantages of the lean satellites, the emerging countries and institutions can now go much more quickly through design, development, launch, and operation [*5*,*6*].

With the increase of the development of such small designs, and due to the high demands for several missions' onboard satellites, several challenges have to be faced and considered carefully. From the mechanical constraints, thermal and power management, until the safety requirements, must be addressed.

The challenge with small/lean satellites is mainly summarized in their small size, which leads to some technological and design challenges, as has been summarized briefly by sub-systems in ***Table I-1***.

Table I-1 Small satellites' challenge by sub-systems with some proposed solutions

Satellite's sub-systems	**Challenges**	**Proposed solutions**
Structure	Heavy and complex	New materials
OBC	Limited memory, and tasks	New processor
Communication	Antenna with limited power and frequency band	Deployable antenna, S-Band
AODC	Bulky	High accuracy small sensors and actuators
Propulsion	Bulky	Electric plasma propulsion
Power	Limited power	Deployable solar panel, high-performance small batteries

As an example, for the satellite's structure it may be more appropriate to gain more weight by using new materials [*7*], (CFRP/CFRTP/CF-PEEK, …), or adopting a new approach with the 3D printed elements that can considerably reduce the weigh with reducing all kinds of fixation mechanism. The Ten-Koh satellite is an example of a small satellite, developed by students at *Okuyama* laboratory at the *Kyushu Institute of technology* in 2017 and launched in 2018, within almost 18 months of time development, the satellite had an external structure made by only Carbon fiber. However, the weight for the only screws and bolts has reached approximately 1Kg, in which the application of the 3D printed elements may reduce considerably the total weight if has been applicable.

In the case of the On-Board-Computer (OBC), some technologies have shown limited memory and number of tasks' execution, as well as sensitivity to radiation

[*8*]. Using a new generation of processors, as a high-performance Microcontroller or the *Raspberry Pi*, may solve some of these problems. The demonstration mission done by *SSTL* onboard DOT-1 satellite, launched in 2019, is a good example of using *Raspberry Pi* in space, as has been reported on *SSTL* and *Raspberry Pi*'s websites which showing an image taken by *Raspberry Pi* camera [*9*,*10*]. Moreover, SPATIUM-II, a 6U satellite designed by students at the *Kyushu Institute of Technology* and planned to be launched in 2021, is another example that will include a *Raspberry Pi* as an on-board demonstration mission [*11*]. However, the application of *Raspberry Pi* as the main Microcontroller for the OBC in space may need more investigations and tests, especially with the radiation issues.

The communication subsystem is another challenge due to the limited frequency band used with the amateur radio UHF/VHF that may require in some cases several passes over the main ground station for collecting data especially for satellites that may have a high-resolution camera. Using the S-Band may be a good alternative. However, it may require more power. The study reported by *Bugryniec. P* is an example showing the requirements of power for telecommunications in CubeSats. It compares two power budgets for two different satellites, one with a positive budget and the other with a negative one, in which most of the power is consumed by the transmitters. The report has been highlighting the high demand for power due to high peak power consumption especially from transmitters in terms of the limited power generation from the electrical power system due to the small size and restricted geometry of the CubeSats [*12*].

To face the challenges of small satellites, many approaches may be proposed, such as the ones represented in ***Table I-1***. Additionally, to face the limited volume issues, all these sub-systems and payloads need to be arranged properly; a better internal configuration of the satellite may lead to more free volume which means more payloads.

However, the compromise between the power required during all the operation time with having a certain number of missions in a small size should be considered too.

Concerning the power management, and including the actual research in this area, the progress to find solutions seems to have some delay. Due to the hostile launch and outer space environments, the requirement related to the design and the safety issues is more severe.

Additionally, according to the survey done by *Martin Langer* about the reliability of CubeSat within 30 days in orbit, it has been shown how each subsystem contributes to the satellite failures: 20% for the On-Board-Computer, 16% for the communication, and 12% for the other unknown reasons. finally, the electrical

power system which has been categorized as the most frequent reason for the failures with 44% [*13*,*14*].

The power system may be the most interesting subsystem to study. However, the complexity of the electrical power system makes the reason for these failures difficult to be detected and leads to a big research area. Improving efficiency can be done in different ways. Several approaches and propositions in this field have been proposed, as an example, the work done by *Gonzalez-Llorente et al.* by selecting operating conditions for power converters [*13*,*15*], or designing a configuration for efficient and reliable solar panel by *Ivo Vertat et al.* [*13*,*16*], and comparison between different deployable solar panels architecture by *Syahrim Azhan Ibrahim et al.* [*13*,*17*]. Even more, the work has done by *Clark. C et al.*in which one of the solutions has been presented with showing the three most common implementation approach for the power system: Direct Energy Transfer (DET) with Battery Bus, DET with Regulated Bus, Maximum Power Point Tracker with Battery Bus (MPPT) [*18*].

In this work, Since the batteries have been classified as fourth on nine top-level categories for causes of power-related satellite failures by *Geoffrey A. Landis* and *Sheila G. Bailey* [*13*,*19*], a different approach of a study looking for suitable technology and design from different kinds of batteries has been proposed. Batteries may be classified and categorized from different aspects: technological, and design, however, in space engineering, the most attractive aspect is technological, looking for more performances rather than the design.

The present work has been presented within seven parts and has been organized as follows, following the introduction in ***Chapter I*** with summarizing the small satellite challenges that have to be faced by each subsystem including some proposed solutions and highlighting the importance of the improvement that has been done and should be done on the electrical power system especially the batteries. The attempts that have been done in this area such as the improvement of the electrical power system architecture.

Chapter II has been more dedicated to the state of the art of small satellite power, including the three main systems that constitute the electrical power system known as power management and distribution system, solar panel, and battery. It has focused mainly on energy storage and especially batteries with their application and brief history for their large use in space. It has included the Solid-Sate-Battery, definition and description of the novel and promising technology for a better battery with their application in space onboard small satellites. The chapter has listed some of the manufacturers of these three parts, including the Solid-State Battery with all its types based on the electrolyte. Finally, two Solid-State-Batteries belong to the *Ceramic* type have been presented, as battery candidates for the outline of the

present work, then, the final battery chosen for the *Modular-Wall-Battery* (*MWB*) which will be included in ***Chapter V***, has been described in detail with the main reason for its selection and application into the *MWB*.

The description of the engineering approach and feasibility study of the Solid-State Lithium-Ceramic-Battery on small satellites has been presented in ***Chapter III***. Including the description of the study case satellite with its electrical power system (EPS) and the kind of battery's technology. The classification and comparison between several kinds of batteries' technology with showing their application in some satellites and the approach followed for their arrangement. The classification of batteries, including the battery candidate, has been done in terms of higher capacity, higher energy, smaller, and lighter. The comparison has been done from different aspects: **First**, all batteries selected for the study have been compared to Ten-Koh's battery in terms of the capacity in order to get the equivalent battery according to Ten-Koh battery. **Then**, the comparison has been done in terms of multiple parameters, one parameter according to the others at a time, in order to study the effect of all parameters on the performances of the battery. **Finally**, for the battery resizing, the battery equivalent has been resizing depending on the initial Ten-Koh battery's capacity, the analysis has been done in order to study the effect of each equivalent resized battery on the satellite' design and operation. The discussion has been done into two different sides, **ones** in terms of the electrical performances' classification, and the complexity of the battery arrangement. **And ones** in terms of the in-orbit thermal management and heathers optimization during eclipse operation. The other side of the study is showing the relationship between the design for the different kinds of batteries, cylindrical and pouch, and the level of complexity on their arrangement onboard the satellite.

Chapter IV has presented the full ground evaluation process of the battery candidate as the first ground evaluation test of the *Ceramic* based *Oxide* type, deals with the description of all the test facilities that have been used and test procedures, it has presented the inputs test condition required for the *launch environment* and the *space environment*, the description in detail of the full test procedure and methodology. The reel test conditions applied on the batteries, with discussion and interpretation of the results test. The chapter has been presented also as a complete guideline for the full ground test and evaluation of batteries target to be used onboard small satellites or as a demonstration mission in orbit.

Then ***Chapter V*** and ***VI*** have summarized the new approach of battery arrangement for small satellites and Nanosatellites, proposed by the author in order to face the small satellite challenge and lack of power, combining the new batteries technology that has been evaluated in ***Chapter IV*** and the new approach of battery arrangement which is the *Modular-Wall-Battery* (*MWB*), that may be the future generation of battery based on the Solid-State Lithium-Ceramic-Battery technology as well as the

All-Solid-State Battery. In *the first part (I)*, ***Chapter V***, the proposed approach has been presented as a list of requirements; the full design has been included, offering the opportunity to be enlarged for other battery technology. Finally, simulation of the concept has been discussed while the application on different sizes of CubeSats from 1U to 6U has been compared with the application of the Lithium-Ion battery. ***Chapter VI***, with *the second part (II)* of the *Modular-Wall-Battery*, has included the description of the *launch* and the *space environment* simulation of the battery pack that has been proposed for this concept as a sample, and discussion of the results with an estimation of the remained capacity of the *Modular-Wall-Battery* after all the simulation.

Finally, ***Chapter VII*** has regrouped all the conclusions from the previous chapters focusing on the future works that have to be continued to enrich more the results related to the *Modular-Wall-Battery* as well as the Solid-State Lithium-Ceramic-Battery for their potential use in space.

After the promising results got from the ground evaluation test, the first flight of the Solid-State Lithium-Ceramic battery onboard a next small satellite has been proposed. The new satellite shall be able to demonstrate the first application of the Solid-State Lithium-Ceramic-Battery in space as well as the *Modular-Wall-Battery* (*MWB*) approach. This one will be presented, as the future work, a mini-project that will list the requirements for the mission demonstration, a proposed mission board block diagram, finally, a data, power and mass budget.

Chapter II

State of The Art of Small Satellites Power & Energy Storages

II. State of The Art of Small Satellites Power & Energy Storages

Any small satellite shall have the three main parts for a complete electrical power system operation, which are: Power Management and Distribution, Solar Panels including Solar Cells, and finally Energy Storage using mainly Secondary Batteries. The two first parts will be briefly introduced by including some examples of companies which provides their services. Then the third part is about the energy storage, which will be more in detail.

II.1. Power management and distribution

The Power Management and Distribution (PMaD) considered as the orderly officer for the electrical power system, its duties are to receive energy from the solar cells, manage and distribute appropriate power for each sub-system and payloads, finally store energy through charging the satellite battery. It is constituted by software and hardware, which are developed and manufactured by the satellite designer according to the need and the requirements of the satellite for the power of each part including the bus and the payload system. However, due that almost all small satellites included such 5 and 3,3 V as a regulated bus, in such a way that may be standard for all satellites, nowadays, some manufacturers started to provide a standard PMaD system that can be integrated into a designated satellite by the designer, in such a way that shall satisfy all the need and requirements. ***Table II-1*** summarizes some of the PMaD system manufacturers listed by *NASA* on their state of the art of small spacecraft technology [***20***]. Some of the manufacturers are not limited to the power distribution and management system but all the electrical power system.

Table II-1 List of some power management and distribution manufacturers
(Data source: NASA. (2020). State of the Art Small Spacecraft Technology [***20***])

Manufacturer	**Product**	**System**
Blue Canyon Tech	BCT CubeSat Electrical Power System	EPS
Pumpkin, Inc.	CubeSat Kit EPS 1	
Endurosat	CubeSat EPS Type I, II and I Plus	
NanoAvionics	EPSL	
Clyde Space	Nanosatellite EPS, Starbuck-MICRO, MINI, NANO, PICO	
Crystalspace	P1U “Vasik”	
SEAKR	3u cPCI Power Supply	
DHV Technology	EPS for 2U, 3U and 6U CubeSats	
ISIS	iEPS	
ibeos	150-Watt SmallSat EPS	
Pumpkin, Inc.	CubeSat Kit EPS 1	

Surrey Satellite Technology, Ltd	LEO PCDU	PMaD
GomSpace	NanoPower P31U	
ÅAC Microtec	PCDU-2100, -2200, -2300	
Tyvak	Power Storage and Distribution	
Clyde Space	Small Satellite PCDU	
Vectronic	Vectronic PCDU	
Magellan Aerospace	Power and Control Unit	

II.2. Solar panels

The other essential part, which may be more able to be standardized, is the solar panels. Its main function is to support the solar cells or photovoltaic cells that will convert the light to an electric current through the semiconductor. Due to the high demand for power generation, the multi-junction solar cells are the most requested in space which their efficiency may reach 30% compared to the ground application that can use only the single junction due to the lower price, however, they have a lower efficiency of about 20%. ***Fig II-1*** represents some examples of available solar cells with their efficiency [***20***].

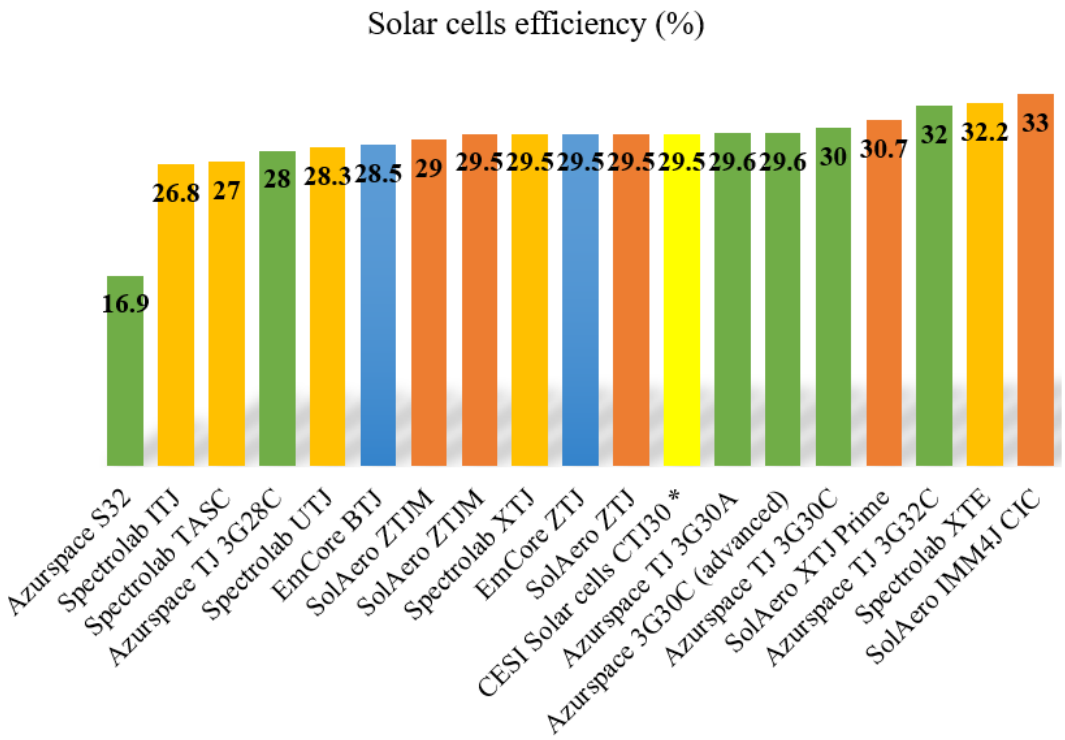

** Same technology of solar cell has been used for the Ten-Koh satellite.*

Fig II-1 List of some solar cell's manufacturers for space application
(Data source: NASA. (2020). State-of-the-Art Small Spacecraft Technology [***20***])

Same as the PMaD system some companies, listed in ***Table II-2***, are manufacturing a full solar panel for 1U, 3U and 12U Nanosatellites using the technology of the solar cell presented in ***Fig II-1***, or more such as *Nanoavionics*, and *Innovation Solution in Space* (*ISIS*) which its solar panel may be compatible *Pumpkin* structures and the *GomSpace* NanoPower EPS [***20***].

Table II-2 List of some solar panel's manufacturers
(Data source: NASA. (2020). State-of-the-Art Small Spacecraft Technology [***20***])

Manufacturers	**Product**	**Solar cells used**
Clyde Space	Solar Panel (0.5- 12U); Deployable Solar Panel (1U, 3U)	SpectroLab UTJ
		SpectroLab XTJ
		AzurSpace 3G30A
DHV Technology	Solar Panel (5 x 5 cm, 1U, 2U, 3U, 6U, 12U)	AzureSpace 3G30C Advanced, and Solaero ZTJ-Ω
Endurosat	Solar Panel	CESI Solar cells CTJ30 *, and AzurSpace 3G30
GomSpace	NanoPower (CubeSat and custom)	AzurSpace 3G30A
MMA DESIGN, LLC	HAWK (High Watts per Kilogram)	SolAero XTJ & Prime, and Spectrolab UTJ
	eHAWK	
SolAero	COBRA	SolAero ZTJ
	COBRA-1U	
SpectroLab	Space Solar Panel	SolAero ITJ
		SolAero UTJ
		SolAero XTJ
		SolAero XTJ Prime
CubeSatshop	DSA/1A	AzurSpace 3G30A
ISIS	CubeSat Solar Panels	AzurSpace 3G30x
NanoAvionics	GaAs Solar Arrays	N/A
Pumpkin	Varies	SpectroLab XTJ Prime

Moreover, with the progress in this area, a new kind of solar cells may be adopted for space application in near future, at least if it can prove its reliability, as the Multi-junction Solar Cells (38% efficiency under laboratory conditions), flexible and thin-film solar cells (22.7% efficiency), and organic solar cells [***20***].

Far from the pure photovoltaic concept as the solar cell, the power generation may be done from the different concept as the Hydrogen Fuel cells, Nuclear Power (Radioisotope Thermoelectric Generators (RTGs)) or the thermophotovoltaic (TPV) battery and the Alpha and Beta-voltaic which are currently in the testing/research phase and has not been integrated yet to small satellites [***20***].

II.3. Energy storages & Space application

Since the space exploration that started in 1958, energy storage devices have been used for several missions, in several ways from a primary source to storing electrical energy. They are divided into four categories including batteries [*13*]:

- Primary (non-rechargeable),
- Secondary (rechargeable),
- Capacitors,
- Fuel cells.

Since 2000, several kinds of rechargeable batteries have been widely used in space: silver-zinc (Ag-Zn), nickel-cadmium (Ni-Cd), nickel-hydrogen (Ni-H2), and lithium-ion (Li-ion), as presented on *NASA* report for energy storage technology for future planetary science missions which summarizes all the kinds of these energy storages used for space mission exploration [*13*,*21*].

For some thermal characteristics, Nickel-Hydrogen Ni-H2 batteries have been the most used for space application, before being replaced by the Lithium-Ion. These ones have become the most used for several missions on several orbits. From ***Table II-3***. we can notice that the Li-Ion technology is still in front of the best battery with their high specific energy. Moreover, some technology of battery may have limited application as the Lithium-Ferrite or the Lithium-Polymer. However, the Li-Ion still presents some limitations: low energy density, sensibility for temperature and safety issues according to specific space missions [*13*].

Even with the long history and large application of the Lithium-Ion batteries, since they have been the most used in large mobile applications: from ground such as cellphones and electrical vehicles, to space with spacecraft and space suits, they have been categorized as hazardous batteries [*22*], especially after a bad manipulation or working under extreme conditions [*23*]. The manufacturers and users have been required to cover several test conditions following different requirements such as vibration and shock to verify their ability to work safely at the nominal level and good performances [*24*].

According to the mechanical design of the Lithium-Ion batteries, the vibration and shock conditions can have a significant effect on the batteries' performances especially during the launch due to the hostile vibration and shock. Concerning these effects, internal shorts may occur which can lead to venting the electrolyte with the possibility of firing and thermal runaway. It may lead to breaking the cells and leakage in the case of liquid or jelly batteries [*25*]. At the work was done by

Lijun Zhang et al., it has been identified that the vibration may lead to a significant increase in discharge resistance [***24***,***26***].

Eventually, the vibration and shock test for batteries became necessary due to the effect which could apport on the performances, like for the study done by *Martin J. Brand et al.*, in which the effect of vibration and shock have been evaluated on two different battery structures: Cylindrical and Pouch, which the results have shown no degradation on the pouch batteries [***27***]. Or the work was done by *James Michael Hooper et al.* on a multi-axis vibration test on the Li-Ion cylindric cells, for their electrical and physical evaluation [***28***,***29***]. Then, the work was done by *J-K Lee et al.* on the Pouch Lithium-Polymer battery in which the accelerated vibration and the charge-discharge cycling have been combined has shown good mechanical and electrical stability of the batteries [***24***,***30***].

However, *Gunnar Kjell* and *Jenny Frodelius Lang* have concluded with the comparison between different vibration test standard limits on the Li-Ion batteries and fatigue damage on the mechanical structure that the standards differ strongly and should be considered for the purpose which the battery will be used [***24***,***31***].

For the space applications, the primary objective is to ensure that the satellite and all components have passed the qualification test and free from workmanship defects. That is why all kinds of energy storage including the batteries should be qualified for space used, otherwise, they should be evaluated and tested before launch to space [***24***].

These are some examples of the qualification test done on the batteries for small satellites including the *launch environment*, in which *K-H. Park et al.* have presented the qualification test for the secured reliability of the Lithium-Ion batteries [***32***], moreover, the test was done by *Saft* and *ESA* for the qualification and life testing of the Saft Li-ion batteries [***24***,***33***]. Or the evaluation of variable cylindric cells by *Jonghoon Kim et al.*, in which several batteries have been tested to evaluate their capacity and internal resistance [***34***], and another work for a battery certification for small satellite done by *Zachary Cameron et al.*, for the Li-Ion cylindric cells test procedure [***24***,***35***].

Due to the rising demand for safer, higher capacity energy storage with lighter weight and smaller size, the researcher area, which has been limited to only rechargeable batteries, has been enlarged to all kinds of energy storage [***13***]. An alternative solution has been proposed with the application of the electric double-layer capacitors, known as the supercapacitors, some works have started with the ground evaluation testing, as the one has done for Nanosatellites applications by *Muhammad Alkali et al.* [***36***]; some others have worked on the evaluation test under thermal vacuum for space application by *Keith C.Chin et al.* [***13***,***37***]. Finally, the

experimental evaluation at the Low-Earth-Orbit for charge and discharge onboard Ten-Koh satellite [***38***,***39***,***40***], which has shown so far interesting results and have been published by *Jesus Gonzalez et al.* [***13***,***41***].

The Lithium-Sulfur (Li-S) batteries, which are one of the concurrent of the Li-Ion, have been targeted as an alternative replacement for Li-Ion because of their higher energy density. However, the test done by *ESA* on Li-S for liquid electrolyte shows that Li-S has not reached the maturity of Li-Ion yet to be used under the space environment for its poor specific energy at 0°C and a significant increase in internal resistance. However, Li-S is an interesting battery technology to work on, and may be considered as another potential candidate for Low-Earth-Orbit [***13***,***42***].

Another challenge related to the *space environment*'s requirement for the selection of battery is the operating temperature range since the temperature in orbit could reach very low temperature during eclipses, the battery selected should be able to work within a large temperature range, especially within the low temperatures. *Peter. B* reported that the good temperature range for optimal performance should be between +10°C and +30°C, however, during the eclipse the electrolyte starts to solidify with increasing the internal resistance [***12***]. There are many works related to the effect of temperatures on the batteries' performance and safety, as for the work done by *Shuai. M et al.* who reported that the effect of the low temperature and the thermal impact in lithium-ion batteries are mainly the reduction of ionic conductivity and the increase of charge-transfer resistance, that why the temperature range should be between +15°C and +35°C [***43***]. Related to the space application, *NASA* reported that the temperature range should be between +20°C to +40°C, due to the effect of the temperature of charge and discharge on the capacity and voltage characteristics [***44***]. Other work by *SAFT* and *CNES* on the evaluation of a low-temperature Li-ion cell for the specific mission of *NETLANDER*, where the batteries have been charged and discharged at the low temperature around -30°C to -40°C respectively [***45***].

Same as the PMaD system or the solar panel, some companies are providing satellite battery ready for integration within the small satellites, as listed in ***Table II-3***. However, some of the satellite designers still prefer to develop this part by themself using battery cell space qualified as the ones listed in ***Fig II-2***.

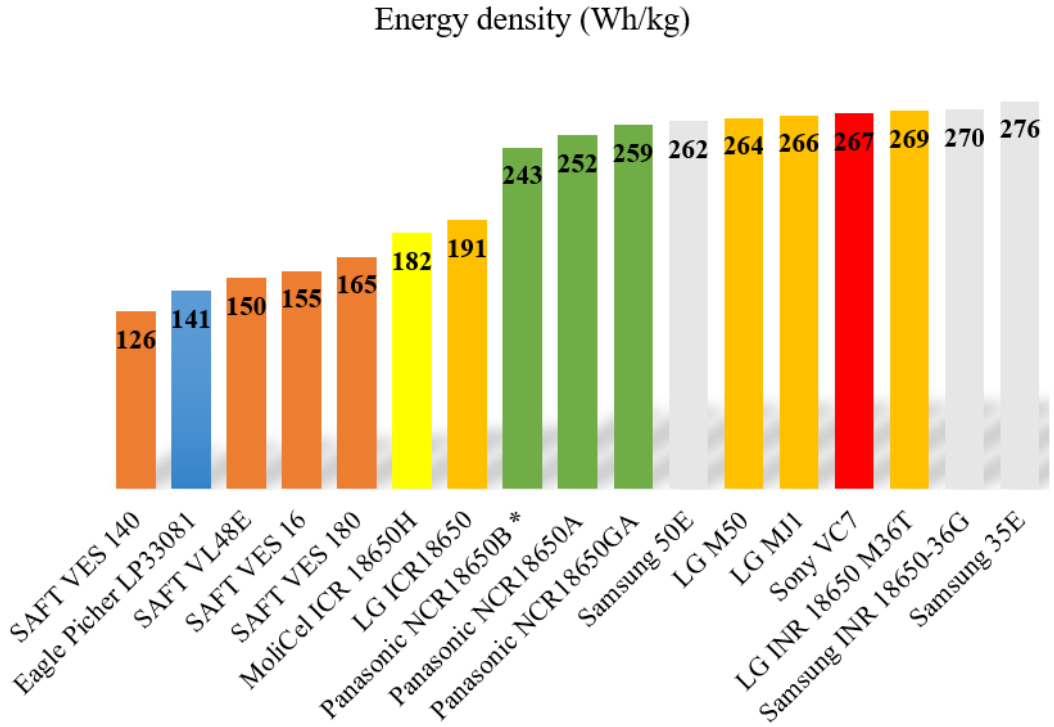

* *Same battery cell has been used for the Ten-Koh satellite as well as during the engineering approach in Chapter III.*

Fig II-2 List of some battery cell's manufacturers for space application
(Data source: NASA. (2020). State-of-the-Art Small Spacecraft Technology [*20*])

Table II-3 List of some satellite battery manufacturers
(Data source: NASA. (2020). State-of-the-Art Small Spacecraft Technology [*20*])

Manufacturer	**Product**	**Cell used**	**Specific energy (Wh/kg)**
Berlin Space Technologies	BAT-100	Lithium-Ferrite (Li-Fe)	58.1
ibeos	Modular SmallSat Battery	Unkn.	109.8
EaglePicher	Rechargeable Space Battery (NPD-002271)	EaglePicher Li-Ion	105–117
AAC-Clyde	40Whr CubeSat Battery	Clyde Space Li-Polymer	119
Blue Canyon Technologies	BCT Battery	Li-Ion or LiFePo4	Unkn.
Canon	BP-930s	four 18650 Li-Ion cells	132
Vectronic	Li-ion Battery Block VLB-X	SAFT Li-ion	Unkn.
GomSpace	NanoPower BP4	GomSpace NanoPower Li-Ion	143
	NanoPower BPX		154
SAFT	4S1P VES16 battery	SAFT Li-ion	155

ABSL	COTS 18650 Li-Ion Battery	Sony, MoliCell, LG, Sanyo, Samsung	90–243
Ultralife Corporation	Li-MnO2 and Li-CFx	Li-MnO2 and Li-CFx	350–450

II.4. Solid-state, ceramic, batteries

The study of the state of art for batteries that have been previously used in space applications and belong to a large category of energy storage has been conducted to focus on a new kind of technology that may be used in the near future for more efficiency and reliability [*13*].

Since 1950, another solution focusing on material properties for ionic conductivity has been proposed. Researchers have started working on a solid electrolyte; however, their limited performances on lithium battery restricted its use on pacemaker with the first practical use [*13*,*46*].

Batteries are mainly composed of the cathode and anode, and these two electrodes are isolated by a separator. The separator is moistened with electrolyte and forms a catalyst that promotes the movement of ions from cathode to anode on charge and in reverse on discharge [*47*].

The separator is the part of the electrochemical cells placed between the positive and negative electrode, or between electrodes with different polarity. Its function is not only limiting to the separation, it prevents the self-discharge of the battery, but simultaneously allows the flow of Ions. Separators can be categorized into: ion-permeable (previous membrane), or ion conductive (solid electrolyte), in which the *Polymer* and the *Ceramic* electrolyte are located [*48*].

A solid electrolyte can be made by *Ceramic* or *Polymer* as shown in ***Table II-4***. The difference between these two materials is mainly summarized in their mechanical properties; while *Ceramic* has high elastic moduli and is more appropriate to work in high temperature, the *Polymer* is more suitable for flexible design with low elastic moduli and cheap cost production [*13*,*49*].

Table II-4 Electrolyte for Lithium Battery [*13*]

Organic Polymer	**Inorganic Ceramic**
Solid Gel	Sulfide **Oxide** Phosphate

With the apparition of a solid electrolyte, the question of safety has not been a problem. All the rechargeable lithium batteries need a protection circuit to control the voltage between 2.5V ~ 4.2V/4.35V and to prevent the battery from over-

charging, and over-discharging to irreversible damaging which may lead to explosion or firing. The work done by *Xin-Rui Li et al.* for the thermal analysis on lithium batteries shows clearly the hazardous of the lithium battery compared to the other kind of batteries [***50***], or more details in the review done by *Dongxu Ouyang et al.* on the thermal hazards of the lithium-ion batteries, where the risks and consequences due to a bad manipulations or an extreme work conditions have been listed [***13***,***51***]. However, the solid-state batteries have shown that after an abnormal charging at DC 6V, 30V, and even AC 110V-220V without the protection circuit, it is still ultra-safe (no fire, no explosion). The biggest challenges of the actual solid-state Li Battery are poor C-rate, and high internal resistance, compared to a Li-ion battery [***13***].

Fig II-3 represents the classification of batteries in terms of their technology, with the comparison of their performance (energy density) for lighter and smaller, it is clearly seen the reason why the Lithium-Ion batteries have monopolizing the market with its application in majorities of the space mission for a long time. However, the researches for the best battery for more performances is still ongoing, with new technology such as the Solid-State Batteries, the review has been done by *J.G. Kim et al.* has listed the lithium-based Solid-State Batteries, and the non-lithium-based systems [***52***]. As one example of the development of ceramic electrolytes, the work done by *J.K. Feng et al.* which has led to the development of a new system with higher conductivity [***52***,***53***]. Since the Solid-State Batteries have been available, they have been targeted to be the future reliable batteries for space use, the reason for their high energy density and ionic conductivity, finally for safety issues.

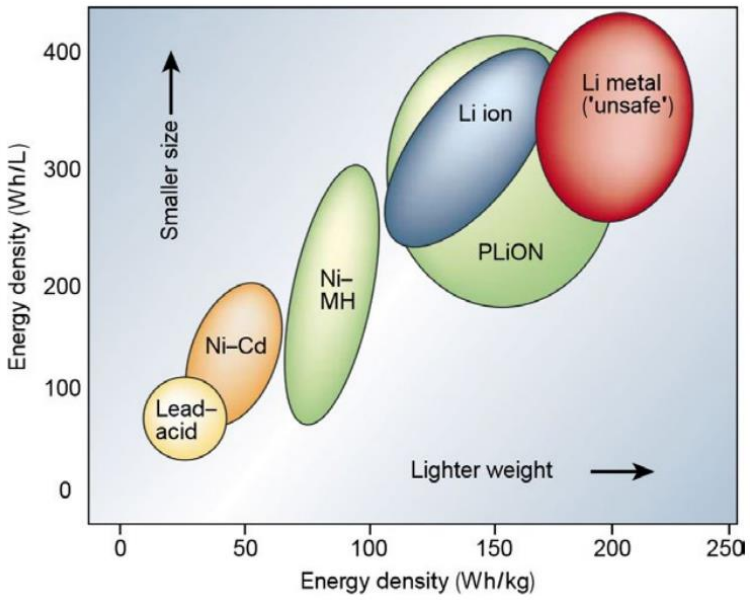

(Creative Commons Attribution License)

Fig II-3 Classification of different batteries technology in terms of lighter and smaller [**54**]

Table II-5 lists some of the manufacturers of the Solid-State Battery all over the world based on the type of its electrolyte, the study done by *ProLogium* company in 2019 and updated in 2021 has reported twenty-one manufacturers between *Polymer* type and *Ceramic* (*Sulfide*, and *Oxide*) type. The last update in 2018 shows that while some manufacturers have chosen to continue with their initial type of electrolyte, others have chosen to switch to the other type of electrolyte or been hybrid as for *Panasonic*. Finally, since 2018 the number of manufacturers working on the Ceramic type, for both *Sulfide* and *Oxide*, has increased, especially for the *Oxide* type where several manufacturers switched from the previous *Polymer* type.

Table II-5 List of some manufacturers of Solid-State-Battery all over the world From 2018 to 2021
(Source: *ProLogium.Co*, 2019 & 2021)

Electrolyte	**Before 2018**	**After 2018**	**Last update 2021**
Solid Polymer	**EMBatt** (Germany), **Solid Energy**, **Ionic Material**, Bosch & Seeo, *Quantum Scape* (USA) **Bollore** (Canada) *WeLion, Qingtao* (China)	**EMBatt** (Germany), **Solid Energy**, **Ionic Material** (USA) **Bollore** (Canada)	**EMBatt** (Germany), **Solid Energy**, **Ionic Material** (USA) **Bollore** (Canada)
Ceramic thick film (***Sulfide***)	**Solid Power** (USA) **CATL (China)** **Samsung SDI**, **LG Chem** (Korea) **Toyota**, **Panasonic**, **Hitachi Zosen** (Japan) *Ganfeg* (China)	**Solid Power** (USA) **CATL (China)** **Samsung SDI**, **LG Chem** (Korea) **Toyota**, **Panasonic**, **Hitachi Zosen** (Japan)	**Solid Power** (USA) **CATL (China)** **Samsung SDI**, **LG Chem** (Korea) **Toyota**, **Panasonic**, **Hitachi Zosen** (Japan)
Ceramic thick film (***Oxide***)	**Prologium** (Taiwan) **muRata – Sony** (Japan)	**Prologium** (Taiwan) **muRata – Sony**, TDK, FDK, NGK, Toyota (Japan) *Quantum Scape* (USA) *Qingtao, WeLion, Ganfeg* (China)	**Prologium** (Taiwan) **muRata – Sony**, TDK, FDK, NGK, Toyota (Japan) *Quantum Scape* (USA) *Qingtao, WeLion, FunLithium* (China)
Ceramic thin film	Apple (IPS), Dayson & Sakti3 (USA)	STMicroelectronics (Switzerland)	STMicroelectronics (Switzerland)

Fig II-4 summarizes only the manufactures from 2018 to 2021, based on the type of the electrolyte used for the battery.

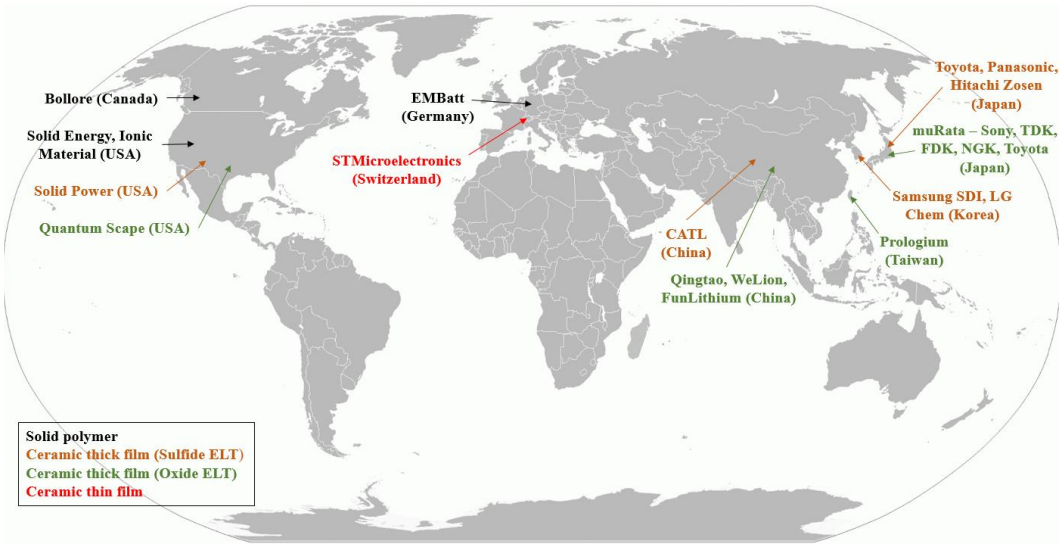

Fig II-4 List of some manufacturers of Solid-State Battery.
(Source: *ProLogium.Co*, 2021)

Several kinds of research have started on the evaluation of Lithium Polymer battery as the work done in 2005 by *Xianming Wang et al.* for the cycle-life simulation of commercial Lithium Polymers cells on Low-Earth-Orbit [*13*,*54*]. In 2007, a ground environmental test and designing power board has been done for a small satellite by *Craig S.Clarkon et al.* [*13*,*56*]. Then, a commercial power system board has been developed using a Lithium Polymer battery by *Clyde Space* in 2008. Again, the characterization of Lithium Polymer batteries for the CubeSat application has been done by *Nimal Navarathinam et al.* [*13*,*57*]. Finally, the work was done by *João P. Monteiro et al.* during the integration, and the verification approach of ISTSat-1 CubeSat is one of many other examples for testing one kind of the Solid-State-Polymer battery for space use [*24*,*58*].

All the previous works on the Lithium Polymer batteries have shown a promising result, which has led to their potential use on small satellites, such as the application in the Low-Earth-Orbit for some recent small satellites listed in ***Table II-6*** [*13*].

Table II-6 List of Small Satellites with Lithium Polymer Batteries [*13*]

Name	**Status in orbit**	**Year**	**Number of Cells**
KySat-1 [59]	Launch failure	2011	4 Cells
Unite [60]	Operational	2018	4 Cells
Libertas [61]	Semi-Operational	2019	1 Cell
Ceres [61]	No signal	2019	1 Cell
CySat [61]	Not launched	2020	1 Cell
Tjreverb [61]	Not launched	2020	2 cells
Colombia 1 [62]	-	-	N/D
Utah Sat [63]	-	-	4 Cells

Concerning the solid-electrolyte made by *Ceramic*, nowadays no work has been done to evaluate its performance and survivability to be used for space application purposes. However, their evaluation for space application will offer a clear vision for the future energy storage that may be used in new missions, starting from a small satellite to a small probe for mission explorations [*13*].

The use of separator-based *Ceramic* has been more attractive comparing to the other material, especially due to the safety. The chemical, mechanical and thermal properties are crucial for the electrochemical cell performances and safe operation. The *Ceramic* has been categorized by higher thermal, chemical and dimensional stability. For those reasons, it has been targeted, and gain interest for the secondary batteries' applications [*48*].

Table II-7 presents a relative comparison done for the solid-state electrolyte showing the differences between the three types: Polymer, *Sulfide*, and *Oxide* in terms of performance, processing; and safety [*64*].

Table II-7 Relative comparison for the different types of solid-state electrolyte
(Data source: [64])

Electrolyte	Performance	Processing	Safety
Polymer	*	***	**
Sulfide	***	**	*
Oxide	**	*	***

* Low, ** Intermediate, *** Excellent.

II.4.1. Batteries' description

Based on the list of different Solid-State-Battery manufacturers in ***Table II-5***, and as a preselection for an engineering demonstrative mission in orbit for a new kind of battery technology, taking into account the small size, which can fit into Nanosatellites from 1U to 6U, two different Solid-State-Batteries based *Ceramic* have been selected as a candidate battery (**SSCB#01** and **#02**). The two batteries, from two different companies, belong to the *Ceramic* type with the difference in the material used for their solid electrolyte, *Sulfide* for **SSCB#01**, and *Oxide* for **SSCB#02**.

The two batteries present an interest for their integration with the *Modular-Wall-Battery*, **First**, with their solid electrolyte which provide more features than the conventional Lithium-Ion battery. **Second**, they have never been used in space, which is a good opportunity to proceed for their evaluation to be used in space as future satellite batteries.

The *Ceramic Sulfide* type **SSCB#01**, is a commercial battery made by *Hitachi Zosen*. This one has been evaluated using several prototypes, so far, without

showing any decrease in the capacity in low temperature at -100°C for 800 hours storage. The same battery has been simulated under the Moon conditions for a temperature range between -40°C to +80°C, 90% remain capacity could be resulted after simulating the 12 cycles of sunlight/eclipse for one year. A battery pack with 2000 mAh with higher capacity could be manufactured following the *Laminated* design of the battery pack [***65***]. ***Table II-8*** presents the specification of the All-Solid-State-Ceramic-Battery based *Sulfide* **SSCB#01**.

Table II-8 All-Solid-State-Battery based *Sulfide* (**SSCB#01**) [***65***]

Specification	**Value**
Size (mm)	50×50
Operation voltage (V)	2.8 to 4.0
Temperature range (°C)	-40 to +80
Capacity (mAh)	150

Finally, due to the market availability comparing to the **SSCB#01** which is still under development, and the reason that the *Ceramic Oxide* type has never been used in space as well as the *Sulfide*, and never been tested on the ground comparing to the **SSCB#01**, three samples of the commercial Solid-State Lithium-Ceramic-Battery (Solid-state LCB) (**SSCB#02**) based *Oxide*, represented in ***Fig II-5*** with different capacities and two different types, Solid-State Flexible-Lithium-Ceramic-Battery (Solid-state FLCB) and Solid-State Pouch-Lithium-Ceramic-Battery (Solid-state PLCB), have been chosen as a sample of *Ceramic*-based batteries to be studied, only the PLCB has been selected for the first full ground evaluation test, from the *launch* to the *space environment* conditions, for Nanosatellite application.

(a)

(b)

(c)

Fig II-5 Solid-State Lithium-Ceramic-Battery based *Oxide* (**SSCB#02**)
((a) PLCB01, (b) PLCB02, (c) FLCB used for the *MWB* pack)

Table II-9 is summarizing all the specifications, mechanical as well as electrical, for all the selected Solid-State Lithium-Ceramic-Batteries based *Oxide* (**SSCB#02**).

Table II-9 Solid-State Lithium-Ceramic-Batteries specification (**SSCB#02**) [***66***]
(Source: Solid-State Lithium-Ceramic-Battery datasheet, *ProLogium.Co*, 2019)

Lithium Ceramic Battery	**PLCB01**	**PLCB02**	**FLCB**
Nominal Voltage (V)	3.75	3.75	3.75
Nominal Capacity (mAh)	1950	1450	90
Energy (Wh)	7.3125	5.4375	0.3915
Operation voltage (V)	4.35~2.75	4.35~2.75	4.35~2.75
Size (mm)	4.5×60×105	6.3×42×88	0.43×51.5×83(76)
Weight (g)	59.5	45	3.1
Operating temperature (°C)	-20〜+60	-20〜+60	-20〜+60

As a preselection for a first evaluation for in orbit demonstrative mission, the capacity has not been the priority as for the FLCB, however, it was better to select the potential candidate for a future application as well as its integration with the *Modular-Wall-Battery* concept, this one using the FLCB pack presented in ***Table II-10***.

Table II-10 includes a different pack of FLCBs that has been customized for the *Modular-Wall-Battery* concept proposal. The FLCB pack will be presented in detail in ***Chapter V*** and ***VI***.

Table II-10 FLCB's pack batteries' specifications (**SSCB#02**)

Li-Ceramic	**Capacity [Ah]**	**Nominal voltage[V]**	**Operation voltage[V]**	**Equivalent size [mm]**	**Weight [g]**
FLCB Pack (9 Cells 90mAh)	0.810	3.75	4.35~2.75	3.87×51.5×83(76)	27.9

II.4.2. Cells' description

Keeping the same principle of operation as a conventional Lithium-Ion battery, the Solid-State Lithium Ceramic Battery (LCB), the selected *Oxide* type battery, is a Lithium-Ion battery cell in which the electrons move from the negative electrode to the positive electrode while the Li+ ions move in the opposite direction through the electrolyte for the electroneutrality equilibrium during operating as a source of energy, and Li+ ions will flow in reversed direction during the charge mode [***13***,***67***].

The Lithium Ceramic Battery (LCB) has a solid *Ceramic* electrolyte instead of liquid such as for the Lithium-Ion (LIB) or gel for the Lithium Polymer battery (LPB). Its solid *Ceramic* electrolyte with high elastic moduli makes the battery

more suitable for high temperature and pressure [*13*,*69*]. There is no leakage and no flammable material inside. Furthermore, with the *Lithium Cobalt Dioxide*, the battery technology is categorized as having high specific energy (capacity), good performance, life span, and specific power [*13*,*67*].

Table II-11 represents the chemical composition of all the selected LCB under evaluation.

Table II-11 Chemical Material Composition for Lithium Ceramic Batteries [*13*]
(Source: *ProLogium.Co*, 2019)

Item	**Material**
Anode (*negative electrode*)	Graphite
Anode current collector	Copper foil
Cathode (*positive electrode*)	Lithium Cobalt Dioxide (LiCoO2)
Cathode current collector	Aluminum foil

Concerning the inorganic *Ceramic* used for the Lithium batteries, the same electrolyte used for the selected battery during the present study, belong to the oxide electrolyte which can be divided into two groups: Crystalline state, and amorphous/glass state. The conductivity of the *Oxide* electrolyte can vary from 10^{-9} to 10^{-3}, however, for only the glass *Oxide* electrolyte, the same material as the selected battery, the conductivity varies from 10^{-9} to 5×10^{-6}. The *Oxide* electrolytes are denoted as Li_2O-MO_x which "M" may be Si, B, P, Ge, etc, as represents in the 2D schematic representation of tetrahedrally coordinated Li_2O–SiO_2 glass by *Ren. Y et al.* [*68*].

Moreover, all rechargeable lithium batteries need a protection circuit to control the voltage between 2.5V ~ 4.2V/4.35V and to prevent the battery from overcharging, and over-discharging to irreversible damaging. But after abnormal charging at DC 6V, 30V, and even AC 110V-220V without the protection circuit, the LCB is still ultra-safe (no fire, no explosion) [*13*].

The biggest challenge of the Solid-State-Ceramic Lithium battery are, additionally to the ones show in ***Table II-7***: First, Poor C-rate, and second, high internal resistance. The company declares on its website that it keeps decreasing internal resistance through developing a new chemical system. Internal resistance of the LCB reached the same level as the LPB in 2017.

Finally, the only concern for all kinds of Solid-State battery, especially the thin ones is the price which makes them relatively expensive than the conventional Lithium-Ion, however, it is expected to be cheaper with time.

II.5. Conclusion

The *Ceramic* type of battery looks to be a good area for development and application, especially whit the features that can be provided as safety, the main concern for many users. Finally, due to the interest by the Japan Aerospace Exploration Agency (*JAXA*), to demonstrate for the first time its *Sulfide type* in space to achieve the targets for application to future planetary exploration missions [***70***,***65***].

The commercial Solid-State batteries, *Oxide type*, as a sample of *Ceramic*-based batteries, selected for the present study should be evaluated carefully, first the *Ceramic* type of battery has been compared to different battery technology including the *Polymer* type following an engineering approach for the feasibility study of the Solid-State Lithium-Ceramic-Battery' application on small satellite presented in ***Chapter III***. Then, following a long evaluation process of ground environmental testing that will be described in detail in ***Chapter IV***. The process has included vibration and shock tests for evaluating the hostile *launch environment* conditions, finally, vacuum and thermal vacuum tests for the *space environment* at Low-Earth-Orbit. According to the *ISO standard 19683:2017(E)*, the radiation test may be optional depending on the satellite mission orbit; however, it will be better to be included according to other orbit or missions, a proposition of procedure has been included within the present study for future investigation.

Chapter III

Engineering Approach, & Feasibility Study of the Solid-State Lithium-Ceramic-Battery' Application

III. Engineering Approach, & Feasibility Study of the Solid-State Lithium-Ceramic-Battery' Application

Chapter III related to the engineering approach and feasibility study of the Solid-State Lithium-Ceramic-Battery application on small satellites consists of a proposition of new methodology of engineering approach in detail for the selection of the appropriate battery and technology following the satellite requirements and missions.

The methodology followed during the study has begun with a selection of a different kinds of batteries' technology, all batteries have been compared to the initial Ten-Koh battery in order to classify them by equivalent capacity. Then the results of this comparison have been taking as inputs for sizing the new battery for Ten-Koh, in order to study the impact of using the Solid-State Lithium-Ceramic-Battery on the design of the satellite compared to the other technology, in terms of the volume and the weight, as well as having enough capacity and to operate safely within all the different satellite operation modes.

Three Solid-State Lithium-Ceramic-Batteries with different capacities have been selected as samples for the study, they belong to the same battery's manufacturer presented in ***Chapter II***.

The engineering approach has also summarized some kinds of batteries' technology with their comparison and showed their application in some satellite's heritages. Finally, the application of the approach on a real case study, Ten-Koh battery resizing, focused on the impact that can lead to the design in terms of simplicity and the in-orbit operation management in terms of decreasing resources needed for the battery's operation.

III.1. Ten-Koh satellite

Ten-Koh satellite that has been launched to the sun-synchronous sub-recurrent orbit on October 29th 2018 as a piggyback satellite [***71***], has been developed at the *Kyushu Institute of Technology* (*Kyutech*) based on the previous deep space probe Shinen-2 [***72***]. The structure, represented in ***Fig III-1***, with 23.5Kg for the total mass consists of a quasi-spherical shape Ø500mm, made mainly by the Carbon Fiber Reinforced Plastic (CFRP), and by the Aluminum for the internal structure [***13***]. The satellite had as a mission to explore the space weather effects in the Low-Earth-Orbit [***73***,***74***], and has focused mainly on the investigation on the change of the physical properties of LATS and CFRP materials additionally to the measurements of changes in the CTE of CF/PEEK composites samples [***75***].

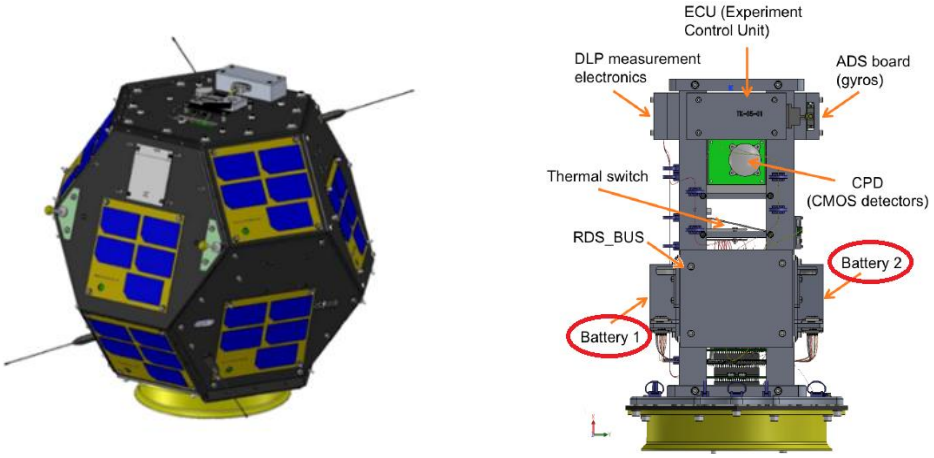

(a) Launch & in orbit configuration

(b) The Inside view of Ten-Koh satellite with batteries' location

Fig III-1 Ten-Koh Satellite [*73*]

The electrical power system of the Ten-Koh satellite consists of twelve *solar module integrated converters* (*SMIC*) connected in parallel [*39*], each panel has contained five triple-junction solar cells for power generation, and for charging batteries.

The battery's technology that has been used in Ten-Koh is a Lithium-Ion (Li-Ion 01), which the specification has been summarized in ***Table III-1***. All batteries have been arranged in two boxes, as represented in ***Fig III-1***, each box has contained four Li-Ions connected in parallel as in ***Fig III-3***, all the eight batteries have been connected in parallel in order to form a total capacity of 12.8Ah.

Table III-1 Ten-Koh battery

Parameter	**Value**
Technology	Li-Ion
Design	Cylindrical
Capacity (Wh)	39.22
Capacity (Ah)	3.2
Nominal voltage (V)	3.6
Max. voltage (V)	4.2
Min. voltage (V)	2.5
At DoD voltage (V)	3.69
Energy (Wh)	11.52
Energy required (Wh)	10
Depth of Discharge (%)	30
Efficiency Charge/Discharge (%)	85
Dimensions (mm)	18.5×18.5×65.3
Weight (g)	48
Temperature Range (°C)	0 to 45

All the power generated has been regulated and distributed to all subsystems, as represented in ***Fig III-2***: 5V for the Communications Control Unit (CCU), Attitude Determination and Control (ADC), On-Board Computer (OBC), Transceivers, Ultra-Double Layer Capacitance (UDLC), then to the payloads, finally 12V to the magnetometer.

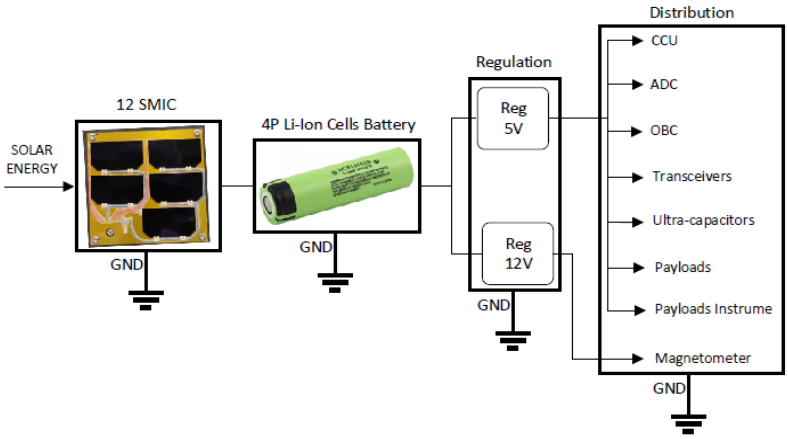

Fig III-2 Ten-Koh satellite EPS simplified block

III.2. Batteries selection

Four different kinds of commercial batteries' technology with flight heritage, at least once a time in flight in the Low-Earth-Orbit onboard small satellites, have been selected for the engineering evaluation and comparison approach, except for the Solid-State Lithium-Ceramic-Battery which have never been used in space, however, they have been evaluated under the space environment for the Low-Earth-Orbit applications and the launch environment, showing so far promising results as have been reported in ***Chapter IV***.

III.2.1. Batteries' arrangement & their heritage

The batteries' arrangement may differ from one satellite to another for different reasons. It may depend on the batteries' technology itself or the design constraint of the satellite, as shown in the following examples.

In the case of the Ten-Koh satellite, in ***Fig III-3***, two boxes in Aluminum have been designed in order to carry in one box four Lithium-Ion (**Li-Ion 01**) batteries connected in parallel. For thermal heat dissipation issues, all batteries have been covered with a layer of the *λ Gel* [*76*], and the inside box has been covered with the *α Gel* [*77*], in order to facilitate the heat transfer. Finally, two heaters in each box are expected to be used for temperatures below 5°C, during the eclipse.

The same approach of having a battery box has been adopted onboard the SPATIUM-I, released from the *International Space Station* (*ISS*) on October 6th, 2018, as presented in ***Fig III-3***. The 2U CubeSat pathfinder mission has been developed in collaboration between *NTU* (*the Nanyang Technological University*) of Singapore and *Kyutech* (*the Kyushu Institute of Technology*) [***78***].

An additional example with a different kind of battery technology is the Nickel-Metal Hydride (**NiMH**) battery which has been used onboard the HORYU-II satellite and launched on May 18th, 2012 [***79***]. Batteries have been arranged as three series and three parallels (3S3P), with a nominal voltage of 3.6V and a capacity of 5.7Ah, packed in a box as presented in ***Fig III-3***. For thermal management, a sheet heater has been used, additionally to the thermo-sensors for temperature monitoring in orbit. Finally, to reduce temperature fluctuation, the battery pack has been isolated from outside temperature using a glass epoxy. The heaters have been planned to work for a temperature below 20°C [***80***]. The same kind of batteries have also been used one more time onboard the HORYU-IV, launched on February 17th, 2016 [***81***,***82***].

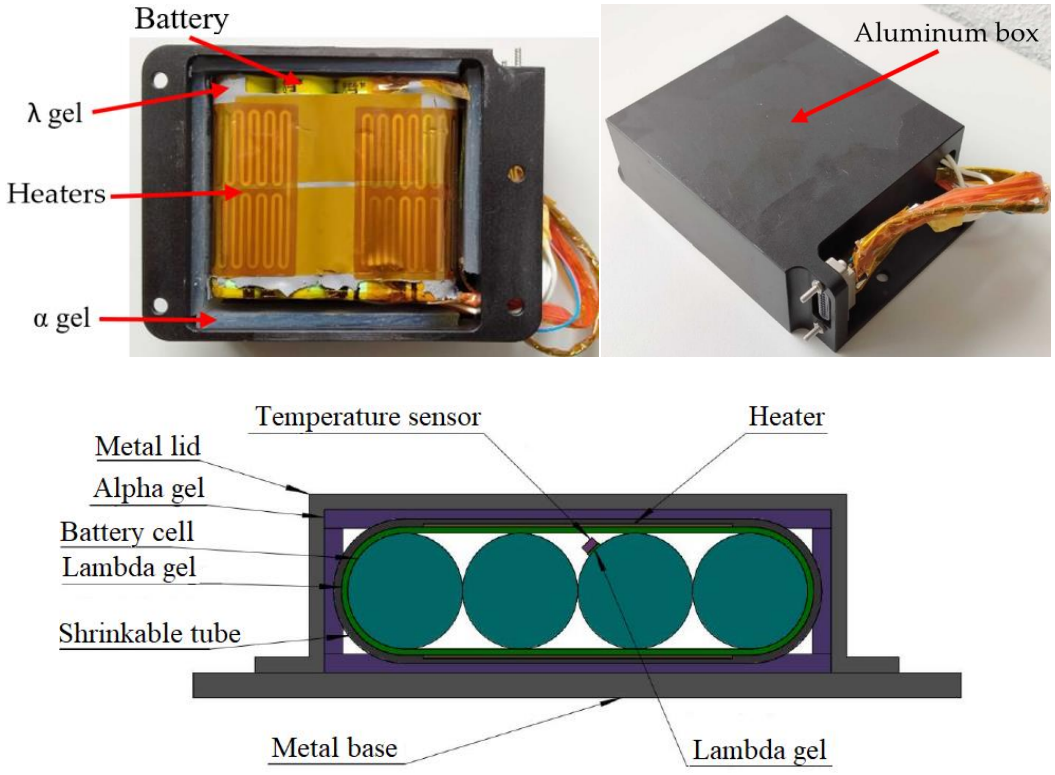

(Ten-Koh project source)

Fig III-3 Satellite battery *box concept arrangement*
The same concept has been followed onboard the Ten-Koh satellite

Another kind of mechanism has been needed to support and fix the cylindrical form of batteries following different approach, the battery's *mechanical structural concept arrangement* as for the EQUiSat satellite, launched on May 21th, 2018, and deployed from the *International Space Station* (*ISS*) on July 13th 2018 [***83***], two different kinds of batteries have been used, one set of two Lithium-Ion (Li-Ion 02), and another set of four Lithium-Iron Phosphate (**LiFePO4**), as a first demonstration and use in space [***84***]. The arrangement of batteries has been less voluminous than Ten-Koh, SPATIUM-I, or HORYU satellites.

The Upsat 2U CubeSat, launched in 2017, shows almost the same approach used onboard the EQUiSat with some mechanical support fixed on the electronic boards [***85***].

Another example with Lithium-Ion battery is the ESTCube-1, launched on April 7th 2013 [***86***]. It does not show any mechanism or box for the two batteries, which have been glued to the power board and fixed on another board. All boards have been assembled using vertical connections [***87***]. The battery used in the ESTCube-1 has almost the same specifications as the Lithium-Ion (**Li-Ion 02**) used onboard the EQUISat.

With the demonstration module for the in-orbit experiment of the Ionic-Liquid-Lithium-Ion (**IL-LIB**) cells on board the Hodoyoshi-3 microsatellite [***88***], batteries have been arranged differently. The approach has not been used for a real application; however, the demonstration mission may lead to a different approach to fix batteries using Kapton tape especially with the pouch design of the batteries.

Concerning the Solid-State Battery, the ISTSat-1 satellite expected to be launched in 2021, is one example of recent satellites that will use Lithium Polymer (**Li-Polymer**) as a secondary battery [***89***]. The pack of batteries will be put between the electronic boards together with any box or structural mechanism, such as in the previous examples [***90***]. Almost the same arrangement, has been proposed by Clyde Space with the application of the Li-Polymer batteries in space [***91***,***92***].

Using the pouch design with the Solid-State Battery makes the *pouch battery pack concept arrangement* looks simpler than the previous examples, and not as bulky as the case of the cylindrical **Li-Ion 01** or **NiMH** batteries onboard the Ten-Kho, the HORYU-II, or even SPATIUM-I, satellites. Otherwise, the use of heaters and thermo-sensors is still necessary for thermal management and temperature monitoring in space.

III.2.2. Batteries' specification and comparison

All batteries have been classified from higher to lower capacity, as represented in ***Table III-2***. There are two Lithium-Ion batteries with different capacities, the Li-Ion 01 (*NCR18650B*) with a capacity of 3,2Ah and the Li-Ion 02 (*LGABC21865*) with 2,8Ah. Followed by the **Li-Ceramic 03** (*PLCB4360A5AAMA*) 1.95Ah, and

the Nickel Metal Hydride (NiMH) (*HR-3UTGB*) 1.9Ah. Then comes the **Li-Ceramic 02** (*PLCB604288AARA*) 1.45Ah, and the Li-Polymer (*LPP 503759 8HH*) with 1.4Ah, and finally the Lithium-Iron Phosphate (LiFePO4) (*APR 18650*) 1.1Ah, and the **Li-Ceramic 01** (*PLCB475255AANA*) 0.77Ah.

The Li-Polymer battery has been selected, for this study, for two reasons: its flight heritage and its similar capacity to the **Li-Ceramic 02** that has been tested within the ground evaluation test under the launch and the space environments. During the discussion and the conclusion, the **Li-Ceramic 02** is the main battery that has been targeted. The other Li-Ceramic batteries have been selected in order to have one with higher and one with lower capacity.

Table III-2 Batteries' specifications

Batteries	Capacity (Ah)	Energy (Wh)	Energy Density (Wh/L)	Volume (L)	Weight (g)	Temperature range (°C)	Design	Reference
Li-Ion 01	3.2	11,52	676	0.022	48	0 to +45	Cylindrical	NCR18650B
Li Ion 02	2.8	10.416	/	0.022	50	0 to +45	Cylindrical	LGABC21865
Li-Ceramic 03	**1.95**	**7.313**	**300**	**0.028**	**59.5**	**-20 to +60**	**Pouch**	**PLCB4360A5AAMA**
NiMH	1.9	2.28	/	0.010	27	0 to +45	Cylindrical	HR-3UTGB
Li-Ceramic 02	**1.45**	**5.438**	**234**	**0.023**	**45**	**-20 to +60**	**Pouch**	**PLCB604288AARA**
Li-Polymer	1.4	5.18	465	0.011	24.6	0 to +45	Pouch	LPP 503759 8HH
LiFePO4	1.1	3.63	/	0.022	39	-30 to +60	Cylindrical	APR 18650
Li-Ceramic 01	**0,77**	**2,888**	**210**	**0.014**	**30**	**-20 to +60**	**Pouch**	**PLCB475255AANA**

III.3. Engineering approach methodology

The methodology followed during the study is schematically shown in the flowchart given in ***Fig III-4***, summarizing the three steps followed during the engineering approach for the evaluation of the impact of the Solid-State Lithium-Ceramic-Battery on the Ten-Koh's power supply.

After the selection of different kinds of battery technologies. In **Step I**, all those candidate batteries are compared with the initial Ten-Koh battery (Li-Ion 01)

capacity (**3,2Ah**), considered as reference, in order to classify them by equivalent capacity, this one representing how much each battery's capacity is equivalent to the reference battery.

In **Step II**, the results from Step I (***Task #1***) are applied on volume (***Task #2a, line a***), and then on weight (***Task #2b, line b***). Finally, the two results on the two lines have been applied respectively on capacity and weight, then on capacity and volume (***Task #5a*** *and* ***#5b***), respectively.

Within **Step III**, the results of the comparison and final classification are taken as inputs for sizing the new Ten-Koh satellite's battery, in order to study the impact of using the Solid-State Lithium-Ceramic-Battery on the design of the satellite compared to other technologies. The comparison is carried out in terms of volume, weight, and capacity, as well as regards the ability to operate safely within all the different satellite operation modes.

While the discussion has been performed in terms of one battery only, the term battery has been used to refer to the satellite battery's cell. The Ten-Koh satellite has used a pack of four batteries in each box (*main and backup*), with a total of eight batteries connected in parallel, as presented in ***section III.1***. The term satellite battery has been used to refer to the battery pack.

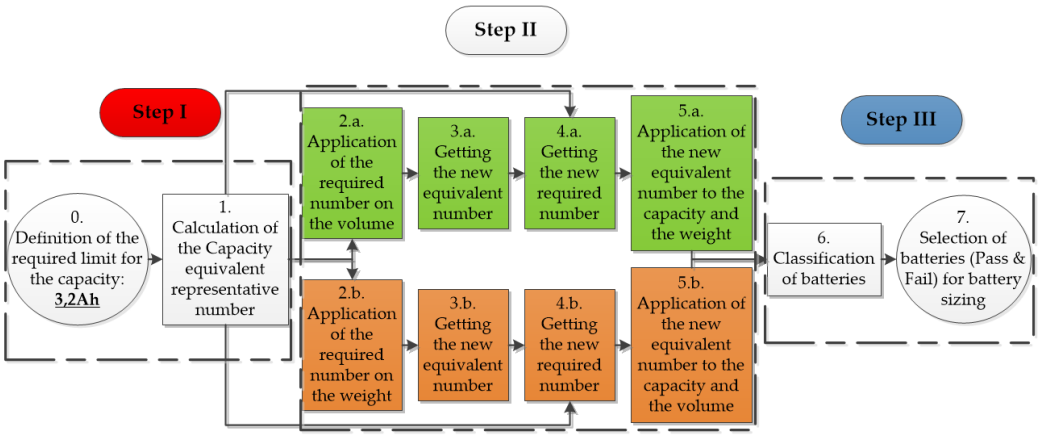

Fig III-4 Methodology flowchart overview

III.3.1. Step I: The capacity equivalent representative number (RNC)

With the first classification of batteries in terms of the equivalent capacity, using only the equivalent number for capacity (**ENC**) in ***Table III-3***, which is defined as the number of batteries that each battery type displays for a difference in capacity equivalent to one Li-Ion 01 battery, without exceeding the max capacity of 3,2Ah. The NiMH, the **Li-Ceramic 03 (1,95Ah)** with one equivalent battery, and LiFePO4 with two equivalent batteries have shown a capacity deficit larger than 1Ah. The

two Solid-State batteries, Li-Polymer and **Li-Ceramic 02 (1,45Ah)** with two equivalent batteries, and the Li-Ion 02 with one equivalent battery, have shown a capacity deficit of less than 0,5Ah. Finally, the **Li-Ceramic 01 (0,77Ah)** with four equivalent batteries has shown about 0,1Ah less than the limit.

The new classification of all batteries in ***Table III-3*** has been computed in terms of the max capacity got after the application of the required number for the capacity (**RNC**), which is defined as the number of candidate batteries equivalent to one Li-Ion 01 in providing the minimum capacity of 3,2Ah. The required number (**RNC**) is thus defined as the equivalent number for capacity (**ENC**) add by one unit. The required number of batteries thus displays a capacity that is equal to, or higher than the required value of 3,2 Ah.

The new classification of batteries changes when compared to the classification in terms of the equivalent capacity. From higher to lower capacity, the Li-Ion 02, with two required batteries, has shown almost double of the reference capacity. The **Li-Ceramic 02** shows an increase of 1,15 Ah and the Li-Polymer of 1Ah, for three batteries equivalent. The **Li-Ceramic 03**, **Li-Ceramic 01**, and the NiMH have shown an excess between 0,6Ah and 0,7Ah, with two, five, and two equivalent batteries, respectively. Finally, the LiFePO4 has shown just 0,1Ah of excess capacity with three equivalent batteries.

Table III-3 The capacity equivalent representative number **(RNC)**
Classification in terms of the maximum capacity (**C/c**)

Battery	**Capacity (Ah)**	**Equivalent Number (ENC)**	**Equivalent capacity (Ah)**	**Difference in capacity (Ah)**	**Capacity equivalent representative number (RNC)**	**Max capacity (Ah)**	**Excess capacity (Ah)**
Li Ion 02	2,80	1	2,80	-0,40	2	5,60	2,40
Li-Ceramic 02	**1,45**	**2**	**2,90**	**-0,30**	**3**	**4,35**	**1,15**
Li-Polymer	1,40	2	2,80	-0,40	3	4,20	1,00
Li-Ceramic 03	**1,95**	**1**	**1,95**	**-1,25**	**2**	**3,90**	**0,70**
Li-Ceramic 01	**0,77**	**4**	**3,08**	**-0,12**	**5**	**3,85**	**0,65**
NiMH	1,90	1	1,90	-1,30	2	3,80	0,60
LiFePO4	1,10	2	2,20	-1,00	3	3,30	0,10

The capacity equivalent representative number (**RNC**) has been used as the input for the second step.

III.3.2. Step II: Compromise of the capacity in terms of volume and weight

III.3.2.1. The new equivalent number for volume and weight (NENV, NENW)

The results for the capacity equivalent representative number (**RNC**), from Step I, have been applied to the two other parameters: the volume and the weight, respectively, in order to get the new equivalent number for volume and weight (**NENV**, **NENW**) specific to the **RNC**. Then the classification has been carried out from the smaller to the larger equivalent volume (**EV**), and from the lighter to the heavier equivalent weight (**EW**).

The equivalent number for volume (**ENV**) in ***Table III-4*** is the ratio of the volume of each battery and the volume of one Li-Ion 01 which is 0,022L (***Eq.III.1***). The equivalent volume (**EV**) for each candidate battery is given by the product of the **RNC** and the unit volume of each battery (***Eq.III.2***). Then, the new volume equivalent number (**NENV**) has been computed as the ratio of the equivalent volume (**EV**) and the volume of one Li-Ion 01 (***Eq.III.3***) in order to define how much each battery is equivalent to one Li-Ion 01 battery, in terms of volume (**V/c**).

$$ENV = \frac{V_i}{V_0} \qquad \textbf{(Eq.III.1)}$$

$$EV = RNC \times V_i \qquad \textbf{(Eq.III.2)}$$

$$NENV = \frac{EV}{V_0} \qquad \textbf{(Eq.III.3)}$$

$V_0 = 0.022L$ *(Li-Ion 01 volume)*

$V_i =$ *Volume of each battery*

For some batteries, the **NENV** is equal to the required number (**RNC**) as for Li-Ion 02, LiFePO4, and **Li-Ceramic 02**, or smaller like for the NiMH, the Li-Polymer, and the **Li-Ceramic 01**. However, for the **Li-Ceramic 03**, it has been difficult to judge for the small change, it can be seen as an increase in terms of capacity as well as for the volume. Finally, the classification from the smaller to the larger equivalent volume (**EV**), has been as follows: NiMH, Li-Polymer, Li-Ion 02, **Li-Ceramic 03**, LiFePO4, and **Li-Ceramic** (**01** and **02**).

The equivalent number for the weight (**ENW**), in ***Table III-4***, is the ratio of the weight of each battery and the weight of one Li-Ion 01 which is 48g (***Eq.III.4***). The product of the **RNC** and the unit weight of each battery lead to an equivalent weight (**EW**) (***Eq.III.5***). Then, the new weight equivalent number (**NENW**) has been computed as the ratio of the equivalent weight (**EW**) and the weight of one Li-Ion 01 (***Eq.III.6***) in order to define the equivalence of each battery with one Li-Ion 01 battery, in terms of weight (**W/c**).

$$ENW = \frac{W_i}{W_0} \quad \textbf{(Eq.III.4)}$$

$$EW = RNC \times W_i \quad \textbf{(Eq.III.5)}$$

$$NENW = \frac{EW}{W_0} \quad \textbf{(Eq.III.6)}$$

$W_0 = 48g$ *(Li-Ion 01 weight)*

$W_i =$ *Volume of each battery*

For all batteries, the new weight equivalent number (**NENW**) is the same as for the new volume equivalent number (**NENV**), except for the LiFePO4 that has shown **NENW** smaller than **NENV**. The classification for the weight, that has been done from lighter to heavier equivalent weight (**EW**), is as follows: NiMH, Li-Polymer, Li-Ion 02, LiFePO4, and **Li-Ceramic** (**03**, **02,** and **01**).

Table III-4 NENV (V/c) and **NENW (W/c)**

Battery	**Volume (L)**	**Equivalent number for volume (ENV)**	**Equivalent volume (L) (EV)**	**New equivalent number (NENV)**	**Weight (g)**	**Equivalent number for weight (ENW)**	**Equivalent weight (g) (EW)**	**New equivalent number (NENW)**
Li Ion 02	0,022	1	0,044	2	50	1	100	2
Li-Ceramic 02	**0,023**	**1**	**0,070**	**3**	**45**	**1**	**135**	**3**
Li-Polymer	0,011	0,5	0,033	1,5	24,6	2	73	1,5
Li-Ceramic 03	**0,028**	**1**	**0,057**	**2,5**	**59,5**	**1**	**119**	**2,5**
Li-Ceramic 01	**0,014**	**0,5**	**0,069**	**3**	**30**	**1,5**	**150**	**3**
NiMH	0,010	0,5	0,021	1	27,0	2	54	1
LiFePO4	0,022	1	0,066	3	39	1	117	2,5

III.3.2.2. The new required number (Optimization phase) (NRNV, NRNW)

As a result of the **RNC** application on all batteries in Step I, all capacities have presented an increase, as may be seen from ***Table III-3***. Then the application of the **RNC** on the volume and weight resulted in the **NENV** and **NENW** that give the volume and weight for the specific **RNC**.

In order to optimize the classification of batteries, the new required numbers (**NRNV** and **NRNW**) for volume and weight, respectively, for each battery to have less volume and weight on behalf of the capacity, have been computed from the two last outputs, the new volume and weight equivalent numbers (**NENV**, and **NENW**), in ***Table III-4***, that have been combined with the required number for the capacity (**RNC**).

These combinations have been presented as a list of conditions based on the difference (**D**) between the **RNC** and the **NENV** and **NENW,** respectively, as follows:

In the case of the volume, the **NRNV**, given in ***Table III-5***, has been estimated from the combination of the required number of the capacity (**RNC**) from Step I, and the new equivalent number for the volume (**NENV**) given in ***Table III-4*** from the application of the (**RNC**) to the volume, such as reducing the number of batteries as well as having high capacity with less volume. Following this criterion, if the new equivalent number for the volume (**NENV**) and the required number for the capacity (**RNC**) are equal, as for the Li-Ion 02, the LiFePO4, or **Li-Ceramic 02**, then the **NRNV** is taken as equal to **RNC**.

In the other case, while "$\mathbf{D_V = RNC - NENV}$" (***Eq.III.7***) is defined as the difference between the **RNC** and the **NENV**, three cases have to be considered:

- If **NENV** is smaller than the **RNC**, $\mathbf{0 < D_V \leq 1}$, as for the NiMH, then the **NRNV** is taken as equal to **NENV**.
- If **NENV** is much smaller than the **RNC**, $\mathbf{D_V > 1}$, as for Li-Polymer, **Li-Ceramic 01**, then the **NRNV** is taken as the average value between **NENV** and **RNC**.
- If **NENV** is higher than **RNC**, $\mathbf{-1 \leq D_V < 0}$, as for the **Li-Ceramic 03**, then the **NRNV** is taken as equal to **RNC**.

Table III-5 NRNV determination the new equivalent volume (V/v)

Battery	Volume (L)	New equivalent number for volume (NENV)	Required number for capacity (RNC)	New required number (NRNV)	New equivalent volume (L) (NEV)
NiMH	0,010	1	2	1	0,01
Li-Polymer	0,011	1,5	3	2	0,022
Li Ion 02	0,022	2	2	2	0,044
Li-Ceramic 01	**0,014**	**3**	**5**	**4**	**0,056**
Li-Ceramic 03	**0,028**	**2,5**	**2**	**2**	**0,057**
LiFePO4	0,022	3	3	3	0,066
Li-Ceramic 02	**0,023**	**3**	**3**	**3**	**0,07**

Following the same approach for weight as for volume, given in ***Table III-5***, the **NRNW** has been estimated from the combination of the required number of the capacity (**RNC**) from Step I, and the new equivalent number for the weight (**NENW**) got in ***Table III-4*** from the application of the (**RNC**) to the weight.

As represented in ***Table III-6***, if the new equivalent number for the weight (**NENW**) and the **RNC** are equal, as for the Li-Ion 02, and the **Li-Ceramic 02**, the **NRNW** is taken as equal to **RNC**.

In the other case, while "$\mathbf{D_w}$ = **RNC - NENW**" (***Eq.III.8***) is defined as the difference between the **RNC** and the **NENW**, three cases have to be considered:

- If **NENW** is smaller than the **RNC**, $\mathbf{0 < D_w \leq 1}$, as for the NiMH, then the **NRNW** is taken as equal to **NENW**. Except for the LiFePO4 in which **D = 0.5**, then the **NRNW** is taken as the lower integer for the **NENW**.
- If **NENW** is much smaller, $\mathbf{D_w > 1}$, than the **RNC**, as for Li-Polymer, **Li-Ceramic 01**, then the **NRNW** is taken as the average value between **NENW** and **RNC**.
- If **NENW** is higher than the **RNC**, $\mathbf{-1 \leq D_w < 0}$, as for the **Li-Ceramic 03**, then the **NRNW** is taken as equal to **RNC**.

Table III-6 NRNW determination for the new equivalent weight (**W/w**)

Battery	**Weight (g)**	**New equivalent number for weight (NENW)**	**Required number for capacity (RNC)**	**New required number (NRNW)**	**New equivalent Weight (g) (NEW)**
NiMH	27,0	1	2	1	27
Li-Polymer	24,6	1,5	3	2	49,2
LiFePO4	39,0	2,5	3	2	78
Li Ion 02	50,0	2	2	2	100
Li-Ceramic 03	**59,5**	**2,5**	**2**	**2**	**119**
Li-Ceramic 01	**30,0**	**3**	**5**	**4**	**120**
Li-Ceramic 02	**45,0**	**3**	**3**	**3**	**135**

The criteria should be defined in such to have a high capacity, small volume, and less weight with a fewer number of batteries. The **NRNV** and the **NRNW** have been defined based only on the possibilities that have been found during the study, otherwise more possibilities may be possible with different batteries, especially if the **NENW** or **NENV** are higher too much than the **RNC**, or in the case when $\mathbf{D_v < -1}$ and $\mathbf{D_w < -1}$, **D = 0.5**, **D = -0.5**, then the new criteria should follow the same philosophy as for the present study.

The new required number (**NRNV**, and **NRNW**) is a transition phase to move to the final optimization of the number of batteries in terms of the technology, depending on their capacity, volume, and weight.

III.3.2.3. Compromise of capacity, volume, and weight in terms of the NRNV, NRNW

The new required numbers, **NRNV** and **NRNW,** have been applied once on the capacity and the weight, then on the capacity and the volume, respectively.

For the first case, the **NRNV** that has been obtained for volume has been applied to capacity (**C/v**), and weight (**W/v**) as in ***Table III-7***.

The classification has been done from higher to lower capacity (C/v). Compared to results in ***Table III-3***, some of the batteries as the Li-Ion 02, **Li-Ceramic 02**, **Li-Ceramic 03**, and LifePO4 have kept the same value for capacity as well as the same required number as **NRNV**, however, some batteries have shown a decrease, as for the Li-Polymer, **Li-Ceramic 01**, and the NiMH, which leads to a new classification as represented in ***Table III-7***.

Concerning the classification in terms of the equivalent weight (W/v), from lighter to heavier, the comparison between results in ***Table III-4*** and ***Table III-7*** has shown the same classification, except for the **Li-Ceramic 02** and the **Li-Ceramic 01** that have been commuted. However, while the Li-Ion 02, **Li-Ceramic** (**03** and **02**), and LiFePO4 kept the same weight, the NiMH, the Li-Polymer, and the **Li-Ceramic 01** have presented a decrease in their equivalent weight.

Table III-7 Equivalent capacity **(C/v)** & Equivalent weight (**W/v**)

Battery	**Equivalent capacity (Ah) (EC/v)**	**New difference in capacity (Ah)**	**Equivalent weight (g) (EW/v)**	**New difference in weight (g)**
Li Ion 02	5,60	2,40	100,0	52
Li-Ceramic 02	**4,35**	**1,15**	**135,0**	**87**
Li-Ceramic 03	**3,90**	**0,70**	**119,0**	**71**
LiFePO4	3,30	0,10	117,0	69
Li-Ceramic 01	**3,08**	**-0,12**	**120,0**	**72**
Li-Polymer	2,80	-0,40	49,2	1
NiMH	1,90	-1,30	27,0	-21

For the second case, the **NRNW** that has been obtained for weight has been applied to the capacity (**C/w**), and volume (**V/w**) as in ***Table III-8***. The classification has been done from higher to lower capacity (**C/w**). Compared to results in ***Table III-3***, only some of the batteries as the Li-Ion 02, **Li-Ceramic 02**, **Li-Ceramic 03** kept the same value for the capacity as well as the same required number as **NRNW**.

However, all other batteries have shown a decrease in capacity, following the new order in ***Table III-8***.

Concerning the classification in terms of the equivalent volume (**V/w**), from smaller to bigger, the comparison between results in ***Table III-4*** and ***Table III-8*** has shown a decrease of the equivalent volume, as for the NiMH, the Li-Polymer, LiFePO4, and the **Li-Ceramic 01**. The other batteries have kept the same equivalent volume. Finally, the classification from the smaller to the bigger volume has been updated keeping the same position for NiMH, Li-Polymer, Li-Ion 02, while the main change in the classification has been for the four other batteries as follows: LiFePO4, **Li-Ceramic 01**, and the **Li-Ceramic 03**, finally the **Li-Ceramic 02** at last position.

Table III-8 Equivalent capacity **(C/w)** & Equivalent volume (**V/w**)

Battery	**Equivalent capacity (Ah) (EC/w)**	**New difference in capacity (Ah)**	**Equivalent volume (L) (EV/w)**	**New difference in volume (L)**
Li Ion 02	5,60	2,40	0,044	0,022
Li-Ceramic 02	**4,35**	**1,15**	**0,070**	**0,048**
Li-Ceramic 03	**3,90**	**0,70**	**0,057**	**0,035**
Li-Ceramic 01	**3,08**	**-0,12**	**0,055**	**0,033**
Li-Polymer	2,80	-0,40	0,022	0,000
LiFePO4	2,20	-1,00	0,044	0,022
NiMH	1,90	-1,30	0,010	-0,012

III.3.3. Step III: Batteries' classification

The final classification of batteries, as result of the step I and II, has been done in order to have a high capacity, small occupied volume, and less weight with fewer batteries. ***Fig III-5*** represents the matrix of the compromise for all the different batteries' technology in terms of their capacity, volume, and weight. It has regrouped in each column all the previous classifications, in order to summarize and highlight the main differences, displaying results for each parameter within each line of the matrix. Each battery's technology has been represented by a different colour in order to follow easily its classification within the matrix. The discussion has been done in terms of a good position, which means the battery that presented the same, an increase in the capacity, or the same, a decrease in the volume and weight, respectively.

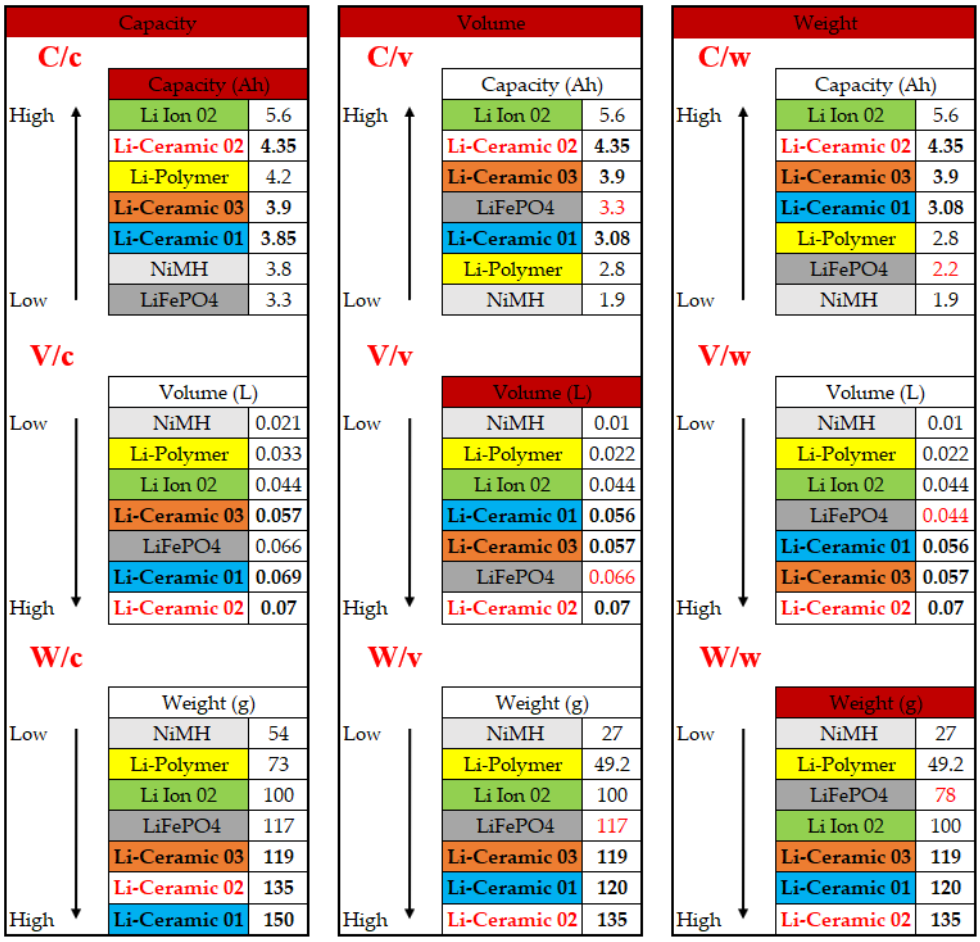

Fig III-5 compromise's matrix for higher capacity, smaller volume, and lighter weight

For the classifications of capacity in line one (L1), the Li-Ion 02 and the **Li-Ceramic 02** have kept all the time the same capacity within the two first positions, then the **Li-Ceramic 03**, between the third and the fourth position, and the **Li-Ceramic 01** between the fourth and the fifth position. The LiFePO4 could keep stability in capacity too, at L1C1 (C/c) and L1C2 (C/v), while only a decrease at L1C3 (C/w). For the Li-Polymer and the NiMH, the classification has not been so good, with a big decrease in capacity almost half, the Li-Polymer moved to the sixth position for C/v and fifth position for C/w, while the NiMH shifted to the last positions for C/v and C/w.

Otherwise, in the classification for volume at L2 and weight at L3, the NiMH and the Li-Polymer have been smaller and lighter, while the Li-Ion 02 has kept the same volume and weight along these two lines. The LiFePO4 has shown a decrease in the volume at L2C3 (V/w), and a decrease in weight at L3C3 (W/w). Finally, the **Li-Ceramic** (**03** and **02**) have kept the same volume and weight, while the **Li-Ceramic 01** has shown a decrease at W/v and W/w. Thus, the position at L2 has been the same for **Li-Ceramic 02** all the time, while the **Li-Ceramic 03** has been

moved to the fifth and sixth position at V/v and V/w, respectively. While, the **Li-Ceramic 01** has shown improvement in its position, shifted to fourth and fifth position at V/v and V/w, respectively. At L3, for weight, the **Li-Ceramic 03** kept the same position, while the **Li-Ceramic 02** and **01** have been commuted within the two last positions at W/v and W/w compared to W/c.

Table III-9 represents the effect of each parameter on the others for the different battery technologies. The table has been organized as follows: each line represents the battery's technology, and each column represents the parameters taken as the input for the required number (***Table III-3*** for the capacity **C/c**, ***Table III-5*** for the volume **V/v**, and ***Table III-6*** for the weight **W/w**) which the two other parameters will be subject to, respectively. Then, the matrix of compromise in ***Fig III-5*** has been used to fill the table after comparing the change of all parameters in terms of being stable (=), increasing (+), or decreasing (-), using the following new terms defined in ***Table III-9*** such as described below for the volume:

- Vc/v: The volume for the capacity V/c (L2C1) compared to the volume V/v (L2C2) in ***Fig III-5***.
- Vc/w: The volume for the capacity V/c (L2C1) compared to the volume V/w (L2C3) in ***Fig III-5***.
- Vw/c: The volume for the weight V/w (L2C3) compared to the volume V/c (L2C1) in ***Fig III-5***.
- Vw/v: The volume for the weight V/w (L2C3) compared to the volume V/v (L2C2) in ***Fig III-5***.

All the other terms, for the capacity and weight, have been defined in the same way.

Table III-9 Effect of each parameter on the others

Battery' technology	**In terms of capacity (C/c)**	**In terms of volume (V/v)**	**In terms of weight (W/w)**
Li-Ion	Vc/v(=), Vc/w(=) Wc/v(=), Wc/w(=)	Cv/c(=), Cv/w(=) Wv/c(=), Wv/w(=)	Cw/c(=), Cw/v(=) Vw/c(=), Vw/v(=)
NiMH	Vc/v(+), Vc/w(+) Wc/v(+), Wc/w(+)	Cv/c(-), Cv/w(=) Wv/c(-), Wv/w(=)	Cw/c(-), Cw/v(=) Vw/c(-), Vw/v(=)
LiFePO4	Vc/v(=),Vc/w(+) Wc/v(=),Wc/w(+)	Cv/c(=),Cv/w(+) Wv/c(=),Wv/w(+)	Cw/c(-), Cw/v(-) Vw/c(-), Vw/v(-)
Li-Polymer	Vc/v(+), Vc/w(+) Wc/v(+), Wc/w(+)	Cv/c(-),Cv/w(=) Wv/c(-),Wv/w(=)	Cw/c(-),Cw/v(=) Vw/c(-),Vw/v(=)
Li-Ceramic	Vc/v(=), Vc/w(=) Wc/v(=), Wc/w(=)	Cv/c(=), Cv/w(=) Wv/c(=), Wv/w(=)	Cw/c(=), Cw/v(=) Vw/c(=), Vw/v(=)

C: capacity; V: volume; W: weight; (=): stable; (+): increase; (-): decrease

From *Table III-9*, the Li-Ion and **Li-Ceramic** have presented the same capacity, volume, and weight, respectively, during all the study, while it has not been the same for other batteries. The capacity (Cv/c and Cw/c) for NiMH, LiFePO4 and Li-Polymer has decreased all the time, except one time for the LiFePO4, for Cv/c, which has been equal to C/c. The capacity in terms of volume and weight, Cv/w and Cw/v, for NiMH and Li-Polymer, have been equal, respectively. While the LiFePO4 capacity has increased for the volume (Cv/w) compared to the weight, in the other way the capacity for the weight has decreased compared to the one for the volume (Cw/v).

The volume in terms of weight (Vw/c), and the weight in terms of volume (Wv/c), for NiMH, Li-Polymer, and LiFePO4, have decreased, except for one time for LiFePO4 with Wv/c which W/v has been equal to W/c.

Meanwhile, the volume in terms of capacity (Vc/v, and Vc/w), and the weight in terms of capacity (Wc/v, and Wc/w), for NiMH, Li-Polymer, and LiFePO4 have increased, except two times for the LiFePO4, with the W/c which kept equal to W/v, and V/c equal to V/v.

In the case of the volume in terms of weight with Vw/v, and weight in terms of volume with Wv/w, for the NiMH and Li-Polymer, the two parameters have been stable. While for the LifePO4, when the weight (Wv/w) increased, the volume (Vw/v) decreased.

III.4. Ten-Koh battery resizing

The previous classification of all batteries summarized in *Fig III-5* has been performed without including the volume of batteries' box and arrangement; represented in *Fig III-3* with the satellite battery's box concept, or with the battery's mechanism structural concept. However, for the battery sizing and the choice of a battery for the Ten-Koh satellite, the constraints of the mechanical arrangement and thermal management in orbit should be taken into consideration.

Moreover, in order to study the impact of the use of the Solid-State Lithium-Ceramic-Battery including all the considered batteries, the input required for the new Ten-Koh satellite battery resizing has to be the same as that employed for the sizing of the Lithium-Ion satellite battery sized using the Li-Ion 01, with 4 battery's cells in parallel in one box, for a total capacity of 12.8Ah.

III.4.1. Electrical performances vs mechanical proprieties

Table III-10 and *Fig III-6* shows the difference between the resized satellite batteries in terms of total weight, volume, capacity, and energy, as compared with the original one, using the Li-Ion 01.

The classification in ***Fig III-6*** has been done, from left to right, in terms of the number of batteries, from lower to higher, for a capacity equal to, or higher, than the requirement of 12.8Ah, the number of batteries has been included with batteries' name. The Ten-Koh satellite battery has its batteries arranged in parallel. Volume and weight have been computed for the satellite batteries, alone with no mechanisms or boxes included.

Table III-10 Resized battery Ten-Koh equivalent

Batteries	Number of batteries	Capacity (Ah)	Energy (Wh)	Volume (L)	Weight (g)
Li-Ion 01	4	12.80	46.08	0.089	192.0
Li Ion 02	5	14.00	52.08	0.109	250.0
Li-Ceramic 03	**7**	**13.65**	**51.19**	**0.198**	**416.5**
NiMH	7	13.30	15.96	0.073	189.0
Li-Ceramic 02	**9**	**13.05**	**48.94**	**0.210**	**405.0**
Li-Polymer	9	12.60	46.62	0.100	221.4
LiFePO4	12	13.20	43.56	0.258	468.0
Li-Ceramic 01	**17**	**13.09**	**49.09**	**0.233**	**510.0**

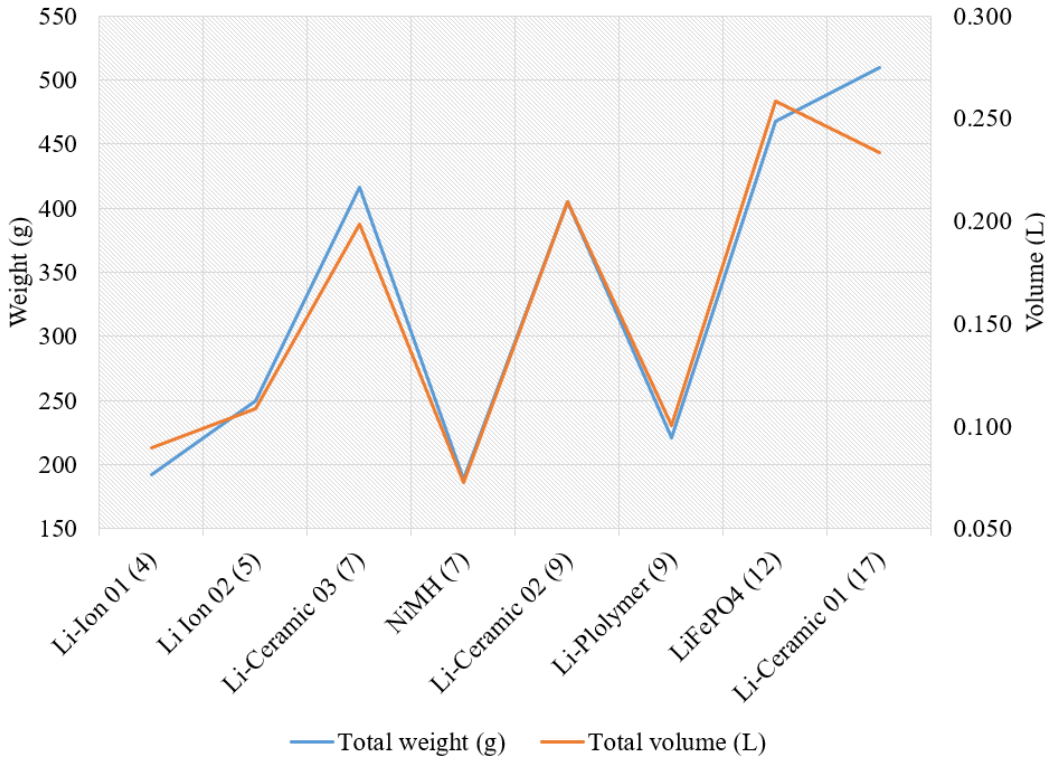

(a) Total Weight and Volume

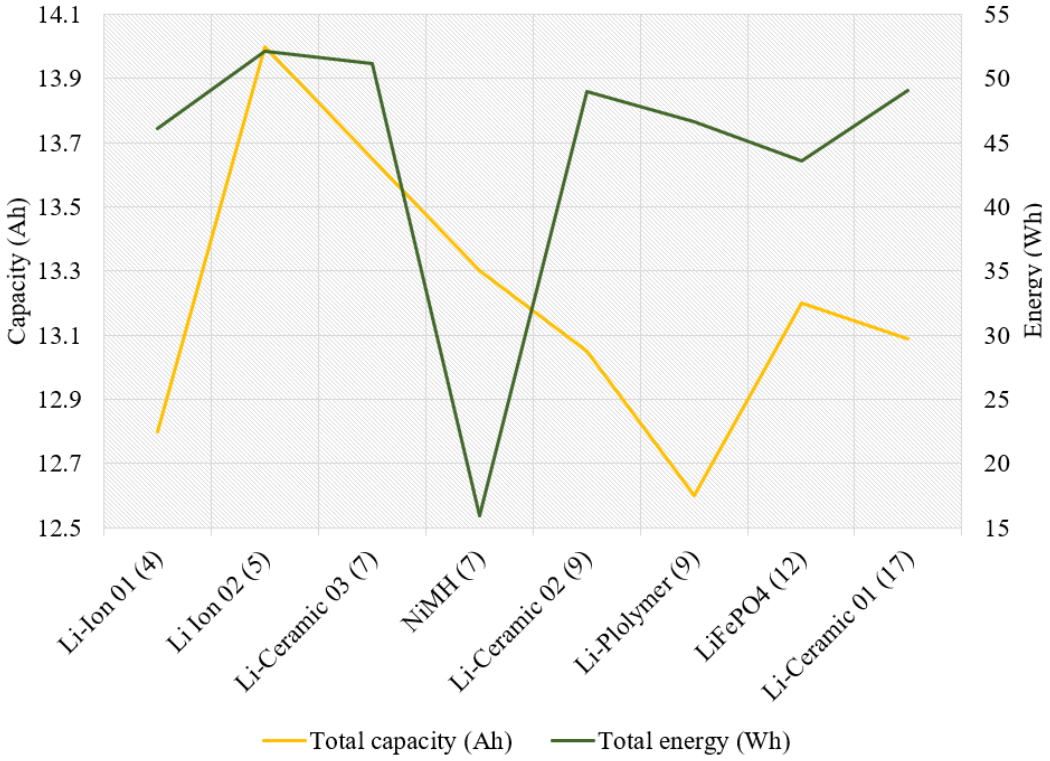

(b) Total Capacity and Energy

Fig III-6 Resized Ten-Koh battery
Total Volume, Weight, Capacity, and Energy representation

However, with the inclusion of the mechanical arrangement of batteries, with the volume and weight of the satellite batteries' boxes, the classification may change.

The total volume including the Aluminum box in Ten-Koh has reached 0.25L. However, with 313g weight for one box, and 192g weight for the four Li-Ion 01, the total weight has reached 505g.

In the case of the HORYU-II, no data have been available for the volume and the weight of the NiMH box. However, an estimation could be computed following the same approach as for Ten-Koh. Since the Ten-Koh satellite batteries' box used 0.25L and weights 313g for every four batteries and the size of one NiMH is half the size of one Li-Ion 01, then the estimated volume could be around 0.22L for the seven batteries. Then, the estimated weight for a box with four NiMH is around 313g/2, which means 156.5g. As the required number of NiMH battery units is seven, the estimated weight for batteries could be around 273.5g and the total weight, including batteries, will increase to 462.5g. Moreover, it may require other connections than parallel batteries because of the low nominal voltage (1.2V), with three cells in series (3S) the voltage will reach 3.6V, the capacity will remain the same as 1.9Ah, then the total number of cells will increase to twenty-one batteries

with three series and seven parallel (3S7P) to reach 3,2Ah, which means everything will increase three times, 0.66L for volume, and 567g without box, then 1387.5g including a box.

The EQUISAT satellite makes use of the Li-Ion 02 and the LiFePO4 in which no box has been used. The estimated volume and weight remain the same as presented in ***Fig III-6*** with five batteries for the Li-Ion 02 and twelve for the LiFePO4.

Following the same approach as for the ESTCube-1, the batteries' position may be seen changed totally compared to the Ten-Koh satellite due to the internal configuration. However, following the box arrangement concept for the satellite battery, the volume and weight for one box will increase considerably. The estimation for volume for box will reach 0.313L for Li-Ion 02, and 0.75L for LiFePO4, while the weight for only the battery box will be 391.25g for Li-Ion 02, and 939g for LiFePO4. Finally, the weight for all the satellite's battery will be increasing including the weight of the battery to: 641.25g for Li-Ion 02, and 1407g for LiFePO4.

The application of the solid-state batteries, Polymer as well as Ceramic, with nine batteries for each, may reduce considerably the complexity of the arrangement, as seen with the pouch battery pack arrangement concept. With any box needed for the thermal protection, as the glace epoxy or additional coating as the α and λ Gel, due to the pouch design of batteries, the mechanical arrangement will be simpler. The total volume and total weight remain almost the same as in ***Fig III-6***.

Finally, the equivalent satellite batteries presented quite similar total energy due to the same calculated total capacity and the same nominal voltage, except for the NiMH due to the low nominal voltage (1.2V).

III.4.2. Thermal management and heater optimization

The temperature in orbit, even for other space missions, may have its word for the selection of the battery. All batteries should have a thermal control system in order to keep a certain operating' range of temperature as obtained by using heaters.

For safety issues, the temperature range recommended by manufacturers for charging the batteries is between 0°C to 45°C for the Lithium-Ion, the NiMH, as well as the Li-Polymer, and higher for the LiFePO4 batteries with +55°C. Concerning the discharging, almost all batteries have a wide range of operation from -20°C to +60°C except for the NiMH batteries which is from 0°C to +50°C. However, due to the safety issues is not recommended to discharge all these batteries at those levels, and it is better to refer to the manufactures for more details, especially for those that probably will be used in space, a different environment than in ground.

The Solid-State Lithium-Ceramic-Battery have shown a wide operating' range of temperature during discharging as well as during charging, they have been able to operate from -20°C to +60°C during the space environment evaluation test within the thermal vacuum at 10^{-4} Pa [*13*].

The use of the Solid-State Lithium-Ceramic battery (SSLCB) may reduce the heaters' work-time according to the low-temperature limit, while the appropriate low-temperature limit for the best performance of the Lithium-ion battery is around +20°C, as discussed in the introduction. The same requirement has been used for the NiMH battery for the HORYU-II. However, for the Ten-Koh satellite, the low-temperature limit for using the heaters has been defined at +5°C. The study was done by *Garzón. A et al.* with the thermal analysis guideline for CubeSats has shown the minimum and maximum battery temperatures' limits that should be kept at Low-Earth-Orbit is from 0°C to +85°C, with the maximum low temperature of -40°C [*93*]. As a comparison between all the previous operating' ranges of temperature for battery in orbit, that have been limited to +20°C, +15°C, +10°C, or even +5°C for the Ten-Koh satellite, as represented in ***Table III-11***. While the lowest temperature has reached -20°C for the solid-state-ceramic battery, the operating' range of temperature in orbit for the heater usage may be considered increased by +20°C for a limit of 0°C, for charge and discharge. Then, increased by +25°C for the case of Ten-Koh. Finally, the temperature range may be seen increased almost twice, with +40°C, compared to the limit set to +20°C as for NiMH battery onboard HORYU-II.

Table III-11 Temperature limit for best battery's performance

Temperature limit (°C)	**The temperature difference with SSLCB (°C)**
+20 [*44*,*80*]	+40
+15 [*43*]	+35
+10 [*12*]	+30
+5 for Ten-Koh	+25
0	+20

The in-orbit temperature record onboard the Ten-Koh for the two boxes of the satellite battery (Box 1, and 2), represented in ***Table III-12***, have shown a variation between +9,09°C to +10.88°C for the lowest temperature, and +16,99°C to +18,6°C for the highest temperature. Finally, the heater has never been used. The reason may be due to the usage of the battery box concept arrangement, including all the material used for heat dissipation protection. However, it has been seen that the concept may be heavier, voluminous, and complex for such small satellites design. The other reason may be due to the CFRP material, for the structure, that may have an additional effect that improved the environment onboard the satellite, while the

temperature of the OBC board has reached +16,27°C, the external PCB has reached -36,51°C.

Table III-12 Ten-Koh in-orbit temperature records

Position	Min (°C)	Max (°C)
OBC PCB	+16.27	+28.48
Battery 1	**+10.88**	**+18.60**
Battery 2	**+9.09**	**+16.99**
Solar Panel	+80.91	+89.13
ADS PCB	+27.00	+47.00
External PCB	-36.51	+12.05

In another point of view in terms of the heaters' work-time that depends on the eclipse's duration. The maximum calculated power consumption for Ten-Koh has been 1.7Wh using the heaters below +5°C, and the total duration for one eclipse at the Low-Earth-Orbit (LEO), has been about 2100 Sec. As an estimation using the SSLCB with the new limit of -20°C, the worktime of the heaters could be delayed until the temperature reaches -20°C, in order to reduce the power consumption of the heaters during the eclipse. This assumption may be demonstrated and studied more in detail as future tasks by the authors.

III.5. Discussion

The engineering approach presented in this study has shown, from a different perspective, the effect of different battery technologies on the design of small satellites, to face the new challenges related to the power supply, showing the compromise among capacity, volume, and weight.

As the main outcome of the study, ***Fig III-7*** summarizes the classification of batteries that has been achieved following the proposed methodology criteria, considered as the main rule of an appropriate battery's selection, in terms of stability or increase of the capacity, and stability or decrease of the volume and the weight. Results that have presented a decrease in the capacity or an increase in the volume and weight have not been included.

While the capacity has been computed in terms of volume and weight, the Li-Ion and the **Li-Ceramic** batteries' capacity has remained the same within all the comparisons, respectively. In which the volume and weight did not affect the capacity. However, it has not been the same for other batteries, in which the capacity has been decreased in some cases, and kept the same in others, or even increased. The LiFePO4 presenting an increase of the capacity in terms of the volume compared to the capacity in terms of the weight Cv/w, has kept the same capacity for Cv/c while decreasing for Cw/c. The NiMH and Li-Polymer batteries

had similar results, decrease in capacities Cv/c and Cw/c while keeping the same capacity Cv/w.

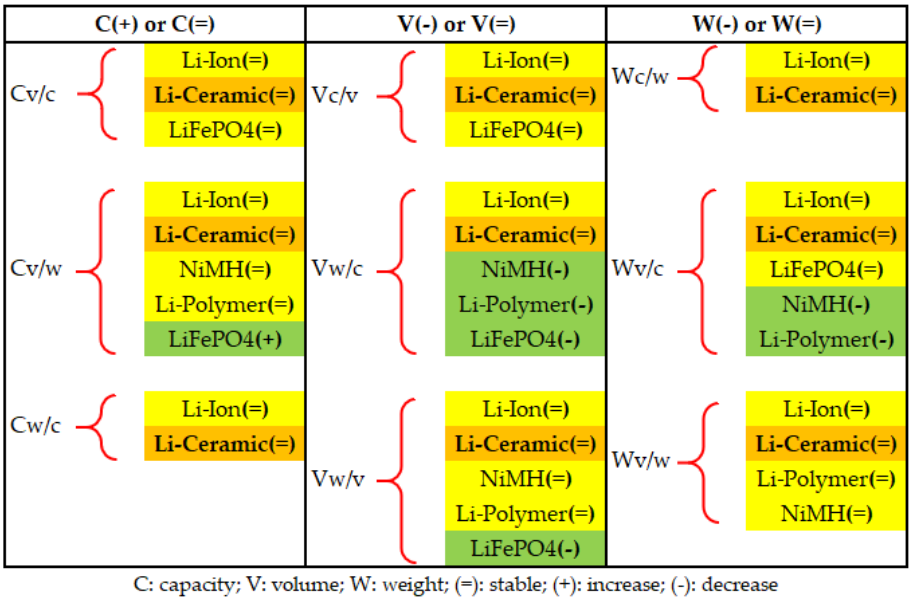

Fig III-7 Classification in terms of higher capacity, smaller size, and lighter weight

For the volume, the Li-Ion and the **Li-Ceramic** batteries kept the same volume respectively within all the classification, the same as for the capacity. The volume has not been affected by the capacity or weight. Concerning the other batteries, the NiMH, Li-Polymer, and the LiFePO4, have presented a decrease in the volume in terms of the weight compared to the volume in terms of capacity Vw/c, while an increase for the volume Vc/v, and stability for the volume Vw/v. As an exception, the LiFePO4 battery has shown the same volume for Vc/v, and a decrease for Vw/v. The change of the weight, for the Li-Ion and the **Li-Ceramic** batteries, has been the same as for the volume and capacity. For the other batteries, only the NiMH and Li-Polymer decreased in weights for Wv/c, while they increased for Wc/w. Finally, keep the same weight for Wv/w. The LiFePO4 had a different variation for the weight, keeping stable for Wv/c, while increasing for Wc/w and Wv/w.

Compared to the other battery technologies that have presented a variation in their parameters even if it has shown a decrease in the volume and the weight, the result for the **Li-Ceramic** has been very similar to the Li-Ion within all the study. For the final classification in ***Table III-13***, it has been considered that the battery that has shown stability within all the study has the first position, as for the Li-Ion and the **Li-Ceramic** in terms of higher capacity and lighter weight. Then, the LiFePO4 in terms of smaller volume, which could be a good selection for the compromise of volume, however, it is still in the second position in terms of the weight or even the capacity. The Li-Polymer, the second solid-state-battery, selected for the study, has

shown acceptable results for the weight, while has got the last position for the capacity and volume. Finally, the NiMH has presented the last position for the volume and the capacity, while the second position for the weight.

Table III-13 Battery technology final list

No	Higher capacity	Smaller volume	Lighter weight
1	Li-Ion, **Li-Ceramic**	LiFePO4	Li-Ion, **Li-Ceramic**
2	LiFePO4,	Li-Ion, **Li-Ceramic**	Li-Polymer, NiMH
3	Li-Polymer, NiMH	Li-Polymer, NiMH	LiFePO4

With the application of battery technology other than the conventional Lithium-Ion, it has been shown the impact that can occur with using the solid-state-lithium-ceramic batteries on a real case study with the Ten-Koh satellite. The application of these batteries and their impact on the satellite have been presented in terms of the challenge in the capacity needed, the volume occupied, and the weight, and finally the safety.

So far, using the Solid-State Battery as well as the solid-state-ceramic battery could reduce significantly the batteries' arrangement complexity, which may lead to removing some mechanical parts and making the power system lighter. Otherwise, another improvement could be done with the optimization of the use of the heaters during the eclipse in orbit.

On another side, two different designs of the batteries have been presented, the cylindrical as for the Li-Ion, NiMH, and LiFePO4, and the pouch as for the solid-state battery (Polymer and **Ceramic**), while the cylindrical requires some special arrangement like boxes, or more space even without boxes, the pouch design is more suitable for a simple arrangement and more flexible for packing.

III.6. Conclusion

During the proposed engineering study, a set of different batteries' technology has been compared in terms of the compromise between the capacity, the volume, and the weight in order to propose a solution for the power storage challenge for small satellites. Then, the impact of those batteries on a real satellite case study has been presented with focusing on the new advanced battery technology based on the Lithium-Solid-State-Ceramic.

Using the solid-state-ceramic battery may have a good impact on the small satellite design especially with the Nanosatellites. Taking into account their pouch design, the wide operating temperature range, finally the safety with no liquid inside, the

electrical power system may be on one side simpler with no need for a complex arrangement, and on another side, it may be seen as improved with the high performances of the new batteries' technology.

Another outcome of the study has been related to the temperature in orbit, the Solid-State Lithium-Ceramic-Battery could have their part to improve and optimize the thermal management. The heater consumption optimization may be done in two ways, one is reducing the heater consumption by reducing the maximum power by increasing the temperature range of the battery as for the Solid-State Lithium-Ceramic-Battery to -20°C, which leads to reducing the worktime of the heater. It may require good monitoring of temperature in orbit, to power on the heater at a certain level of temperature and then keep it at much lower until the end of the eclipse. Or using a different approach with new material for the structure, as the Carbon Fiber Reinforced Plastic that has shown a good temperature inside the satellite around +9°C.

Otherwise, the optimization for the use of heaters during the eclipse may need more investigation, as the next step, the actual Solid-State Lithium-Ceramic-Battery should be tested under different low temperature, before proceeding with their real integration within a demonstration mission in orbit.

Chapter IV

Ground Evaluation Test & Guideline, from Launch to Space Environment, of the Solid-State-Ceramic Battery based Oxide

This part is a preprint of the two articles published in PRAISE WORTHY PRIZE S.r.l. (PWP) publisher the International Review of Aerospace Engineering (IREASE).

The two different articles have been presented as follows:

"Space Environment Evaluation Test of Solid-State-Ceramic Battery Advanced Energy Storage Under Vacuum and Thermal Vacuum", International Review of Aerospace Engineering (IREASE), 13 (2), pp. 68-79, 2020. [13]
https://doi.org/10.15866/irease.v13i2.18582

"Launch Environment Ground Test Evaluation with Multi-axis Vibration and Shock for Pouch Solid-State-Ceramic Battery Advanced Energy Storage", International Review of Aerospace Engineering (IREASE), 13 (4), pp. 126-134, 2020. [24]
https://doi.org/10.15866/irease.v13i4.18949

IV. Ground Evaluation Test & Guideline, from Launch to Space Environment, of the Solid-State-Ceramic Battery based Oxide

The selected Solid-State Lithium-Ceramic-Battery, described in ***Chapter II*** including the **Li-Ceramic 02** discussed within the engineering approach in ***Chapter III***, have been tested within two different environments: the *launch environment*, in which batteries have endured all kinds of vibrations (sine burst, sine wave, and random) and shock, then the *space environment* for the Low-Earth-Orbit vacuum conditions and within two temperatures limits, cold and hot.

IV.1. Ground evaluation test description

IV.1.1. The launch environment test

IV.1.1.1. Test's preparation

The *launch environment* test, also called the dynamic testing, is a key phase for spacecraft and different space-flight components. It is conducted to simulate the launch conditions of vibration and shock over a wide range of frequencies according to the rocket requirements provided by the launcher.

The purpose of the *launch environment* evaluation test is to check the ability of the Solid-State Lithium-Ceramic-Battery to withstand the conditions during the launch and the separation from the rocket. The hostile shock and vibration conditions have been applied according to the defined H2A Japanese rocket requirements [*24*].

During the test, a group of the six Solid-State Lithium-Ceramic-Battery (Solid-state LCB) have been tested during two steps: once the group has been exposed to the shock conditions, and then it has been tested under several vibration environments: P1X, P1Y, and P1Z for the **PLCB01**; P2X, P2Y, and P2Z for the **PLCB02** [*24*].

Fig IV-1 SSLCBs group selected for the *launch environment* ground evaluation test [*24*]

The robustness of the Solid-State Lithium-Ceramic-Battery has been evaluated carefully. Before and after each test, the Solid-State Lithium-Ceramic-Battery have been inspected with a visual check, measurement of physical properties: weight, length, width, and thickness, then the electrical measurement of the open-circuit voltage, finally charged and discharged during several cycles as a functional test for checking their discharge capacity [*24*].

Fig IV-2 Solid-State-Ceramic battery functional test
Charged and discharged before and after each test [*24*].

Discharged with a constant current (CC) (Discharge Capacity: 0.5C, End of Discharge: 2.8V) and charged with a constant-current constant-voltage (CC/CV) (Charge Capacity: 0.5C, Charge Voltage: 4.35V, End of Charge PLCB01: 97.5mA, PLCB02: 72.5mA) [*13*]

To support all batteries during the shock and vibration test, a tailor-made jig has been designed at the *Kyushu Institute of Technology* according to the test facility conditions, with a natural frequency of 2981 Hz. The performance of the jig has been checked with simulation for the three-axis and different modes using *SolidWorks* software to confirm its ability to waistband the test conditions and support all the batteries safely [*24*].

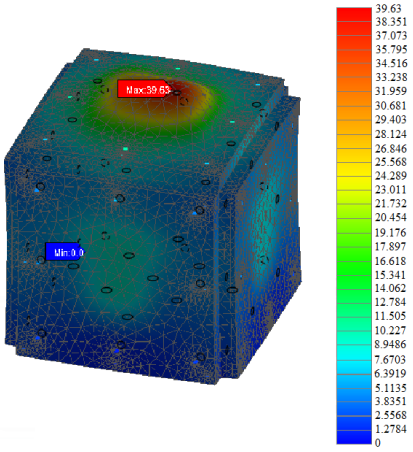

Fig IV-3 Jig natural frequency and deformation simulation [*24*]

Since the Solid-State Lithium-Ceramic-Battery are planned to be launched on the same rocket as the Ten-Koh satellite, the Japanese rocket H2A [*94*,*95*], the same approach for the launch conditions previously adopted by *Jesus Gonzalez et al.* for the solar modules integrated converters [*39*], as well as the Lithium-Ion battery pack for the Ten-Koh satellite and all its subsystems [*38*,*40*], have been reproduced as the input's requirements for the launch environment ground test [*24*].

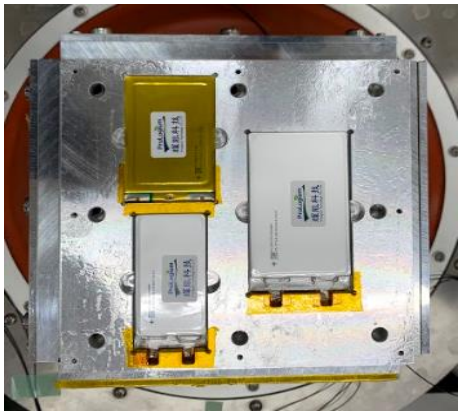

Fig IV-4 Solid-State Lithium-Ceramic-Battery configuration on the jig (Top view of the jig at the vibration facility) [*24*]

Two different test facilities have been selected to satisfy the test conditions. ***Table IV-1*** summarizes the specification for all the test equipment, first for the facility used for the shock test then the vibration facility which has the capability for testing under sine and random vibrations [*24*].

Table IV-1 List of the equipment used during the evaluation test [*24*]

Name	**Type**	**Range**
Shock machine	CeNT [*96*]	4000G
Vibration machine	A30 (TBD-A30)	5Hz to 2600Hz
Cubed jig	TCJ-B200-A30-A	DC ~ 2000Hz
SSB Jig	Jig for SSB (Original)	2981Hz

IV.1.1.2. Test's conditions

IV.1.1.2.1. The shock test

For the high frequency from 100 to 5000Hz, the shock test is needed to simulate the conditions during the rocket stage, fairing and satellite separation. The six Solid-State Lithium-Ceramic-Battery have been distributed in three different groups or three jigs and then exposed to a short shock duration with more than 1000G [*24*].

The accelerometers have not been attached to the test article directly but to the support jig, because battery survival is the main concern for the test. Thus, only the input shock spectrum has to be measured [*24*].

Fig IV-5 The shock test's jig with pickup sensors configuration [*24*]

The inputs shock spectrums conditions for the shock evaluation test are the qualification level (QT) of the H2A rocket which is represented in ***Table IV-2***. Typically, the required shock level is between 1000 to 4000G within the frequency range from 100 to 5000Hz [*24*,*97*].

Table IV-2 Inputs test condition for the shock test [*24*,*39*]

Axis	**Frequency range (Hz)**	**Shock Response Spectrum (SRS)**	**Number of tests**
X (longitude)	100～2600	+6dB/octave 2000G	2 times
Y and Z (lateral)	2600～5000		

IV.1.1.2.2.The vibration test

The purpose of the vibration test is to check the compliance of the Solid-State Lithium-Ceramic-Battery with the vibration that may occur during the launch, they should be able to keep at least the same performances without degradation or malfunctions for the operation in orbit [*24*].

During the vibration test, the launch environment conditions defined as the qualification test level (QT) for batteries required by *JAXA* for the H2A rocket, have been reproduced as the input required for the test [*24*].

The Solid-State Lithium-Ceramic-Battery have been tested under the low and high frequencies:

- **Quasi-static or sine-burst:**
  Demonstration against the static acceleration in the longitudinal and lateral direction. The maximum quasi-static acceleration is a combination of static

acceleration and low-frequency dynamic acceleration [*24*,*94*]. Typically, the number of cycles is 3 to 5. A sin-burst is often selected reason for the difficulty to get the static acceleration in one direction. The test's frequency should be lower than the item's natural frequency [*24*].

Table IV-3 Sine burst inputs testing parameters [*24*,*39*,*98*]

Direction	Frequency [Hz]	Acceleration	Excitation time [sec]
X axis	20	58.8 m/s0-p2	1
		7.5 G0-p	
Y, Z axis		49 m/s0-p2	
		6.25 G0-p	

- **Sinusoidal:**
  It is often standardized rather than quasi-static acceleration conditions with a low frequency (from 5 to 100Hz) within 2 minutes in the longitudinal and lateral direction [*24*].

Table IV-4 Sinusoidal vibration inputs testing parameters [*24*,*39*,*98*]

Direction	Frequency [Hz]	Level	Excitation time [oct/min]
X axis	5-7.1	0.02 m0-p	2 (UP and DOWN)
	7.1-100	30.7 m/s0-p2	
		3.13 G0-p	
Y, Z axis	5-6.3	0.02 m0-p	
	6.3-100	24.5 m/s0-p2	
		2.5 G0-p	

- **Random:**
  The random vibration environment is imposed on the spacecraft, subsystems and equipment due to the lift-off acoustic field, aerodynamic excitations, and transmitted structure-borne vibration [*24*,*99*]. For the high frequency (from 20 to 2000Hz), it is caused by the acoustic noise [*24*,*39*]

Table IV-5 Random vibration inputs testing parameters [*24*,*39*,*98*]

Direction	Frequency [Hz]	Level	Excitation time [sec]	RMS value
3 Axis	20-200	+3 dB/oct	120	11 Grms
	200-2000	0.064 G2/Hz		

IV.1.1.3. Procedure

The Solid-State Lithium-Ceramic-Battery have been divided into three jigs, each jig has contained one battery from each sample, and it has been tested three times once for the shock test following the conditions previously presenting.

Then for the vibration test which three configurations with different distribution have been adopted. The following distribution allowed to test the three axes for all batteries sequentially during the vibration.

During the first configuration, the Solid-State Lithium-Ceramic-Battery have been mounted into the three jigs (1, 2, and 3) where the tested axes for batteries (x, y, and z) have followed respectively the vibration machine axes (X, Y, Z) in which the vibration has been applied (X for jig 1, Y for jig 2, and then Z for jig 3) [*24*].

After each test's sequence (sine burst, sinewave and random), the three jigs have to be rotated, which the following tested axis for the battery should be respectively (Y for jig1, Z for jig2, and X for jig3); finally, the last rotation [*24*].

Fig IV-6 and ***Table IV-6*** summarize all the three configurations with the three rotations for each test's sequence.

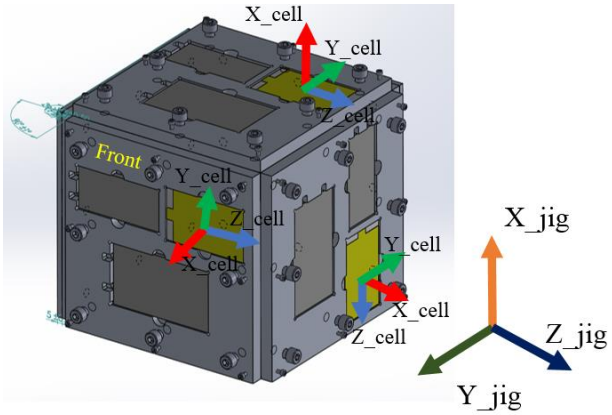

(a)

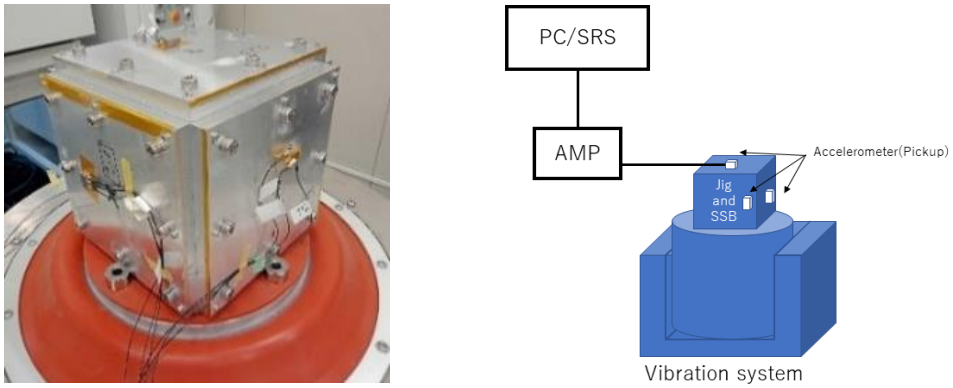

(b)

Fig IV-6 Solid-State Lithium-Ceramic-Battery' configuration during the vibration test
(a) Solid-State Lithium-Ceramic-Battery' configuration inside the jig during the three axes rotations, (b) The pickup sensors' configuration for the three jigs [*24*].

Vibration test procedure:

The following test sequence has been carried out during all the three rotations for the vibration test [*24*]:

1. *Solid-State Lithium-Ceramic-Battery should be mounted according to the first configuration (**Table IV-6**).*
2. *Start the first sequence for the x-axis:*
    - *Perform x-axis Sine burst vibration.*
    - *Perform x-axis Sine wave vibration.*
    - *Perform x-axis Random vibration.*
3. *Change to the second configuration (**Table IV-6**), then the sequence at step 2 should be repeated for the y-axis.*
4. *Finally, repeat the sequence at step 2 for the last configuration for the z-axis.*

Table IV-6 Vibration test's Solid-State Lithium-Ceramic-Battery distribution For the three configurations during the three test's sequence: sine burst, sinewave and random [*24*]

(a) Vibration spectrum's configuration for each SSLCB's axes respectively

	X_jig	**Y_jig**	**Z_jig**
SSLCB x,y,z (Cell)	Spectrum X	Spectrum Y	Spectrum Z
SSLCB y,z,x (Cell)	Spectrum Z	Spectrum X	Spectrum Y
SSLCB z,x,y (Cell)	Spectrum Y	Spectrum Z	Spectrum X

(b) Three jigs configuration

Configuration	**Jig 1**			**Jig 2**			**Jig 3**		
# 1	P1x	P2x	Fx	P1y	P2y	Fy	P1z	P2z	Fz
# 2	P1y	P2y	Fy	P1z	P2z	Fz	P1x	P2x	Fx
# 3	P1z	P2z	Fz	P1x	P2x	Fx	P1y	P2y	Fy

(c) Solid-State Lithium-Ceramic-Battery' axes configuration

Configuration	**PLCB 1950mAh**			**PLCB 1450mAh**			**FLCB 90mAh**		
# 1	P1,1x	P1,2y	P2,1x	P2,2y	P2,3z	P1,3z	F1,1x	F2,2y	F3,3y
# 2	P1,1y	P1,2z	P2,1y	P2,2z	P2,3x	P1,3x	F1,1y	F2,2z	F3,3z
# 3	P1,1z	P1,2x	P2,1z	P2,2x	P2,3y	P1,3y	F1,1z	F2,2x	F3,3x

Fig IV-7 summarizes in fourth steps the all the *launch environment* test: with the before test preparation and measurement, the shock test procedure, the vibration test steps, then the after-test measurement for comparison with the before test measurements that have been used for further analysis. The quasi-static acceleration test has been carried out by replacing it with a sine burst test.

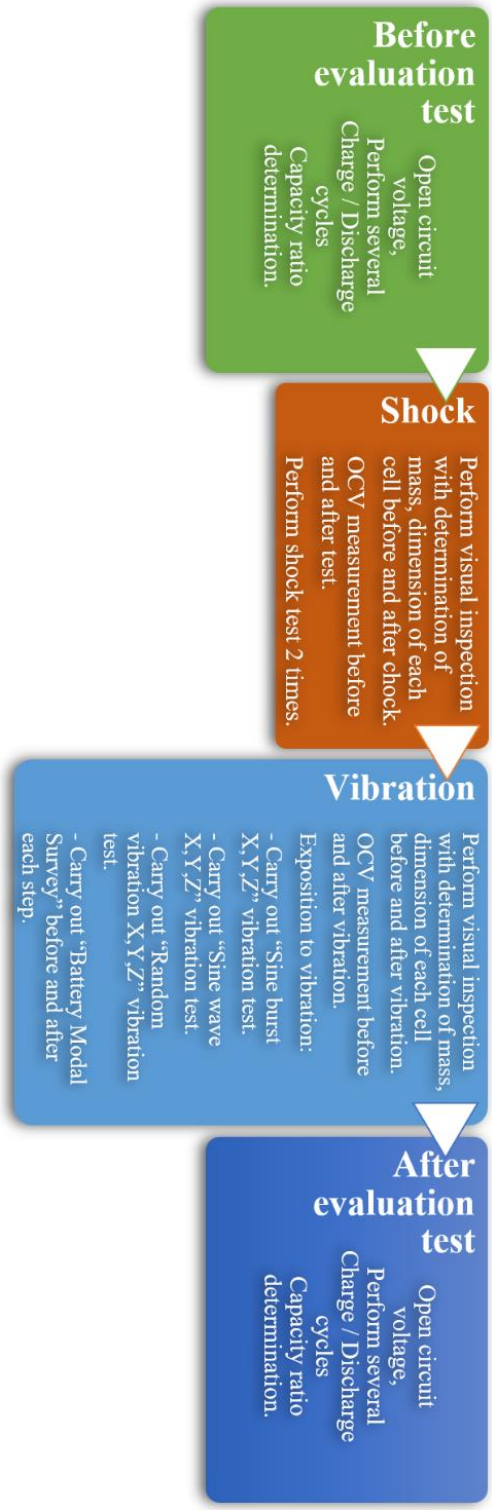

Fig IV-7 The *launch environment* test flowchart [*24*]

IV.1.2. The space environment test

The *space environment* test is an important phase for each qualification test. It allows simulating the outer-space conditions including a wide range of temperature and different levels of pressure and radiation where the performances of the items under test will be evaluated carefully carrying out under a minimum level of safety the functional test at the nominal and critical conditions.

The purpose of the *space environment evaluation* is to check the ability of the Solid-State Lithium-Ceramic-Battery to withstand the *space environment* for the Low-Earth-Orbit operation. Batteries have been tested once under the vacuum and then under the thermal vacuum environment.

Concerning the radiation test, according to the *ISO standard 19683:2017(E),* the radiation test may be optional depending on the satellite mission orbit, additionally to the *Ceramic* material properties which lead to its use for many applications and industrial domains such as an immobilization form for radioactive wastes, inert fuel matrices for actinide transmutation, cladding materials for gas-cooled fission reactors, and structural components for fusion reactors as reported by *Thomé. L. et al.* [***100***]. Finally, the selected Solid-State-Ceramic battery has not been evaluated directly under the radiation environment. However, based on how the radiation may result on every material's properties especially the *Ceramic* [***100***,***101***], and to compare with the radiation effect on the Lithium-Ion battery [***102***,***103***], a procedure test under the *Gamma irradiation* environment corresponding to the equivalent total dose (TID) at the Low-Earth-Orbit has been proposed. More details about the test conditions have been summarized in the following sections.

IV.1.2.1. Test's preparation

All the Solid-State Lithium-Ceramic-Battery with different capacities have been tested with a total number of four: P1, P2, P3, and P4 for **PLCB01** and **PLCB02**, simultaneously at the vacuum and the thermal vacuum conditions, respectively. One-cell FLCB has been included in the evaluation test, finally, the results have not been presented within the present chapter, however, they have been used for further analysis in ***Chapter IV***.

Before and after each test, the Solid-Stat-Ceramic batteries have been inspected with a visual check, measurement of physical properties: weight, length, width, and thickness, then the electrical measurement for the open-circuit voltage and the discharge capacity. Finally, the internal resistance measurement has been done at the beginning and the end of all the evaluation *space environment test* [***13***].

In order to control the temperature inside the chamber, two heaters for each set of batteries have been put on the top, and one thermocouple has been put on each battery's side for temperature monitoring as shown in ***Fig IV-8*** [*13*].

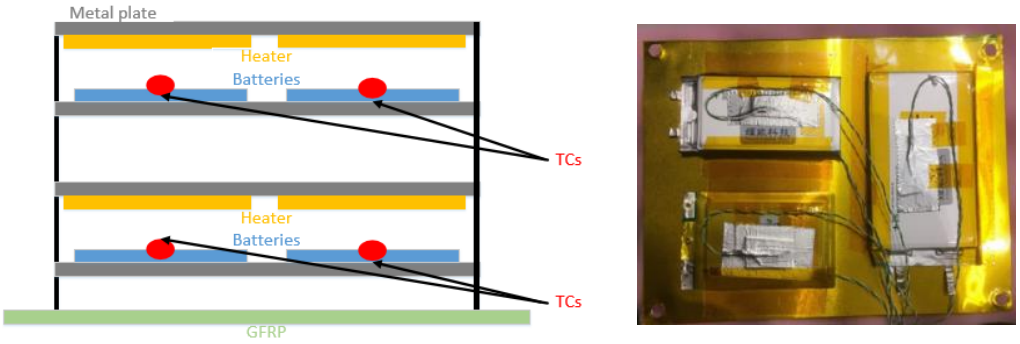

Position of the two heaters on the top of each set including thermocouples on the top side of Solid-State Battery

Fig IV-8 Solid-State battery configuration inside TVCH [*13*]

Fig IV-9 gives an overview of the thermal vacuum test setup with hardware for data acquisition and command. The test equipment used during the test are listed in ***Table IV-7***.

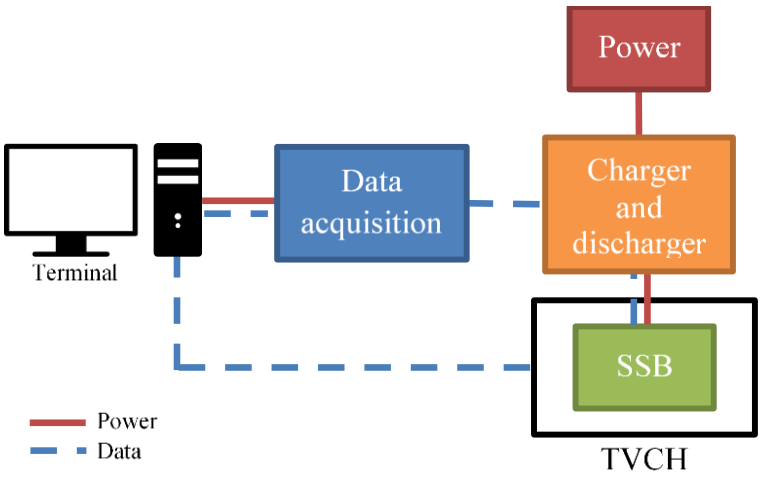

Fig IV-9 Overview of the thermal vacuum test setup [*13*]

Table IV-7 List of Equipment Used for the Thermal Vacuum [*13*]

Name	**Type**	**Range**
Thermal vacuum shock test machine	ULVAC Small TVAC [*96*]	10^{-5} ~10^{-3} Pa
Heater	ps50200-100/12	100V 108.2W
Power Source	Agilent U8001A	0-30V 3A

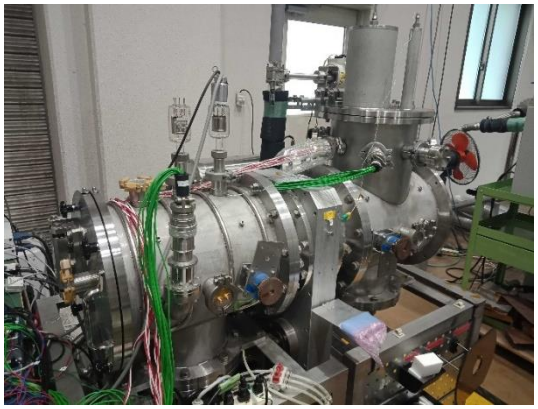

Fig IV-10 Thermal Vacuum Chamber (TVAC)
The *Kyushu Institute of Technology LaSEINE laboratory* [*13*,*96*]

The same batteries tested, previously, during the vacuum test have been tested again under the thermal vacuum, when one sample from each kind will be tested for the functional test, the other samples have been kept as reference batteries inside the thermal vacuum chamber [*13*].

IV.1.2.2. Test's conditions

IV.1.2.1.1.Vacuum

During the non-functional test for vacuum, Solid-State Lithium-Ceramic-Battery has been exposed to pressure around 2×10^{-4} Pa close to the Low-Earth-Orbit pressure [*104*], at the *Center for Nanosatellite Testing* at the *Kyushu Institute of Technology*, where all test has been recorded and monitored during the 24 hours [*13*].

The purpose of the vacuum test is to check the survivability of the batteries under a vacuum environment with no leakage or damage before proceeding to the functional test under the thermal vacuum [*13*].

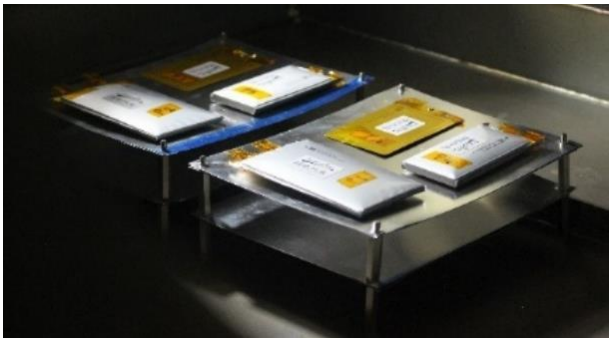

Fig IV-11 Solid-State Lithium-Ceramic-Battery (PLCB) during the vacuum test showing some swelling during the vacuum test [*13*]

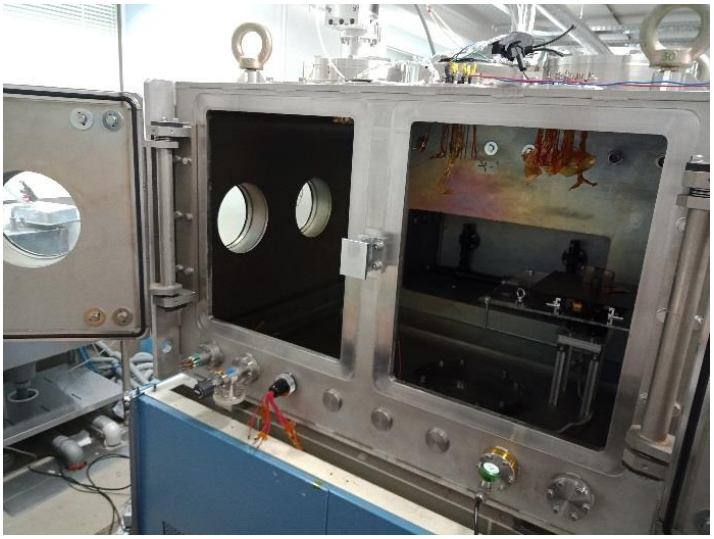

Fig IV-12 Vacuum chamber
The *Kyushu Institute of Technology La SEINE laboratory* [***13***,***96***]

IV.1.2.1.2. Thermal vacuum

During the thermal vacuum test, the ability of the Solid-State Lithium-Ceramic-Battery to withstand the *space environments* conditions have been checked. They have been discharged and charged several times between two temperature limits -20°C and +60°C under the same pressure as the vacuum, about 1×10^{-4} Pa [***13***].

The test conditions have been defined based on the *JAXA* requirement. As for the conditions of the battery assembly, the allowable temperature range from -20°C to +60°C is used as the worst hot and cold dwell temperatures. *JAXA* also requires a minimum heating/cooling rate of 1°C /min [***13***,***105***].

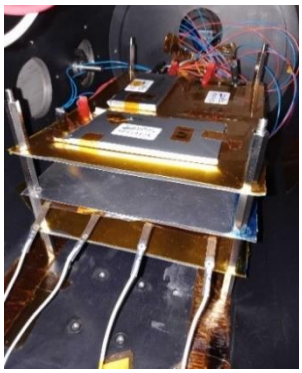

Fig IV-13 Solid-State Lithium-Ceramic-Battery inside TVAC
at the *Kyushu Institute of Technology* [***13***]

IV.1.2.1.3. Radiation

The test conditions proposed for the radiation test evaluation test have been defined to cover at least a total irradiation dose (TID) of more than one year at the Low-Earth-Orbit, which is equivalent to 12 krad for 1 h, as represented by *Masaki YAMAGATA et al.* while testing the first Lithium-Ion battery with ionic liquid electrolyte demonstrated in the extreme *space environment* [***106***]. Other works have supported the same radiation level, as the work done by *Michael Xapsos et al.* which showed in his article, as in ***Fig IV-14 (a)***, the total dose probability distributions for one-year inclination Low-Earth-Orbit mission [***107***]. Or as reported by *Flemming Hansen et al.* for the typical radiation tolerances of COTS Parts that is from 10^3 rads to 10^4 rads [***108***].

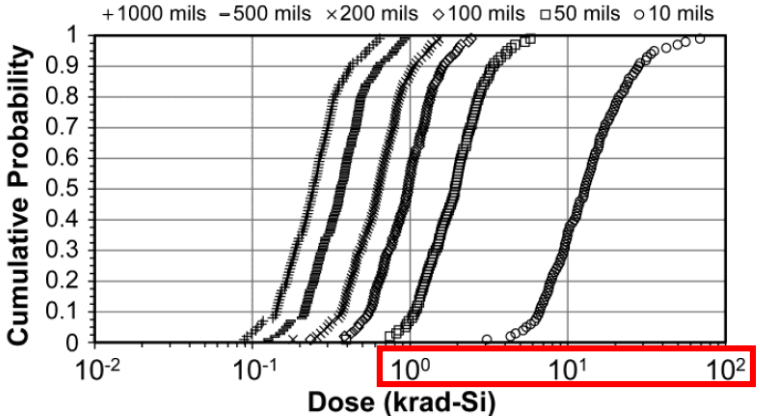

(Work of the US Gov. Public Use Permitted)

TID probability distributions for a 1-year LEO mission
Each curve contains 99 points corresponding to confidence levels ranging from 1 to 99%. Shielding levels for the curves, from right to left, are 10, 50, 100, 200, 500 and 1000 mils equivalent to 0.254, 1.27, 2.54, 5.08, 12.7, and 25.4 mm Al [***107***]

Fig IV-14 Total Irradiation Dose & Typical Radiation Tolerances [***107***].

Other approaches for testing have included the condition of the dose rate as by *B. V. Ratnakumar et al.* at the *Jet Propulsion Laboratory* for testing the Li-Ion cells in a high-intensity radiation environment [***109***].

However, the radiation test for the *Polymer* battery has been done by *C.Clark et al.*, which has presented a different total dose and dose rate using a Cobalt irradiation source, from 10 to 500 Krad at 50 rad/min (0.833 rad/s) [***56***].

Following all the previous works, and based on the total dose of 12 Krad/h with 3,33 Krad/s which is equivalent to one year in LEO, three different dose rates have been targeted. ***Table IV-8*** represents the reached TID for each dose rate, **Dose 1** is for one full Discharge/Charge cycle, then **Dose 2** for one Discharge and one Charge

cycle, respectively, the duration for discharge and charge has been estimated equal (3.5 h), the limit for TID has been fixed to 12 Krad. The first and second dose rate has been defined as low dose rate, however, the final dose rate (**Dose 3**) has been defined as a very high dose rate reaching 84 Krad with 3.33 rad/s continuously for the TID per one full discharge/charge cycle equivalent to seven hours irradiation.

Table IV-8 Gamma irradiation dose rate

	Dose Rate (Krad/s)	**TID limit (Krad/cycle)**	**Cycle duration (h)**	**TID reached (Krad)**
Reference	3.33	12	1	12
Dose 1	0.48	12	7	12
Dose 2	0.95	12	3.5 (7/2)	24
Dose 3	3.33	/	7	84

IV.1.2.3. Procedure

First, the group of Solid-State Lithium-Ceramic-Battery have been checked under the vacuum only, under a pressure close to 10^{-4} Pa.

Then, they have been tested during one week and seven cycles: two cycles under ambient temperature and five cycles, within eight discharge/charge cycles, under thermal vacuum around 1×10^{-4} Pa during 120 hours. They have been discharged with a constant current (CC) (Discharge Capacity: 0.5C, End of Discharge: 2.8V) and charged with a constant-current constant-voltage (CC/CV) (Charge Capacity: 0.5C, Charge Voltage: 4.35V, End of Charge **PLCB01**: 97.5mA, **PLCB02**: 72.5mA) [*13*].

a- Thermal vacuum test procedure

The following test sequence has been carried out during the thermal vacuum test [*13*]:

1. *Pumping down to create vacuum condition with pressure around ~1×10^{-4} Pa.*
2. *Adjusting the temperature to reach +20°C.*
3. *Performing a minimum of one discharge/charge cycle under vacuum at +20°C.*
4. *Decreasing temperature to reach -20°C.*
5. *Performing a minimum of one discharge/charge cycle under vacuum at -20°C.*
6. *Increasing temperature to reach +60°C.*
7. *Performing a minimum of one discharge/charge cycle under vacuum at +60°C.*
8. *Repeating the cycle -20°C, +60 °C, 2 times.*
9. *Increasing temperature to reach +20°C.*
10. *Performing a minimum of one discharge/charge cycle under vacuum at +20°C.*
11. *Stopping vacuum and return to normal pressure.*

Fig IV-15 summarizes the test procedure and shows the temperature profile during thermal vacuum.

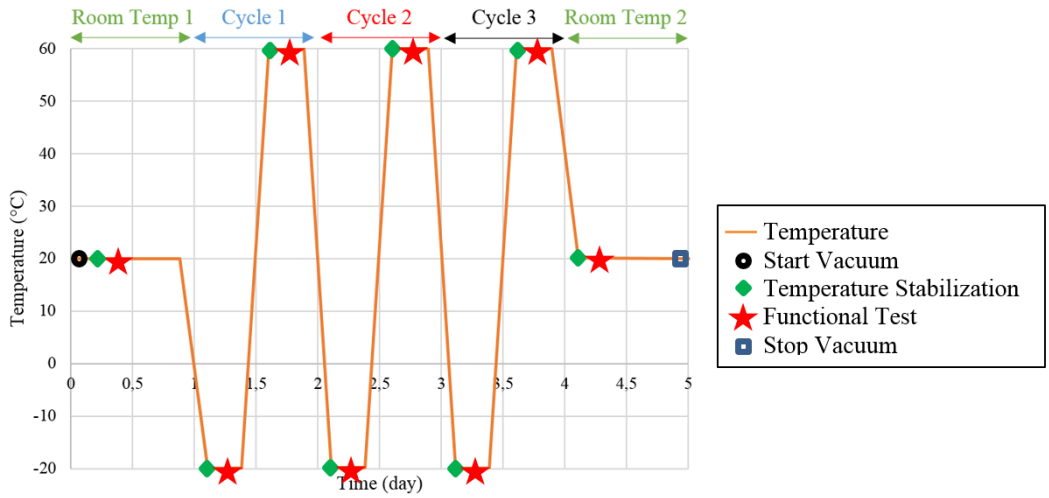

Fig IV-15 Temperature profile during the thermal vacuum test summarizing the main step for the test procedure [*13*]

b- Radiation test procedure

The following test sequence has to be carried out during the radiation test:

1. *Visual inspection for all SSLCBs, with OCV, IR, capacity, mechanical properties measurements.*
2. *Perform a minimum of one discharge and charge cycle for SSLCBs before the evaluation test,*
3. *Put all SSLCBs close to the radiation source (Gamma), according to the dose rate 1,*
4. *Start irradiation with dose rate 1,*
5. *Perform at least one complete cycle discharge and charge,*
6. *Change the SSLCBs and update the position according to the dose rate 2,*
7. *Perform only discharge (step 1 in **Table IV-9**) SSLCBs, then change SSLCBs and only charge (step 2 in **Table IV-9**), during dose 2,*
8. *Change the SSLCBs and update the position according to the dose rate 3,*
9. *Repeat step 4 and 5 for dose rate 3,*

Table IV-9 Radiation test procedure for different dose rate

SSLCBs	Dose1	Dose2		Dose3	Total SSLCBs needed
		Step 1	Step 2		
FLCB Pack (810mAh)	1	1	1	1	**4(+2)**
PLCB (1450mAh)	1	1	1	1	**4(+2)**

Note: *The radiation should be measured and recorded during all phases and doses rate.*

10. *Visual inspection for all SSLCBs, with OCV, IR, capacity, mechanical properties measurements.*
11. *Perform a minimum of one discharge and charge cycles for SSLCBs after the evaluation test.*
12. *Take pictures of all SSLCBs.*

Fig IV-16 summarizes in fourth steps all the *space environment* test, excluding the radiation test, of the selected Solid-State Lithium-Ceramic-Battery: before the test with the preparation and all the necessary measurements, vacuum, thermal vacuum, and after the test measurement.

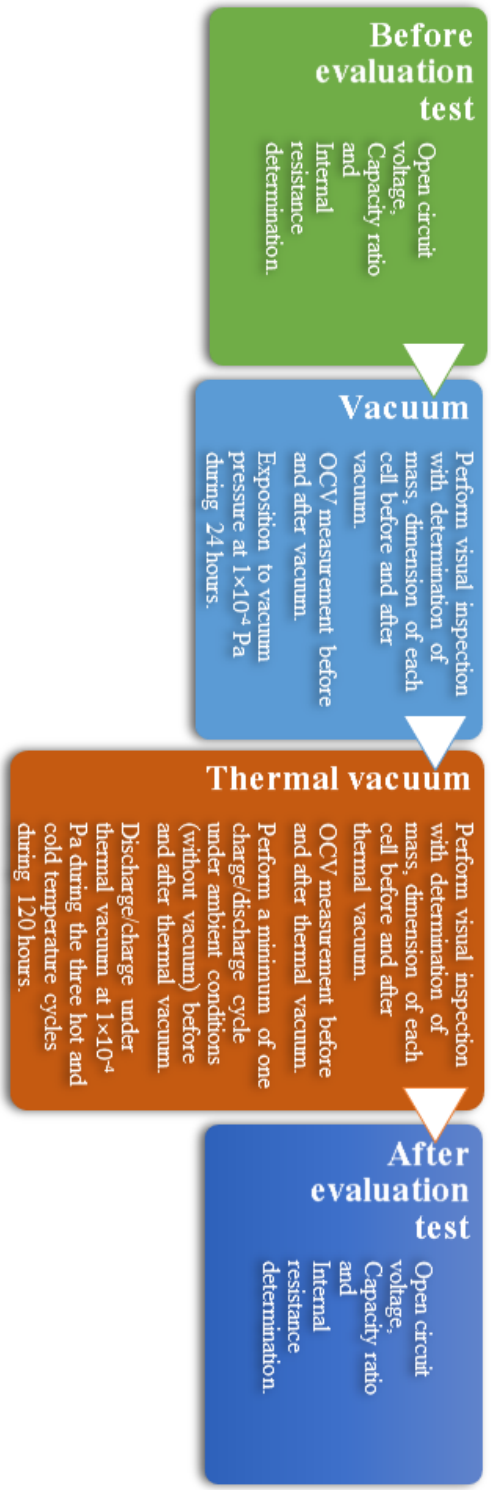

Fig IV-16 The *space environment* test flowchart excluding the radiation test [*13*]

IV.2. Charge and discharge test board description

During the evaluation test, the Solid-State Lithium-Ceramic-Battery have been discharged and charged before and after each test. Two different charge and discharge boards have been designed and manufactured for the two different batteries capacities, the main change between the testing boards has been in the charge and discharge current. All boards have followed a modular approach, which makes them more suitable to be customized and repaired, if necessary, all boards can be used with any batteries as well as the currents have been adjusted as the desired value.

Fig IV-17 shows the functional block diagram for each test board which is divided into four parts: charger (***Module 1***), discharger, sensors (***Module 2 &3***), and relay. The test board has been controlled and monitored by an 8-bit microcontroller "*ATmega32U4*" [***110***], then connected to a terminal for data collection [***13***].

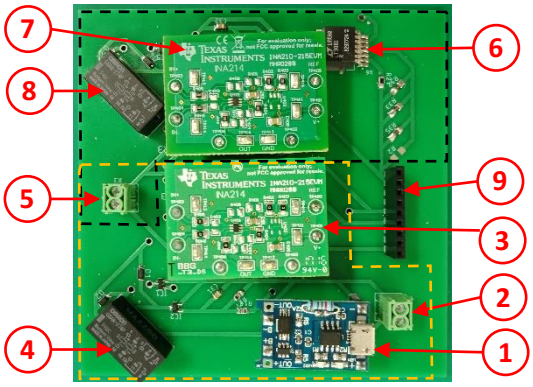

1- Charger
2- Charge port
3- Charge sensor
4- Charge switch
5- Battery port
6- Discharger
7- Discharge sensor
8- Discharge relay
9- Comm port
- - Charge circuit
- - Discharge circuit

(a) Experimental test board's hardware

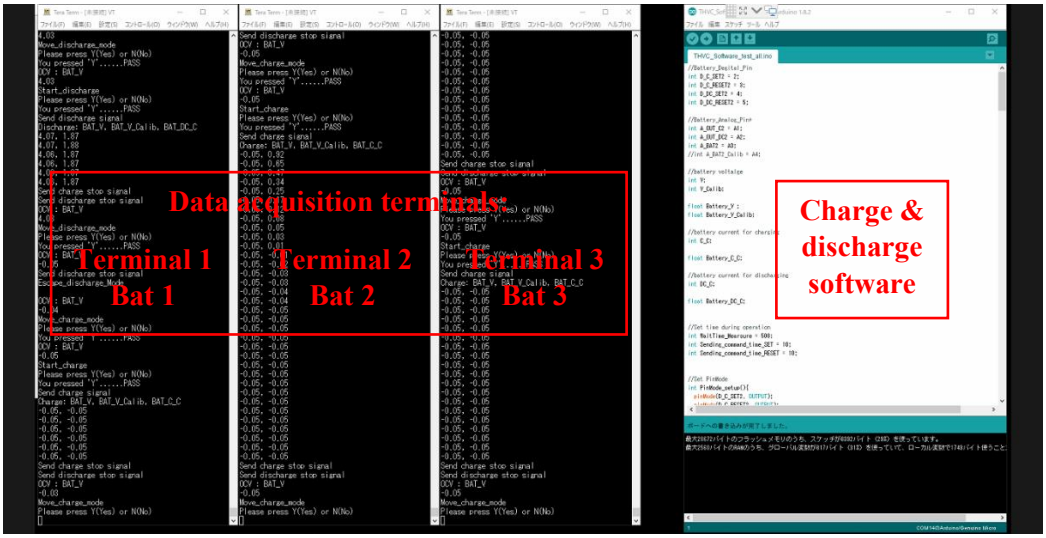

(b) Experimental test board's software

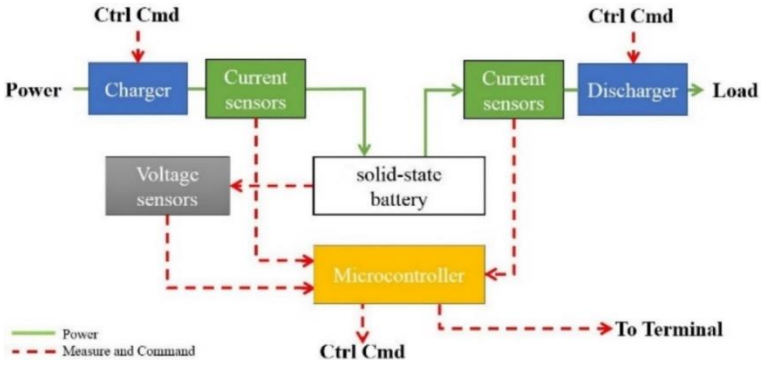

(c) Test board functional block diagram [13]

Fig IV-17 Experimental test board setup
Used for charge and discharge of the Solid-State Lithium-Ceramic-Battery
within all the evaluation tests

The charger used for the test is *TP4056* a constant-current/constant-voltage CC/CV linear charger for single-cell Lithium-Ion and Polymer batteries, programmable charge current up to 1000 mA [***13***,***111***]. Battery protection from over-charge, over-discharge, and/or over-current for one-cell *IC DW01-P*, which has not been used during the test, is included [***13***,***112***]. The charge current varies from each circuit according to each Solid-State-Ceramic battery [***13***].

The discharger is *LT3081* a 1.5A low dropout linear regulator with a constant current [***13***,***113***].

The charge and the discharge current are measured with a voltage-output current-shunt sensor *INA21X* [***13***,***114***].

In order to switch between charge and discharge cycle, two low signal relays *G6A* have been used [***13***,***115***].

Finally, the charge and the discharge rate have been defined at 0.5C [***13***].

Before proceeding to the evaluation test, the test board has been integrated with the Solid-State batteries and all the experimental setup as shown in ***Fig IV-18***, several cycles (charge and discharge) have been performed to check its functionalities for monitoring, controlling and reading data [***13***].

Fig IV-18 Testing the test board with Solid-State-Ceramic battery
The same setup used during the charge and discharge before and after each test [*13*]

IV.3. Results and discussion

IV.3.1. Launch environment test results and discussion

Considering the vibration and shock as a circumstance that may happen simultaneously or consecutively, the results of the two evaluation tests are discussed in the same section. However, during the *launch environment* evaluation test, the two groups have been tested separately under shock then the vibration [*24*].

IV.3.1.1. Criteria

During the launch ground test's result evaluation, the criteria used during the space evaluation for the vacuum and the thermal vacuum test have been used. As well as some other criteria listed in ***Table IV-10*** for the change in values after each environmental test for the open-circuit voltage, internal resistor, mass, and capacity:

Such as some projects at *NASA* have used criteria (***#1*** *in* ***Table IV-10***) for the change in values before and after each environmental test as following: the change should be less than 0.1% for OCV and internal resistance, between 0.1% and 1% for mass and less than 5% for capacity [*13*,*116*]. Another pass/fail criterion (***#2*** *in* ***Table IV-10***) for the qualification test for COTS battery mentions that the change should be less than 0.5% for OCV and mass, and less than 3% for capacity [*13*,*117*].

During our analysis, the criteria (***#3*** *in* ***Table IV-10***) have been adopted, which is a combination of the two previous criteria.

Table IV-10 Pass/fail criteria for the *launch environment* test [*24*]

Criteria	OCV	IR	Mass	Capacity
#1	< 0.1%	< 0.1%	0.1 to 1%	< 5%
#2	< 0.5%	/	< 0.5%	< 3%
#3	0.1 to 0.5%	< 0.1%	0.1 to 0.5%	3 to 5%

IV.3.1.2. Outputs test's conditions

For each group, ***Fig IV-19*** shows the reel spectrum for the applied shock during the test, following the same test condition in ***Table IV-2***. The pickup sensors show that the acceleration during the test has exceeded the upper limit, because of the difficulty of the tuning, while it is still higher than the lower limit which is more important for the credibility of the test. However, we could say that the batteries were exposed to an accepted shock level test even if the upper limit was exceeded [*24*].

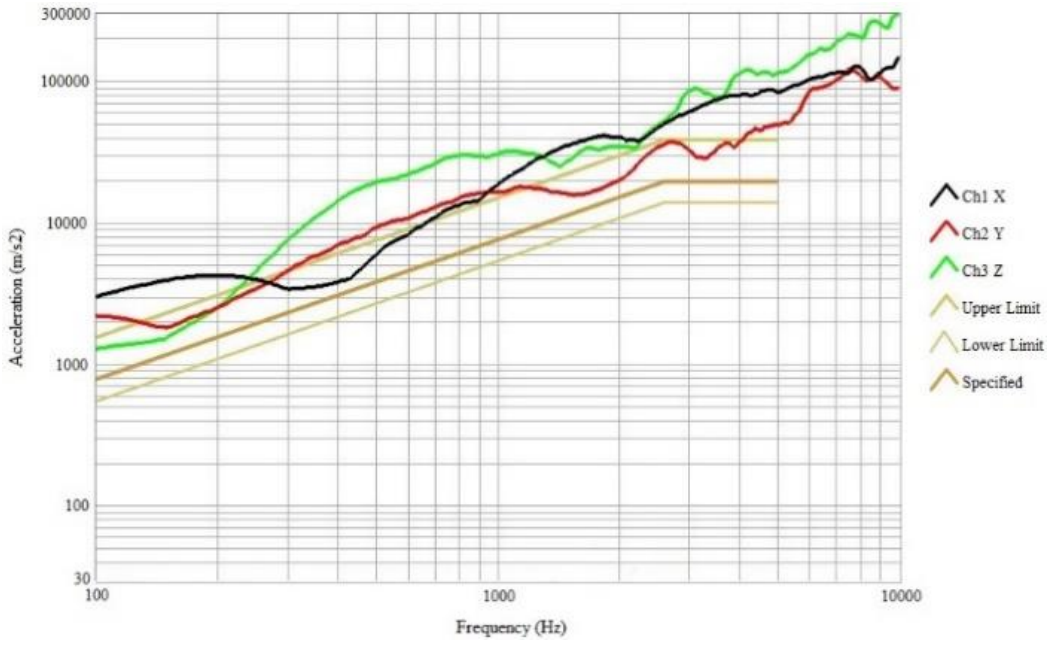

Fig IV-19 Shock test pickup sensors' outputs spectrum [*24*]

During the vibration test for the sine burst, the pickup sensors' records for CH2, CH6, and CH7; could reach the required limit at 7.5G with more than 10 cycles (*typically only 3 to 5 are required*), as represented in ***Fig IV-20***. CH2, CH6, and CH7 are respectively the records for the axes that have been exposed to the same sine burst excitation's direction during the second configuration, the same results have been obtained during the other configurations [*24*].

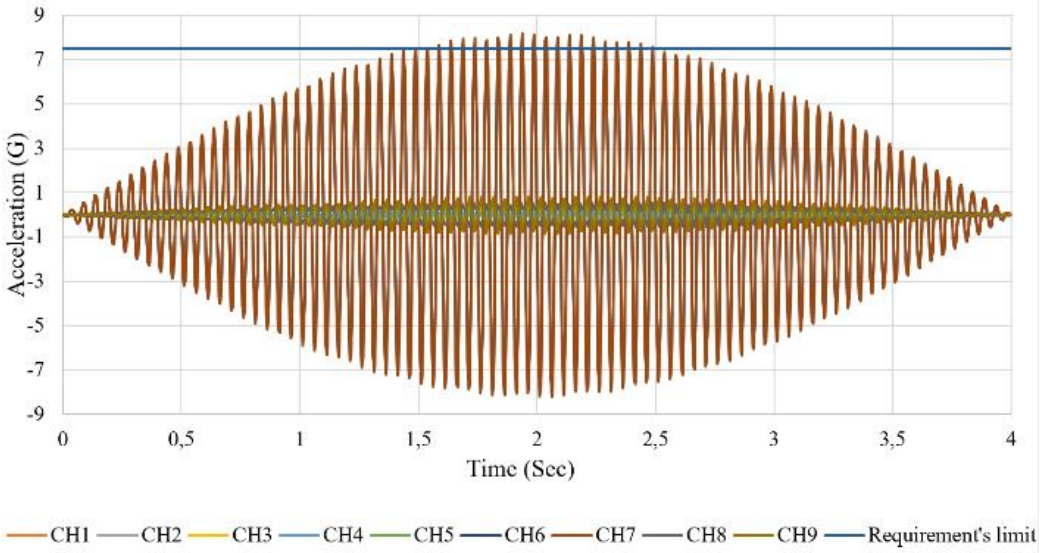

Fig IV-20 Sine burst test pickup sensors' outputs
Jig 1 (CH:1,2,3), Jig 2 (CH:4,5,6), and Jig 3 (CH:7,8,9) [*24*]

For the sinewave, ***Fig IV-21*** shows the real condition during the test where all the Solid-State Lithium-Ceramic-Battery' jigs have been exposed during the low frequencies from 5 to 100 Hz [*24*].

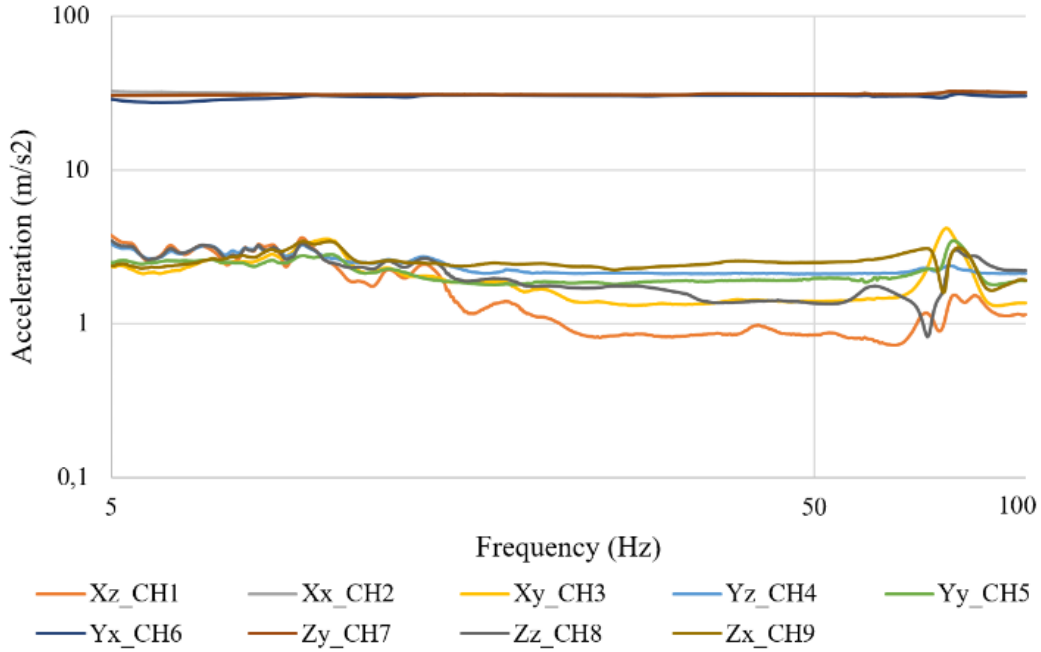

Fig IV-21 Sinewave test pickup sensors' outputs
Recorded for the Solid-State Lithium-Ceramic-Battery following the inputs' condition [*24*]

Finally, with the high frequencies, during the random vibration, ***Fig IV-22*** shows the real test spectrum generated during the test, following the inputs parameter

required in ***Table IV-5***, in which the batteries have been exposed to the random vibration between 20 and 2000 Hz within 2 minutes [*24*].

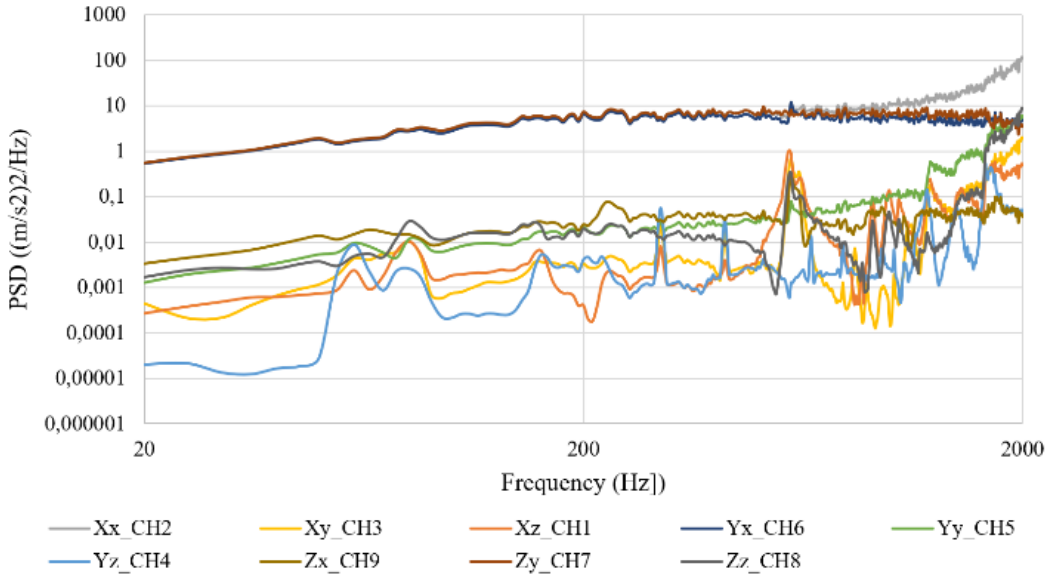

Fig IV-22 Random test pickup sensors' outputs
For the three jigs during the first configuration [*24*]

IV.3.1.3. Visual inspection, weight, and open-circuit voltage measurements

At the end of the test with the non-functional check, no physical damage has been observed related to the fatigue, none of the batteries has shown a change in dimensions or weight, ***Table IV-11*** summarizes the weight measurement before and after all the launch environment test. Otherwise, the change of value for the OCV measurements shows a variation exceeding the criteria's limits for some batteries (**PLCB02**) with 0.2% excess as shown in ***Table IV-12*** [*24*].

Table IV-11 Weight measurement before and after test [*24*]

	PLCB					
	01#1	**01#2**	**01#3**	**02#1**	**02#2**	**02#3**
Before (g)	58,32	58,38	58,18	45,44	45,56	45,46
After (g)	58,33	58,37	58,17	45,43	45,56	45,45
Difference (%)	0,02	0,02	0,02	0,02	0,00	0,02

Table IV-12 OCV measurement before and after test [*24*]

	PLCB					
	01#1	**01#2**	**01#3**	**02#1**	**02#2**	**02#3**
Before (V)	4,21	4,21	4,23	4,28	4,28	4,28
After (V)	4,19	4,21	4,21	4,25	4,25	4,25
Difference (%)	0,48	0,00	0,47	**0,70**	**0,70**	**0,70**

After comparing the measurements between after the shock; which the results have shown no significant variation in value at the order of 10^{-3}; and after the vibration, it has been concluded that the change of the value has been induced by the vibration and not the shock. However, the exceeding could not be used for judgment until the functional test has been done which would give the more significant interpretation [*24*].

IV.3.1.4. Functional test results

After the batteries have been exposed to the shock and vibration test, several charges and discharges cycles have been performed showing that batteries have been able to operate several cycles in normal conditions, which means that the hostile environment did not affect the charge mode of batteries [*24*].

During the result discussion, the capacity before the test is considered as the *reference capacity*, according to the test conditions, it is given in mAh and calculated from the current discharge. The *capacity ratio*, the percentage of the capacity compared to the capacity before the test, is another term that will be used for comparison during each cycle [*13*].

As shown in ***Fig IV-23*** and ***Fig IV-24*** for the PLCBs batteries (01 & 02), the constant-current constant-voltage (CC-CV) mode has been perfectly followed, starting charging with a constant-current (CC) at ~1.3A and a voltage at ~3.4V for PLCB01, and ~0.8A and ~3.3V for PLCB02, the constant-current has been switched to the constant-voltage (CV) at ~4.1 to 4.2V, then the charge stopped when the batteries have been fully charged [*24*].

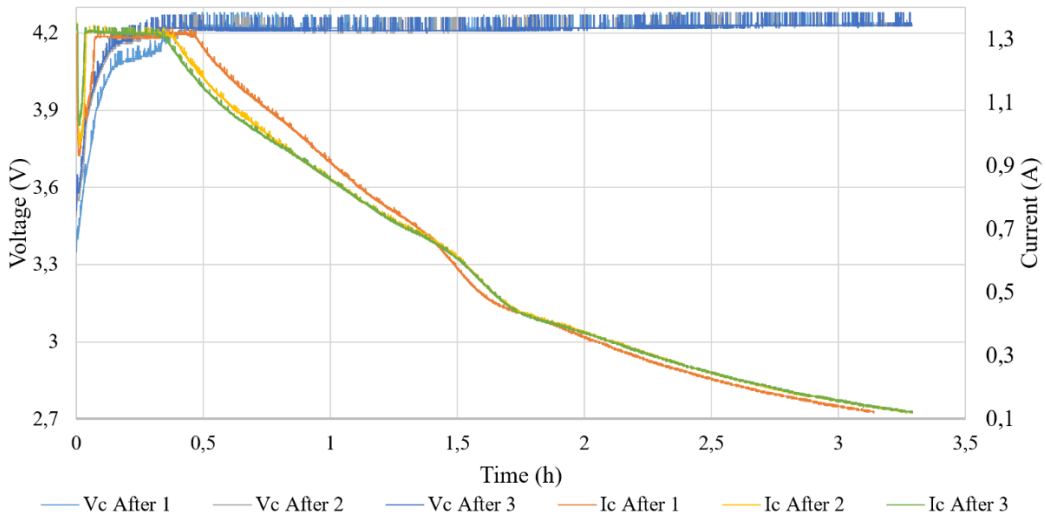

Fig IV-23 Charge cycles for PLCB01 1950 mAh after the launch evaluation test Group's samples for one jig [*24*]

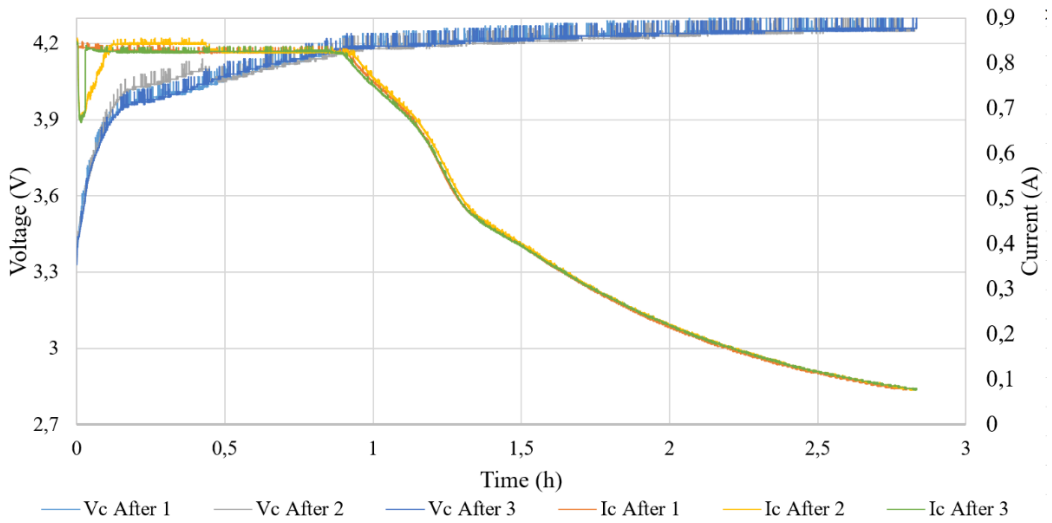

Fig IV-24 Charge cycles for PLCB02 1450 mAh after the launch evaluation test Group's samples for one jig [*24*]

All batteries have been charged following the CC-CV mode perfectly without showing any malfunctions, except for some perturbations due to some noises.

However, for the discharge mode and the capacity evaluation, ***Fig IV-25*** and ***Fig IV-26*** represent the result of the discharge capacity after the shock only, and after all the test compared to the before test discharge capacity. All PLCBs batteries have been discharged at the required discharge current: ~0.92A for PLCB01 and ~0.72A for PLCB02, with the same discharge rate of 0.5C [*24*].

It has been noticed that the PLCB01 batteries showed more stability according to the total number of samples that have been tested and the numbers of samples that have been passed the test, with a decrease in capacity so far not exceeding the limit of 3% after the shock and vibration only, and between 3% to 5% after all the test. All the results have been summarized in the following figures: ***Fig IV-25 (a, b, and c)*** [*24*].

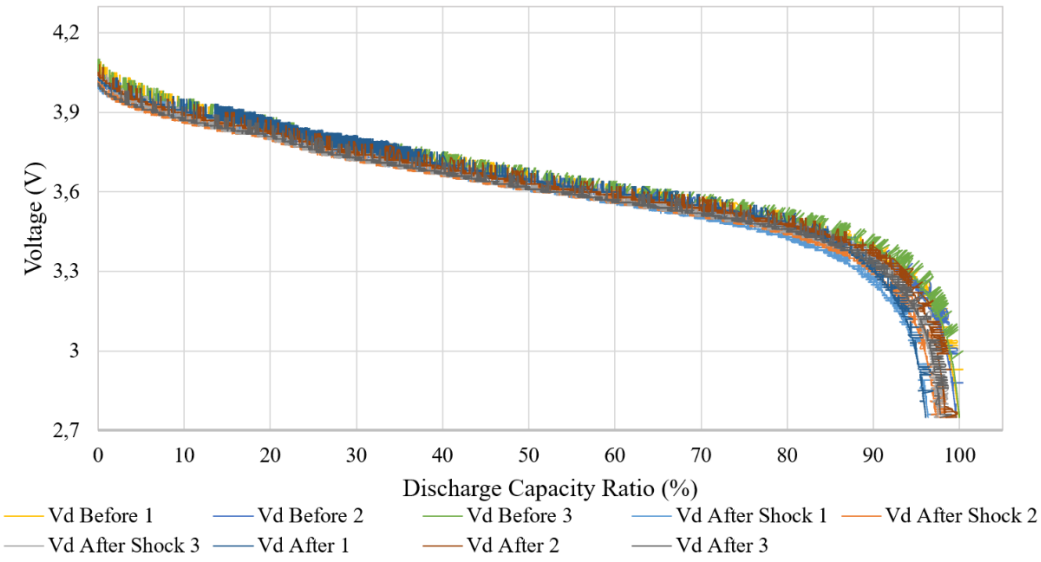

(a) Jig's group 1

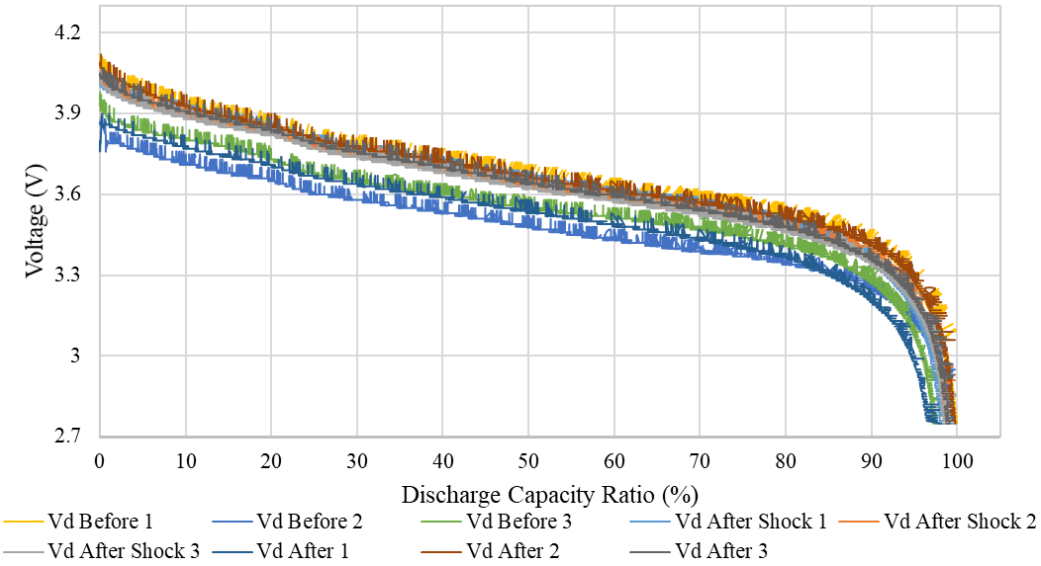

(b) Jig's group 2

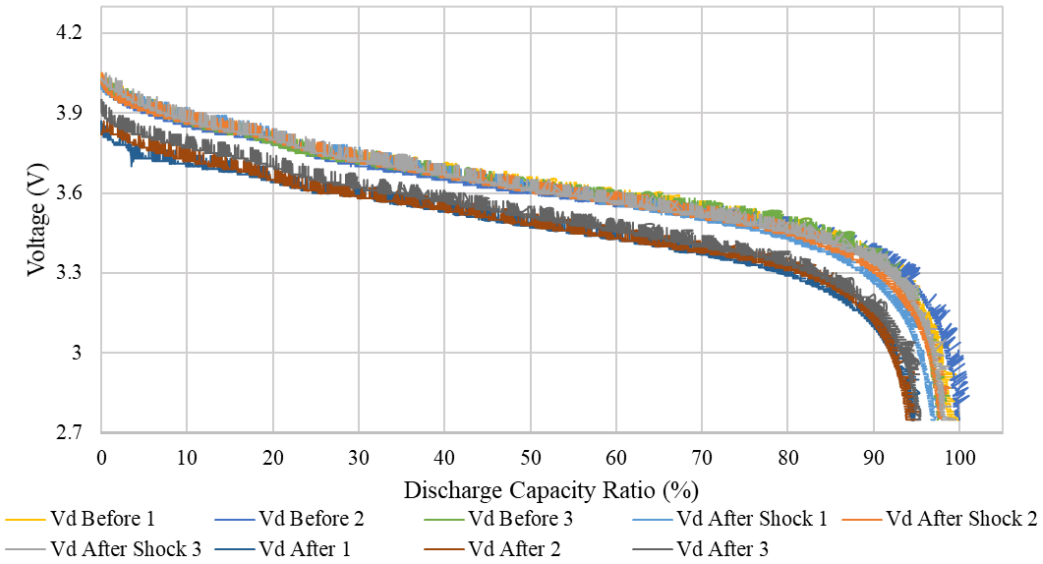

(c) Jig's group 3

Fig IV-25 Discharge voltage vs discharge capacity ratio for PLCB01 1950 mAh.
Group's samples for the three jigs (groups): before, after the shock tests and after the 3 axis vibration tests [*24*]

While the only exception is for one PLCB02 battery which has shown a decrease of more than 5% after all the test, as represented in ***Fig IV-26 (a)*** and ***Fig IV-26 (c)***, during two or three cycles, it may be due that the battery was already in bad condition or manufacturing defect, the others PLCB02 show no significant loose in capacity, less than 3% after the shock, between 3% to 5% after the vibration and all the test as shown in ***Fig IV-26 (b)*** [*24*].

However, it can be concluded that all PLCBs has passed the launch environment successfully, including the results that have been got for some groups with exceeding the limits.

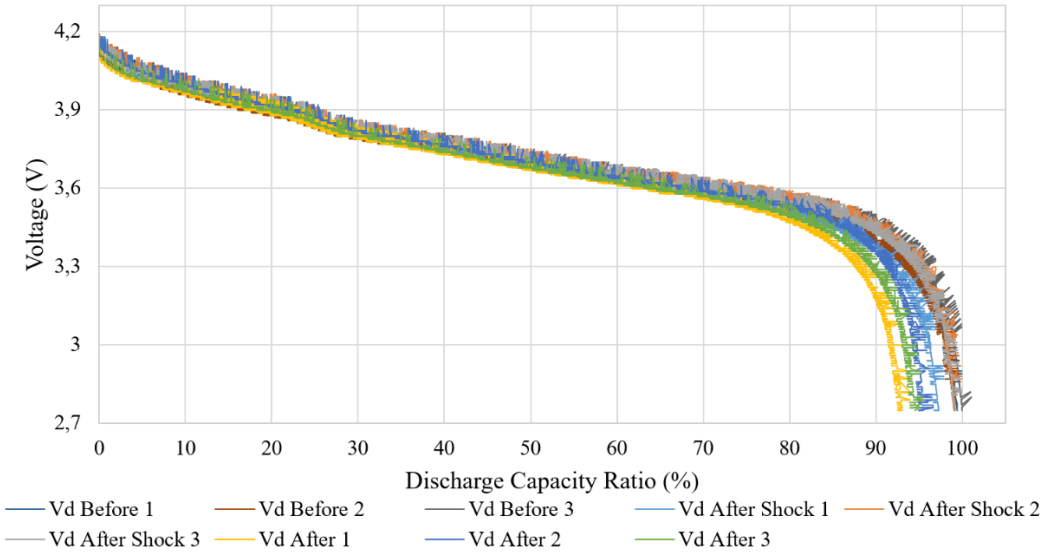

(a) Jig's group 1

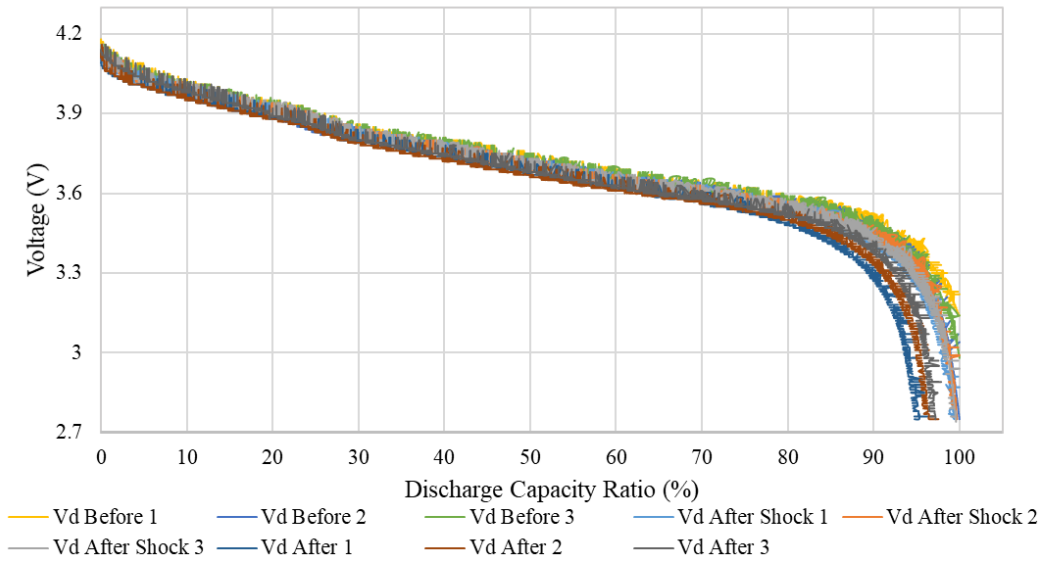

(b) Jig's group 2

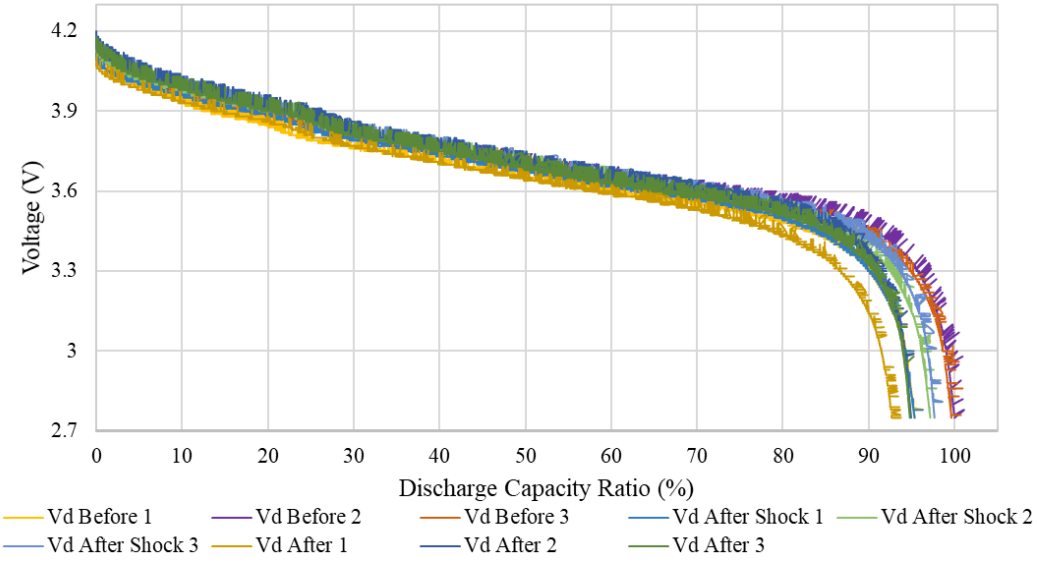

(c) Jig's group 3

Fig IV-26 Discharge voltage vs discharge capacity ratio for PLCB02 1450 mAh.
Group's samples for the three jigs (groups): before, after the shock tests and after the 3 axis vibration tests [*24*].

From another point of view, the complete discharge charge cycle for the two SSLCBs has been reproduced in order to compare the results between the before and after the test. ***Fig IV-27***, and ***Fig IV-28*** have reproduced some of these cycles as examples.

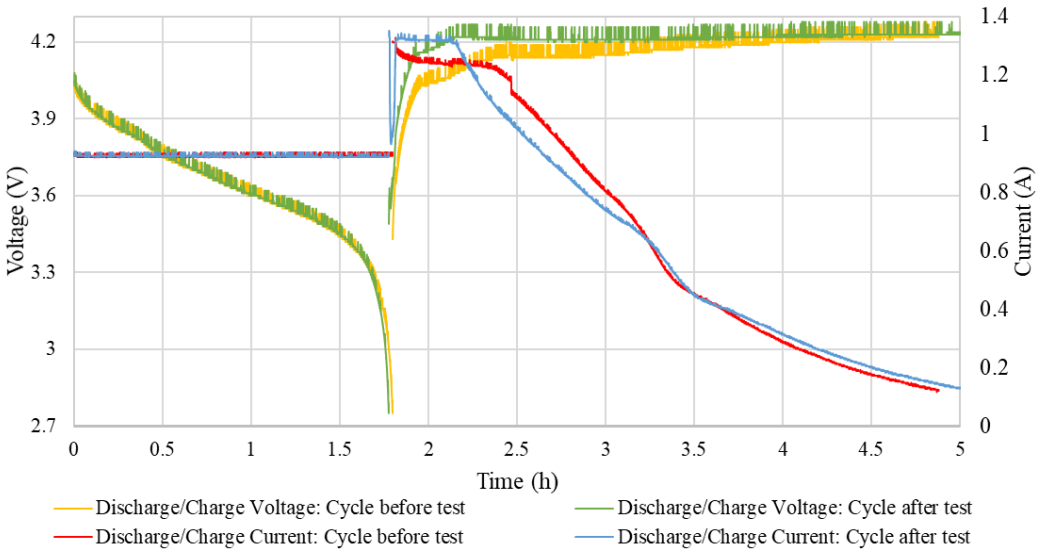

Fig IV-27 Charge/Discharge cycle for the PLCB01 1950mAh
Before and After the test

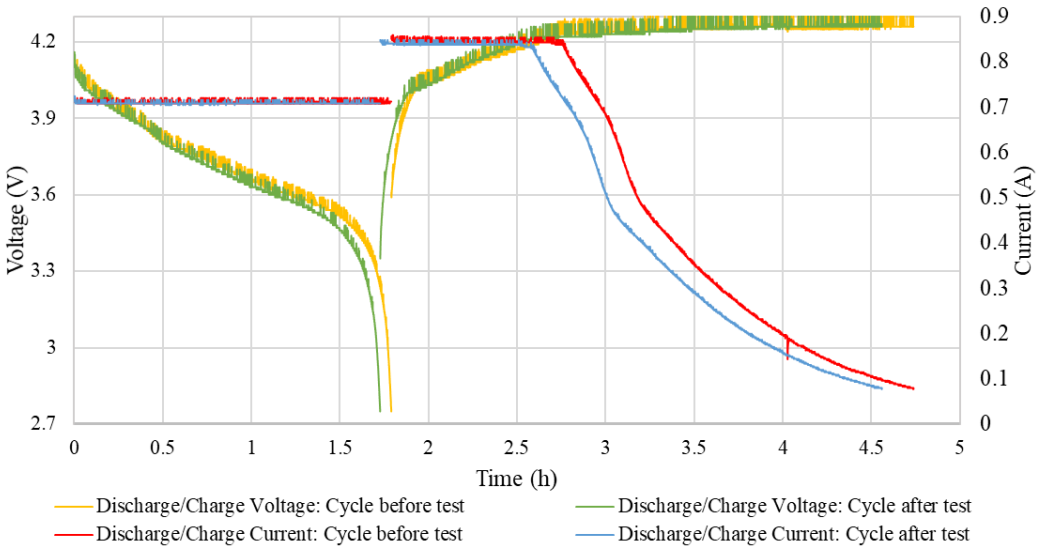

Fig IV-28 Charge/Discharge cycle for the PLCB02 1450mAh
Before and After the test

IV.3.2. Space environment test results and discussion

For the results discussion and the evaluation of batteries after the test, some guidelines from *NASA* and *ISO standards* cited previously in the literature, and used previously at the launch environment results analysis have been used (***Table IV-10***) [***13***]:

- The criteria used by *NASA* for the change in values before and after each environmental test: the change should be less than 0.1% for OCV and internal resistance, between 0.1% and 1% for mass and less than 5% for capacity [***13***,***116***].
- The pass/fail criterion for the qualification test for COTS battery: the change should be less than 0.5% for OCV and mass, and less than 3% for capacity [***13***,***117***].

Additionally, the *ISO standard 17546:2016* related to the design and verification requirements for the Lithium-ion battery on space vehicles in which it is saying: "***If the total change in mass of the batteries exceeds 0.2%, the batteries are considered as failure and unfit for development***" [***13***].

IV.3.2.1. Vacuum

Fig IV-29 represents the variation of the pressure during the vacuum test inside the chamber for a total duration of 24 hours, vacuum started at $1{,}7\times10^{-3}$ Pa then stopped at 2×10^{-4} Pa.

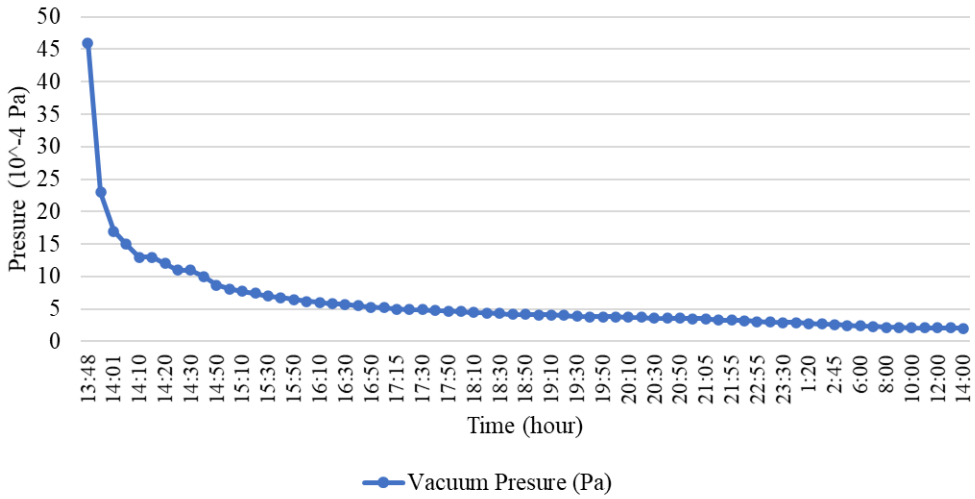

Fig IV-29 Variation of pressure inside the vacuum chamber (Pa)

Based on the measurements for the length, width, and thickness done before and after the vacuum test represented in ***Fig IV-30***, batteries show no significant change in their physical properties except during the vacuum where the two PLCBs show some swelling as figured in ***Fig IV-11***; due to the difference of pressure between inside the battery and the chamber, finally it returns to the normal condition after the pressure goes normal [*13*].

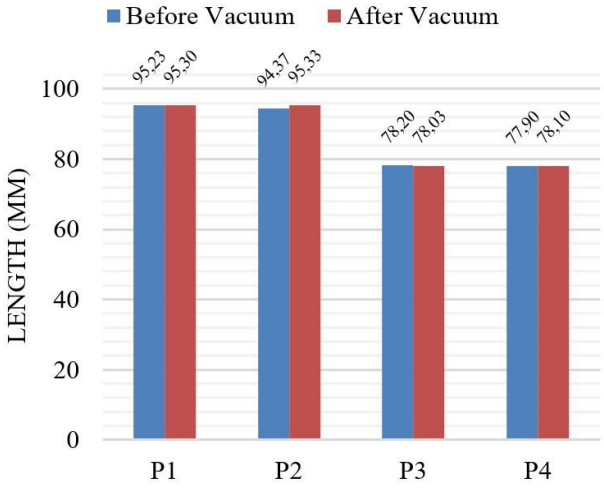

(a) Length (mm)

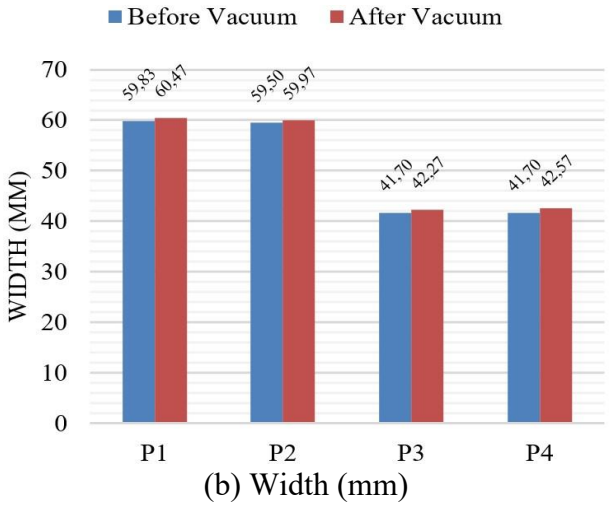

(b) Width (mm)

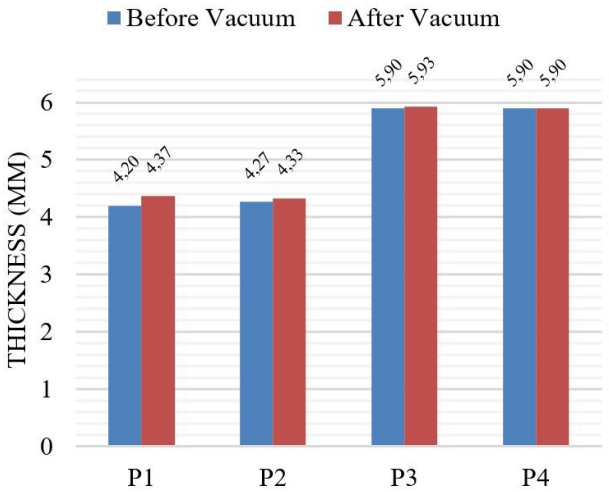

(c) Thickness (mm)

Fig IV-30 Physical properties before & after vacuum test ((a) Length, (b) Width, (c) Thickness) [*13*]

For the open circuit measurement in ***Fig IV-31***, the Solid-State batteries have kept almost the same voltage before and after the exposition to the vacuum pressure [*13*].

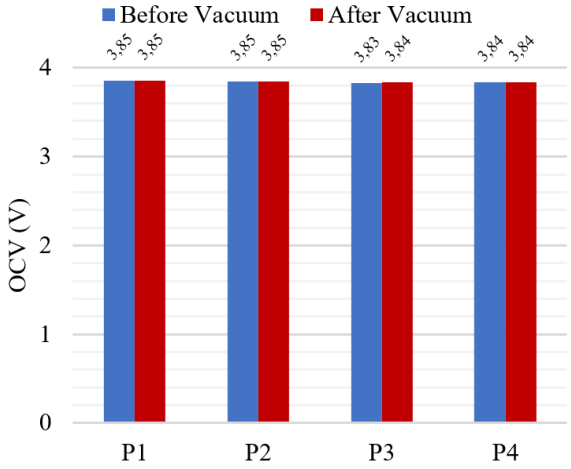

Fig IV-31 Open circuit voltage before & after vacuum test (V) [*13*]

Finally, based on the weight measurement of the Solid-State Lithium-Ceramic-Battery after the vacuum test, where the results are clearly represented in ***Fig IV-32***, show a difference in weight of 0.02% for PLCB01 (P1, P2), 0.01% for PLCB02 (P3, P4), that can be neglected compared to the criteria, which leads to the fact that all the batteries have passed the first step and are ready for the functional test at the thermal vacuum [*13*].

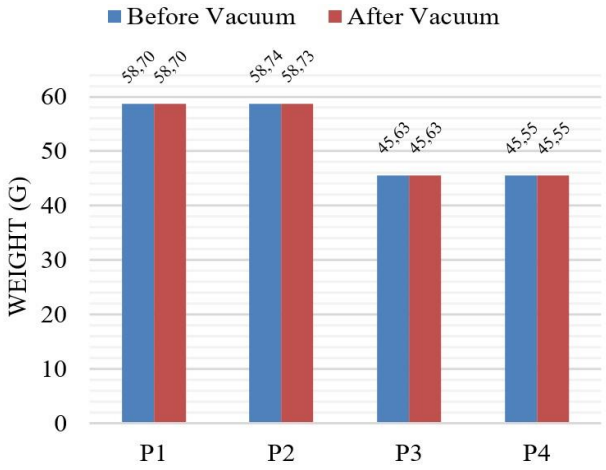

Fig IV-32 Weight before & after vacuum test (g) [*13*]

IV.3.2.2. Thermal vacuum

For the second part of the evaluation test, the Solid-State battery P1 and P3 were discharged and charged as described in the test procedure, results for the thermal vacuum test have been divided into three categories [*13*]:

First, with the electrical properties summarized on the open-circuit voltage for all batteries, **then** the discharge capacity ratio comparison for the Solid-State Lithium-Ceramic-Battery: P1 and P3 which have been discharged and charged as described

at the test procedure during the eight cycles at the three different temperatures: cold with -20°C, room temperature with +20°C and hot with +60°C [*13*].

Finally, with the physical properties' measurement for all batteries done before and after the test [*13*].

Fig IV-33 represents the real temperature profile during all cycles, in which the temperature reading on the top and the bottom thermocouples for P1 and P3 during all the cold cycles, show a generation of heat and an increase of temperature, which is clearly seen in the ***Fig IV-33***, the reason may be due to the high capacity with the high discharge current for the tow PLCBs [*13*].

During the first cold cycle at -20°C, the Solid-State Lithium-Ceramic-Battery (FLCB) could not be discharged and charged properly, which lead to adding a new pre-charge step to cycle 2 and 3, between -20°C and +60°C, the pre-charge step is to make sure that the batteries could be able to charge fully before being discharged at the next cycle [*13*].

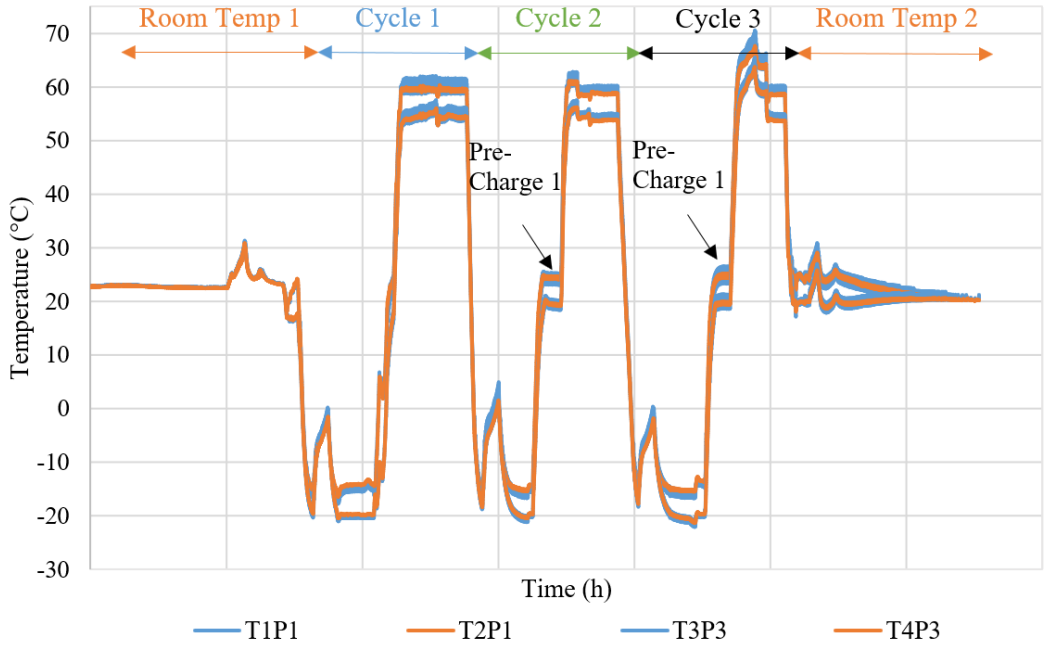

Fig IV-33 Thermal Vacuum's real temperature profile (T1 and T3 for the top; T2 and T4 for the bottom) for P1 & P3 with showing the heat dissipation during discharge [*13*].

During the result discussion, the capacity before the test is considered as the *reference capacity*, according to the test conditions, it is given in mAh and calculated from the current discharge. The *capacity ratio*, the percentage of the

capacity compared to the capacity before the test, is another term that will be used for comparison during each cycle [*13*].

For the Solid-State Lithium-Ceramic-Battery P1 and P3, the results are quite similar. During all the cycles except for the cold ones, the capacity ratio has not shown a big difference between the capacity before and after the test with ~5% of loose, while the capacity has been decreasing during the cold cycles with less than ~20 % as shown in ***Fig IV-34*** [*13*].

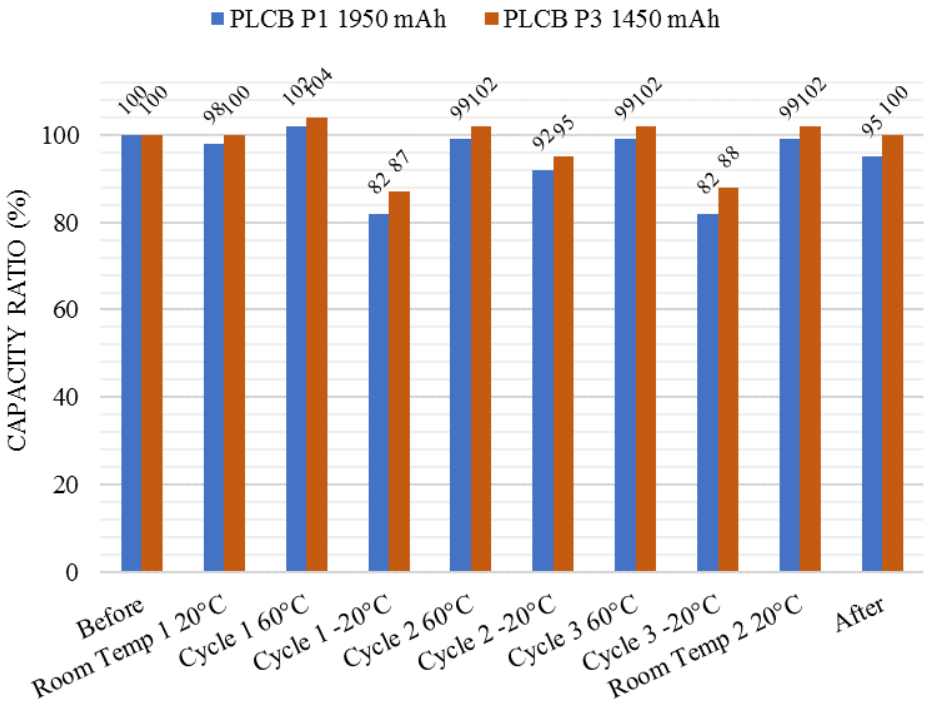

Fig IV-34 Capacity ratio comparison between P1 & P3 [*13*]

Fig IV-35 and ***Fig IV-36*** represent the relationship between the discharge voltage and the discharge capacity ratio for the Solid-State batteries P1 and P3 respectively. Each figure contains five plots that compare the discharge voltage and the discharge capacity ratio before and after the test with the discharge voltage during the hot, cold and the room temperature cycle [*13*].

Concerning the hot and room temperature cycles, the Solid-State-Ceramic battery P1 has shown ~1% capacity loss comparing to the capacity before the test. ***Fig IV-35 (a)*** and ***Fig IV-35 (b)*** show that for the hot and room temperature, the battery keeps almost the same discharge profile, it starts discharge form: ~4.2V and stopped at 2.8V with 0.96A for discharge current, except for the last test, due to some reasons related to the test condition the current has been increasing to ~1.2A, and the discharge starts from low value: ~3.87V for voltage. The discharge after the test has been repeated two times in order to confirm the result, which keeps the same

discharge current and voltage with the same capacity. However, the result does not conclude to any capacity degradation for P1 and it may need more investigation on the battery itself [*13*].

During the cold cycle, P1 shows a decrease in capacity with ~18% of loss as shown in ***Fig IV-35 (c)***, which is normal due to the low temperature around -20°C. The discharge has started from ~3.6V for voltage with a discharge current that is the same as the other cycles with 0.96A [*13*].

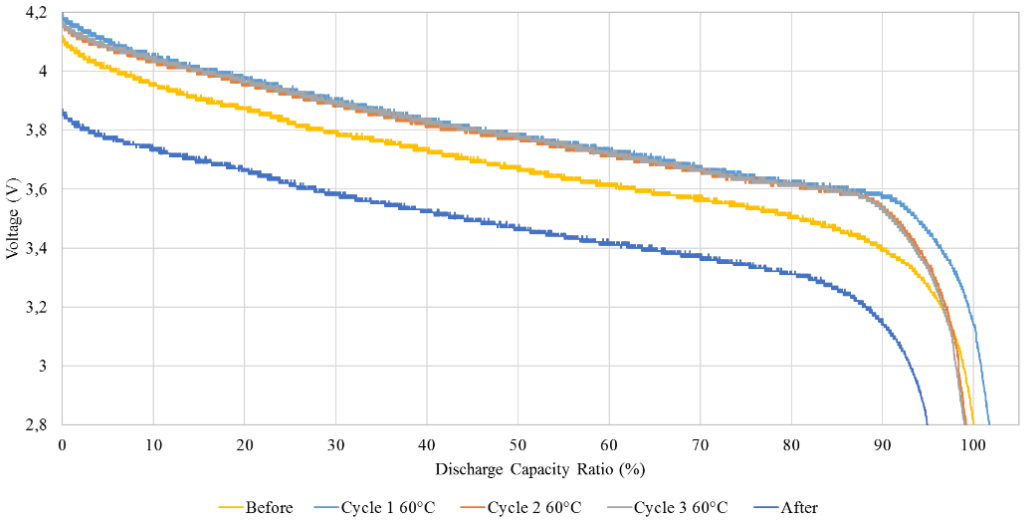

(a) Hot temperature

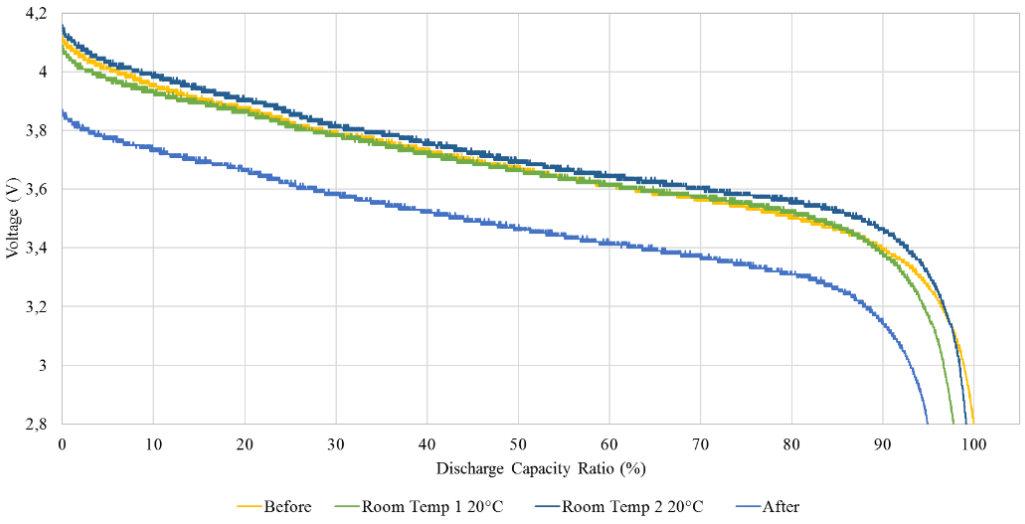

(b) Room Temperature

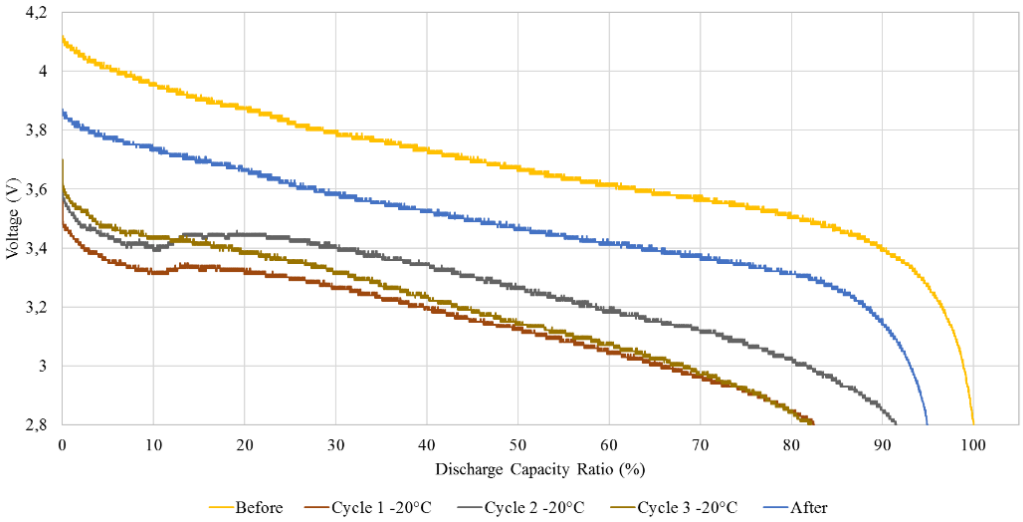

(c) Cold Temperature

Fig IV-35 Discharge voltage vs capacity ratio for P1 (PLCB01) 1950 mAh ((a) Hot temperature, (b) Room Temperature, (c) Cold temperature) [*13*]

For the second Solid-State-Ceramic battery P3, ***Fig IV-36 (a)*** and ***Fig IV-36 (b)*** show that the hot temperature has not affected its performance, as for the room temperature which the capacity is more stable and shows no difference compared to P1, it has the same discharge voltage from ~4.1V with the same current ~0.73A during all cycles [*13*].

For the cold cycles in ***Fig IV-36 (c)***, starting discharge from ~3.5V, the capacity has been decreased ~13% compared to the capacity before the test, in the same way as the battery P1 but with 5% lower [*13*].

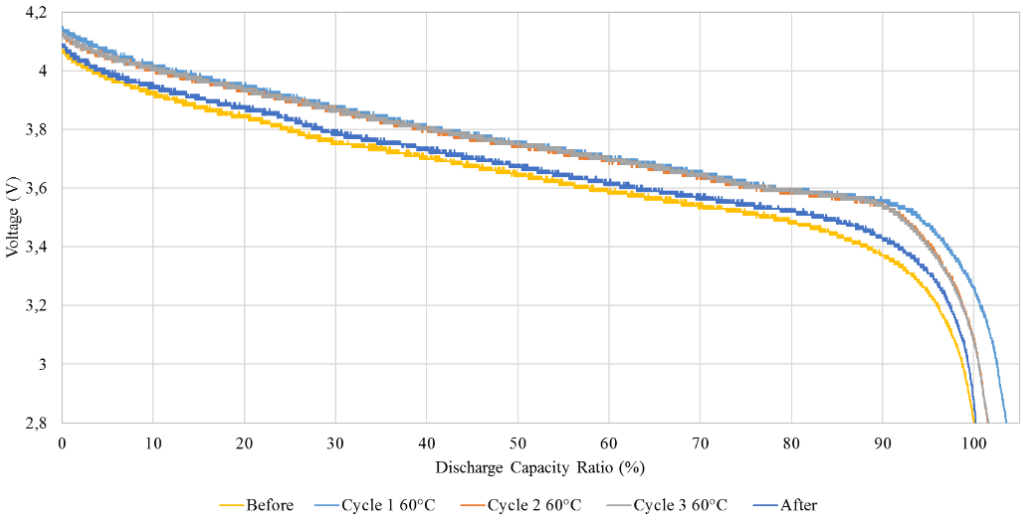

(a) Hot temperature

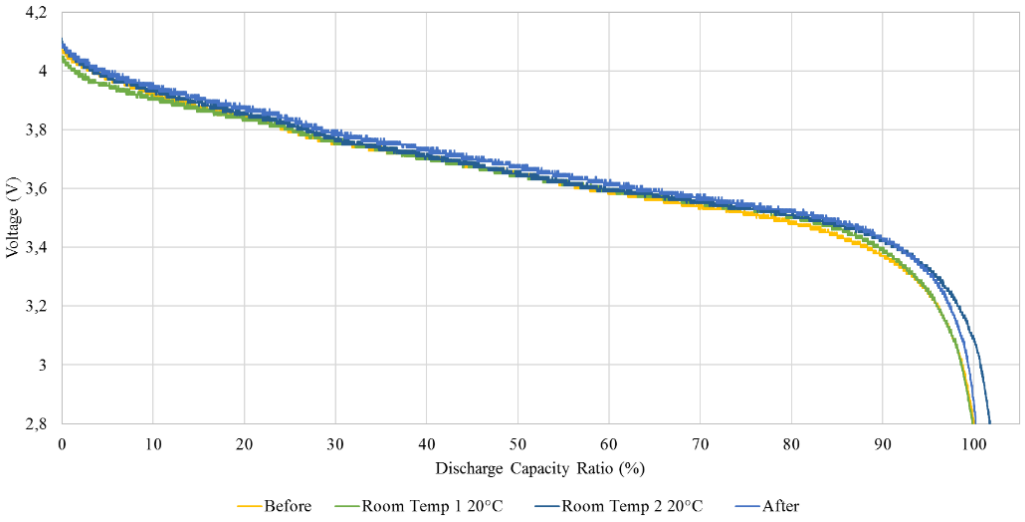

(b) Room Temperature

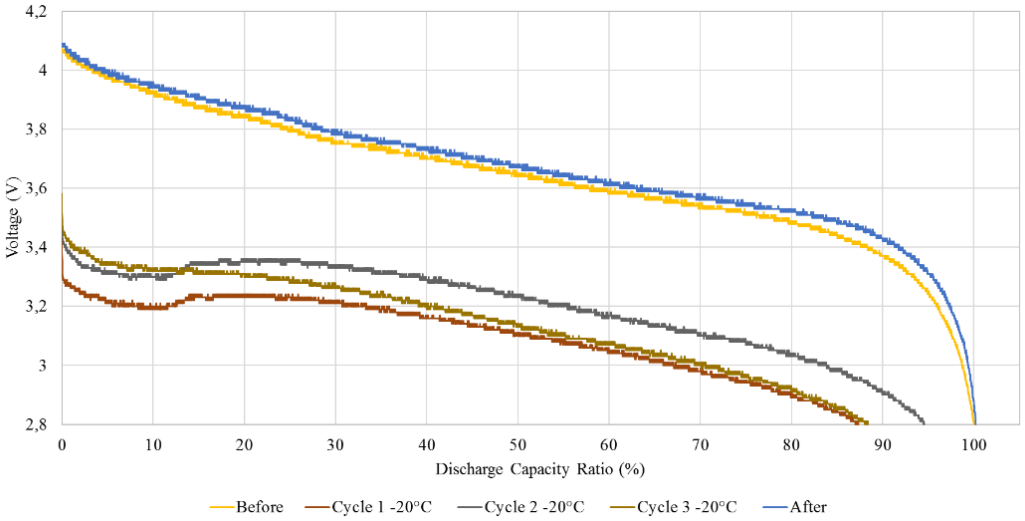

(c) Cold Temperature

Fig IV-36 Discharge voltage vs capacity ratio for P3 (PLCB02) 1450 mAh ((a) Hot temperature, (b) Room Temperature, (c) Cold temperature) [*13*]

Comparing the capacity ratio variation from the beginning to the end of the test, the Solid-State Lithium-Ceramic-Battery P1 and P3 keep almost the same capacity, which is a good result, even after enduring a big change of temperature from -20°C to +60°C during several cycles of discharge and charge, P1 and P3 keep so far same performances [*13*].

Concerning the open circuit measurement, ***Fig IV-37*** shows good stability with almost the same value for all batteries [*13*].

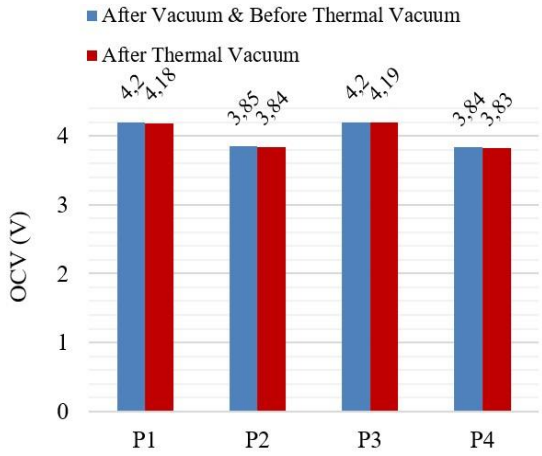

Fig IV-37 Open circuit voltage before & after the thermal vacuum test (V) [*13*]

Fig IV-38 for physical properties with length, width and thickness, have shown that there is no change, the batteries show no degradation or damage [*13*].

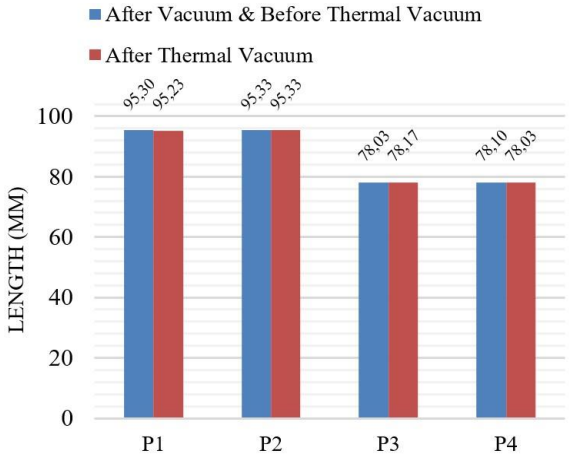

(a) Length (mm)

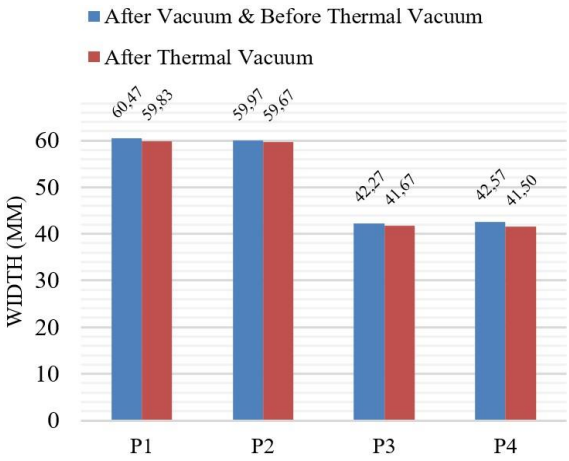

(b) Width

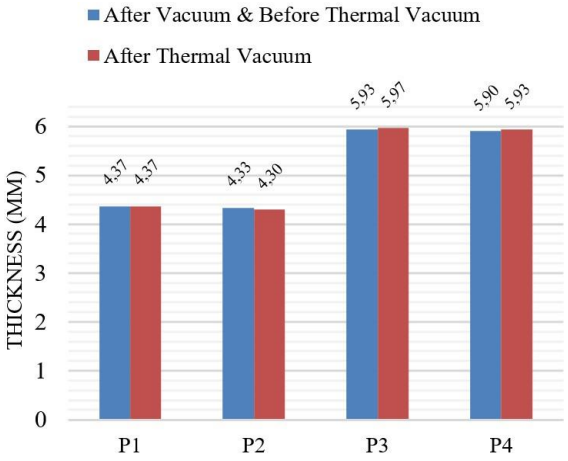

(c) Thickness

Fig IV-38 Physical properties before & after thermal vacuum test ((a) Length, (b) Width, (c) Thickness) [*13*]

Following the same criteria used for the evaluation during the vacuum test, ***Fig IV-39*** shows that the Solid-State batteries P1 and P3 have not shown any weight change, additionally to their physical or electrical properties, so far not affecting their performances [*13*].

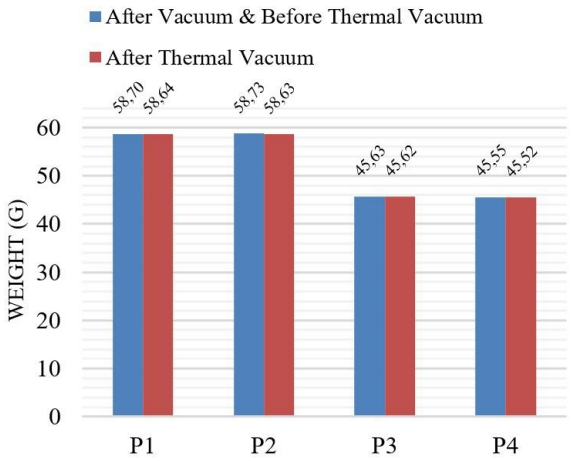

Fig IV-39 Weight before & after the thermal vacuum test [*13*]

More results could be provided by the company like for ***Table IV-13***, which summarizes the test results for the open-circuit measurement and the capacity ratio before and after all the space environment test, which has been done without a vacuum and under ambient temperature in their laboratory [*13*].

The results presented in ***Table IV-13*** agree well with the results obtained after the thermal vacuum test which the two PLCBs could pass the test with no degradation for their performance. The company could confirm the stability for the open voltage measurements and the decrease of capacity with ~6% for booth Solid-State Lithium-Ceramic-Battery PLCB01 and PLCB02. Additionally, for the internal

resistance another key parameter for batteries, the PLCB batteries P1 and P3 keep the same value for their internal resistances [*13*].

Table IV-13 OCV and Internal Resistance Before and After the Evaluation Test [*13*]

SSLCB	Before Evaluation Test			After Evaluation Test			
	IR (Ω)	OCV (V)	C (mAh)	IR (Ω)	OCV (V)	C (mAh)	Ratio (%)
P1	0.0259	3.86	2029	0.0250	3.86	1912	94.2
P3	0.0279	3.84	1503	0.029	3.87	1418	94.3

IV.4. Conclusion

So far, the results from the evaluation within the *launch environment* conditions for the Solid-State Lithium-Ceramic-Battery show that all batteries have not been affected by the high shock and the high vibration level and could withstand the launch environment successfully; at least it could notice on the comparison between the capacity before and after the test that the batteries do not show any significant degradation which 83% of Solid-State Lithium-Ceramic-Battery tested could be able to keep their capacity with 95%, which means in another way that all **PLCB01** and two **PLCB02** have passed the *launch environment* evaluation test, so far within the limits. Additionally, they have not shown any physical degradation [*24*].

The Solid State-Ceramic batteries evaluated under the vacuum and the thermal vacuum conditions, with ~2% mean loss of capacity after all test, have been able to demonstrate their ability to maintain their performances under several cycles of thermal vacuum with a hot temperature reaching +60°C, and a good stability for operating under such as high temperature compared to the other *Lithium Cobalt Oxide* (LiCoO2) batteries which are very reactive and suffer from poor thermal stability. For a low temperature around -20°C, the result shows that the Lithium Ceramic Battery (PLCB) could operate normally with a mean loose of the capacity of ~12%, so far without affecting their performances or showing any physical degradation, which may lead to reduce using heaters and power consumption on small satellite compared to the conventional Lithium-Ion battery [*13*].

Another key parameter, such as the internal resistance, the PLCB have shown no significant change with good stability of about ~4% [*13*].

The chapter has also summarized as a guideline all the main steps for the battery's ground testing from the *launch* to the *space environment* including the main criteria which may be used for the evaluation of results and discussion after the two environment tests. Finally, a procedure for the radiation test under the *Gamma-ray* has been proposed in order to be used for future tests and evaluations.

Chapter V

Nanosatellites Modular-Wall-Battery (MWB) Concept I:

Design & Requirement

V. Nanosatellites Modular-Wall-Battery Concept I: Design & Requirement

The idea of the *Modular-Wall-Battery* (*MWB*) concept starts while investigating and searching for a simple design solution related to small satellite and Nanosatellites challenges, especially for 1U CubeSats, in order to save volume by providing at least the required power to the satellite. The *MWB* design should be simple and totally adaptable to any Nanosatellite while solving the challenge related to the limited size and lack of power.

The *Modular-Wall-Battery* design is defined as a new proposed engineering approach for battery arrangement, combining advanced batteries technology, the Solid-State battery, and the modular philosophy.

V.1. Modular-Wall-Battery (MWB) approach

V.1.1. Design concept definition

When talking about battery, is directly reminded to us the Lithium-Ion cylindrical battery that has been used for a long time and everywhere in our daily life, it is also reminded to us the question of safety, especially with the large expansion of the application on a mobile device and electrical vehicles.

However, the Lithium-Ion is one kind of battery technology between many others, it could be able to keep the first position for many applications, as well as in space, the reason for its electrochemical specification that led to a good performance in terms of electrical characteristics with power, capacity and lifespan.

Based on the batteries' technology, several designs could be found: cylindrical, prismatic or pouch also called *laminated*, as presented in ***Fig V-1***, the other reason for this diversity may be due to the material used in some of the battery parts, as for the cathode, anode, or the most part that many manufactures or researchers are working on, the electrolyte, which leads to the apparition on the market of the Solid-State batteries (*Polymer* and *Ceramic*), even the future All-Solid-State-Battery which may still have limited application, while under improvement and development into laboratories, especially to be integrated into future satellites.

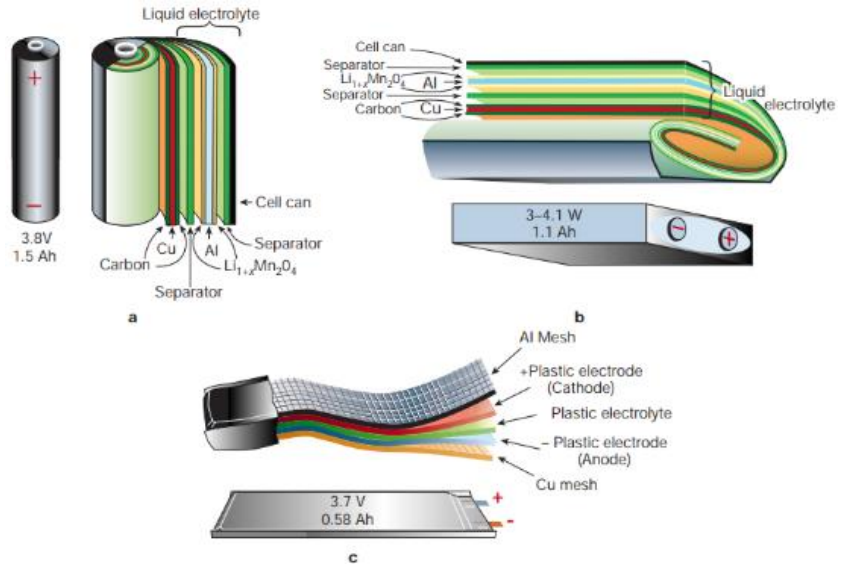

(Open access Creative Common CC BY license)

Fig V-1 Different battery design representation
(a. Cylindrical, b. Prismatic, c. Pouch (*Laminated*)) [*118*]

In space, onboard Nanosatellites, different batteries technology have been used including the Lithium-Ion, however, several approaches have been adopted for batteries arrangement based especially on the cylindrical or pouch design, as summarized in ***Table V-1***, the same batteries have been presented in ***Chapter III***. These approaches could be categorized as follows: *battery box concept arrangement* (***Fig III-3***), *battery's mechanical structural concept arrangement*, and the *pouch battery pack concept arrangement*.

Table V-1 List of some satellite using different battery's arrangement

Satellite	**Battery technology**	**Design**	**Concept**	**Reference**
Spatium	Li-Ion	Cylindrical	Battery box	[*78*]
Equisat	Li-Ion & LiFePO4	Cylindrical	Mechanism structural	[*84*]
Upsat	Li-Ion	Cylindrical		[*85*]
ESTCube-1	Li-Ion	Cylindrical	Other	[*87*]
Hodoyoshi-3	IL-LIB (demo)	Pouch		[*88*]
ISTSat-1	Li-Pol	Pouch	Pouch pack	[*90*]

The modular approach, or the modular design philosophy, seems to be more popular on the electrical power system the reason for the many solutions that can provide, as making the development faster, as for the work done by *Jesus Gonzalez et al.* where it has been adopted for the solar cells with the *Solar Module Integrated Converters* (*SMIC*) as a power generator in small spacecraft [*39*]. Or saving more volume as the work done by *Giorgio Capovilla et al.* on the AraMiS CubeSat

project presented in ***Fig V-2***, an interesting approach using the CFRP material for the structure of the battery arrangement [***119***].

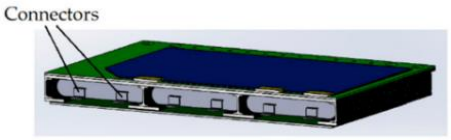

(Open access Creative Common CC BY license)

Fig V-2 AraMiS CubeSat CAD model for the battery's arrangement [***119***]

The Modular Multifunctional Composite Structure for AraMiS CubeSat has been used a CFRP structural/battery array configuration in order to integrate the electrical power system, including commercial Lithium-Polymer batteries, with the spacecraft bus primary structure [***119***].

However, the modular philosophy being a good approach should be able to be adopted to any design philosophy. The idea proposed with the *MWB* concept is to make the electrical power system *simpler*, *more efficient*, with a *minor change*, following the *modular philosophy* too.

The *Modular-Wall-Battery* (*MWB*) follows a new philosophy defined by the author as "*To Be Without Being*". To be more explicit, if we take three examples: one is the satellite structure with all fasteners, and the other is the solar cells or solar panel, finally the harness. All of them have a necessity to be onboard any satellite, we cannot have a satellite without a structure, and neither remove the solar cells, just in case if using another power generation as a nuclear source. Concerning the harness, it may have more signification on big satellites than the Nanosatellites. Finally, they are existing, having weight and occupying a specific space, however, without having a specific volume. The *MWB* is trying to keep using batteries without affecting the volume of the satellite. The approach has been used the *blind spots* usually not used onboard satellites, finally, the battery should occupy space but not a volume.

Batteries will be mounted on the internal panel of the satellite within the allowed area, as defined by the concept and presented in ***Fig V-3 (a)***, ***(b)*** and ***(d)***, however, it should be fixed using *Aluminum* tape including adhesive or glue qualified for space use such as the *RTV Silicone adhesive/sealants* (which could resist to vibration and large temperature range from -59°C to 204°C), using the same approach as for fixing the solar cells on the external panel, more details about the manufacturing process will be presented in ***section V.5***. With such a configuration, every one or two solar cells can be equivalent to one battery's pack as presented in

Fig V-3 (c). This equivalence is not related to the charging but only a physical representation, finally, all the available solar cells will charge all battery packs as for conventional architectures.

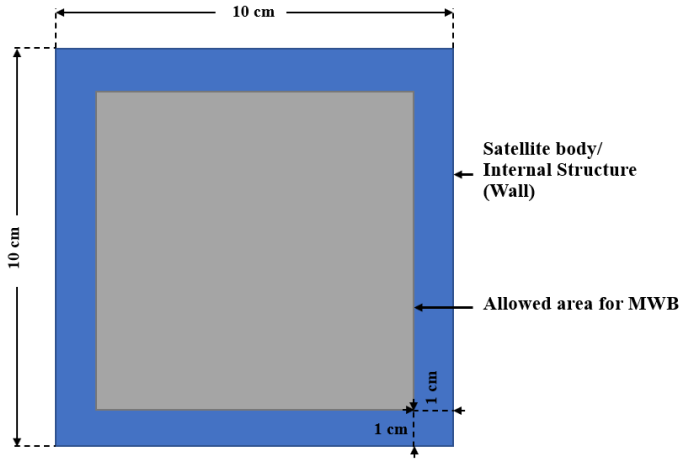

(a) Showing the allowed area based on the *MWB* requirement

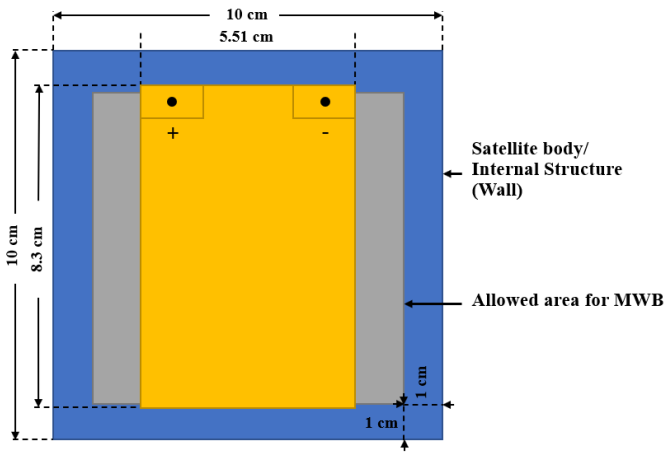

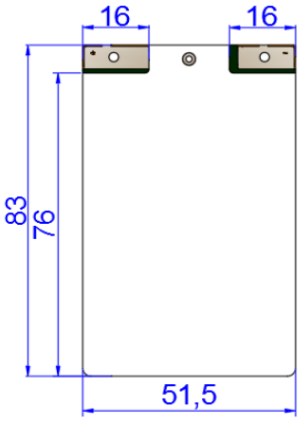

(One-cell size, ±0.5 mm)

(b) Using the proposed battery

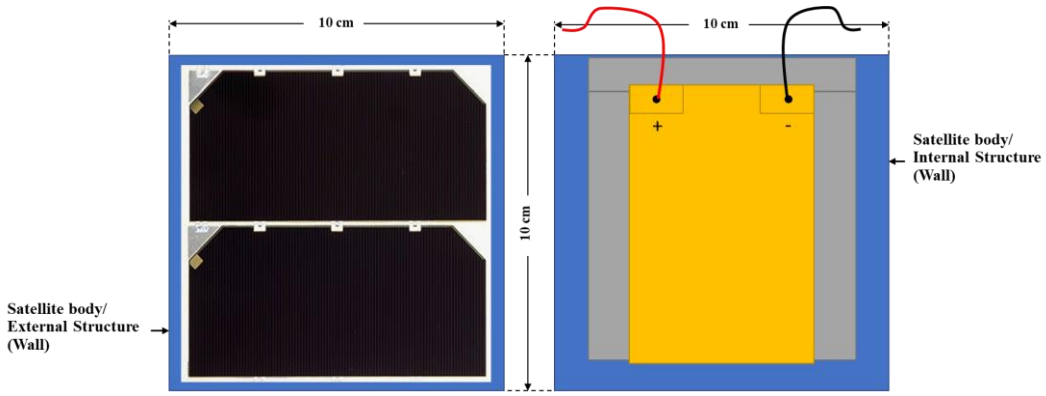

(c) *MWB* concept design

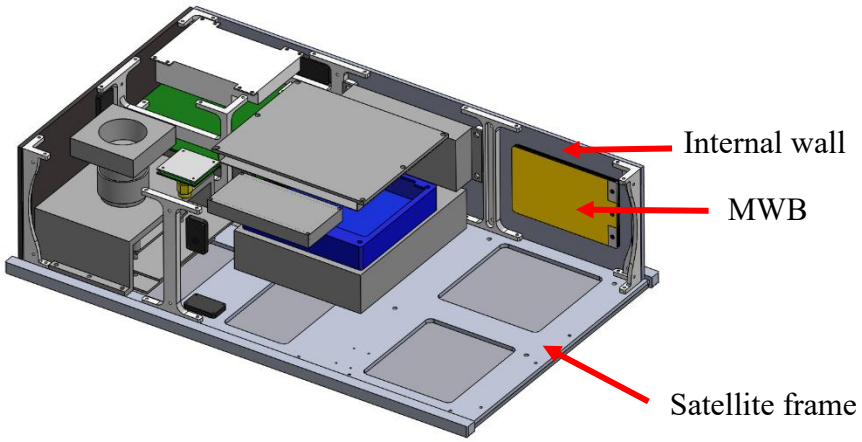

(d) 6U Nanosatellite's *MWB* representation sample

Fig V-3 *Modular-Wall-Battery* approach conceptual representation

Fig V-4 presents a mock-up representation for the *Modular-Wall-Battery* concept using the proposed customized battery pack FLCB 810 mAh on a 2U Nanosatellite model (real scale) [***120***].

The two packs present a good integration with the 2U Nanosatellite structure, so far without affecting the volume dedicated for the electronics boards. As defined by the *MWB* philosophy, the battery pack is occupying a space but not a volume.

The two terminals of the battery pack (positive and negative) presented in ***Fig V-4 (a)***, have been included for simulation purposes only, may be removed as for the one-cell FLCB 90 mAh in order to make the design smaller.

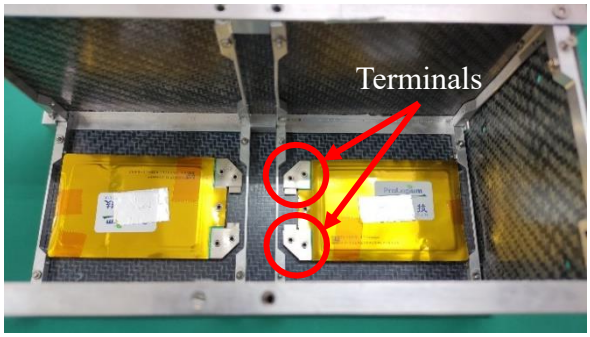

(a)

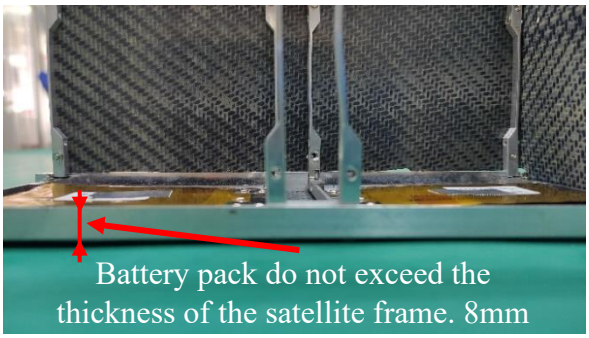

(b)

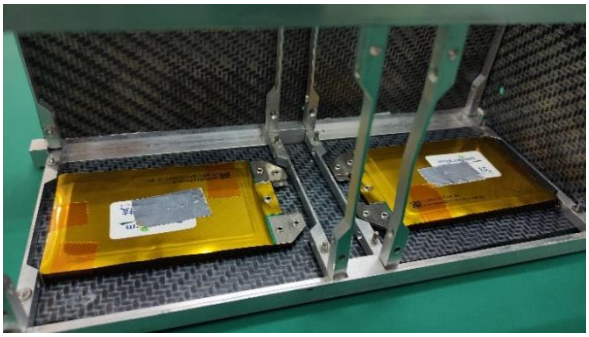

(c)

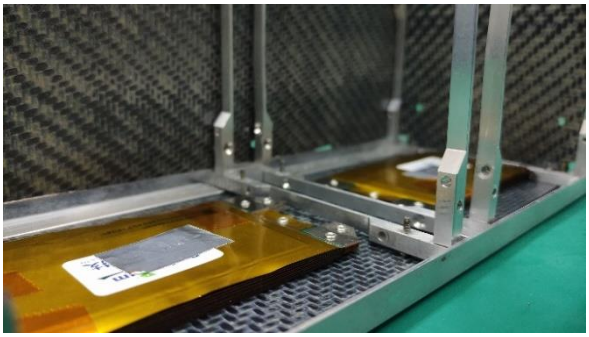

(d)

Fig V-4 *Modular-Wall-Battery* concept for 2U Nanosatellite mock-up

V.1.2. Requirements

In order to make the present concept applicable onboard Nanosatellites while using any kind of battery that can fulfil the need, a preliminary list of requirements has to be defined carefully following the standards of Nanosatellites, by including specific ones to the concept.

A list of requirements specific to the concept's philosophy related to development, safety and design has been presented in ***Table V-2***.

Table V-2 The *Modular-Wall-Battery* concept's requirements

Code	Requirements
MWB-01-R	The *MWB* concept shall use CubeSat standards for the mechanical interface and size.
MWB-02-R	The electrical power source and OBC communication interfaces shall use CubeSat standards.
MWB-03-R	The *MWB* design shall include deployment switches between each battery pack and the loads, and the solar panels and the battery. The switches shall prevent any of the loads from being powered.
MWB-04-R	The *MWB* boards shall include deployment switches that will disconnect the board ground from the system ground.
MWB-05-R	The *MWB* concept shall have a power control unit and management, in order to control the charge and discharge of the battery packs. *
MWB-06-R	The *MWB* concept shall have a software unit for the battery software management, in order to monitor the battery pack for a safer and optimized operation. *
MWB-07-R	The *MWB* board shall contain a communication interface to the OBC, which will be used to transfer telemetry and commands. *
MWB-08-R	The *MWB* board shall notify the OBC about critical subsystem events. *
MWB-09-R	The *MWB* design shall include a switch that shall permanently disconnect the solar panel output from the battery packs positive terminal and the loads, this one will be used at the end-of-life of the satellite.
MWB-10-R	The *MWB* design shall include a battery heater.
MWB-11-R	The *MWB* concept shall turn the heater according to the selected battery operating temperature range.
MWB-12-R	The *MWB* concept shall ensure all thresholds related to the over-voltage (4.2V) and under-voltage protection (2.8V). In that case, the battery pack may be disconnected from the load. **
MWB-13-R	The threshold related to the over-voltage protection shall be defined based on the selected battery.
MWB-14-R	The threshold related to the under-voltage protection shall be defined based on the selected battery.
MWB-15-R	The battery pack shall only be charged when battery voltage is between 2.8V and 4.2 V. **
MWB-16-R	The *MWB* concept shall provide the measurements of battery status: current, voltage, and temperature of each pack.
MWB-17-R	The *MWB* shall include a backup data bus, a hot redundancy shall be considered.
MWB-18-R	The *MWB* concept shall be compatible with any electrical power system of the satellite.
MWB-19-R	The selected battery shall be qualified to withstand the launch and the space environments. (*Space qualified or at least tested*)

MWB-20-R	The selected battery shall have enough capacity and energy in order to ensure continuous power to all the satellite during the eclipse.
MWB-21-R	The max thickness of the selected battery shall be no more than 4 mm. ***
MWB-22-R	The size of the selected battery shall be able to fit within the allowed represented area.
MWB-23-R	The selected battery shall have a wide operating temperature range, due that will be mounted on the internal panel.
MWB-24-R	The selected battery shall be available in the market.

Note:

* *It may be included with the electrical power system of the satellite.*

** *It may be defined based on the selected battery specifications.*

*** *Limit defined by the author following the proposed battery (SSLCB).*

V.1.3. Battery pack technology

The selected commercial batteries proposed for this concept is the Solid-State Lithium-Ceramic-Battery (Solid-state LCB) based *Oxide*, it has so far never been used in space; however, the battery technology has been evaluated under the *launch* and the *space environment* as presented in ***Chapter IV***, showing a promising result same battery has been planned to be evaluated in real space conditions at the Low-Earth-Orbit onboard a Nanosatellite as the first engineering mission demonstration [*132*].

The proposed battery has been selected for:

1. *Its availability, (Mass Production (MP)),*
2. *Wide operating temperature range: -20°C to +60°C, comparing to the conventional Lithium-Ion battery.*
3. *The battery presents a good result at the launch and space environment evaluation test (**Chapter IV**).*
4. *The customized battery pack presents flexibility due to its modularity in terms of total capacity and power per one pack.*
5. *Never been tested or planned for use in space, a novelty in the research community.*
6. *Furthermore, with the Lithium Cobalt Dioxide, the battery is categorized as having high specific energy (capacity), good performance, life span, and specific power [**13**].*

The *Modular-Wall-Battery*'s pack may be made by one Solid-State Pouch-Lithium-Ceramic-Battery (Solid-state PLCB) already manufactured by the company as for the 1450 mAh and tested within the *launch* and *space environment* conditions, or

several Solid-State Flexible-Lithium-Ceramic-Battery (Solid-state FLCB) as the 90 mAh (*customize pack*), to be tested within the *MWB* simulation, the two kinds of batteries belong to the same battery technology.

Furthermore, the *MWB* aims to adopt any other kind of batteries that could fulfil the requirements (***Table V-2***) as the *Polymer* type or any Pouch (*Laminated*) design battery.

However, during the study, due to the flexibility that the FLCB battery could provide for the capacity, weight, and volume, for the battery pack, a customized FLCB battery pack has been defined which the specifications are summarized in ***Table V-3***. The concept of the FLCB pack is more flexible and able to be modulable (*Laminated*) and designed based on the power requirements of the user while connecting several FLCB cells in parallel.

Table V-3 Proposed *MWB* pack's specifications (*customize pack*)

Battery's technology	**Lithium-Ceramic battery**
Design	*Laminated*
Nominal Voltage (V)	3.75
Nominal Capacity (mAh)	810 (*9 cells 90 mAh connected in parallel*)
Energy (Wh)	3.0375
Operation voltage (V)	4.35~2.75
Size (mm)	3.87×51.5×83(76)
Weight (g)	27.9
Operating temperature (°C)	-20〜+60

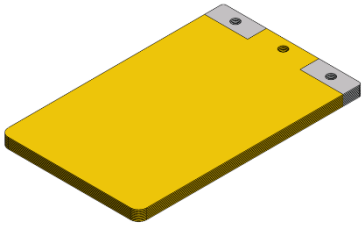

(a) CAD model

(b)

(c)

(d)

(e)

(f)

Fig V-5 Lithium-Ceramic battery customized pack 810 mAh.

V.2. Modular-Wall-Battery feasibility study

A 1U, 3U, and 6U CubeSats have respectively 1000, 3000, and 6000 cm^3, as represented in ***Table V-4***, which means that the volume is strictly limited. On the other hand, the weight seems to be more flexible, however, the *JAXA* requirement has limited on their standards that the satellite mass of 3U or less shall be not less than 0.13 Kg and not more than 1.33 Kg per 1U. In addition, for 6U size satellites, it should be 14 Kg or less [***120***], the same limits have been cited by *NASA* for 1U CubeSat [***121***].

Table V-4 Nanosatellite's size, volume, and weight

Satellite	**1U**	**3U**	**6U**
Size (cm)	10×10×10	10×10×30	10v20×30
Volume (cm^3)	1000	3000	6000
Wight (Kg)	1.33	1.33/1U	14

In order to study the impact of the *MWB* on Nanosatellites, **the first step** was to estimate the total equivalent capacity that the *MWB* could provide for different Nanosatellite's sizes. ***Table V-5*** summarizes all the possible configurations with their minimum and maximum equivalent capacity for 1U, 3U, and 6U Nanosatellites respectively.

The maximum capacity has been estimated using all the internal panels of the satellite, concerning the minimum capacity, the minimum number of batteries' pack used for the following Nanosatellite (from 1U, 3U to 6U) is the maximum number of the previous Nanosatellite, as following: starting with only two packs for 1U, then 6 packs for 3U, and 14 packs for 6U Nanosatellite. However, the most important amount of total equivalent capacity/power has been targeted with the maximum value which could be provided. Finally, the *MWB* with six-packs of batteries may be used for 1U with a total capacity of 4860 mAh, fourteen packs with 11340 mAh for 3U, and twenty-two packs with 17820 mAh for 6U.

Table V-5 *Modular-Wall-Battery* equivalent capacity

Capacity (mAh)	1U (6)	3U (14)	6U (22)
Minimum	1620	4860	11340
Maximum	4860	11340	17820

Into the second step, the Li-Ceramic pack has been compared to three other Lithium battery technology: Li-Ion (*LG LGABC21865*), LiFePO4 (*APR 18650*), and the Li-Polymer (*Varta LPP 503759 8HH*) presented in ***Table V-6***.

Table V-6 Batteries specification

Specifications	LG LGABC21865 Li-Ion	APR 18650 LiFePO4	Varta LPP 503759 8HH Li-Polymer
Capacity (Ah)	2.8	1.1	1.4
Nominal voltage (V)	3.72	3.3	3.7
Max. voltage (V)	N/D	2	4.275
Min. voltage (V)	N/D	1.6	2.3
Energy (Wh)	10.416	3.63	5.18
Temperature Range (°C)	0 to +45	-30 to +60	-20 to +60
Length (mm)	18.29×18.29×65.05	18.2×18.2×64.95	59
Width (mm)			37
Thickness (mm)			5.1
Volume (L)	0.022	0.022	0.011
Weight (g)	50	39	24.6

Their comparison result has been presented in ***Fig V-6***. Concerning the volume and weight, the difference in volume may not be clear in the figure, comparing to the weight, however, the two Solid-State batteries showed a smaller volume and lighter weight.

Almost all batteries may be operated at a high temperature, while for the Li-Ion is about +45°C, with the +60°C, operating some batteries at this temperature may cause fire, even risk of explosion as presented within ***Chapter I***. Additionally, the temperature in orbit may changes faster, from lower to higher or inverse, due to the gradient of temperature which will be discussed in ***section V.4***, this change may affect the performances of the battery especially the non-solid-state one.

For the low-temperature limit, while only 0°C for the Li-Ion battery, the lowest one that could be recorded is about -20°C for the Solid-State batteries, and -30°C for the LiFePO4 according to the datasheet. Additionally, the selected Solid-Stat Lithium-Ceramic battery could operate at -20°C including vacuum conditions, so far, reaching the Low-Earth-Orbit conditions (***Chapter IV***).

Additionally to the discussion in ***Chapter III***, ***section III.4.2***, and even with those low limits of temperature, each battery should be evaluated before being used in space, since the condition in the ground may be different than the one in orbit around the Earth, or other planets, batteries may be unable to operate at their max limits or even not operate at all, with the possibility to have irreversible damage on the battery.

Finally, almost all batteries have the same capacity as well as energy, the Li-Ion battery showed the highest value, while for the Li-Ceramic showed the lowest value due to the selected pack of 0.81 Ah. However, with the advantage of the flexibility in terms of modularity of the pack in terms of the number of cells, which may have a customized capacity by adding more cells in parallel, finally, the capacity may be increased. The defined pack has been tailor-made for evaluation purpose, finally, in order to fulfil the *MWB* concept requirements (***Table V-2***), especially for the thickness limits.

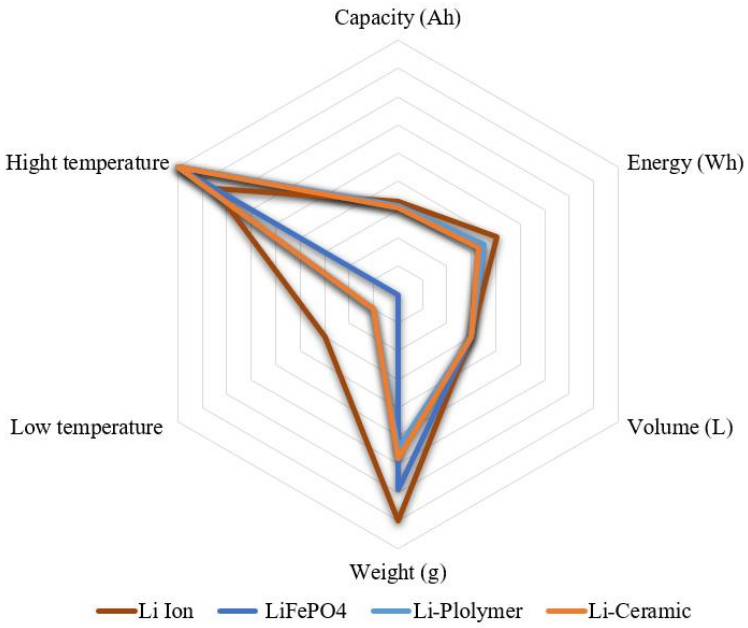

Fig V-6 Batteries comparison

Finally, the last step was to compare the *MWB* and the Li-Ion application on the different Nanosatellite sizes. The FLCB's pack has been compared to a Lithium-Ion battery with good flight heritage, the *Panasonic NCR18650B*, which has been used onboard the Ten-Koh satellite for Low-Earth-Orbit mission as main battery [***38***], moreover, the same battery has been listed by *NASA* in ***Fig II-2***. ***Table V-7*** presents a comparison between the specifications of the two different batteries.

Table V-7 Li-Ion and SSLCB batteries' specifications

Specifications	**Battery 1**	**Battery 2**
Battery technology	Li-Ion	Li-Ceramic
Design	Cylindrical	Laminated
Capacity (Ah)	3.2	0.81
Nominal voltage (V)	3.6	3.75
Voltage range (V)	2.5 to 4.2	2.7 to 4.35
Energy (Wh)	11.52	3.0375
Dimensions (mm)	18,5×18,5×65,3	3.87×51.5×76
Weight (g)	48	27.9
Temperature Range (°C)	0 to +45	-20 to +60

For the comparison, the initial input was the equivalent capacity which has been defined based on the total number of capacities that could provide the FLCB 810 mAh packs to the 1U, 3U, and 6U Nanosatellites respectively.

Table V-8 summarizes the steps that have been followed for sizing the satellite battery using the Li-Ion in order to define the equivalent capacities. Then, the equivalent capacities have been defined as the maximum capacities that the Li-Ion may provide because of the lower value of the minimum ones that cannot be compared to the FLCB 810 *MWB* packs.

Table V-8 Li-Ion satellite battery sizing for 1U, 2U, and 6U Nanosatellites

		Max	**Min**	**Max using MWB**
1U	**Number of batteries**	2	1	6
	Equivalent weight (g)	96	48	167
	Equivalent volume (cm3)	45	22	91
	Total capacity (Ah)	6	3.2	4.86 (***5***)
3U	**Number of batteries**	4	3	14
	Equivalent weight (g)	170	144	391
	Equivalent volume (cm3)	89	67	212
	Total capacity (Ah)	13	9.6	11.34 (***11***)
6U	**Number of batteries**	6	5	22
	Equivalent weight (g)	288	240	614
	Equivalent volume (cm3)	134	112	333
	Total capacity (Ah)	19	16	17.82 (***18***)

Finally, the total capacities using the *MWB* FLCB packs have been rounded to an integer for the presentation in ***Fig V-7***.

The final result could show that the challenge of the volume seems to be not solved with the increase in the number of FLCB's pack, it has clearly seen that the cylindrical Li-ion could show a good result, more efficient with its big capacity and

energy per one cell, which has affected the number of required cells, and finally, the total equivalent weigh. Finally, the total capacity remains almost the same for both batteries as has been defined as the input.

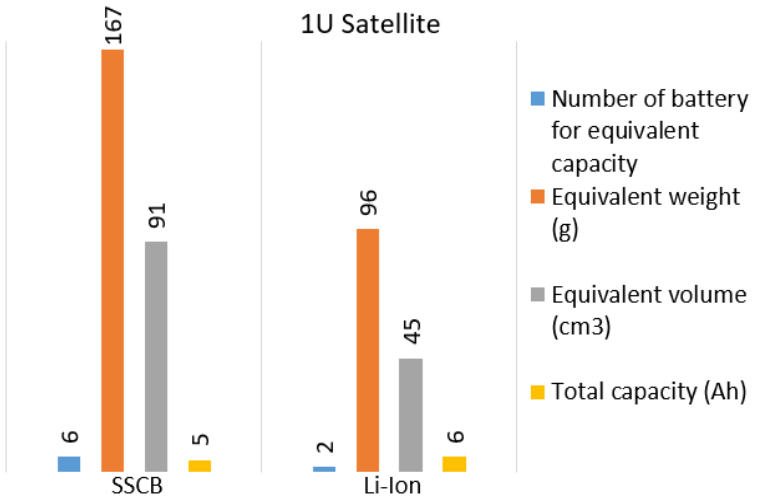

(a) 1U satellite

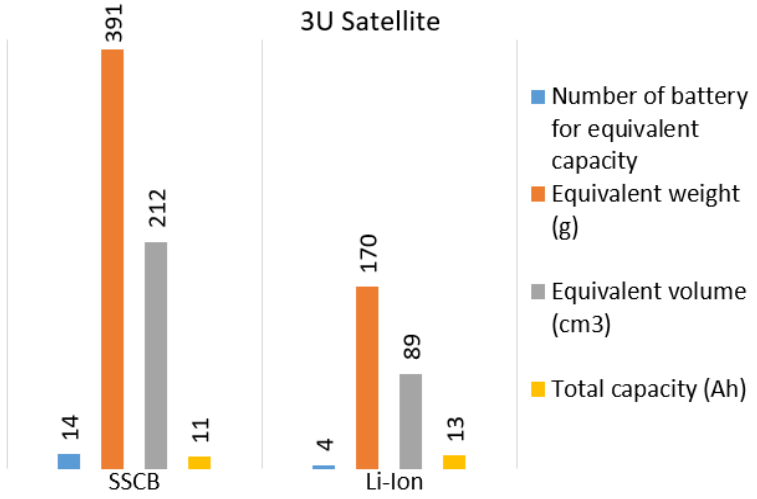

(b) 3U satellite

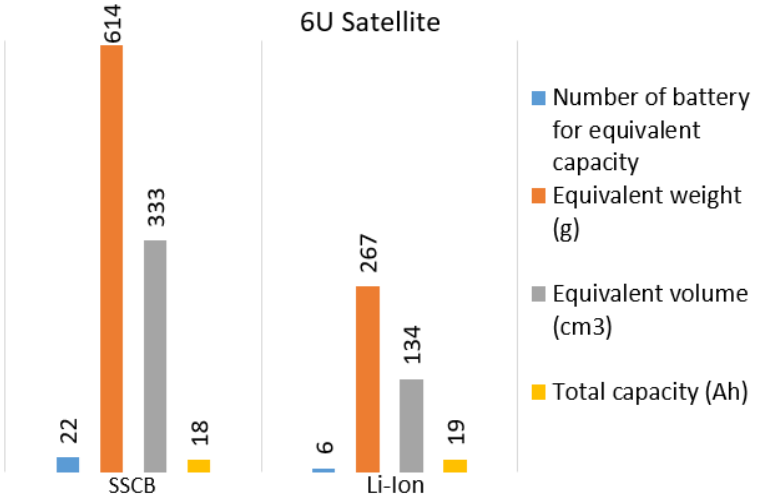

(c) 6U satellite

Fig V-7 Li-Ion vs SSLCB application effect on different Nanosatellite size

However, within the *Modular-Wall-Battery* approach conceptual graphic representation for the different Nanosatellite size: 1U, 3U, and 6U in ***Fig V-8***, the judgment should be reconsidered, in terms of the point of view that the *MWB* could save more volume compared to the Li-Ion.

Almost 99% of the volume has been free for other electronics boards, adding more payloads may be possible with the space availability. The mechanical specification (length, high, and thickness) for the Nanosatellites, including all the mechanical parts used for the design in ***Fig V-8*** have followed the CubeSat standards and have been summarized in ***Table V-9***. Initially, five electronics boards have been included as an example, however, they may have several possible configurations according to each CubeSat layout.

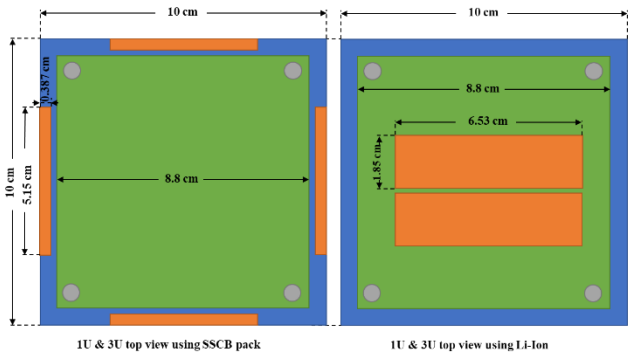

(a) 1U and 3U up view *MWB* vs Li-Ion configuration

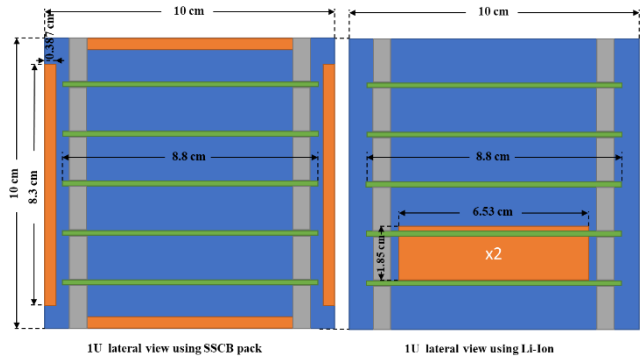

(b) 1U lateral view *MWB* vs Li-Ion configuration

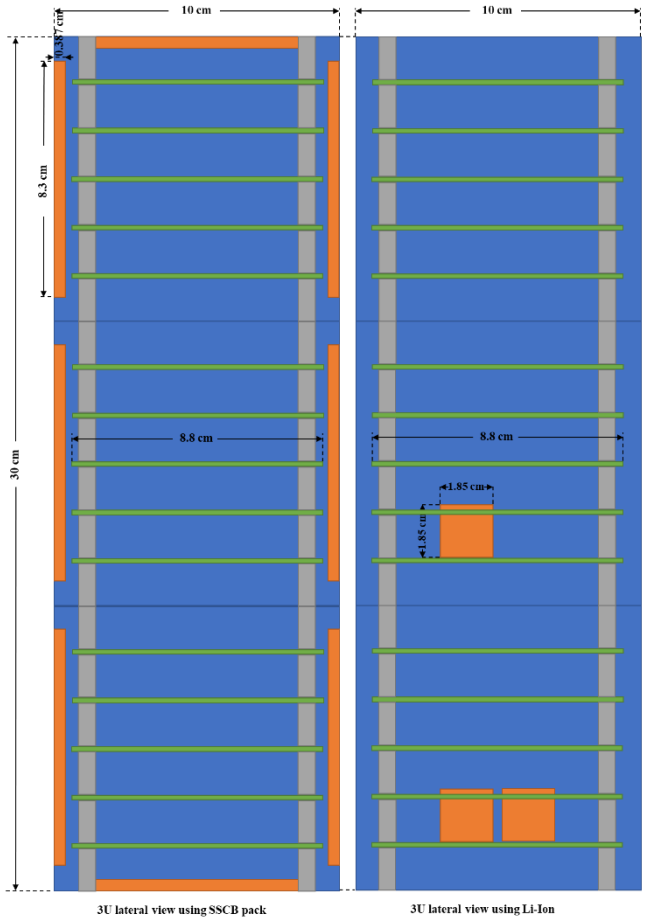

(c) 3U lateral view *MWB* vs Li-Ion configuration

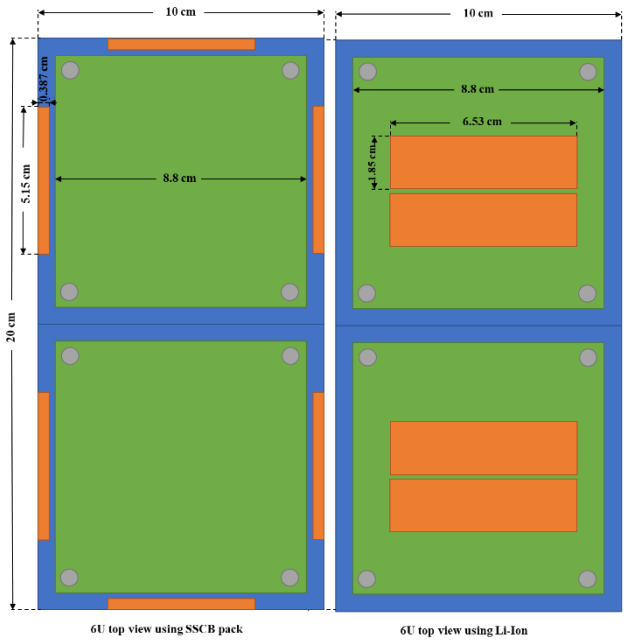

(d) 6U up view *MWB* vs Li-Ion configuration

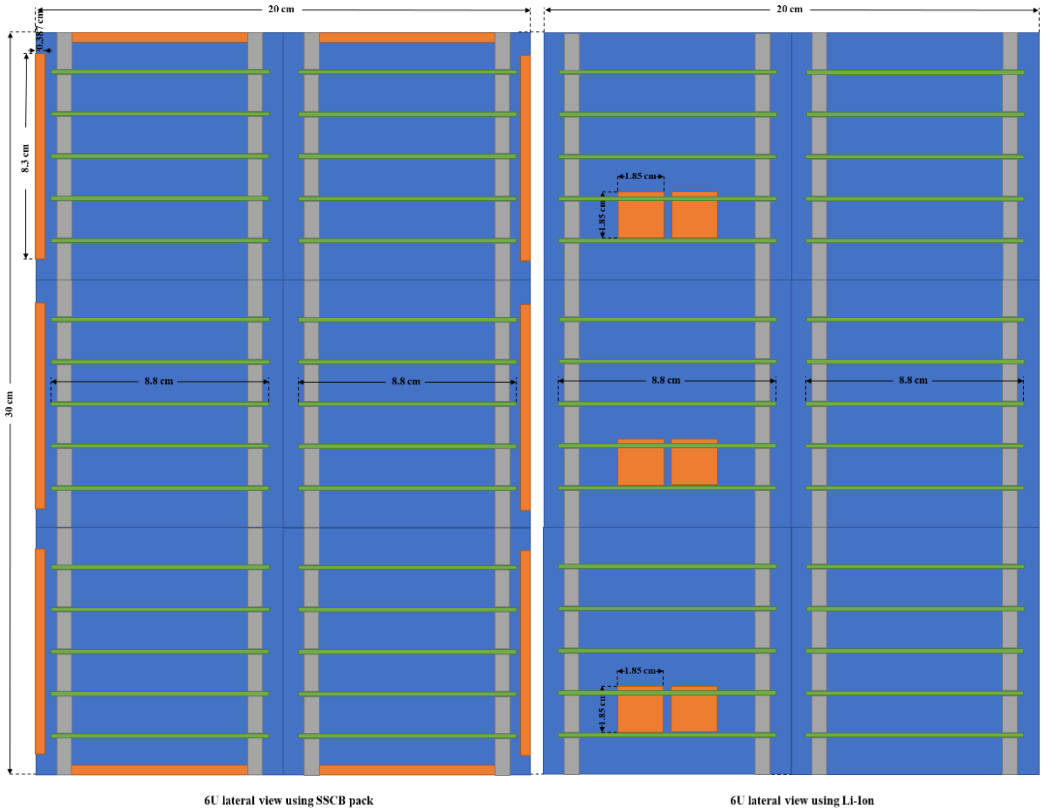

(e) 6U lateral view *MWB* vs Li-Ion configuration

Fig V-8 *Modular-Wall-Battery* approach graphical conceptual Representation for different Nanosatellite sizes: 1U, 3U, and 6U

Table V-9 Mechanical specification for CubeSat standards used in ***Fig V-8***

Item	Specification (mm)
1U CubeSat	100×100
Electronics board	88×88×1.6
Spacer between electronics board	15×6

Fig V-9 presents an estimation of the available area on the internal wall of the 6U Nanosatellite sample with the integration of the *Modular-Wall-Battery*. Finally, from seven to eight packs may be used with a capacity from 5670 to 6480 mAh. The estimation of the number of available *MWB* packs has been done based on the Nanosatellite structure and layout design, in order to not affect the initial design and layout, however, if the satellite requires more power, the structure design and layout should be considered for an update and then more packs may be included as defined in ***Table V-5*** with the maximum number of *MWB* packs of twenty-two packs, finally, with these number of packs, redundancy may be included too.

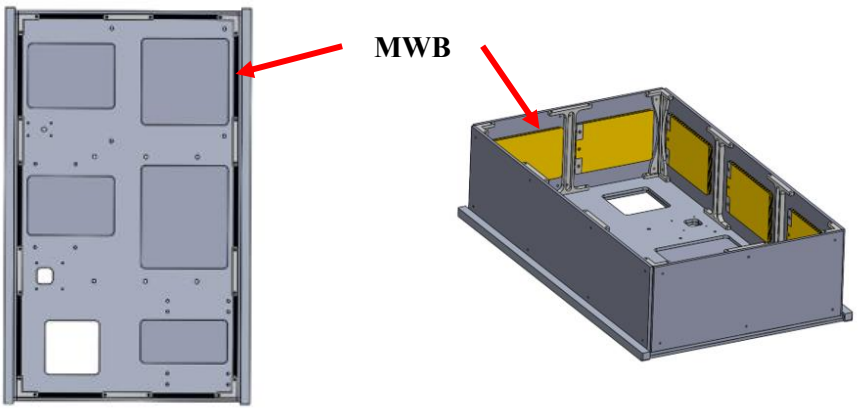

(a) *MWB* location onboard 6U Nanosatellite from different side views

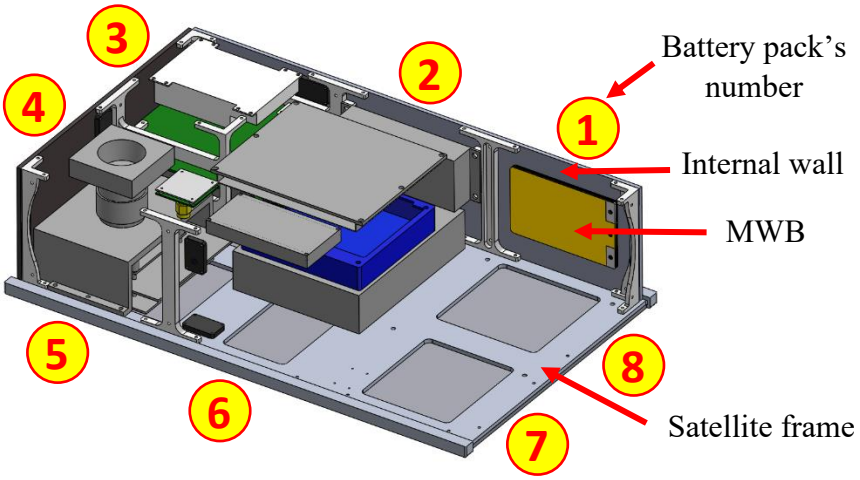

(b) Estimated number of *MWB* pack (Real case)

Fig V-9 6U *MWB* pack integration (Real case)

Initially, the same satellite has been planned to use two Li-Ion batteries, the *Panasonic NCR18650B* 3200 mAh, with a total capacity of 6400 mAh including one *Aluminium* box (**Fig *V-10***).

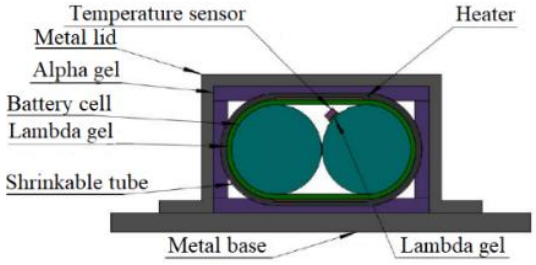

Fig V-10 6U Nanosatellite battery box (Preliminary design)

The estimation for the total weight in ***Table V-10*** shows a decrease in terms of using the *MWB* packs instead of the Li-Ion battery. Finally, the *Modular-Wall-Battery* could provide the same capacity while saving more volume as well as if a different approach has to be used than the *box concept arrangement* or the *mechanical structural concept arrangement*.

Table V-10 6U *MWB* pack's weight estimation (Real case)

	Li-Ion	**FLCB pack**
Number of batteries	2	8
Weight for one battery (g)	96	223.2
Weight for box (g)	156.5	0 (*No box*)
Total weight (g)	252.5	223.2
Total capacity (mAh)	6400	6480

The comparison between the *MWB* and the other battery arrangement which have been introduced within the introduction has led to conclude that the concept may look simpler, no need for a battery box or mechanism, or even a CFRP structural/battery array as for the proposed Modular Multifunctional Composite Structure used for the *Polymer* batteries. Saving more volume, the new available volume that has been occupied previously by batteries may be used for having more payloads.

Finally, the battery's pack may be customized with having several thicknesses according to the number of batteries required for a certain amount of needed power and capacity. The thickness's limit for the proposed CFRP structural/battery array is 4.5 mm, however, for the *MWB* it has been defined initially as only 3.87 mm (±0.2) by using the 0.81 Ah FLCB's customized pack.

V.3. Modular-Wall-Battery architecture and reliability

In order to have a complete design of the *Modular-Wall-Battery* concept that can be considered for integration into the Nanosatellite Electrical Power System, finally, the BUS system, some architectures may be proposed. Moreover, in order to ensure the reliability of the battery packs, isolation and redundancy shall be included. The requirements listed in ***Table V-2*** shall be considered too.

To avoid the balancing process for batteries that may make the design more complex and increase the risk of failures with decreasing the battery pack efficiency, *Modular-Wall-Batteries* have been designed to be connected in parallel, in that case, the balancing may be avoided.

Battery balancing is usually used for batteries connected in series, in order to equalize the voltages and state of charge among the battery cells when they are at a full charge, also to increase each cell's longevity.

In the case of one cell or many cells has shown degradation with a decrease in capacity or voltage, then the total capacity will be affected, voltage too. Also, it may lead to an over-charge or over-discharge of other batteries which are still presenting higher capacity, finally, the battery pack may be at risk of thermal runaway, fire or explosion.

In the case, if the battery pack requires a series connection, then the balancing process may be done in two different ways, depending on the complexity of the design and coast:

1- *Passive balancing: the most charged cell will dissipate energy as heat, through resistors.*
2- *Active balancing: the most charged cell will transfer energy to the low charged cells, it may be done using DC-DC converters.*

Since the *Modular-Wall-Battery* adopts a parallel connection instead of series, balancing is not required, while parallel cells will balance each other with mutually applied voltage.

V.3.1. Proposed architectures

Based on the CubeSat size, 10×10×10 cm, the *MWB* concept design will have one battery pack equivalent to two solar cells as presented in ***Fig V-3 (c)***.

For the present proposed design, the *MWB* concept, two different architectures (***Case 1*** and ***2***) may be possible using a parallel connection for battery packs,

additionally, in order to ensure reliability, battery isolation and the redundancy for packs shall be included.

a- <u>Case 1</u>:

Following the same CubeSat design used for the battery controller, this one will be integrated into the EPS. All battery packs will be controlled with the same battery controller.

Finally, no major modification is needed except for adding more harnesses according to the number of packs defined by the satellite designer, as well as following the four steps for integration and assembly (***section V.5***), this one is the major criteria of the *MWB* concept that can be integrated within any Nanosatellite with a minor change.

Fig V-11 is presenting an example of 1U CubeSat, this one having six faces, only three packs as the main battery have been used for demonstration, the other three packs may be considered redundant.

The electrical power system (EPS) shall include a battery controller for monitoring, charging and discharging all packs simultaneously. The *MWB* will have the battery pack, initially designed using a conventional cylindrical battery (***Fig V-11 (a)***), splitted into several packs equivalent to the initial battery sizing (***Fig V-11 (b)***).

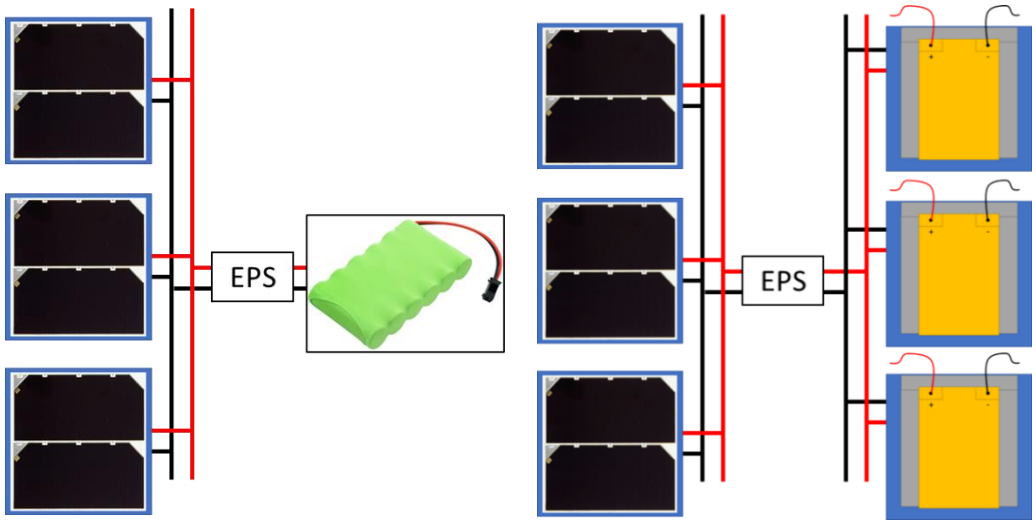

(a) CubeSat philosophy (b) *MWB* philosophy

Fig V-11 *MWB* architecture ***Case 1***

b- Case 2: (*Advanced*)

Following a different design philosophy, each battery pack may be controlled with its controller, this one may be located in the EPS or integrated into the *MWB*.

a. In the case, if the battery controller will be integrated with the EPS, still, the EPS will be in charge of the monitoring, charging and discharging of battery packs, the design will be quite similar to ***Case 1***, instead of having one battery controller, then several battery controllers should be designated for one battery pack or more, the final design may vary from satellite to other according to the satellite designer philosophy. ***Case 2 (a)*** may be considered as a step to go forward ***Case 2 (b)***.

b. In the case, if the battery controller will be integrated into the *MWB*, ***Fig V-12 (b)***, the EPS may be in charge only of monitoring and discharging battery packs to be used later for the BUS system. The charging will be accomplished by the *MWB* boards, in this situation the architecture is considered as an *advanced* one comparing to the two previous, it will require an appropriate IC charger and more space on the wall in order to support the circuit and all components that will be in charge of charging. However, this configuration may not be suitable for all 1U size but a bigger size of Nanosatellite. The charging board may be located near the battery pack that will be controlled, mounted on the internal wall as well. Moreover, the controller may control more than one pack in order to save space and weight.

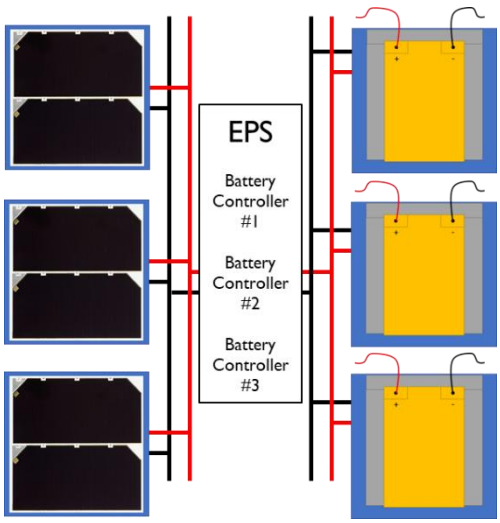

(a)

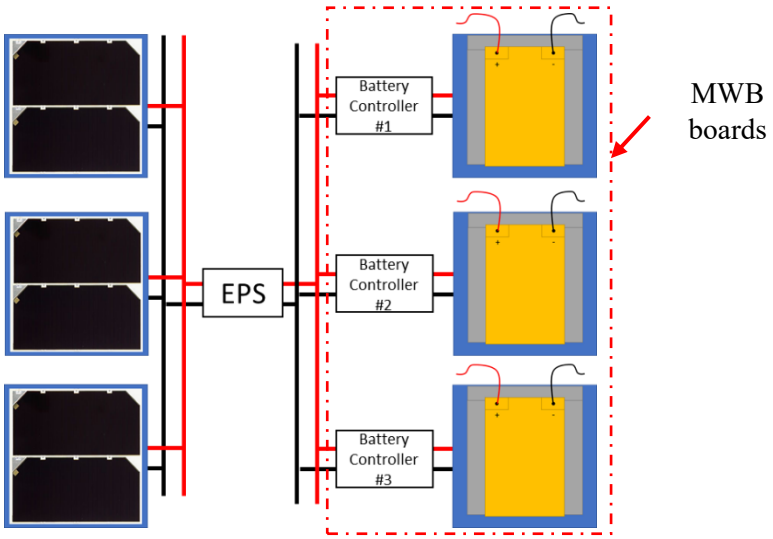

(b) (*Advanced*)

Fig V-12 *MWB* architecture ***Case 2***

c- Architecture's comparison

Table *V-11* presents a comparison between the two previous architectures and the conventional one used in almost all CubeSats as well as Nanosatellites. The comparison has been listed into five axes in terms of simplicity or complexity, since the conventional architecture has been used in several Nanosatellites, it may be considered to have positive effects on the Nanosatellites architecture as well as having been adopted in several designs, the proposed *Modular-Wall-Battery* (*MWB*) concept aims to improve some of those axes, as well as providing solutions for the Nanosatellites challenges.

In terms of simplicity of the design, the *MWB* has to be simpler while adopting the *Pouch Battery Concept Arrangement* with no box or any mechanism, compared to the conventional one which may require mechanisms to support the cylindrical battery or even boxes. However, ***Case 2*** (***b***) may be complex than the previous cases while more boards are required to integrate the battery controller within the *MWB* board, finally more appropriate to bigger Nanosatellites for 2U size and more.

The *MWB* architectures are more complex for the system, especially with the inclusion of switches that are required for safety and good operation, or even the increase of using harnesses due to the increase of modular battery packs. The complexity may vary for each case, ***Case 1*** is simpler than ***Case 2***, while the only difference of ***Case 1*** with the conventional architecture is the modularity of the battery, finally, not the same result for ***Case 2*** (***a***) while each battery pack has a battery controller, or ***Case 2*** (***b***) while additional boards are required for the battery controller within the *MWB* board.

All architectures may have the same level of simplicity in terms of development and integration except for ***Case 2*** (***b***) in terms of the development due to the *MWB* board.

Finally, in terms of reliability for the system, the *MWB* provides an easy way to adopt redundancy for the battery controller as well as the battery pack, without taking into account the increase in weight or making the design complex, additionally to be adaptative to any Nanosatellites without affecting the design.

Table V-11 *MWB* vs convention architecture

	Conventional	**MWB architecture**		
		Case 1	**Case 2 (A)**	**Case 2 (B)**
Simplicity (Design)	O / X	O	O	O / X
Complexity (System)	O	X	XX	XXX
Development	O	O	O	X
Integration	OO	OO	OO	O
Reliability (System)	O	OO	OO	OO

O: Yes, X: No

V.3.2. Isolation and redundancy

Following the modular philosophy for the battery pack, the reliability may be improved at the *system level*. Moreover, with the laminated FLCB packs, using several cells in parallel within each pack may increase the reliability of the packs too at the *component/part level*, as well as for the battery controller for the *MWB advanced* architecture ***Case 2***.

Since one *Modular-Wall-Battery* pack is constituted by several cells in parallel, in a different way the battery pack is *laminated* (*battery pack design in **Fig V-5**, customized pack, 9 cells connected in parallel used as a sample*), the battery satellite's power and capacity are no more condensed in a few numbers of cells but split into several packs (***Fig V-11***), finally, the reliability may be seen increased.

> *"For example, if two components are arranged in parallel, each with reliability R1 = R2 = 0.9, that is, F1 = F2 = 0.1, the resultant probability of failure is F = 0.1 × 0.1 = 0.01. The resultant reliability is R = 1 – 0.01 = 0.99. The probability of failure has thus dropped 10 times. This feature is sometimes used for reliability increasing by using redundant parts [122]."*

In order to improve more the reliability of the *MWB* as a system, redundancy for battery packs should be included based on the total available packs and the required power for the satellite. ***Table V-12*** presents examples of the number of redundant packs that have been defined based on the total *MWB* pack that may be used for several Nanosatellite sizes (1U, 3U and 6U).

The total number of battery packs has been divided into two, then the remained capacity for the BUS system will be half of the maximum capacity that the *MWB* could provide using all the internal walls of the Nanosatellite, so far, this amount of capacity may still be enough for the BUS system's required power.

Table V-12 *MWB* proposed redundancy configuration

Nanosatellite size	**1U (6)**	**3U (14)**	**6U (22)**
Total number of packs	6	14	22
Total capacity (mAh)	4860	11340	17820
Number of redundant packs	**3**	**7**	**11**
Capacity (*Total capacity/2*) (mAh)	**2430**	**5670**	**8910**

Additionally, to the redundancy, each pack may include an *Isolation Switch*, additionally to the *Remove Before Flight* and the *Kill Switch* for the end of the mission which shall be included with the EPS, in this case, if one pack is out of service for some reasons, then this one may be *isolated* (*disconnected*) from the EPS and the BUS system, in order to avoid overheating the pack in case a short-circuit acquires. This action may be done according to the data received from each battery pack that should be monitored separately. Finally, the command shall be sent from the ground station.

Fig V-13 is presenting an example of one battery pack, following ***Case 1*** for the battery pack architecture, that has been deteriorated while losing performances, then this one has been disconnected or isolated from the BUS system which has been presented a risk for the satellite. The same approach could be adopted for ***Case 2*****,** as well as any other possible architecture.

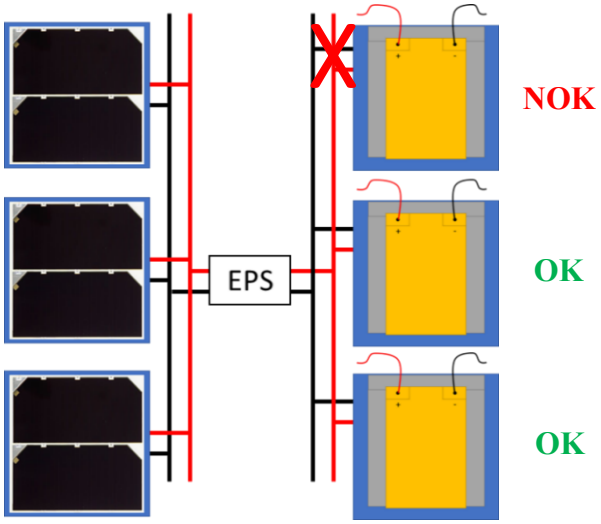

Fig V-13 *MWB* architecture, ***Case 1***, failure case with isolation

V.4. Temperature issue and alternative proposed battery

V.4.1. Temperature issue

Since the temperature in the Low-Earth-Orbit can vary from about -120°C to +120°C [***123***,***124***], so far, none of the actual battery technology could operate, or even operate with low performances especially during the charging mode, unless proven otherwise, waiting for the promising battery.

However, researchers are pushed to developing such as the technology to be able to withstand a wide temperature ranges, with the available batteries, the lowest temperature that could be registered is -40°C during testing with the Lithium-Ion [***45***], and the widest temperature range that could be reached for prototyping is from -40°C to +80°C or +100°C with the All-Solid-State-Battery technology [***65***].

M. Von Lukowicz et al. could present in their work the typical temperature in Low-Earth-Orbit which may vary from about +10°C to +50°C [***125***]. *Sieger L. et al.* presented the temperature record varying from +8°C to +30°C for electronics boards onboard VZLUSAT-1 CubeSat [***126***].

Based on the work done by *Kakimoto. Y. et al.* with the in-orbit temperature data of BIRDS-2 and SPATIUM-I, the temperature for batteries that could be reached at its lowest level were about +5°C for BIRDS-2, and +10°C for SPATIUM-I [***127***]. Moreover, according to the Ten-Koh satellite in-orbit temperature record presented in ***Table III-12***, it has presented around +9.09°C for the battery. Since the three satellites had following the *battery box concept arrangement* for batteries, while could be considered as a good concept for the battery arrangement, so far, these temperatures may not be considered as good references for the lowest temperature

of batteries at the Low-Earth-Orbit for the present concept, which the temperature may be affected by the *battery box arrangement*, as well as the *MWB* pack will be located very close to the satellite panels.

However, with the BIRDS-2 backplane in-orbit temperature data results, the temperature that could be reached at its lowest level was between -10°C and -20°C at the lowest beta angle, the backplane board is located very close to one of the panels [***127***]. Moreover, the minimum temperature for the external PCB for the Ten-Koh satellite, which was spinning in its orbit, was about -36.51°C, while the maximum was +12.05°C (***Table III-12***).

Additionally, the work done by *S. Corpino et al.* with the thermal design and analysis of a Nanosatellite in the Low-Earth-Orbit showed, so far, a good temperature range for the battery, especially for the selected one for the present study, comparing to the Lithium-Polymer battery, the same battery technology that has been used for the thermal analysis by *S. Corpino* [***128***]. The first simulation results could not satisfy the lowest temperature range for charging the Lithium-Polymer which was from -10°C to 0°C, instead of 0°C to 45°C, however, with the *Ceramic* type (*Sulfide* or *Oxide*) battery, especially the selected battery (*Ceramic Oxide* type) the temperature range could be satisfied within the limit of the simulation, as the battery could be operated within all the temperature range going from -20°C to +60°C, during the discharge as well as the charge [***13***].

In order to avoid the gradient of temperature between the outside and the inside of the Nanosatellite, and to prevent any change of the temperature, the application of the *Multi-Layer-Insulator* (*MLI*) may be adopted especially for the surface which is not covered by the Solar cells, additionally to the internal isolation proposed by the concept at the *Isolation Process* (*IP*) step (***Section V.5***). Moreover, with the thermal analysis and research ongoing with the amelioration and improvement of the optical and thermal properties of the surfaces, many alternative solutions may be found.

According to the 6U Nanosatellite under development, a preliminary estimation is expecting that the satellite will be exposed to a temperature range between -40°C to +60°C around the *International Space Station* orbit.

For such as a situation presented in ***Fig V-14***, the satellite energy balance could be used to estimate the average temperature of the Nanosatellite using ***Eq.V.1***, useful for the preliminary design in order to define the boundary of the operating temperature range of the satellite, as well as the battery. ***Eq.V.1*** is the simplified version of ***Eq.V.2*** for the energy balance equation [***129***].

$$\varepsilon_s \sigma A_s T_s^4 = \varepsilon_s \sigma A_s F_{s,e} T_e^4 + Q_{sun} + Q_{er} + Q_i \qquad \textbf{(Eq.V.1)}$$

$$Q_{sun} + Q_{er} + Q_i = Q_{ss} + Q_{se} \qquad \textbf{(Eq.V.2)}$$

Q_{sun} : ***Solar input to spacecraft***, $\sigma_s A \perp I_{sun}$

Q_{er} : ***Earth-reflected solar input***, $a\sigma_s F_{s,e} A_s I_{sun}$

Q_i : ***Internally generated power***

Q_{ss} : ***Net power radiation to Space***, $\sigma_s F_{s,s} A_s (T_s^4 - T_{space}^4)$

Q_{se} : ***Net power radiation to Earth***, $\sigma_s F_{s,e} A_s (T_s^4 - T_e^4)$

a : ***Earth albedo***, *Range from 0.07 to 0.84.*

α_s : ***Spacecraft surface absorptivity***.

ε_s : ***Spacecraft surface emissivity***.

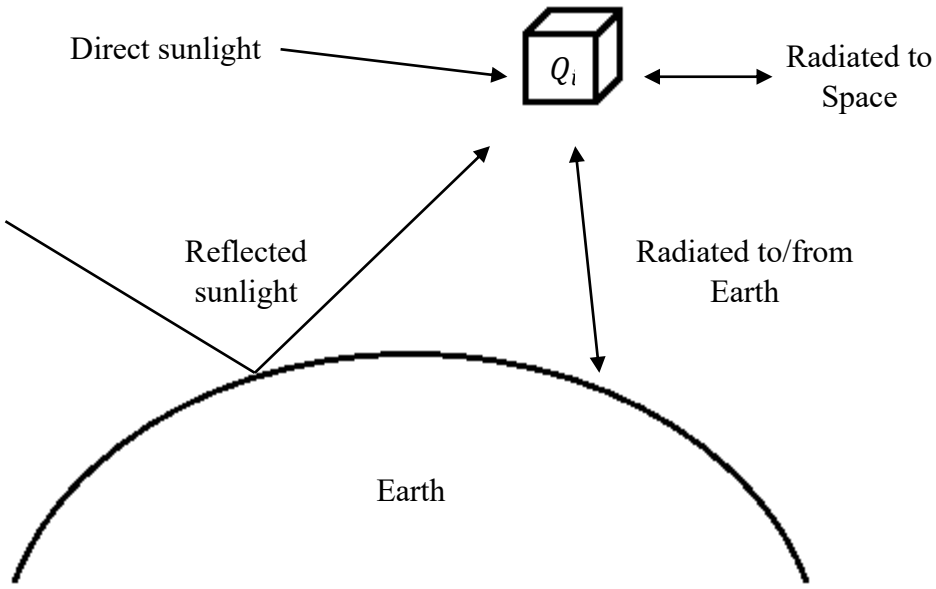

Fig V-14 Nanosatellite energy balance in orbit

Finally, based on the calculation and thermal analysis of the 6U Nanosatellite using the *Thermal Desktop* Software, the temperature range could be defined.

V.4.2. Alternative proposed battery

Basically, the *MWB* has been proposed using the same battery preselected during the ground evaluation test, the *Ceramic Oxide* type with its first evaluation to be used in space, while the customized pack could offer flexibility in terms of the capacity and power as well as thickness of packs due to the laminated pack using several Solid-State Flexible Lithium-Ceramic-Battery (Solid-State FLCB) (90 mAh × 9 = 810 mAh/Pack).

Since the *MWB* concept has been defined to use any pouch/*laminated* battery design, moreover, for the present study, any other *Laminated* battery could be adopted for the *MWB* concept. The Solid-State Pouch-Lithium-Ceramic-Battery (Solid-state PLCB) already manufactured by the company and evaluated within ***Chapter VI***, the 1450 mAh, may be considered as well.

Moreover, the *MWB* is aimed to be not limited to the *Ceramic* type only but any pouch/*laminated* battery, the Solid-State-Battery (*Polymer* and *Ceramic*), as well as the All-Solid-State-Battery. An alternative battery may be proposed, the *Ceramic Sulfide* type, a commercial battery made by *Hitachi Zosen*, nowadays under development, only prototypes may be available for testing [***65***].

Comparing the performances of the two packs in ***Table V-13*** that may be adopted for the *MWB* concept (**#1** proposed pack made by the proposed *Ceramic Oxide* type, **#2** alternative pack made by the alternative *Ceramic Sulfide* type), and based on the limit for the pack's thickness defined by the concept to *4 mm*, the total capacity has been calculated including the total weight according to the equivalent number of cells that should be connected in parallel. Concerning the size, the alternative battery's size could be within the limit defined by the allowed area for the *MWB* presented in ***Fig V-3***.

The alternative battery pack using Battery (**#2**) has using the specification provided by *JAXA*, fifteen 140 mAh cells may be connected in parallel for getting about 2.1Ah [***70***]. Results in ***Table V-13*** shows that the customized pack (**#1**) proposed in the presented study could show good results regarding the weight, about 30 g compared to 50 g for (**#2**), for a capacity of 810 mAh compared to 280 mAh, respectively. However, the proposed alternative battery (**#2**) has a higher operating temperature range, from -40°C to +80°C comparing to -20°C to +60°C for (**#1**).

Table V-13 *MWB* Concept (proposed vs alternative) batteries pack selection

Battery	Capacity /Cell (mAh)	Size/Cell (mm)	Number of cells/Pack	Weight/ Pack (g)	Capacity/ Pack (mAh)
#1	90	0.43×51.5×83	9	27.9	810
#2	140	2.7×52×65	2	50	280

As the alternative pack (**#2**) shows three times lower in capacity than the proposed one, finally, all the estimation of the total capacity done for different sizes of Nanosatellite (1U, 3U and 6U) within the feasibility study section will be decreased three times too.

This comparison is presenting the effect of the size on capacity, and finally the selection of the battery following the engineering approach proposed in ***Chapter III***. When Battery (**#2**) presents a high capacity per one cell comparing to Battery (**#1**), the pack using Battery (**#1**) presented higher capacity and lighter weight compared to using Battery (**#2**), which the size has been affected by the two other parameters; the capacity and weight. Finally, affecting the integration of the battery back into the Nanosatellite.

Since the temperature at the wall could be about -40°C at its lowest level, then the *Sulfide* Ceramic battery (**#2**) may be a better selection for the *MWB* concept as has been simulated from -40°C to +100°C with a remaining capacity of 90% [***65***].

However, the proposed alternative battery is still under development and need more time to be tested in space. Waiting for the result, it may be considered to be used with the *MWB* concept in the future with the *Ceramic Oxide* type.

Finally, the *MWB*'s pack may be made by any battery technology/type that can fulfil the requirements listed in ***Table V-2***, as well as enlarged to future battery technologies.

V.5. Modular-Wall-Battery assembly & integration process

The proposed design of the concept may be assembled and integrated on any Nanosatellite which fulfils the requirements (***Table V-2***), the procedure for the assembly and integration has been summarized within *four main steps*, however, in order to have a safe design of the *Modular-Wall-Battery*, the following materials will be needed:

- Thin-film isolator,
- RTV Silicone adhesive,
- Kapton tape,
- Aluminum tape.

The following *four steps* are summarizing for a wall-size 10×10 cm, 1U CubeSat size as an example. Then, the *Modular-Wall-Battery* may be ready for its full and final integration within any Nanosatellite.

Step 1: Defined as the ***Isolation Process (IP)***, the first important step in the process, the thin film isolator should be put on the allowed area defined for the battery in ***Fig V-3*** as in ***Fig V-15***. The isolator has two functions:

- *To isolate the battery from the wall in order to avoid any short-circuit between the positive and negative terminals and the main body of the satellite.*
- *To reduce the gradient in temperature between the outside and the inside environment.*

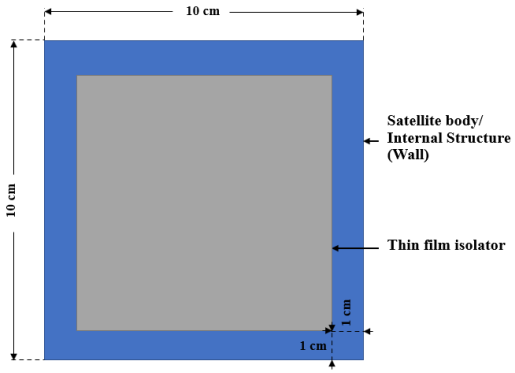

Fig V-15 Isolation Process (IP)

Step 2: The ***Surface's Processing (SP)***, before the assembly of the battery pack on the wall, the allowed area and the battery pack should be prepared with the *RTV Silicone* adhesive. Moreover, the two terminals should be extended for later connection with the power line. The two steps are presenting in ***Fig V-16***.

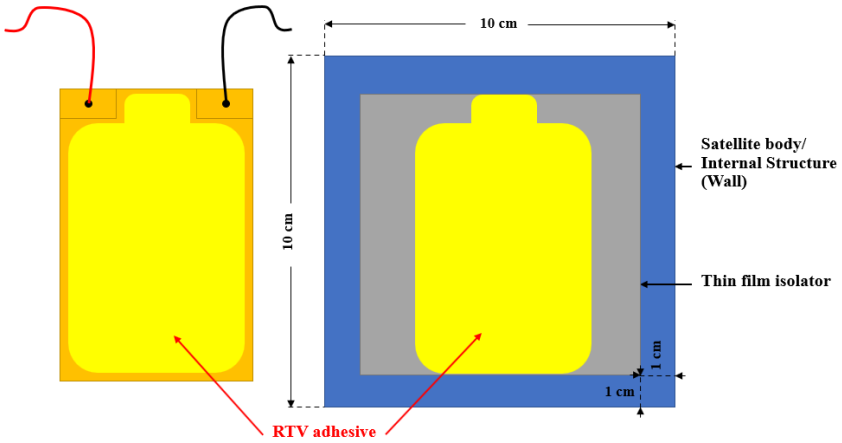

Fig V-16 Surface's Processing (SP)

Step 3: ***Battery Pack & Wall Assembly (BP&WA)***, the battery terminals should be already included an extension of wires for later connection with the power line and isolated with Kapton tape. Finally, the assembly may be done as in ***Fig V-17***.

Note: *An extension of the thin film isolator may be needed according to the size of the battery pack within the limits.* ***Fig V-17*** *presents an example of this extension based on the selected battery, the FLCB customized pack.*

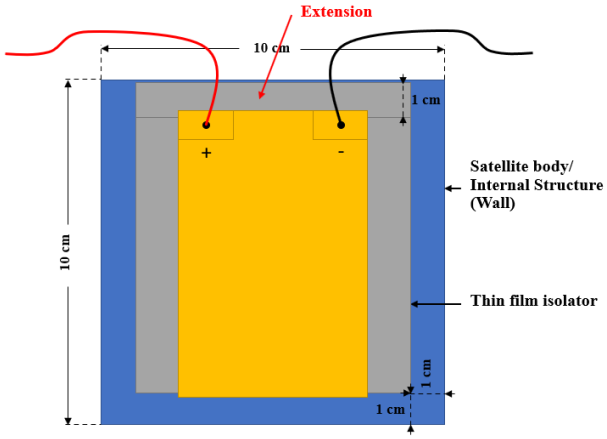

Fig V-17 Battery Pack & Wall Assembly (BP&WA)

Step 4: ***Assembly Packing (AP)***, all the assembly should be covered with the Kapton tape then the Aluminum tape, the same thin-film used for the isolation in

Step 1 may be included too, in order to ensure a good fixation and thermal conductivity as in ***Fig V-18***.

Note: *All battery pack may be covered with the Aluminum tape in case if the two battery pack terminals have been properly isolated.*

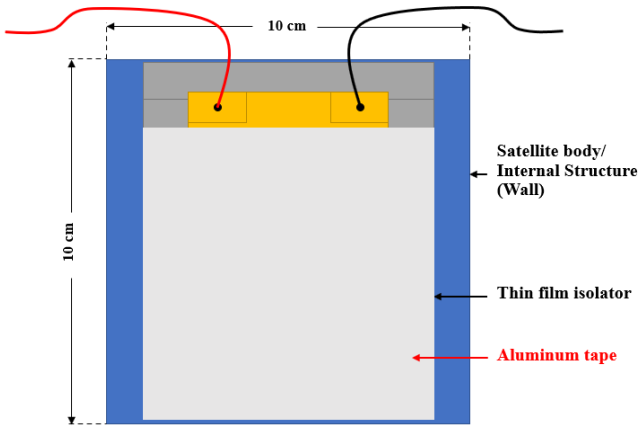

Fig V-18 Assembly Packing (AP)

V.6. Conclusion

The *Modular-Wall-Battery* (*MWB*) looks to be a good solution for the challenge that the Nanosatellites are facing, with the limited size and lack of power. The approach of combined the modular philosophy with the Solid-State-Ceramic battery pouch/*laminated* design shows an increase in capacity provided for the satellite system, the battery can be customized by the user for its modular cells. Finally, with the specific features that the *Ceramic* battery is characterized, including the ability to operate under very low temperature reaching -20°C for the *Oxide*, even more, -40°C for the *Sulfide* (prototype), due to its Solid *Ceramic* electrolyte that solved the issue of the low temperature, additionally to be good for the high temperature.

Moreover, with the *laminated* FLCB packs, using several cells in parallel within each pack may increase the reliability of the packs at the component/part level, additionally to the redundancy of the packs too, at the *MWB* system level.

It may be a good solution for the attitude control challenge and the mechanical design with the center of gravity, the symmetric design gives a good weight's distribution on the panel. Batterie packs may be not affecting anymore the attitude stability of the satellite; however, they should be still included within the calculation of the center of gravity and the inertial matrix.

The *MWB* is not limited to only the *Ceramic* battery technology but it is generic to any other battery that can fulfil the requirements. It can be generalized and adopted for any pouch/*laminated* cell battery design as well as the Solid-State-Battery Polymer or Ceramic (*Oxide* or *Sulfide*).

Table V-14 *Modular-Wall-Battery* advantages & inconvenient

Advantage	Inconvenient
Increase the power and capacity Save 99% of the volume Simple design for satellite structure Generic design for all satellites Wide temperature range using the SSLCB Improving the center of gravity Safe	Increase in the number of batteries Increase in weight Require a specific battery technology and design (*pouch/laminated*) It may increase the cost Increase in using harness System complex

Concerning the increase in weight that may be the big challenge with the application of the *MWB* on Nanosatellites, ***Fig V-19*** represents the estimated total weight for different CubeSats sizes related to their maximum limits required by *JAXA* and *NASA*, including a full design with the conventional Lithium-Ion batteries, it is showing the available margin that can be used to reach the maximum limit which is 12.67Kg for 1U, 10.01Kg for 3U, and 6,02Kg 6U. The *MWB* has to be flexible in terms of limited weight for Nanosatellites.

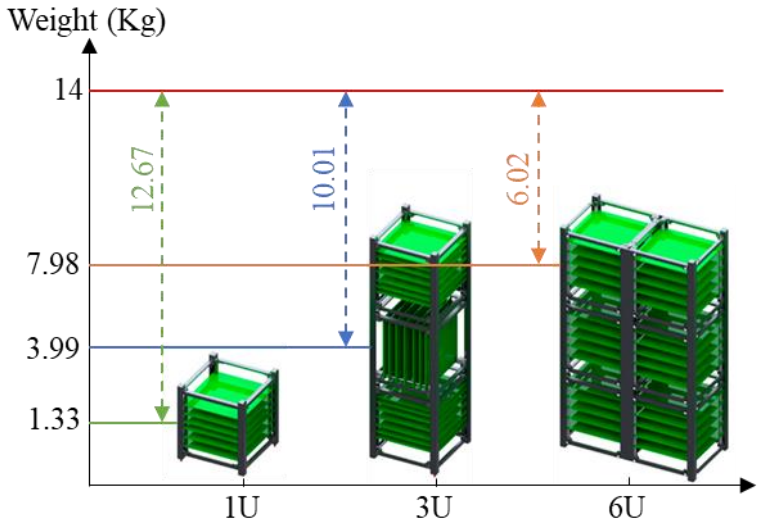

Fig V-19 Nanosatellite weight standards (*JAXA* & *NASA*)

Chapter VI

Nanosatellites Modular-Wall-Battery (MWB) Concept II:

Simulation, Result & Discussions

VI. Nanosatellites Modular-Wall-Battery Concept II: Simulation, Result & Discussions

The following chapter is summarizing the results and discussion of the *Modular-Wall-Battery* simulation which has been used the proposed *Ceramic Oxide* type Solid-State-Lithium-Battery technology that has been evaluated in ***Chapter IV***.

Results are presented in two sections, simulation of the *launch environment* using one-cell FLCB instead of a pack, and simulation of the *space environment* using a complete pack with the 9 cells FLCB.

VI.1. MWB Concept's simulation

VI.1.1. Mechanical structure analysis

The proposed battery pack for the *MWB* has been simulated with software, once itself including battery pack (9 cells) only, then one cell only in order to compare the two natural frequencies, finally, using one pack mounted into a 6U Nanosatellite, in order to calculate the natural frequencies of the proposed battery pack.

The analysis has been done as part of the future integration of the *MWB* concept as a mission demonstration onboard a Nanosatellite, this one using only one pack. The results will be used for further analysis after the vibration test could be done. ***Table VI-1*** summarizes all the natural frequencies got from the simulation in ***Fig V-1***.

Table VI-1 Result of natural frequencies analysis

Item	Frequency (Hz)
1 cell	1.645×10^{6}
9 cells	91454
Pattern #1	622
Pattern #2	657
Pattern #3	608
Pattern #4	594
Pattern #5	594
Pattern #6	606
Pattern #7	649
Pattern #8	605
Pattern #9	595

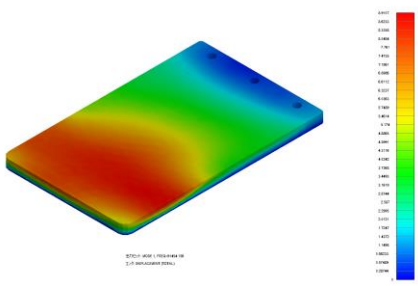

(a) *MWB* pack (9 cells)

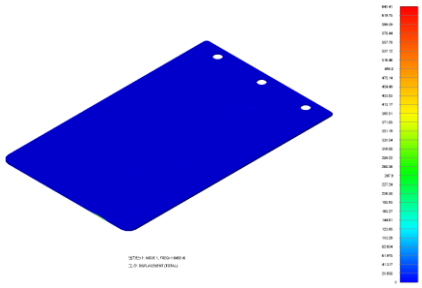

(b) One-cell

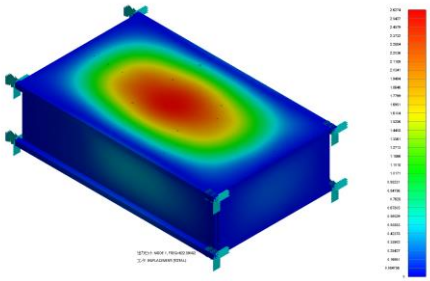

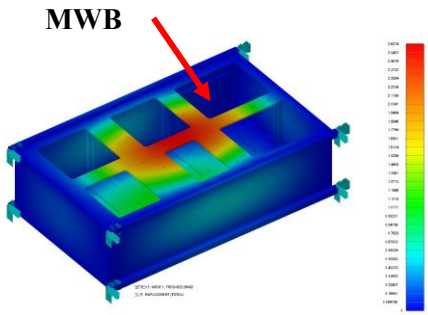

(c) Pattern #1

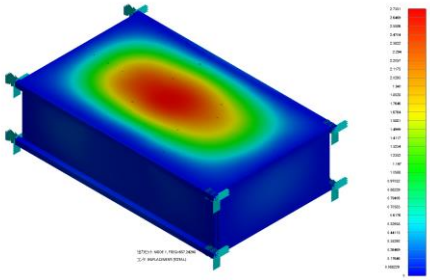

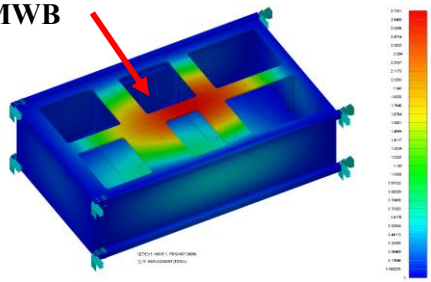

(d) Pattern #2

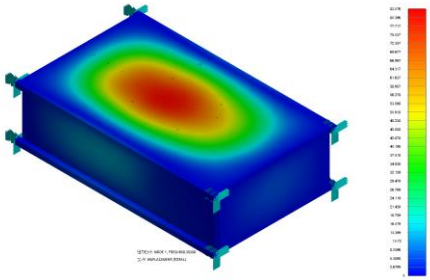

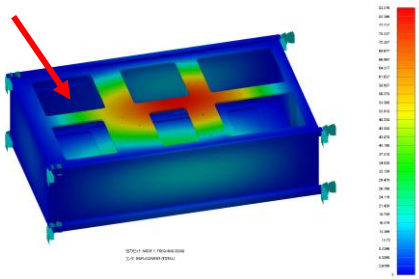

(e) Pattern #3

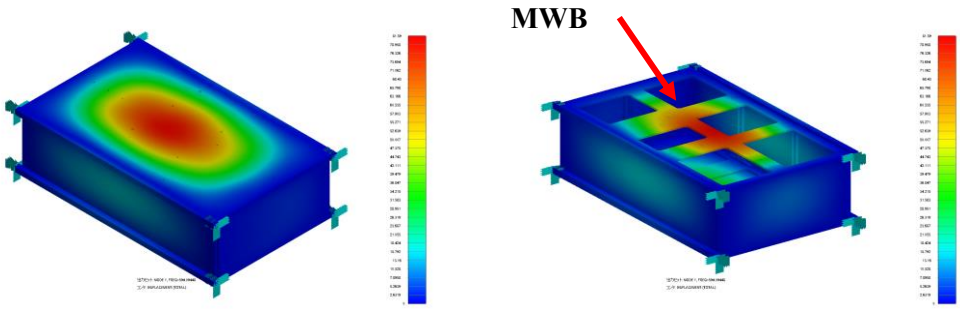

(f) Pattern #4

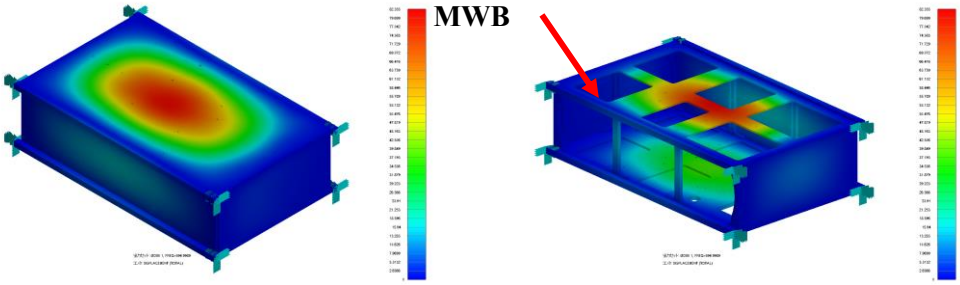

(g) Pattern #5

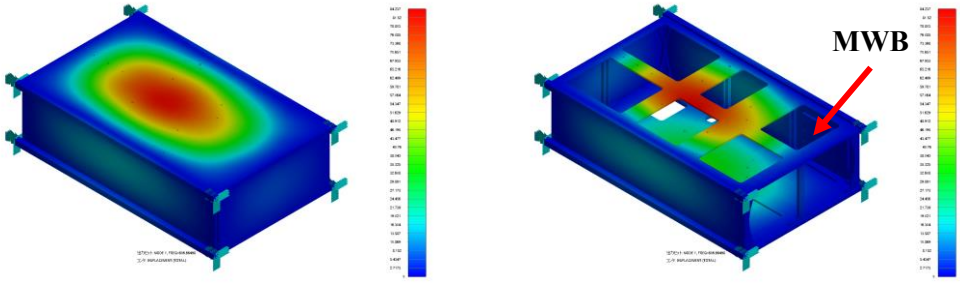

(h) Pattern #6

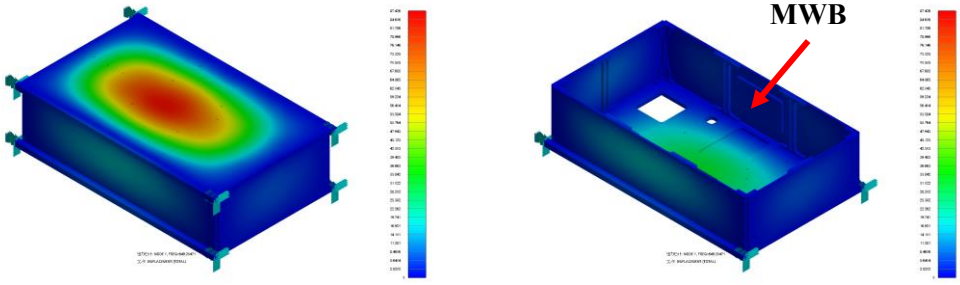

(i) Pattern #7

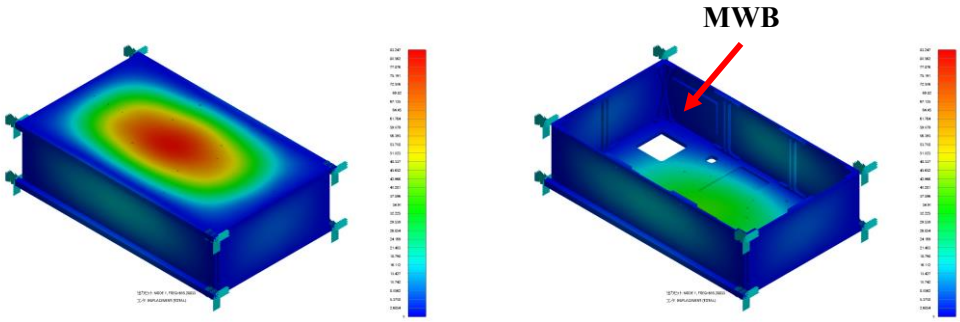

(j) Pattern #8

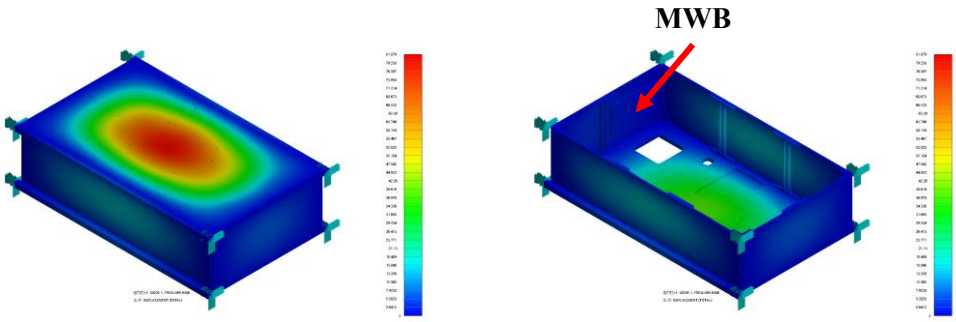

(k) Pattern #9

Fig VI-1 Natural frequencies' result's simulation

Table VI-2 presents the material properties used for the simulation.

Table VI-2 Materials properties

Item	Material	Density (kg/m3)	Youngs module (GPa)	Poisons ratio
MWB	Graphite	2.49×10^{-6}	27.6	0.19
	Copper foil	8960	128	0.34
	Lithium cobalt dioxide	4790	191	0.24
	Aluminium foil	2725	70	0.33
Nanosatellite	CFRTP	1400	49.8	0.3
	AlSi10Mg	2670	67.5	0.33
	A2024	2800	73	0.33

VI.1.2. Launch environment

During the *launch environment* simulation of the *MWB* concept, the *launch environment* of the FLCB battery has been simulated during the evaluation test of the battery technology using one FLCB cells (90 mAh) instead of the FLCB packs as has been proposed during this chapter, in order to check the withstandability of one cell. Please refer to ***Chapter IV***, ***section IV.1.1.2*** for the test conditions.

VI.1.3. Space environment

During the *space environment MWB* simulation, a specific configuration to 1U CubeSat including the redundancy architecture defined in ***Table V-12*** has been used as an example. Six packs of FLCBs have been included (***Fig VI-2***), while the three packs (P1, P2 and P3) with a total capacity of 2430 mAh, considering as the main battery pack (P), have been discharged and charged several times inside a small thermal vacuum chamber as represented in ***Fig VI-3***. The three other packs (RP1, RP2, and RP3) have been not being discharged and charged during the simulation but discharged and charged only before and after the simulation for evaluation and comparison purposes, finally, they have been considering as the redundant battery pack (RP), as well as reference packs.

FLCB packs 810 mAh
Main (P), Redundant (RP)

Fig VI-2 *MWB* packs selected for the simulation

Concerning the simulation condition, the same thermal vacuum conditions and profile previously followed at the evaluation test have been reproduced, however, during the simulation different facility has been used (***Fig VI-3***), the pressure could reach 10^{-5} Pascal instead of 10^{-4} Pascal. Additionally, no pre-charge steps have been used from -20°C to +60°C as for the evaluation test.

Table VI-3 summarizes the similarities and dissimilarities between the two test conditions.

Table VI-3 *MWB* simulation vs evaluation test

Evaluation (***Chapter IV***)	**Simulation**
SSLCB (*Oxide*)	SSLCB (*Oxide*)
PLCB & FLCB one-cell	FLCB one-cell & **FLCB's packs**
Three temperature levels (-20°C, +20°C, and +60°C)	Three temperature levels (-20°C, +20°C, and +60°C)
Include pre-charge step	**No** pre-charge step
Only evaluation	**Simulation** and evaluation
Facility 1	**Facility 2**
Vacuum pressure $\mathbf{10^{-4}}$ Pascal	Vacuum pressure $\mathbf{10^{-5}}$ Pascal
>4 days	>4 days

Please refer to ***Chapter IV***, ***section IV.1.2.2*** for all the evaluation test conditions.

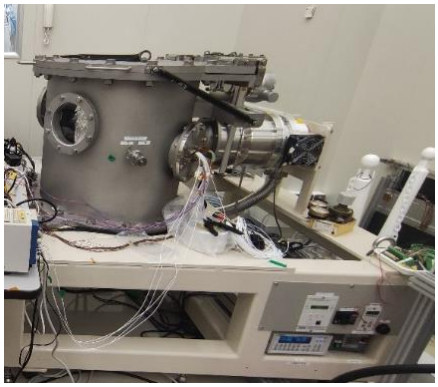

(a) Thermal vacuum chamber at *Wel Research Company* [***130***]

(b) FLCB's packs during thermal vacuum simulation

Fig VI-3 *Space environment* simulation, thermal vacuum

Fig VI-4 presents the temperature profile record for the thermal vacuum simulation including all the FLCB's packs temperature variation during discharge and charge cycles. The temperature has been varying between -20°C and +60°C during three consecutive cycles. The total time of the simulation has been between three days, for three cycles, to four days, including the room temperature (+20°C) cycles at the beginning and the end of the simulation.

Table VI-4 summarizes the equivalent number of minutes and orbits of the thermal vacuum conditions for only the three days cycles that the FLCB's packs have been enduring according to a Low-Earth-Orbit duration between 84 to 127 minutes/one orbit.

Table VI-4 Orbits' simulation

Orbit	LEO			
Number of days	3		4	
Total time (mn)	4320		5760	
Minutes/one orbit	84	127	84	127
Number of orbits	51	34	69	45

Fig VI-4 FLCBs packs temperature profile during simulation

VI.2. Result and discussion

VI.2.1. Launch environment

At the end of the simulation with the non-functional check, no physical damage has been observed related to the fatigue, none of the batteries has shown a change in dimensions or weight, ***Table VI-5*** summarizes the weight measurement before and after all the *launch environment* simulation.

Table VI-5 Weight measurement before and after test

	FLCB		
	00#1	**00#2**	**00#3**
Before (g)	3.34	3.33	3.32
After (g)	3.33	3.33	3.32
Difference (%)	0,30	0,00	0,00

Otherwise, the OCV (Open-Circuit-Voltage) measurements show a variation exceeding the criteria's limits for only one cell of the FLCB with 0.2% excess as shown in ***Table VI-6***, the same results as the PLCB02. However, the excess could not be used for judgment until the functional test has been done which would give the more significant interpretation.

Table VI-6 OCV measurement before and after test

	FLCB		
	00#1	**00#2**	**00#3**
Before (V)	4,25	4,22	4,23
After (V)	4,22	4,22	4,22
Difference (%)	**0,70**	0,00	0,24

On the other side, in ***Fig VI-5***, the FLCB has shown good result at the charge profile, using the same charge (end of charge) and discharge (end of discharge) limits as PLCBs. The charge started at ~ 3.4V, corresponding to ~0.055A for the current, until has been decreasing and switched to the constant voltage mode of about 4.1V.

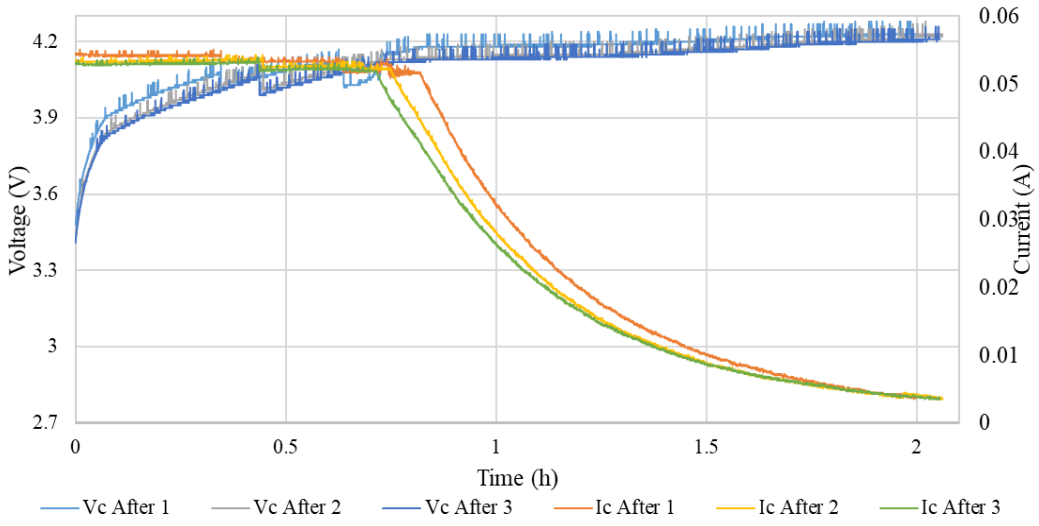

Fig VI-5 Charge cycles for FLCB 90 mAh after the *launch evaluation* test Group's samples for one jig

Fig VI-6 represents the discharge capacity ratio for all the three jigs with the three FLCB's groups. Between 90% and 95% of discharge capacity has been kept after all the *launch environment*, as represented in ***Fig VI-6 (a)*** and ***Fig VI-6 (c)*** for the group 1 and 3 respectively, however, the group 2 in ***Fig VI-6 (b)*** has shown a decrease in capacity to almost 85% during the two last discharge cycle after the test.

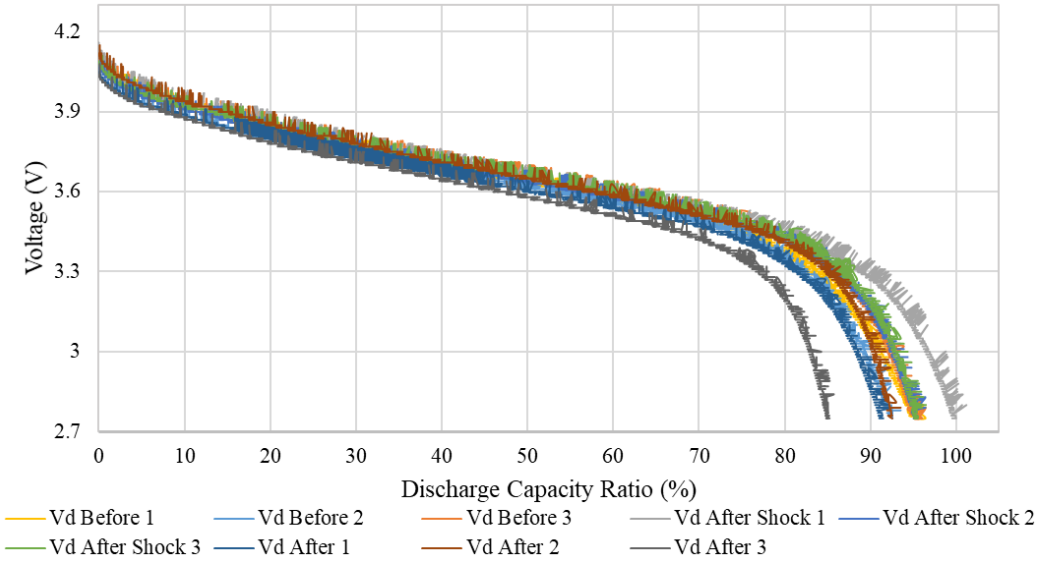

(a) Jig's group 1

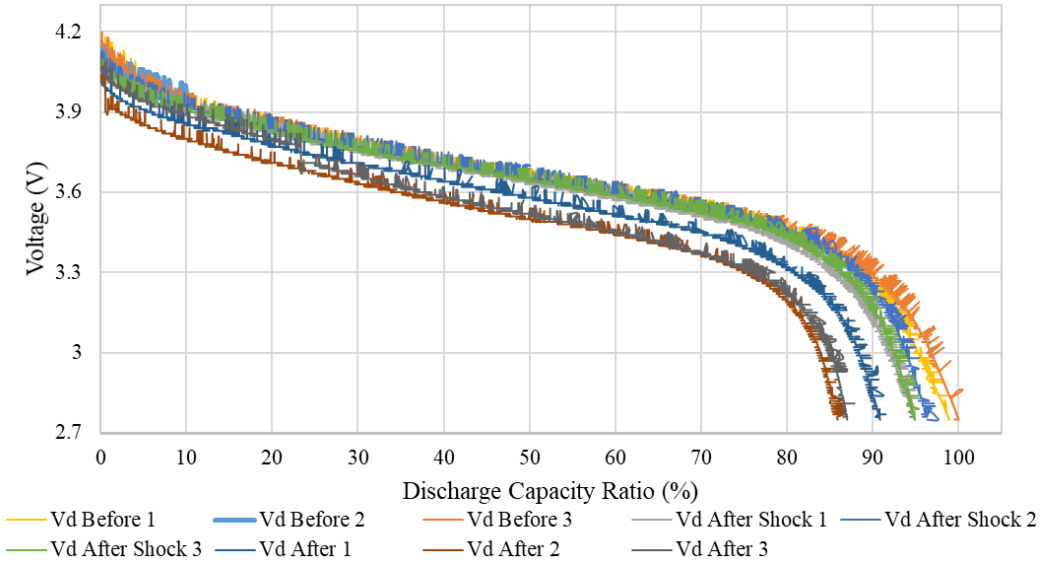

(b) Jig's group 2

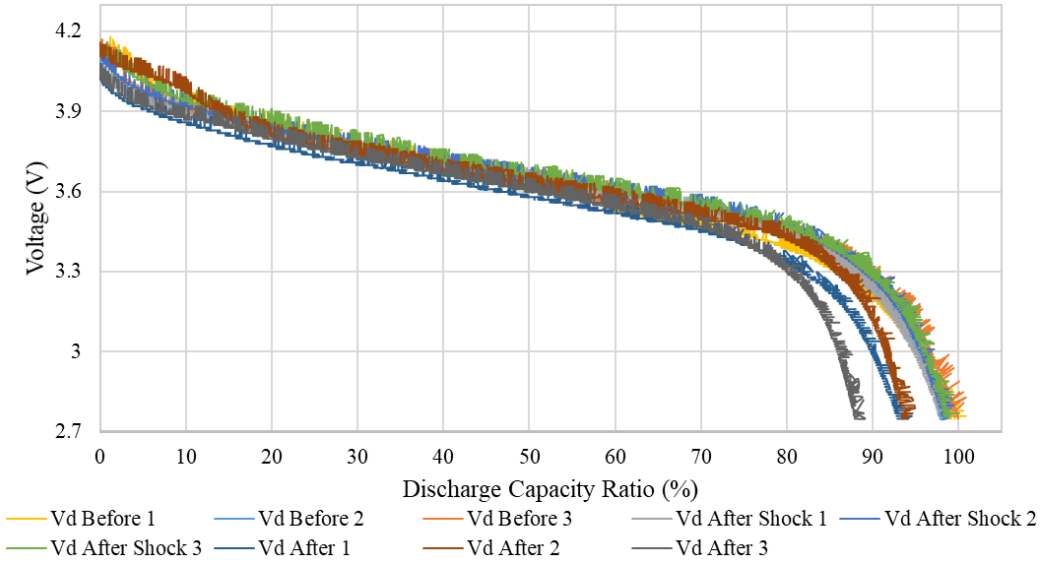

(c) Jig's group 3

Fig VI-6 Discharge voltage vs discharge capacity ratio for FLCB 90 mAh. Group's samples for the three jigs (groups): before, after the shock tests and after the 3 axis vibration tests

From another point of view, and better representation, the complete discharge charge cycle for the FLCB has been reproduced in order to compare the results between the before and after the test. ***Fig VI-7*** have reproduced some of these cycles as examples.

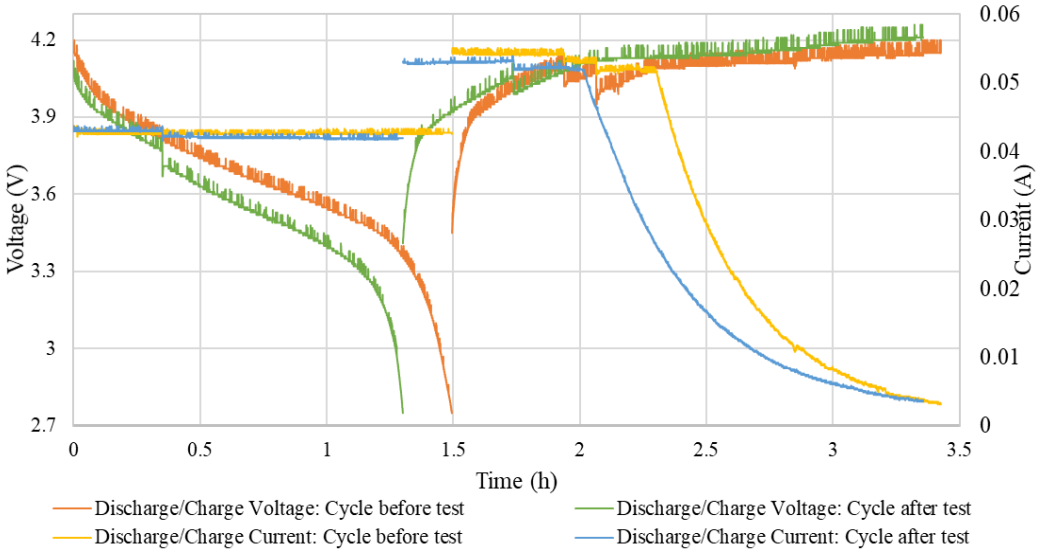

Fig VI-7 Charge/Discharge cycle for the FLCB 90mAh before and after the test

Finally, all cells could show their ability to withstand the hostile *launch environment*, including the capacity ratios and all the electrical and mechanical properties results.

Please refer to ***Chapter IV*** for more details about the PLCBs *launch environment* evaluation test results and discussion.

VI.2.2. Space environment

For the *space environment* simulation, each battery has been weighted three times, then the two mean weights have been computed, finally, the difference (*Before - After*) has been subject to the *ISO 17546:2016(en)* "*Space systems — Lithium-Ion battery for space vehicles — Design and verification requirements*", the same standard used in ***Chapter IV***, in order to define the state of each battery results.

The checking of weight in ***Table VI-7*** shows the difference between the before-test and the after-test weight for each pack.

Table VI-7 Weight results for FLCB packs

Battery	Before	After	Difference (g)	Difference (%)
RP1	32.41	32.45	-0.04	**-0.11**
P1	32.62	32.68	-0.06	**-0.19**
RP2	32.41	32.41	0.003	**0.01**
P2	32.48	32.59	-0.11	**-0.34**
RP3	32.33	32.29	0.03	**0.10**
P3	32.35	32.47	-0.12	**-0.38**

The FLCB packs with 9 cells results have been so far within the limit, of about 0.1%, as for RP1, RP2 and RP3. Finally, P1, P2 and P3 could be considered in pending, the conclusion could not be done due to the negative value, between -0.4% and -0.1%, waiting for the discharge capacity and charge results that may apport more valuable data to the final decision.

The results of the discharge capacity ratios and the charge cycles have been organized as follows: the three FLCB packs P1, P2, and P3 in ***section VI.2.1.a*** for the discharge capacity ratios. Full charge cycle for the three FLCB packs in ***section VI.2.1.b***. Then, the estimated total remaining capacity over all the simulation including the full discharge and charge cycle for the three FLCB packs in ***section VI.2.1.c***. Finally, the results of the physical and appearance checking after the simulation in ***section VI.2.1.d***.

The results for the RP packs have been presented in ***Annex VI.1*** and ***Annex VI.3*** as a reference, they have included several cycles before the test and several cycles after the test, as well as ***Annex VI.2*** and ***Annex VI.4*** for the P packs.

For the discussion section, only one cycle has been used for comparison with the *space environments* cycles simulation, for the before-test and after-test, these cycles have been selected based on the highest capacity that could be obtained, they have been mentioned in each figure by (***B***) or (***A***) referring to ***Before*** and ***After***, respectively.

a. <u>810 mAh FLCB's packs discharge capacity ratio</u>

The results from the simulation could show that the FLCB packs 810 mAh could be operated during all the simulation inside the chamber, however, with a decrease in the capacity.

Fig VI-8 presents the results of the discharge capacity for the three packs 810 mAh (P1, P2, and P3). Almost the two packs (P2 and P3, ***Fig VI-8 (b)*** and ***(c)***) could perform the same operation, between 40% to 80% of remain capacity during the cold cycles, 80% to 100% of remain capacity within the hot cycles. Concerning the +20°C, from 80% to 90% for the capacity could be remained at the last cycle, while the first one showed no decrease comparing to the before the test, almost 100%. Finally, for the after-test cycle, P2 could have 95% of capacity, while P3 has about 85% of capacity.

Concerning pack P1 (***Fig VI-8 (a)***), the results may be different especially for the cold cycles, about 50% of the capacity for the first cycle, while the decrease for less than 5% at the two last cycles. From 40% to 60% for the hot cycles, and about 30% for the last +20°C cycle, while between 90% to 95% for the first one. Finally, the capacity has decreased to less than 65% after all the test.

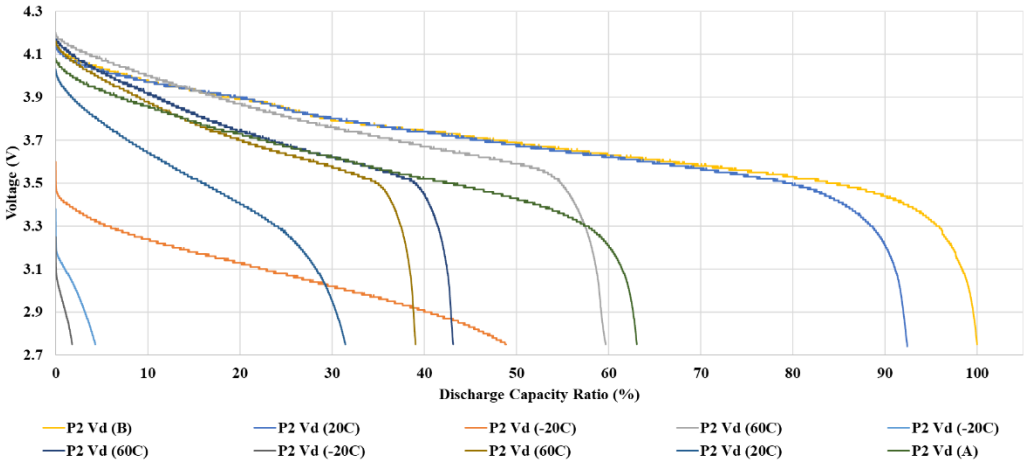

(a) P1 pack

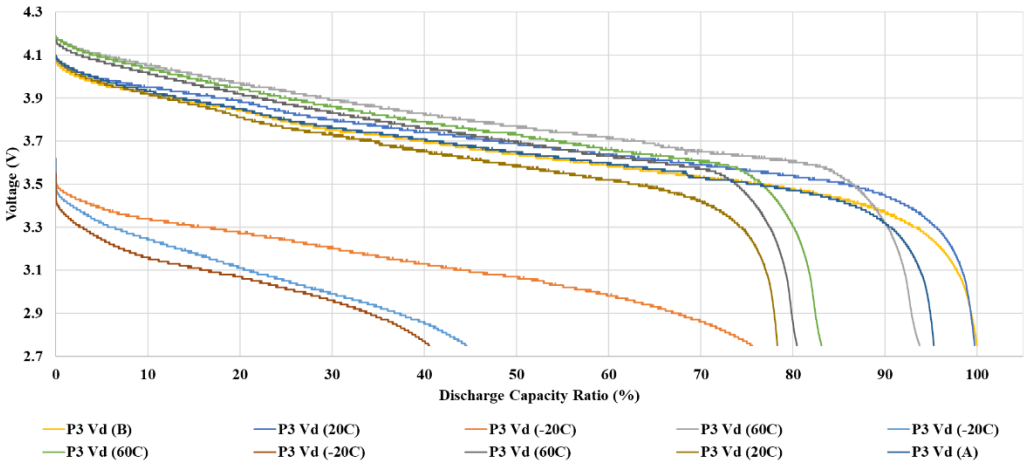

(b) P2 pack

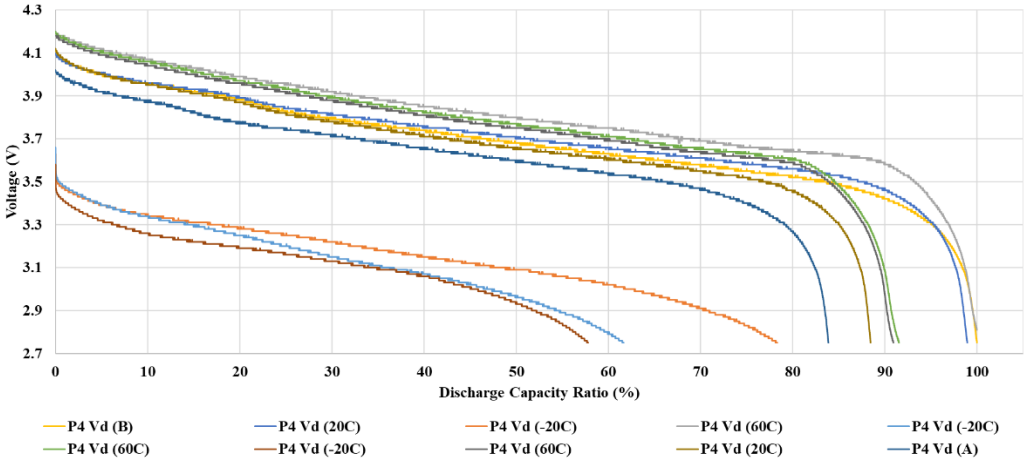

(c) P3 pack

Fig VI-8 FLCBs' 810 mAh packs discharge simulation results
Before, during & after simulation discharge capacity ratios

b. 810 mAh FLCB's packs full charge cycle

Concerning the charge cycles, all packs could be able to operate normally with showing a decrease in time as for the discharge. P2 and P3 have almost the same charge profile, while P1 has shown a fast charge due to the decrease in its capacity since the first +60°C cycle.

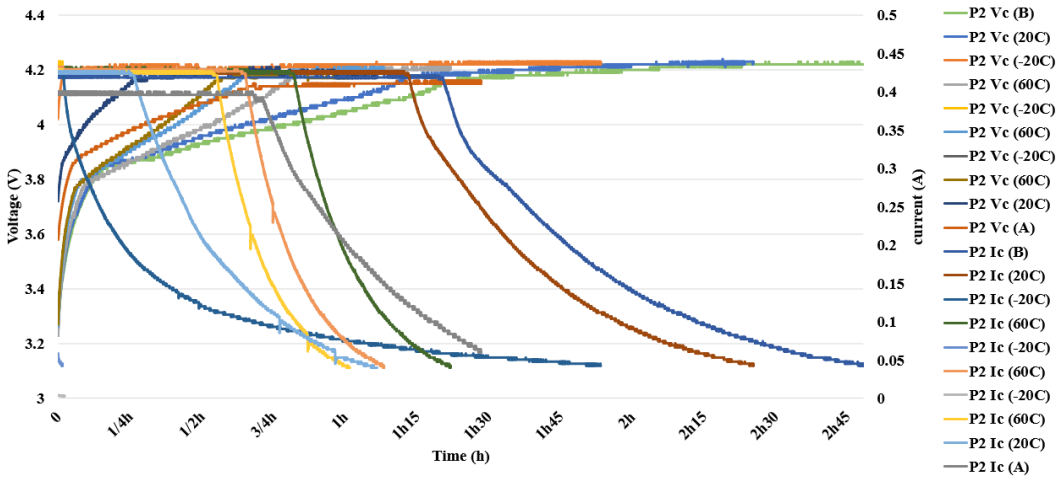

(a) P1 pack

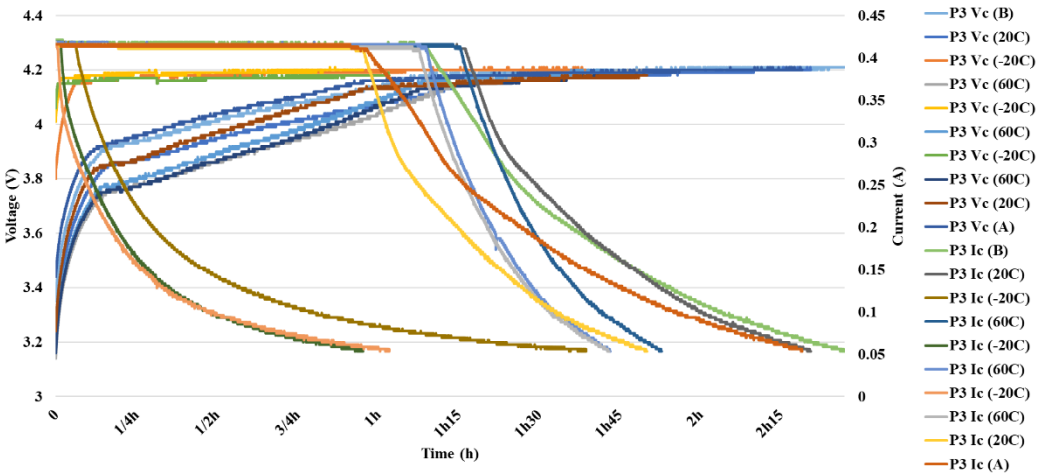

(b) P2 pack

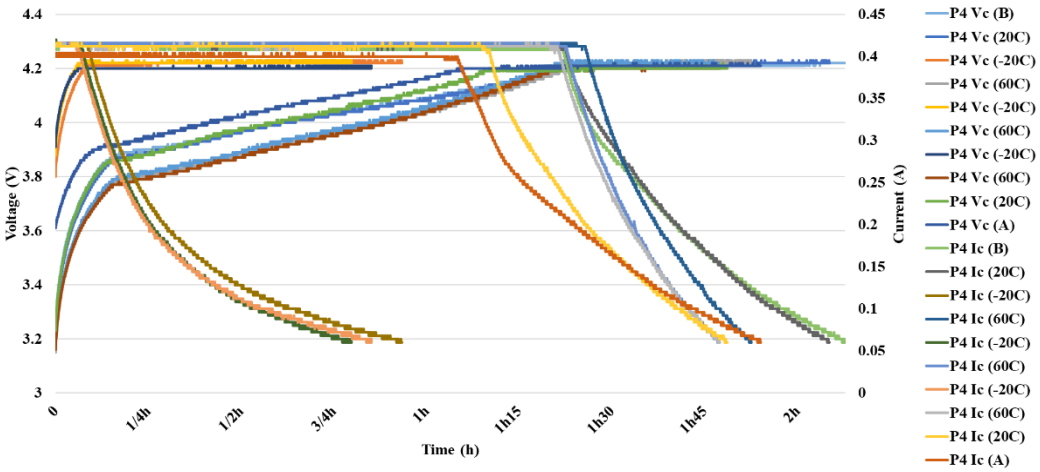

(c) P3 pack

Fig VI-9 FLCBs' 810 mAh packs charge simulation results
Before, during & after simulation full charge cycles

c. The estimated total remaining capacity over the simulation

The previous results of the capacity ratios have been used to estimate the total remained capacity of the three packs over all the simulation and for different temperature levels.

The estimated total capacity for the full simulation is presented in ***Table VI-8 (b)***. ***Table VI-8 (a)*** presents the capacity ratios for each cycle and each sub-cycle, this one is used for the estimation of the minimum and maximum total capacity that could be provided during the simulation. The minimum capacity has been taken as the lowest capacity got during the last sub-cycles for each cycle, the maximum is the highest capacity got at the first sub-cycle for each cycle. Sub-cycles are defined as the discharge/charge cycles performed during a full cycle of temperature from -20°C to +60°C including +20°C within the first and the last cycle.

Table VI-8 Simulation estimated remain capacity

(a) Estimated remain capacity by cycles

Capacity / Cycle	P1 (%)			C P2 (%)			P3 (%)		
-20°C	49	4	2	76	45	40	78	62	58
+20°C	92	31		100	78		99	88	
+60°C	60	46	39	94	83	80	100	92	91

(b) Estimated total remaining capacity

Cycles	Capacity (mAh)		Capacity (%)	
	Min	Max	Min	Max
Cold temperature (-20°C)	810.0	1644.3	33.33	67.67
Room temperature (+20°C)	1595.7	2357.1	65.67	97.00
Hot temperature (+60°C)	1701.0	2057.4	70.00	84.67
Total (*mean between the 3 cycles*)	**1368.9**	**2019.6**	**56.33**	**86.11**
Nominal	**2430**		**100**	

Within all the simulation, the remaining capacity for the three packs combined was more than 50%, from 56% to 86% for the total range, with 1368.9 mAh to 2019.6 mAh, respectively. It could be almost the same for the two temperature levels +20°C and +60°C, from 65% to 70% for the minimum value, and from 85% to 97% for the maximum value. However, lower for the cold temperature (-20°C), less than 50%, from 33% to 67% for the total range, which the total capacity was equivalent to one equivalent pack to operate for the minimum case, and about two packs for the maximum case.

Fig VI-10 summarizes all cycles performed during the simulation with voltage and current for the discharge and charge. The measurement by the software of the discharge current showed a decrease for P1 with time almost the same profile as the voltage, however, after checking with the real-time measurement, the value of the current was constant, this failure has appeared just before the test and could not be improved. Finally, the test could be conducted by ignoring the reading of the current.

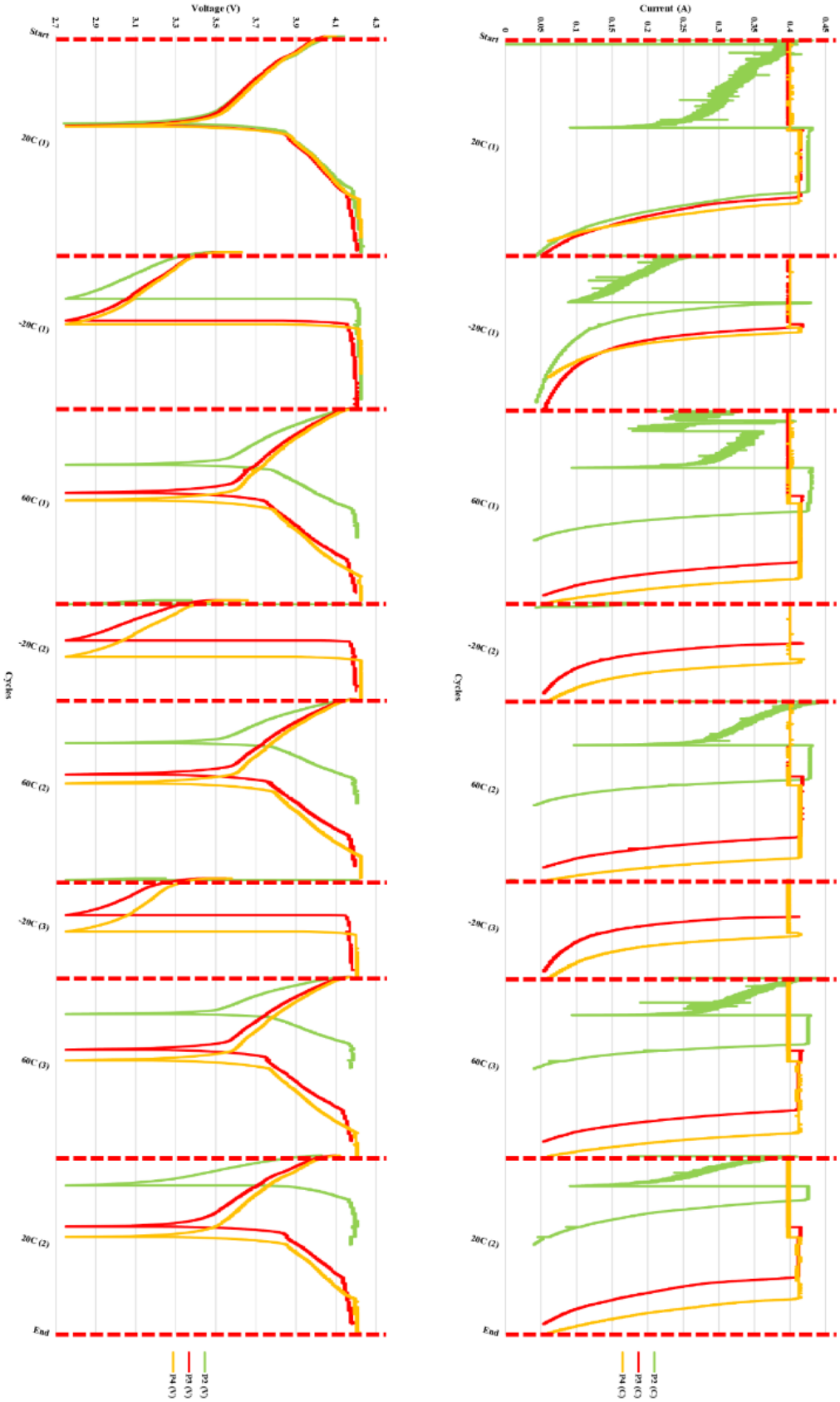

Fig VI-10 Complete discharge/charge simulation cycles

d. Physical and appearance checking after simulation

As presented during the test procedure, each battery and pack has been checked before and after the test in order to verify any change or degradation on their appearance. ***Fig VI-11*** presents all pictures taken after the test for all packs including the one-cell FLCB (FLCB & RFLCB).

Comparing to the appearance in ***Fig V-5*** before the test, even almost all packs present a deformation or degradation, while some have slight deformation as P1, P2, and RP3, other packs presented more deformation as P3, RP1, and RP2 as well as one-cell FLCB and RFLCB.

However, all FLCB's Packs could be able to be charged and discharged after the simulation, additionally, no leakage or fire has occurred, and without risk of explosion, which may make the battery safer for the satellite and the user as well.

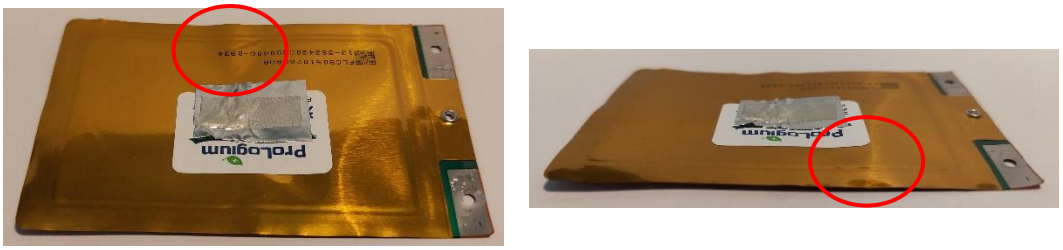

(a) FLCB (one-cell)

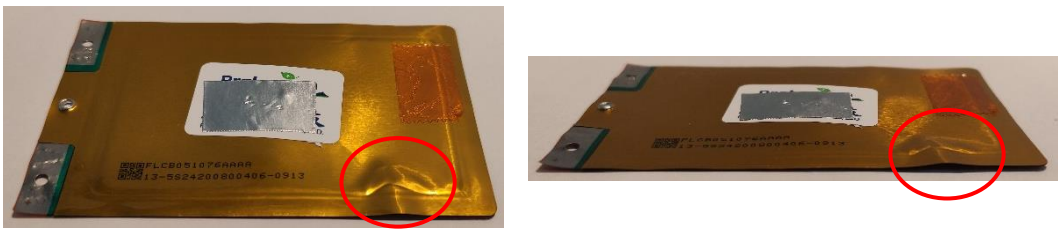

(b) RFLCB (one-cell)

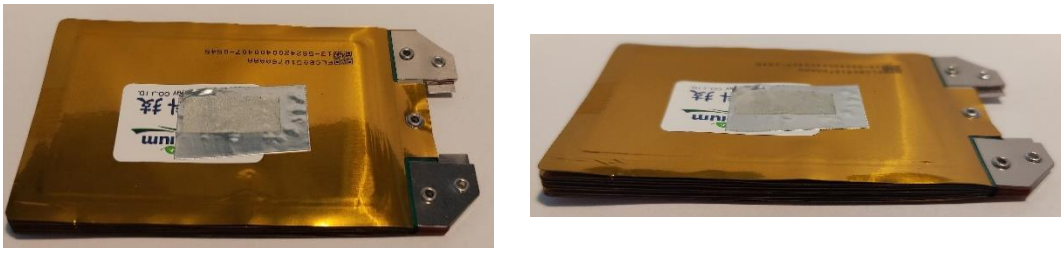

(c) FLCB pack P1

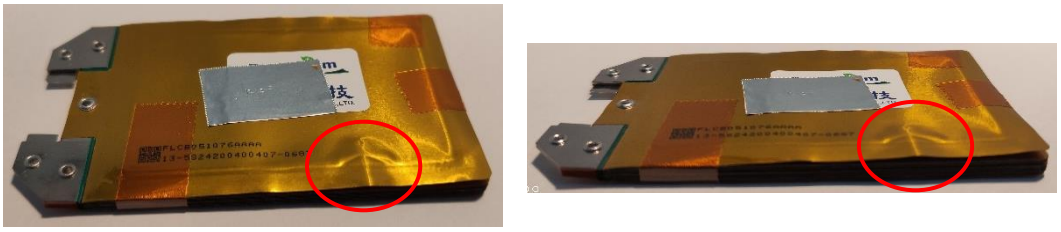

(d) FLCB pack RP1

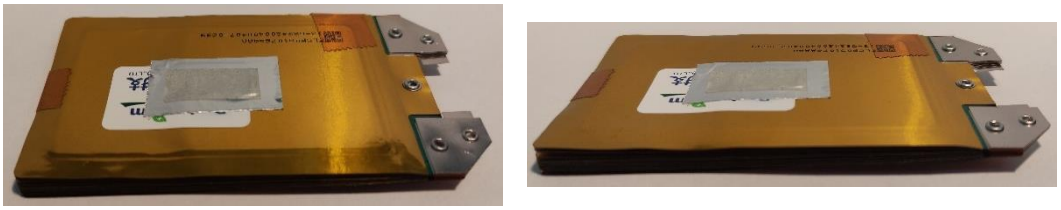

(e) FLCB pack P2

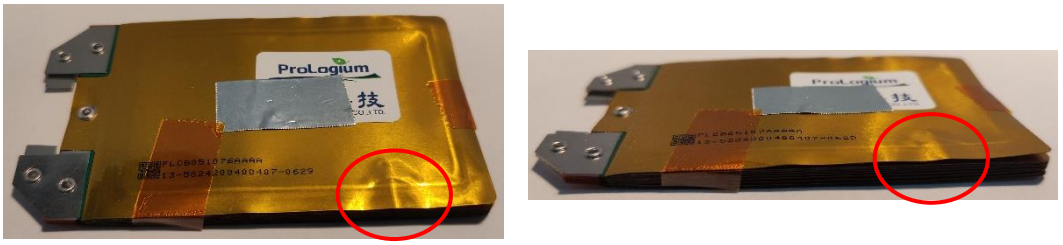

(f) FLCB pack RP2

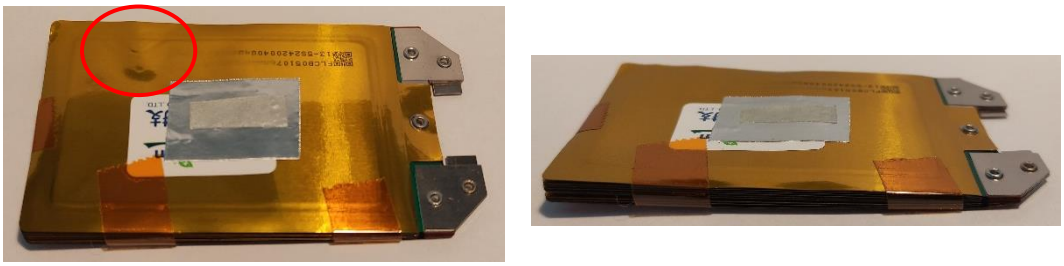

(g) FLCB pack P3

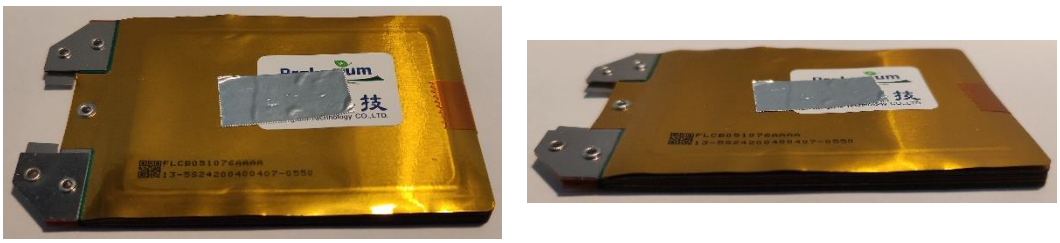

(h) FLCB pack RP3

Fig VI-11 FLCB packs appearance after simulation

VI.3. Conclusion

The simulation of the *Modular-Wall-Battery* including the proposed battery pack as a sample could present, so far, good results, as has been presented for a 1U CubeSat configuration, using six packs (three main packs, and three redundant packs). The remaining capacity at the low temperature (-20°C) could be from 33% to 67% of the total capacity including the three packs, which may be considered as a good step in comparison with the conventional Lithium-Ion batteries. Finally, the remaining capacity for the three packs combined was more than 50%, with 1368.9 mAh to 2019.6 mAh, respectively. It could be almost the same for the two temperature levels +20°C and +60°C.

Since the proposed battery pack may be integrated onboard Nanosatellite, and in order to prevent any malfunction or decrease in its performances due to the gradient of temperature, some solutions may be proposed:

First, the same approach used by the company for the PLCB battery, while in ***Chapter IV*** presented a good result, the coating used by the company may have a positive effect on the isolation and protection of the battery from the external environment.

Second, based on the material used for the battery packing (***Fig VI-12***), several services may be proposed for this purpose, the *Aluminum Laminate Film* is the most used to build a sealing battery packing for the Lithium battery pouch design [***131***]. **Finally**, using a material for the heat transfer, the *Lamda* (λ) Gel may be proposed [***76***], however, this approach may need further tests and analysis.

Moreover, with the thermal analysis and research ongoing with the amelioration and improvement of the optical and thermal properties of the surfaces, many alternative solutions may be found.

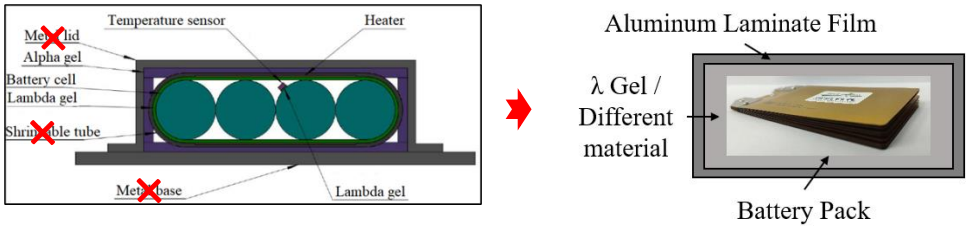

MWB Concept using 90 mAh FLCB pack, a different approach than the manufacturer following Ten-Koh satellite approach for the battery box

Fig VI-12 Proposed solution for the *MWB* packs

As the selected battery has already been evaluated in ***Chapter IV*** with showing so far good results with a remained capacity of more than 90%, the selected battery

may be adopted to any Nanosatellite following its conventional integration into the BUS system while no box needed.

However, for the *MWB* concept integration within Nanosatellites, while using the customized pack, the integration may need to wait for further investigations which may be published later in subsequent publication until the real test will be done onboard a Nanosatellite, this one for further analysis, as well as for comparison reason with in-orbit results.

Annex VI.1. RP pack results before the simulation. Discharge capacity ratios & full charge cycles.

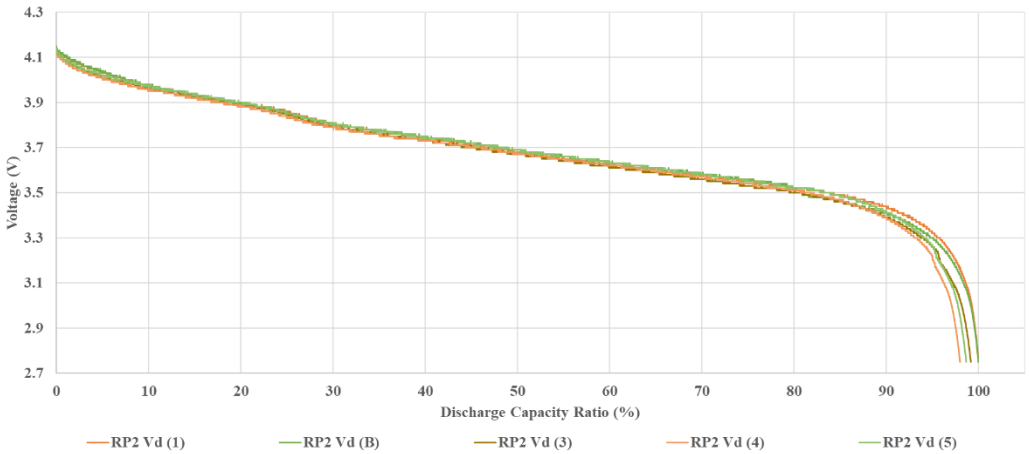

(c) RP1 discharge capacity ratios

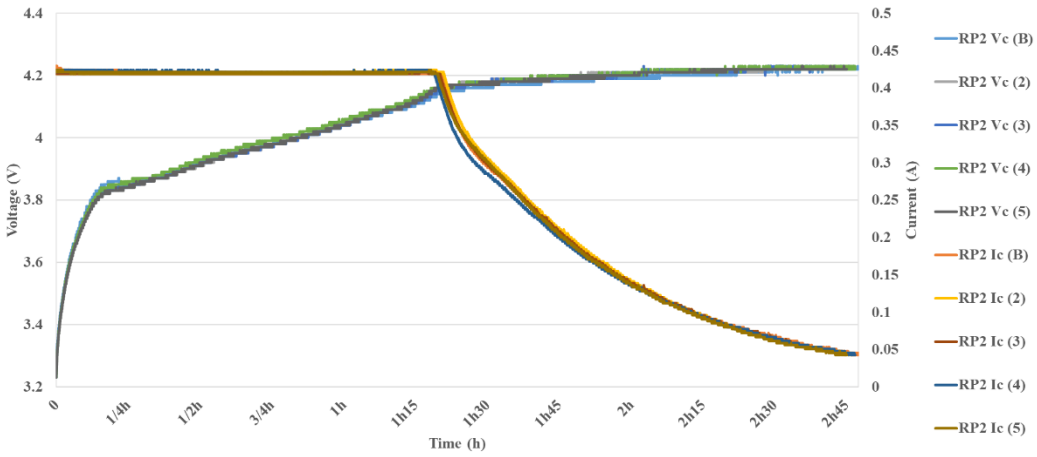

(d) RP1 full charge cycles

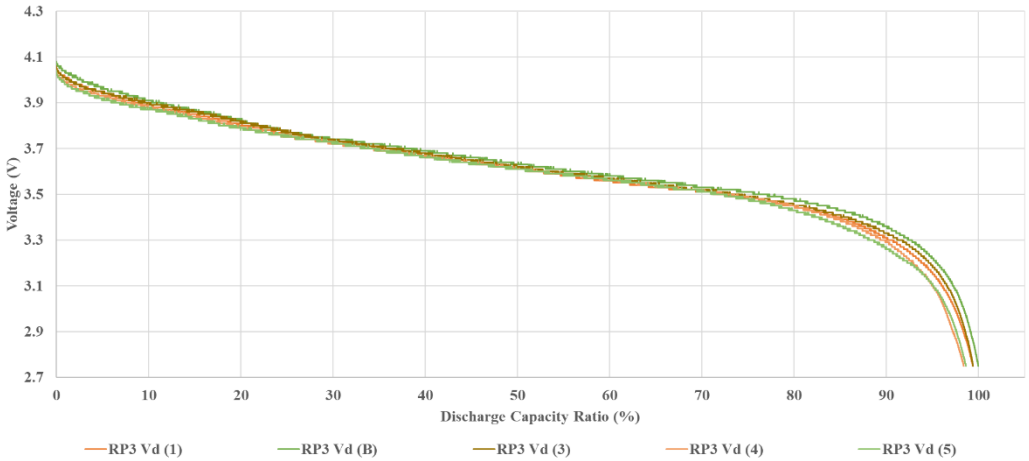

(e) RP2 discharge capacity ratios

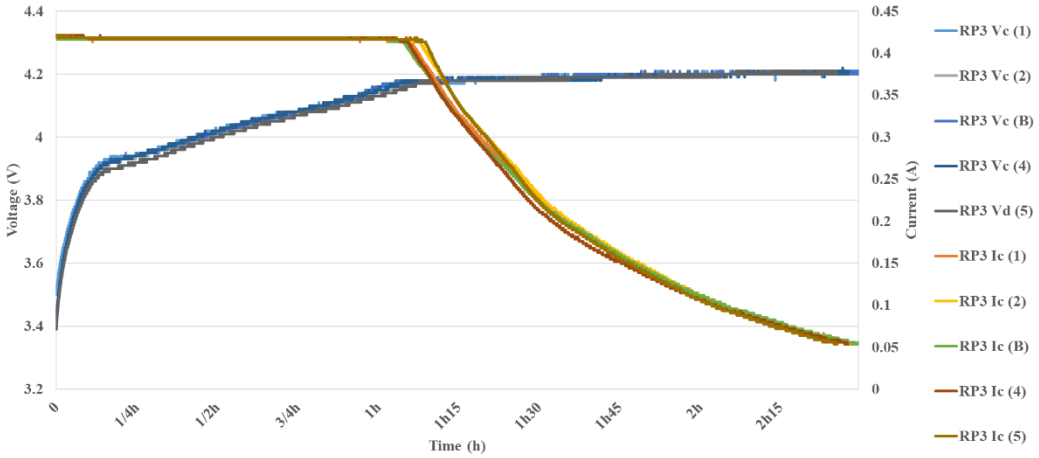

(f) RP2 full charge cycles

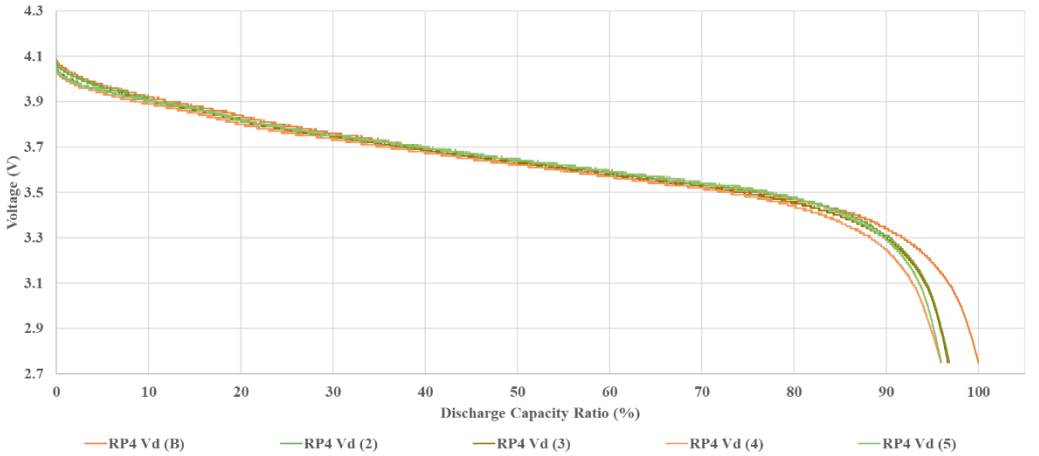

(g) RP3 discharge capacity ratios

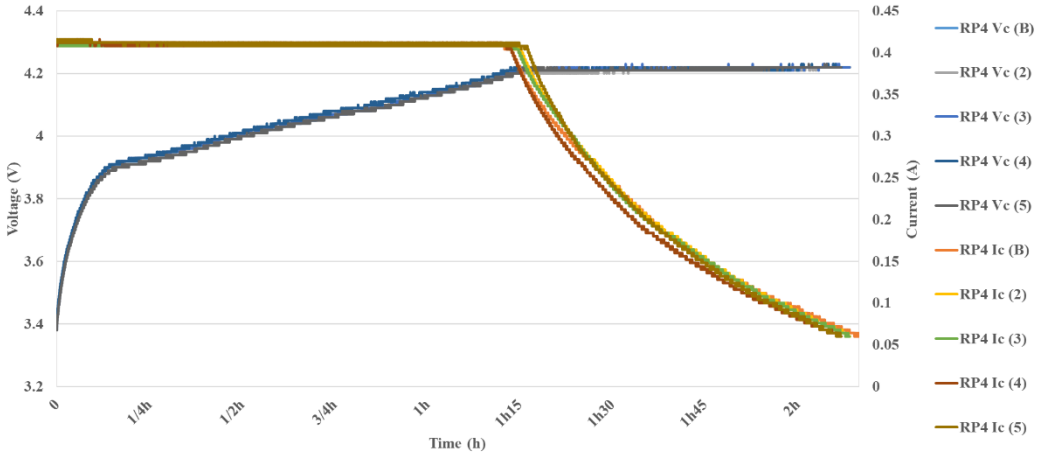

(h) RP3 full charge cycles

Annex VI.2. P pack results before the simulation. Discharge capacity ratios & full charge cycles.

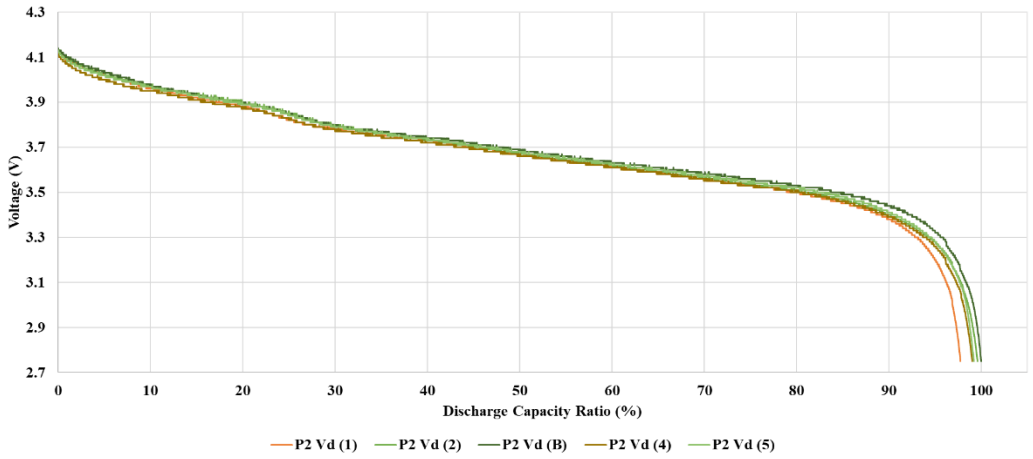

(c) P1 discharge capacity ratios

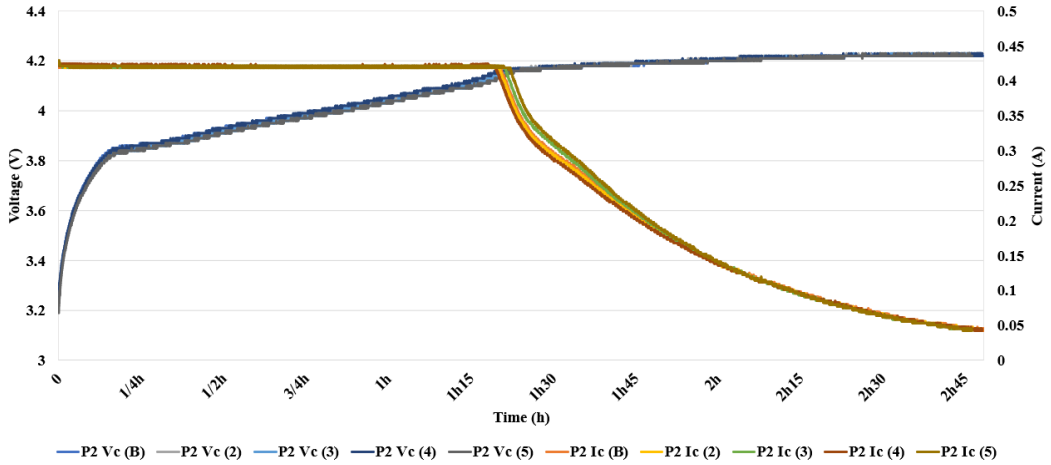

(d) P1 full charge cycles

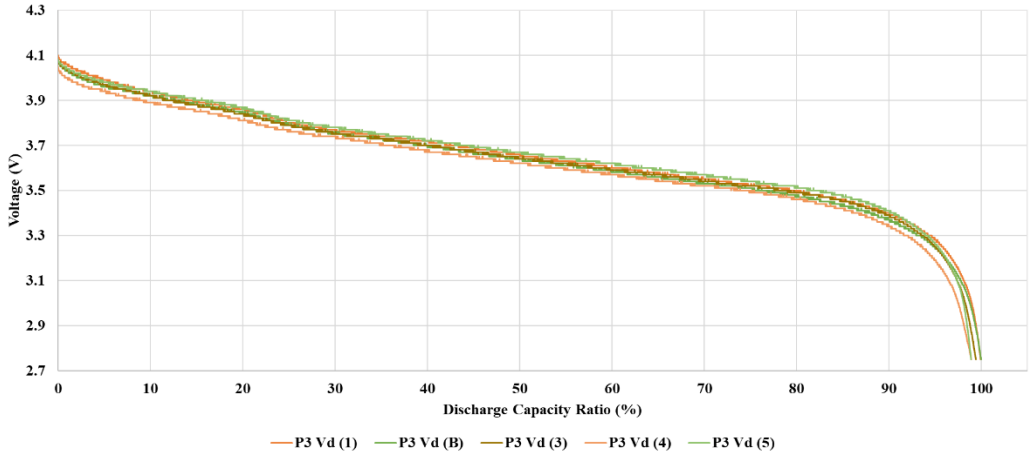

(e) P2 discharge capacity ratios

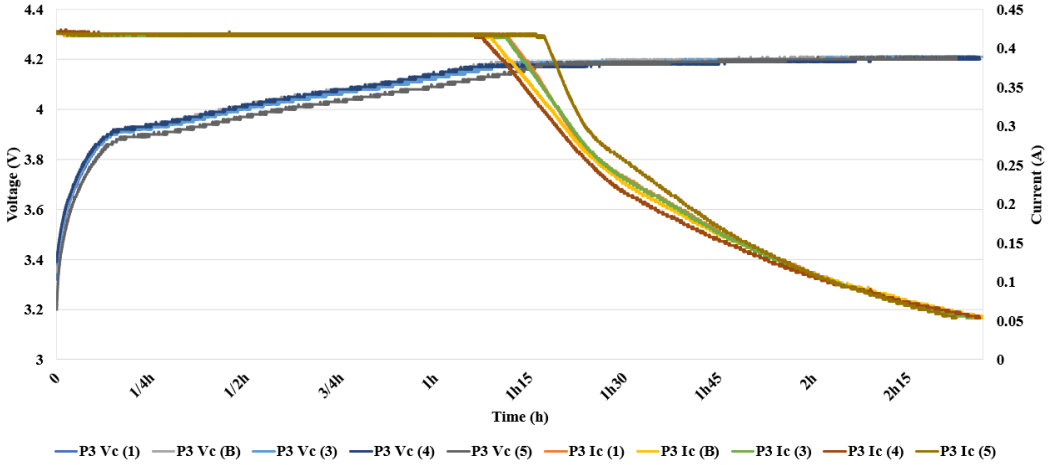

(f) P2 full charge cycles

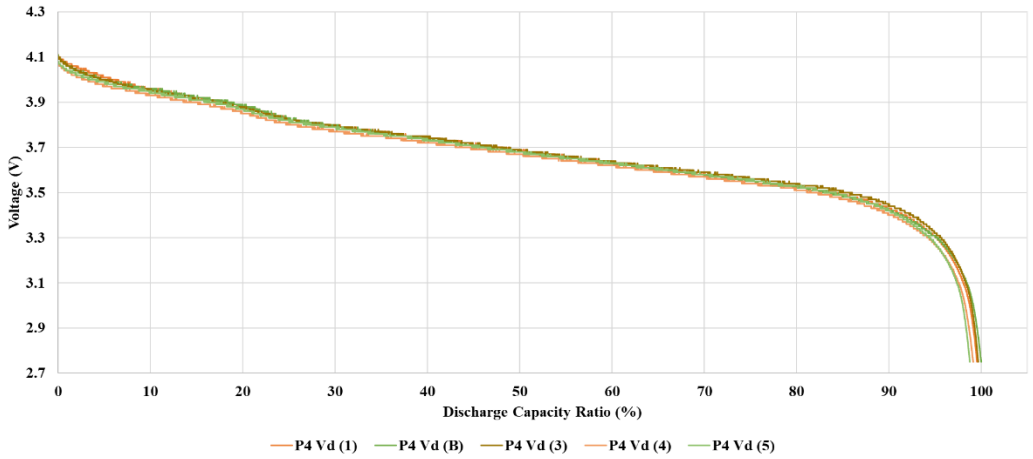

(g) P3 discharge capacity ratios

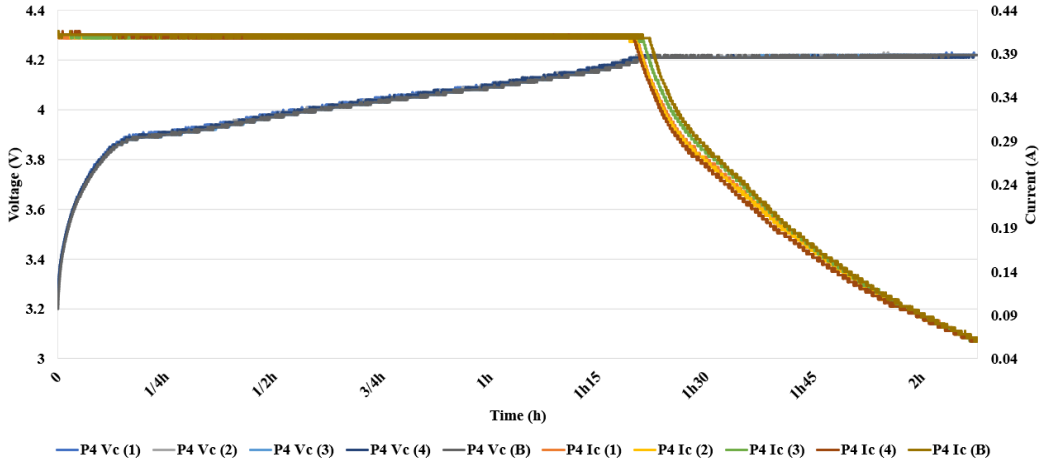

(h) P3 full charge cycles

Annex VI.3. RP pack results after the simulation. Discharge capacity ratios & full charge cycles.

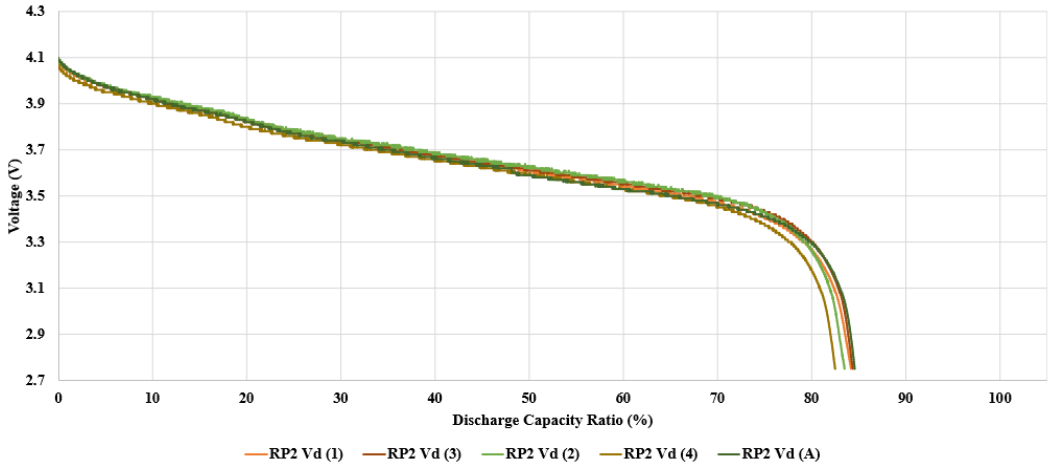

(c) RP1 discharge capacity ratios

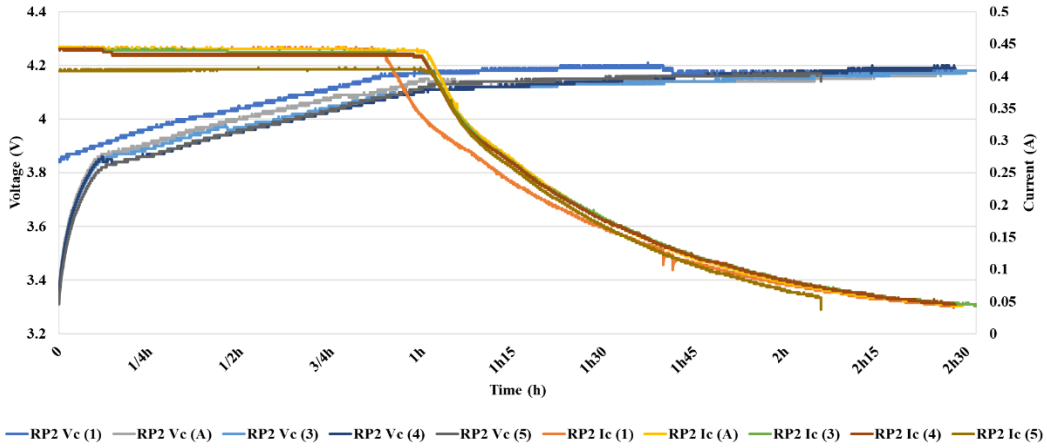

(d) RP1 full charge cycles

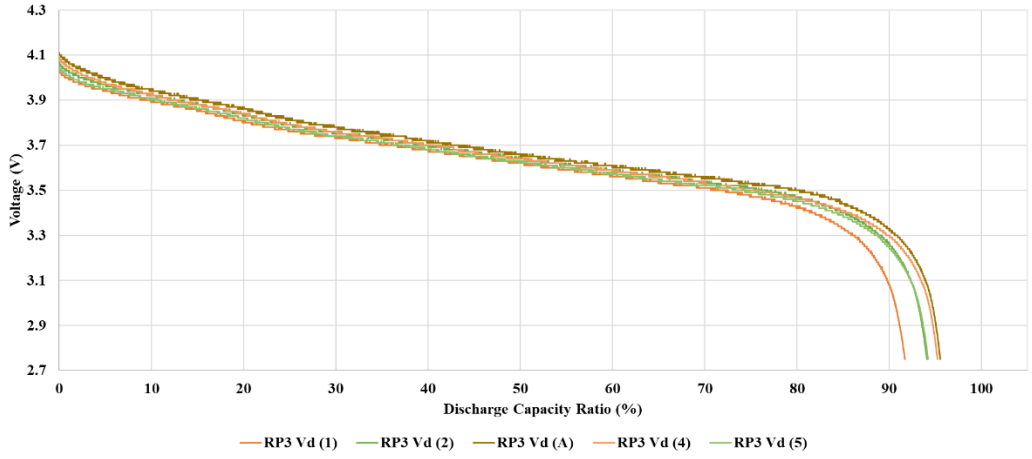

(e) RP2 discharge capacity ratios

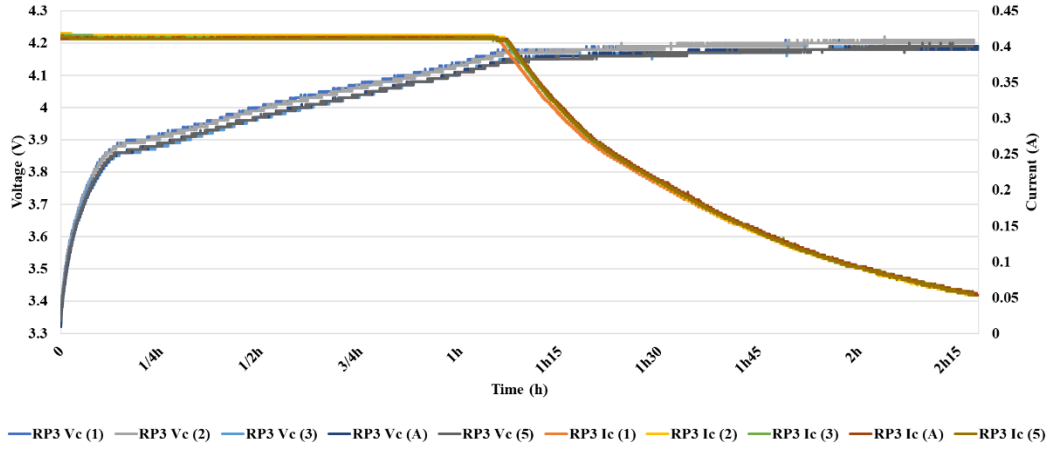

(f) RP2 full charge cycles

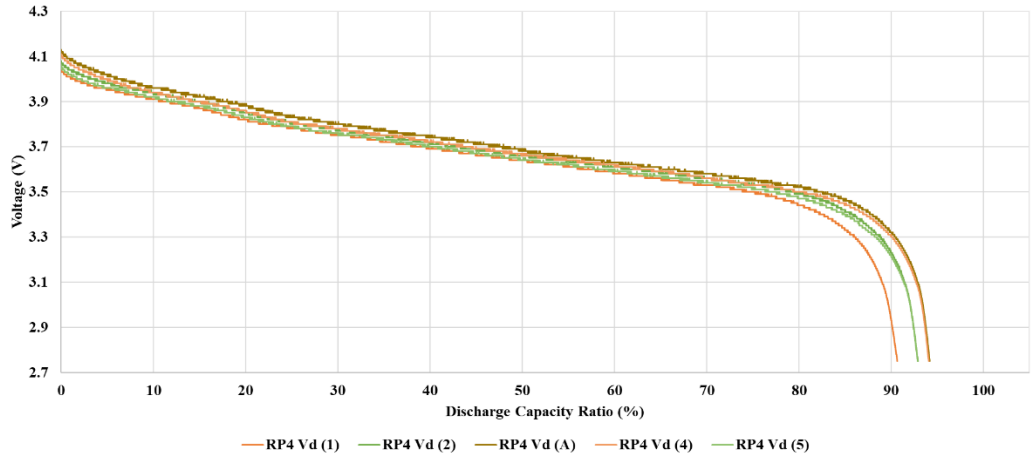

(g) RP3 discharge capacity ratios

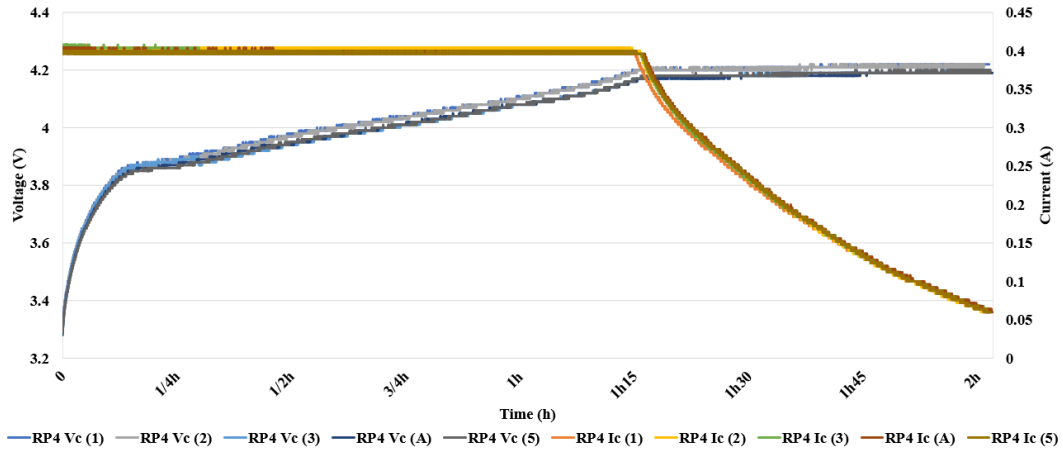

(h) RP3 full charge cycles

Annex VI.4. P pack results after the simulation. Discharge capacity ratios & full charge cycles.

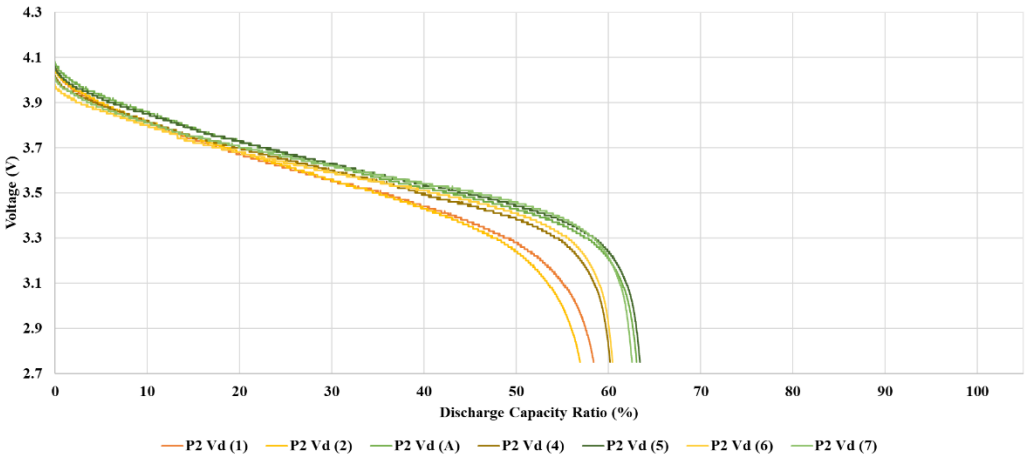

(c) P1 discharge capacity ratios

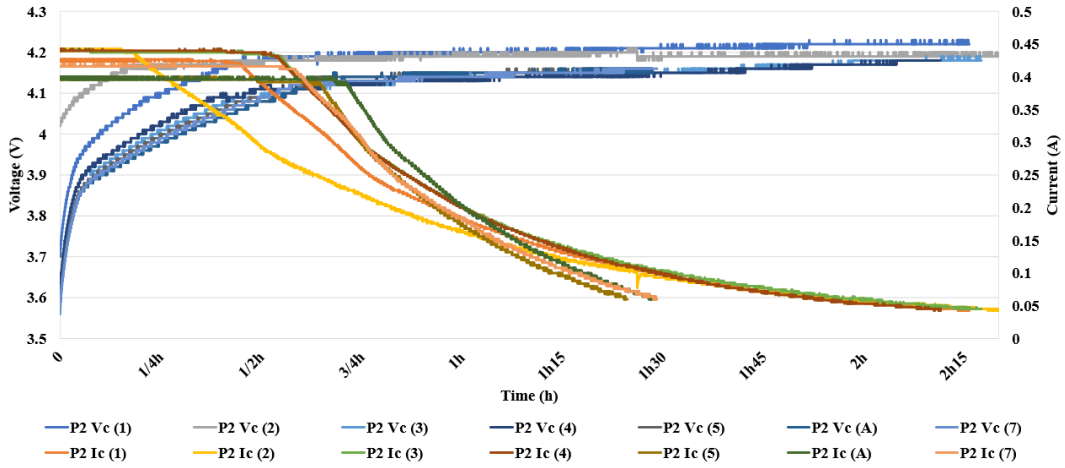

(d) P1 full charge cycles

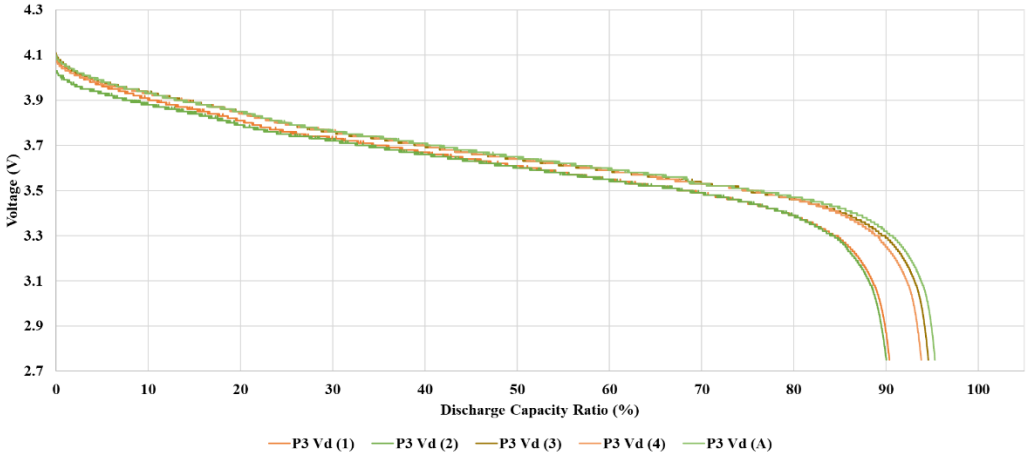

(e) P2 discharge capacity ratios

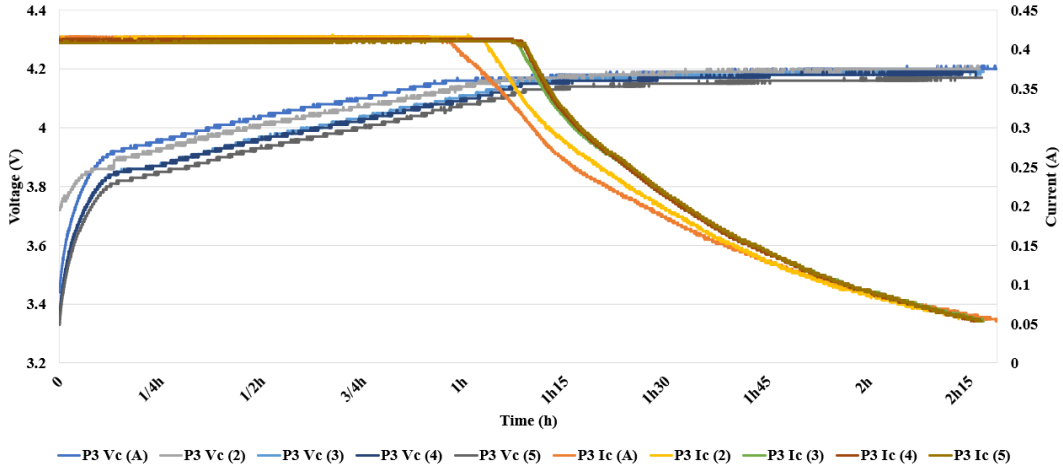

(f) P2 full charge cycles

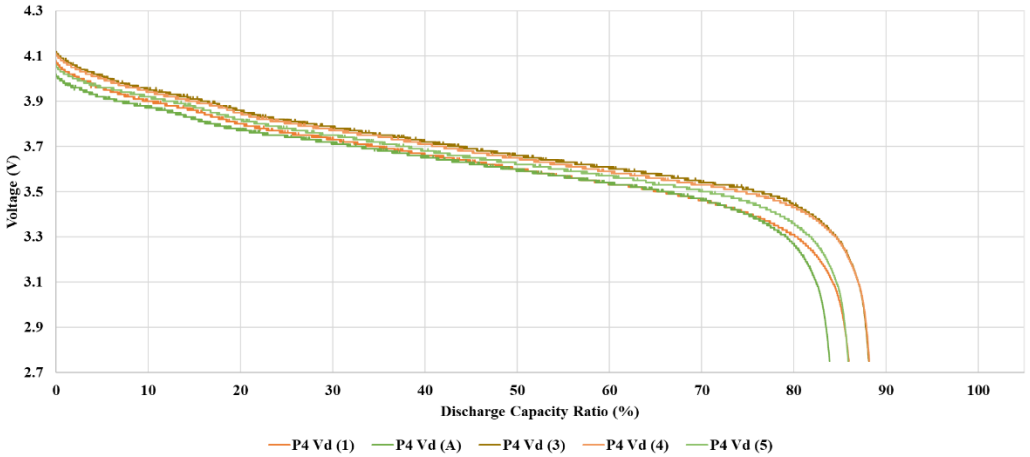

(g) P3 discharge capacity ratios

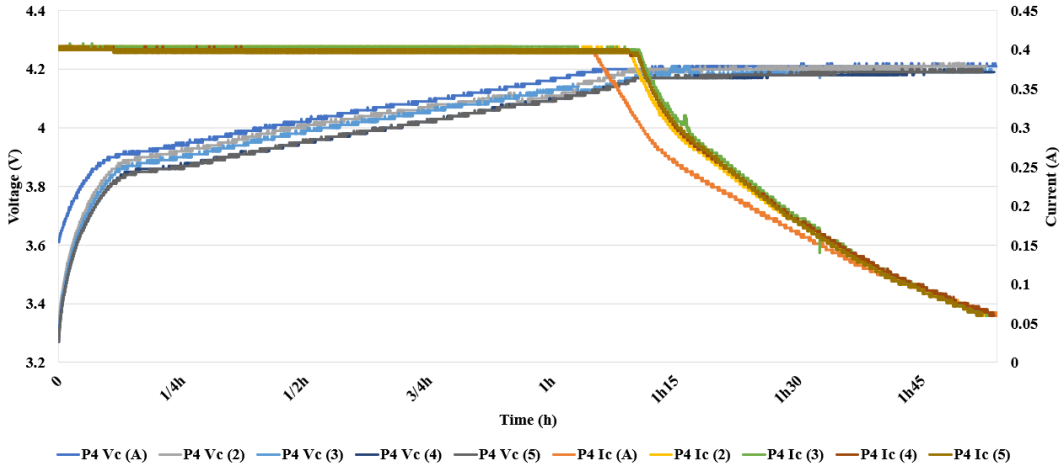

(h) P3 full charge cycles

Chapter VI

Conclusion

VII. Conclusion

The *Ceramic* type of battery looks to be a good area for development and application in space, especially whit the features that can be provided as safety, the main concern for many users. Finally, due to the exclusivity that has been given by the Japan Aerospace Exploration Agency (*JAXA*) to demonstrate for the first time the *Sulfide type* in space to achieve the targets for application to future planetary exploration missions.

The commercial Solid-State batteries, *Oxide type*, as a sample of *Ceramic*-based batteries, selected for the present study have been evaluated carefully, first the *Ceramic* type of battery has been compared to different battery technology including the *Polymer* type following an engineering approach for the feasibility study of the Solid-State Lithium-Ceramic-Battery' application on small satellite presented in ***Chapter III***. Then, following a long evaluation process of ground environmental testing described in detail in ***Chapter IV***. The process has included vibration and shock tests for evaluating the hostile launch environment conditions, finally, vacuum and thermal vacuum tests for the *space environment* at Low-Earth-Orbit. According to the *ISO standard 19683:2017(E)*, the radiation test may be optional depending on the satellite mission orbit; however, it will be better to be included according to other orbit or missions, a proposition of procedure has been included within the present study for future investigation.

During the proposed engineering study, a set of different batteries' technology has been compared in terms of the compromise between the capacity, the volume, and the weight in order to propose a solution for the power storage challenge for small satellites. Then, the impact of those batteries on a real satellite case study has been presented with focusing on the new advanced battery technology based on the Lithium-Solid-State-Ceramic.

Using the Solid-State-Ceramic battery may have a good impact on the small satellite design especially with the Nanosatellites. Taking into account their pouch design, the wide operating temperature range, finally the safety with no liquid inside, the electrical power system may be on one side simpler with no need for a complex arrangement, and on another side, it may be seen as improved with the high performances of the new batteries' technology.

Another outcome of the study has been related to the temperature in orbit, the Solid-State Lithium-Ceramic-Battery could have their part to improve and optimize the thermal management. The heater consumption optimization may be done in two ways, one is reducing the heater consumption by reducing the maximum power by increasing the temperature range of the battery as for the Solid-State Lithium-

Ceramic-Battery to -20°C even -40°C, which leads to reducing the worktime of the heater. It may require good monitoring of temperature in orbit, to power on the heater at a certain level of temperature and then keep it at much lower until the end of the eclipse. Or using a different approach with new material for the structure, as the Carbon Fiber Reinforced Plastic that has shown a good temperature inside the satellite around 9°C.

Otherwise, the optimization for the use of heaters during the eclipse may need more investigation, as the next step, the actual Solid-State Lithium-Ceramic-Battery should be tested under different low temperature, before proceeding with their real integration within a demonstration mission in orbit.

So far, the results from the evaluation within the *launch environment* conditions for the Solid-State Lithium-Ceramic-Battery show that all batteries have not been affected by the high shock and the high vibration level and could withstand the *launch environment* successfully; at least it could notice on the comparison between the capacity before and after the test that the batteries do not show any significant degradation which 83% of Solid-State Lithium-Ceramic-Battery tested could be able to keep their capacity with 95%, which means in another way that all PLCB01 and two PLCB02 have passed the *launch environment* evaluation, so far within the limits. Additionally, they have not shown any physical degradation [***24***].

The Solid State-Ceramic batteries evaluated under the vacuum and the thermal vacuum conditions, with ~2% mean loss of capacity after all test, have been able to demonstrate their ability to maintain their performances under several cycles of thermal vacuum with a hot temperature reaching +60°C, and a good stability for operating under such as high temperature compared to the other *Lithium Cobalt Oxide* (LiCoO2) batteries which are very reactive and suffer from poor thermal stability. For a low temperature around -20°C, the result shows that the Lithium Ceramic Battery (PLCB) could operate normally with a mean loose of the capacity of ~12%, so far without affecting their performances or showing any physical degradation, which may lead to reduce using heaters and power consumption on small satellite compared to the conventional Lithium-Ion battery [***13***].

Another key parameter, such as the internal resistance, the PLCB have shown no significant change and good stability with ~4% [***13***].

A guideline summarizing all the main steps for the battery's ground testing from the *launch* to the *space environment* including the main criteria which may be used for the evaluation of results and discussion after the two environment tests have been presented. Finally, a procedure for the radiation test under the *Gamma-ray* has been proposed in order to be used for future tests and evaluations.

The *Modular-Wall-Battery* (*MWB*) looks to be a good solution for the challenge that the Nanosatellites are facing, with the limited size and lack of power. The approach of combined the modular philosophy with the Solid-State-Ceramic battery pouch/*laminated* design shows an increase in capacity provided for the satellite system, the battery can be customized by the user for its modular cells, finally, with the specific features that the *Ceramic* battery is characterized, with the ability to operate under very low temperature reaching -20°C for the *Oxide*, even more, -40°C for the *Sulfide* (prototype), due to its solid *Ceramic* electrolyte that solved the issue of the low temperature, additionally to be good for the high temperature.

Moreover, with the *laminated* FLCB packs, using several cells in parallel within each pack may increase the reliability of the packs, additionally to the redundancy of the packs too.

It may be a good solution for the attitude control challenge and the mechanical design with the center of gravity, the symmetric design gives a good weight's distribution on the panel. Batterie packs may be not affecting anymore the attitude stability of the satellite; however, they should be still included within the calculation of the center of gravity.

The *MWB* is not limited to only the *Ceramic* battery technology but it is flexible to any other battery that can fulfil the requirements. It can be generalized and adopted for any pouch cell *laminated* battery design as well as the Solid-State-battery *Polymer* or *Ceramic* (*Oxide* or *Sulfide*).

Concerning the increase in weight that may be the big challenge with the application of the *MWB* on Nanosatellites, ***Fig V-19*** represents the estimated total weight for different CubeSats sizes related to their maximum limits required by *JAXA* and *NASA*, including a full design with the conventional Lithium-Ion batteries, it is showing the available margin that can be used to reach the maximum limit which is 12.67Kg for 1U, 10.01Kg for 3U, and 6,02Kg 6U. The *MWB* has to be flexible in terms of limited weight for Nanosatellites.

The simulation of the *Modular-Wall-Battery* including the proposed battery pack as a sample could present, so far, good results, as has been presented for a 1U CubeSat configuration, with using six packs (three main packs, and three redundant packs). The remaining capacity at the low temperature (-20°C) could be from 33% to 67% of the total capacity including the three packs, which may be considered as a good step in comparison with the conventional Lithium-Ion batteries. Finally, the remaining capacity for the three packs combined was more than 50%, with 1368.9 mAh to 2019.6 mAh, respectively. It could be almost the same for the two temperature levels +20°C and +60°C.

Since the proposed battery pack may be integrated onboard Nanosatellite, and in order to prevent any malfunction or decrease in its performances due to the gradient of temperature, some solutions may be proposed: **First**, the same approach used by the company for the PLCB battery, while the results in ***Chapter IV*** showed a good result, the coating used by the company may be has a positive effect on the isolation and protection of the battery from the external environment. **Second**, based on the material used for the battery packing, several services may be proposed for this purpose, the *Aluminum Laminate Film* is the most used to build a sealing battery packing for the Lithium battery pouch design [***131***]. **Finally**, using a material for the heat transfer, the *Lamda* (λ) Gel may be proposed [***76***], however, this approach may need further tests and analysis.

Moreover, with the thermal analysis and research ongoing with the amelioration and improvement of the optical and thermal properties of the surfaces, many alternative solutions may be found.

After the *launch* and the *space environment*, ground evaluation test has been done successfully, the next step is an orbit demonstration of the Solid-State-Ceramic battery on a real application onboard a Low-Earth-Orbit small satellite, in which the battery will be able to be tested at the real conditions during more than one year in orbit.

As the selected battery technology for the *MWB* concept has already been evaluated in ***Chapter IV***, the evaluation of the battery technology, with showing so far good results, the selected battery may be adopted to a Nanosatellite following the conventional integration into the BUS system.

However, for the *MWB* concept integration within Nanosatellites, while using the customized pack, the integration may need to wait for further investigations which may be published later in subsequent publication until the real test will be done onboard a Nanosatellite, this one for further analysis, as well as for comparison reason with in-orbit results.

As **future works**, the Solid-State-Ceramic battery may be tested under the *radiation environment* first, as was suggested in ***Chapter IV*** for the high and low irradiation for Low-Earth-Orbit application and the planetary mission, following the proposed dose levels according to the procedure. The same battery technology may be subject to a ground test evaluation for a lower temperature levels, more than -20°C, as a potential use for planetary mission and deep space exploration as well as the *Modular-Wall-Battery* concept.

The *Modular-Wall-Battery* concept will be tested within the vibration test environment including a Nanosatellite structure, the results will be used for

confirmation of the structural analysis and the natural frequencies calculation done in ***Chapter V***. Then, it may be integrated onboard a future Nanosatellite as the first demonstration of the concept in real conditions.

The selected battery for the mission demonstration may be the same one evaluated within the present work or another Solid-State-Battery that could fulfil the requirements listed by the concept, as well as its ability to withstand the *launch environment*, finally, the ability to work under the *space environment* without degradation on its performances.

However, the *MWB* approach is planned to be tested in orbit. One pack of FLCB 810 mAh or more will be included to the one of the mission objectives of the Nanosatellites.

The mission demonstration will have the following objectives:

- Integration of the *MWB* in Nanosatellite (1U to 6U).
- Application of the *MWB* approach under the real condition in space.
- The operation at high and low temperature (*MWB* will be put on the wall very close to the external *space environment*).

Batteries will be charged and discharged using a mission board designed for this purpose presented by the author in the work entitled: "*One Step Away from The Reliable Batteries for Small Spacecrafts with Solid-State-Ceramic Batteries*" which the preliminary mission board design has been described [***132***].

All the results from the in-orbit engineering demonstration shall be analyzed and compared to other battery technology, as well as the *MWB* simulation and the Solid-State-Ceramic-*Sulfide* battery, waiting for the final selection of battery that can be integrated with the *Modular-Wall-Battery* philosophy as a final main battery for the next Nanosatellite generation.

End of the document

References

1. *Martin N. Sweeting. (2018). Modern Small Satellites-Changing the Economics of Space. Proceedings of the IEEE, 106(3), 343–361. https://doi.org/10.1109/JPROC.2018.2806218*
2. *Hyun, C. D., Choi, W. S., Kim, M. K., Kim, J. H., Sim, E., & Kim, H. D. (2019). High-Resolution Image and Video CubeSat (HIREV): Development of space technology test platform using a low-cost CubeSat platform. International Journal of Aerospace Engineering, 2019. https://doi.org/10.1155/2019/8916416*
3. *Erik Kulu, Nanosats Database. Available online: https://www.nanosats.eu/ , accessed on 07 January 2020.*
4. *Cho, M., Hirokazu, M., & Graziani, F. (2015). Introduction to lean satellite and ISO standard for lean satellite. RAST 2015 - Proceedings of 7th International Conference on Recent Advances in Space Technologies, 789–792. https://doi.org/10.1109/RAST.2015.7208447*
5. *POLANSKY, J., & CHO, M. (2016). Classification of Countries Worldwide according to Satellite Activity Level. Transactions of the Japan Society for Aeronautical and Space Sciences, Aerospace Technology Japan, 14(ists30), Pv_7-Pv_16. https://doi.org/10.2322/tastj.14.pv_7*
6. *Polansky, J. L., & Cho, M. (2016). A university-based model for space-related capacity building in emerging countries. Space Policy, 36. https://doi.org/10.1016/j.spacepol.2016.01.001*
7. *G. Capovilla, E. Cestino, L. M. Reyneri, &, G. Romeo (2020). Modular multifunctional composite structure for cubesat applications: Preliminary design and structural analysis. Aerospace, 7(2), 1–15. https://doi.org/10.3390/aerospace7020017*
8. *Rafael. B., Rodriguez. A. R., Apia. I. F. A. T., Rakami. N. U., & Sami. K. A. (2019). Radiation Effects Tolerances in different COTS Micro-Computers Architectures for a Nano-Satellite Mission, The International Symposium on Space Technology and Science (ISTS) 31, 2019-f-93, 2019.*
9. *Surrey Satellite Technology Ltd. Available online: https://www.sstl.co.uk/media-hub/images/dot-1/dot-1-raspberry-pi-image-of-earth accessed on 4 April 2020.*
10. *The Raspberry Pi Foundation official website, Available online: https://www.raspberrypi.org/blog/raspberry-pi-in-space/, accessed on 26 January 2021.*
11. *Elmegharbel. H. A., Kishimoto. M., Orger. N. C., R-schulz. V., Rahmatillah. R., Teramoto. M., Cho. M., Chow. C. L., Tse, M. S., & Li, H (2020). IONOSPHERE MEASUREMENT: POINT-TO-POINT TOTAL ELECTRON CONTENT ESTIMATION USING UHF INTER-SATELLITE RANGING FOR CUBESAT CONSTELLATION. Proceedings of the 71st International Astronautical Congress – The CyberSpace Edition, IAC, Paper ID 56349, 2020-October.*
12. *Bugryniec, P. (2016). CubeSat: The Need for More Power to Realise Telecommunications Overview of CubeSats Aims & Objectives (Issue June). Available online: http://www.energystorage-cdt.ac.uk/outputs/cohort-2/Bugryniec+mini+project+report.pdf*
13. *Limam L, Hatanaka K, Gonzalez-Llorente J, Chikashi T, Maeda C, Okuyama K-I, "Space Environment Evaluation Test of Solid-State-Ceramic Battery Advanced Energy Storage Under Vacuum and Thermal Vacuum", International Review of Aerospace Engineering (IREASE), 13 (2), pp. 68-79, 2020.* https://doi.org/10.15866/irease.v13i2.18582

14. *M. Langer and J. Boumeester, Reliability of CubeSats – Statistical Data, Developers' Beliefs and the Way Forward, 30th Annual. AIAA/USU Conference of Small Satellite, Logan, UT, paper ID: SSC16-X-2, pp. 1–12, August 2016.*
15. *J. Gonzalez-Llorente, D. Rodriguez-Duarte, S. Sanchez-Sanjuan, and A. Rambal-Vecino, Improving the efficiency of 3U CubeSat EPS by selecting operating conditions for power converters, 2015 IEEE Aerospace Conference, vol. 2015-June. March 2015.* https://doi.org/10.1109/AERO.2015.7119122
16. *I. Vertat and A. Vobornik, Efficient and reliable solar panels for small CubeSat picosatellites, International Journal of Photoenergy, vol. 2014, pp. 8, 2014.* https://doi.org/10.1155/2014/537645
17. *S. A. Ibrahim and E. Yamaguchi, Comparison of Solar Radiation Torque and Power Generation of Deployable Solar Panel Configurations on Nanosatellites, Journal of Aerospace (MDPI), vol. 6, no. 5, pp. 50, 2019.* https://doi.org/10.3390/aerospace6050050
18. *Clark, C. S., & Mazarias, A. L. (2006). Power system challenges for small satellite missions. European Space Agency, (Special Publication) ESA SP, 625 SP.*
19. *G. A. Landis, Tabulation of power-related satellite failure causes, 11th International Energy Conversion Engineering Conference, July 2013.* https://doi.org/10.2514/6.2013-3736
20. *NASA. (2020). State-of-the-Art Small Spacecraft Technology | NASA: Vol. NASA/TP—20 (Issue October).* https://www.nasa.gov/sites/default/files/atoms/files/2020soa_final.pdf
21. *M. Smart, J. Castillo, and T. Yi, NASA's Technical Report, Energy Storage Technologies for Future Planetary Science Missions, issue December, pages 65, 2017.* https://solarsystem.nasa.gov/resources/549/energy-storage-technologies-for-future-planetary-science-missions/
22. *Xin-Rui Li, H. Koseki, Thermal Analysis on Lithium Primary Batteries, International Review of Energy Conversion (I.R.E.CON), vol. 2, no. 4, 2014.*
23. *Dongxu Ouyang, Mingyi Chen, Jian Wang, Que Huang, Jingwen Weng, Zhi Wang, Jian Wang, A Review on the Thermal Hazards of the Lithium-Ion Battery and the Corresponding Countermeasures, Journal of Applied Sciences (MDPI), vol. 9, no. 12, pp. 2483, 2019.* https://doi.org/10.3390/app9122483
24. *Limam, L., Hatanaka, K., Gonzalez-Llorente, J., Miyazaki, M., Chikashi, T., Okuyama, K., Launch Environment Ground Test Evaluation with Multi-axis Vibration and Shock for Pouch Solid-State-Ceramic Battery Advanced Energy Storage, (2020) International Review of Aerospace Engineering (IREASE), 13 (4), pp. 126-134.* https://doi.org/10.15866/irease.v13i4.18949
25. *B. Mckissock, P. Loyselle, E. Vogel, Guidelines on Lithium-ion Battery Use in Space Applications, NASA Center for AeroSpace Information, May 2009.* https://ntrs.nasa.gov/archive/nasa/casi.ntrs.nasa.gov/20090023862.pdf
26. *L. Zhang, Z. Ning, H. Peng, Z. Mu, & C. Sun, Effects of vibration on the electrical performance of Lithium-ion cells based on mathematical statistics. Journal of Applied Sciences (MDPI), vol. 7, no. 8, pp. 802, 2017.* https://doi.org/10.3390/app7080802
27. *M.J. Brand, S.F. Schuster, T. Bach, E. Fleder, M. Stelz, S. Gläser, J. Müller, G. Sextl, A. Jossen, Effects of vibrations and shocks on lithium-ion cells, Journal of Power Sources (Elsevier), vol. 288, pp. 62-69, 2015.* https://doi.org/10.1016/j.jpowsour.2015.04.107
28. *J.M. Hooper, J. Marco, G.H. Chouchelamane, J.S. Chevalier, D. Williams, Multi-axis vibration durability testing of lithium-ion 18650 NCA cylindrical cells, Journal of Energy Storage (Elsevier), vol 15, pp. 103-123, 2018.* https://doi.org/10.1016/j.est.2017.11.006

29. *J.M. Hooper, J. Marco, G.H. Chouchelamane, C. Lyness, Vibration durability testing of nickel manganese cobalt oxide (NMC) lithium-ion 18,650 battery cells, Journal of Energies (MDPI), vol 9, n.1, pp. 52, 2016.* https://doi.org/10.3390/en9010052
30. *Zhang L, Ning Z, Peng H, Mu Z, & Sun C, Effects of vibration on the electrical performance of Lithium-ion cells based on mathematical statistics. Journal of Applied Sciences (MDPI), vol 7, n.8, pp. 802, 2017.* https://doi.org/10.3390/app7080802
31. *G. Kjell, J.F. Lang, Comparing different vibration tests proposed for li-ion batteries with vibration measurement in an electric vehicle, 2014 IEEE Conference: Electric Vehicle Symposium and Exhibition (EVS27), pp. 1-11, 2014.* https://doi.org/10.1109/EVS.2013.6914869
32. *K-H. Park, & K-H. Yi, Space Qualification of Small Satellite Li-ion Battery System for the Secured Reliability. Journal of the Korean Society for Aeronautical & Space Sciences, vol. 42, n.4, pp. 351–359, 2014.* https://doi.org/10.5139/jksas.2014.42.4.351
33. *S. Remy, S. Lawson, S. Lefeuvre, E. Mosset, & M. Nestoridi, Qualification and Life Testing of Li-Ion Ves16 Batteries. E3S Web of Conferences, 16(1), 17009, 2017.* https://doi.org/10.1051/e3sconf/20171617009
34. *J. Kim, P.Y. Lee, C.O. Youn, W. Na, M. Jang, Environmental tests and evaluations of variable 18650 cylindrical Li-Ion cells for space cell's qualification establishment, 2017 IEEE Energy Conversion Congress and Exposition (ECCE), pp. 1010-1015, 2017.* https://doi.org/10.1109/ECCE.2017.8095897
35. *Z. Cameron, C.S. Kulkarni, A.G. Luna, K. Goebel, S. Poll, A battery certification testbed for small satellite missions, 2015 IEEE Auto Test Conference, 2015-December, pp. 162-168, 2015.* https://doi.org/10.1109/AUTEST.2015.7356483
36. *M. Alkali, M. Y. Edries, and A. R. Khan, Design Considerations and Ground Testing of Electric Double-Layer Capacitors as Energy Storage Components for Nanosatellites, Journal of Small Satellites, vol. 4, no. 2, pp. 387–405, 2015.*
37. *K. C. Chin, N. W. Green, and E. J. Brandon, Evaluation of supercapacitors for space applications under thermal vacuum conditions, Journal of Power Sources (Elsevier), vol. 379, pp. 155-159, 2018.* https://doi.org/10.1016/j.jpowsour.2018.01.038
38. *I. Fajardo et al., Design, Implementation, and Operation of a Small Satellite Mission To Explore the Space Weather Effects in Leo, Journal of Aerospace (MDPI), vol. 6, n. 10, pp. 108, 2019.* https://doi.org/10.3390/aerospace6100108
39. *J. Gonzalez-Llorente, A. A. Lidtke, K. Hatanaka, R. Kawauchi, and K.-I. Okuyama, Solar Module Integrated Converters as Power Generator in Small Spacecrafts: Design and Verification Approach, Journal of Aerospace (MDPI), vol. 6, no. 5, pp. 61, 2019.* https://doi.org/10.3390/aerospace6050061
40. *Bendoukha, S., Tapia, I., Okuyama, K., Cho, M., An Experimental and Theoretical Study of Spatial Langmuir Probe Plasma System for a Small Lean Satellite Called Ten-Koh, (2019) International Review of Aerospace Engineering (IREASE), 12 (3), pp. 131-140.* https://doi.org/10.15866/irease.v12i3.15927
41. *Gonzalez-Llorente J, Lidtke A-A, Hatanaka K, Limam L, Fajardo I, and Okuyama K.-I, "In-orbit feasibility demonstration of supercapacitors for space applications," Acta Astronautica., vol. 174, pp. 294–305, 2020.* https://doi.org/10.1016/j.actaastro.2020.05.007
42. *M. Nestoridi and H. Barde, Beyond Lithium-Ion: Lithium- Sulphur Batteries for Space?, E3S Web Conference, vol. 16, no. 1, pp. 2-6, 2017.* https://doi.org/10.1051/e3sconf/20171608005

43. *Ma, S., Jiang, M., Tao, P., Song, C., Wu, J., Wang, J., Deng, T., & Shang, W. (2018). Temperature effect and thermal impact in lithium-ion batteries: A review. Progress in Natural Science: Materials International, 28(6), 653–666. https://doi.org/10.1016/j.pnsc.2018.11.002*
44. *McKissock, B., Loyselle, P., & Vogel, E. (2009). Guidelines on Lithium-ion battery use in space applications. In NASA Engineering and Safety Center Technical Report (Issue May). http://ntrs.nasa.gov/archive/nasa/casi.ntrs.nasa.gov/20090023862.pdf*
45. *Gave, G., Borthomieu, Y., Lagattu, B., & Planchat, J. P. (2004). Evaluation of a low temperature Li-ion cell for space. Acta Astronautica, 54(8), 559–563. https://doi.org/10.1016/j.actaastro.2003.06.001*
46. *K. Takada, Progress in solid electrolytes toward realizing solid-state lithium batteries, Journal of Power Sources (Elsevier), vol. 394, pp. 74-85, 2018.*
47. *Battery University, https://batteryuniversity.com/, accessed on 01 September 2020.*
48. *Nestler, T., Schmid, R., Münchgesang, W., Bazhenov, V., Schilm, J., Leisegang, T., & Meyer, D. C. (2014). Separators - Technology review: Ceramic based separators for secondary batteries. In AIP Conference Proceedings (Vol. 1597, Issue February 2015). https://doi.org/10.1063/1.4878486*
49. *J. W. Fergus, Ceramic and polymeric solid electrolytes for lithium-ion batteries, Journal Power Sources (Elsevier), vol. 195, no. 15, pp. 4554-4569, 2010. https://doi.org/10.1016/j.jpowsour.2010.01.076*
50. *Li, X., Koseki, H., Thermal Analysis on Lithium Primary Batteries, (2014) International Journal on Energy Conversion (IRECON), 2 (4), pp. 133-136. https://doi.org/10.1016/j.jpowsour.2018.05.003*
51. *Dongxu Ouyang, Mingyi Chen, Jian Wang, Que Huang, Jingwen Weng, Zhi Wang, Jian Wang, A Review on the Thermal Hazards of the Lithium-Ion Battery and the Corresponding Countermeasures, Journal of Applied Sciences (MDPI), vol. 9, no. 12, pp. 2483, 2019. https://doi.org/10.3390/app9122483*
52. *J. G. Kim, B. Son, S. Mukherjee, N. Schuppert, A. Bates, O. Kwon, M. J. Choi, H. Y. Chung, & S. Park (2015). A review of lithium and non-lithium based solid-state batteries. Journal of Power Sources, 282, 299–322. https://doi.org/10.1016/j.jpowsour.2015.02.054*
53. *Feng, J. K., Lu, L., & Lai, M. O. (2010). Lithium storage capability of lithium-ion conductor Li1.5Al 0.5Ge1.5(PO4)3. Journal of Alloys and Compounds, 501(2), 255–258. https://doi.org/10.1016/j.jallcom.2010.04.084*
54. *Deng, D. (2015). Li-ion batteries: Basics, progress, and challenges. Energy Science and Engineering, 3(5), 385–418. https://doi.org/10.1002/ese3.95*
55. *X. Wang, Y. Sone, and S. Kuwajima, Effect of operation conditions on simulated low-earth orbit cycle-life testing of commercial lithium-ion polymer cells, Journal of Power Sources (Elsevier), vol. 142, no. 1-2, pp. 313-322, 2005. https://doi.org/10.1016/j.jpowsour.2004.10.014*
56. *C. S. Clark and E. Simon, Evaluation of Lithium Polymer Technology for Small Satellite Applications, 21st Annual. AIAA/USU Conference of Small Satellite, paper ID: SSC07-X-9, August, pp. 1–11, 2007.*
57. *N. Navarathinam, R. Lee, and H. Chesser, Characterization of Lithium-Polymer batteries for CubeSat applications, Journal Acta Astronautical (Elsevier), vol. 68, no. 11-12, pp. 1752-1760, 2011. https://doi.org/10.1016/j.actaastro.2011.02.004*
58. *Monteiro J. P, Rocha R. M, Silva A, Afonso R, & Ramos N, Integration and verification approach of ISTSat-1 CubeSat. Journal of Aerospace (MDPI), vol 6, n. 12, 2019. https://doi.org/10.3390/aerospace6120131*

59. *J. Claricoats, S.M. Dakka, Design of Power, Propulsion, and Thermal Sub-Systems for a 3U CubeSat Measuring Earth's Radiation Imbalance, Journal of Aerospace (MDPI), Vol. 5, n. 2, pp. 63, 2018. https://doi.org/10.3390/aerospace5020063*
60. *G. Kissel, R. Loehrlein, N. Kalsch, W. Helms, Z. Snyder, S. Kaphle, UNITE CubeSat: From Inception to Early Orbital Operations, Small Satellite Conference, Utah State University, Logan, UT, article ID SSC19-WKI-08, 2019.*
61. *Scott Higginbotham, MissidAManager, NASA KSC VA — C, FCC's report, Orbital Debris Assessment for The CubeSats on the CRS OA—10/ELaNa—21 Mission, 2018. https://fcc.report/ELS/Old-Dominion-University/0255-EX-CN-2018/217003*
62. *J. Oyola Alvarado, J. Rodríguez Mora, Designs and Implementations for CubeSat Colombia 1 Satellite Power Module, International Journal of Applied Engineering Research, vol. 12, n. 18, pp. 7360–7371, 2017.*
63. *Burt Robert, Distributed Electrical Power Systems in Cubesat Application, Master's Thesis, Master of Science in Electrical engineering, Utah State University, Logan, UT, USA, December 2011.*
64. *The Faraday Institution. (2020). Solid-State Batteries: The Technology of the 2030s but the Research Challenge of the 2020s. June 2006. https://faraday.ac.uk/wp-content/uploads/2020/04/Faraday-Insights-5_Updated.pdf*
65. *Shimada, T., Hoshino, T., Naito, H., & Shimada, S. (2017), Development of all-individual lithium-ion secondary batteries. Presented at the 36th ISAS Space Energy Symposium, 24th February, 2017Available online: http://id.nii.ac.jp/1696/00007845/ accessed on 9 March 2021.*
66. *Prologium Company website: http://www.prologium.com/, accessed on 07 January 2020.*
67. *A.Y. Yu Miao, Patrick Hynan, Annette von Jouanne, Current Li-Ion Battery Technologies in Electric Vehicles and Opportunities for Advancements, Journal of Energies (MDPI), vol. 12, n. 6, pp. 1074, 2019. https://doi.org/10.3390/en12061074*
68. *Ren, Y., Chen, K., Chen, R., Liu, T., Zhang, Y., & Nan, C. W. (2015). Oxide Electrolytes for Lithium Batteries. Journal of the American Ceramic Society, 98(12), 3603–3623. https://doi.org/10.1111/jace.13844*
69. *Xin-Rui Li, H. Koseki, Thermal Analysis on Lithium Primary Batteries, International Review of Energy Conversion (I.R.E.CON), vol. 2, no. 4, 2014.*
70. *Japan Aerospace Exploration Agency (JAXA), Press Release, Available online: https://global.jaxa.jp/press/2021/02/20210202-1_e.html accessed on 9 March 2021.*
71. *Keiichi Okuyama-Lab. Available online: http://kit-okuyama-lab.com/en/ten-koh/ accessed on 1 April 2020*
72. *Bendoukha, S. A., Okuyama, K. I., Bianca, S., & Nishio, M. (2016). Control System Design of an Ultra-small Deep Space Probe. Energy Procedia, 100(September), 537–550. https://doi.org/10.1016/j.egypro.2016.10.216*
73. *Fajardo, I., Bendoukha, S. A., Okuyama, K. I., González-Llorente, J., Saganti, P., & Limam, L. (2019). Development of a set of instruments for a small satellite mission to observe the LEO environment in the presence of a decreasing solar cycle. Proceedings of the International Astronautical Congress, IAC, 2019-Octob(June).*
74. *Sidi, B., Bendoukha, A., Tapia, I. F., & Okuyama, K. (2019). Double Langmuir Probe System Measurements For Nanosatellite in LEO Plasma. 1–7.*
75. *Abdullah, F., Okuyama, K., Fajardo, I., & Urakami, N. (2020). In Situ Measurement of Carbon Fiber / Polyether Ether Ketone Thermal Expansion in Low Earth Orbit. 1–24. https://doi.org/10.3390/aerospace7040035 https://doi.org/10.15866/irease.v13i4.18949*
76. *αGEL Solution (Heat Dissipation) (taica.co.jp) Available online: https://taica.co.jp/gel/en/solution/thermal_interface_material.html accessed on 16 February 2021.*

77. *αGEL Industries (Automotive) (taica.co.jp) Available online: https://taica.co.jp/gel/en/application/automotive.html accessed on 16 February 2021.*
78. *Chow, C., Zhang, Y., Tse, M., Li, K., Aheieva, K., Rahmatillah, R., Ninagawa, R., Adebolu, I., Kim, S., Kakimoto, Y., Yamauchi, T., Masui, H., and Cho, M.: Overview of Project SPATIUM – Space Precision Atomic-clock Timing Utility Mission, Small Satellite Conference, Paper ID SSC19-WKVII-07, 2019. https://digitalcommons.usu.edu/smallsat/2019/all2019/123*
79. *Nanosatellite & CubeSat Database. Available online: https://www.nanosats.eu/sat/horyu-2 accessed on 12 March 2020.*
80. *OKADA, K., SERI, Y., SHIBAGAKI, R., Satellite Project, K., MASUI, H., & CHO, M. (2014). Ground Tests and In-Orbit Results for the Horyu-II Nanosatellite Power System. Transactions of the Japan Society for Aeronautical and Space Sciences, Aerospace Technology Japan, 12(ists29), Tf_49-Tf_56. https://doi.org/10.2322/tastj.12.tf_49*
81. *EDRIES, M. Y., TANAKA, A., & CHO, M. (2016). Design and Testing of Electrical Power Subsystem of a Lean Satellite, HORYU-IV. Transactions of the Japan Society for Aeronautical and Space Sciences, Aerospace Technology Japan, 14(ists30), Pf_7-Pf_16. https://doi.org/10.2322/tastj.14.pf_7*
82. *Nanosatellite & CubeSat Database. Available online: https://www.nanosats.eu/sat/horyu-4 accessed on 12 March 2020.*
83. *Nanosatellite & CubeSat Database. Available online: https://www.nanosats.eu/sat/equisat accessed on 12 March 2020.*
84. *BROWN SPACE ENGINEERING. Available online: https://brownspace.org/power/ accessed on 12 March 2020.*
85. *Ampatzoglou, A., & Kostopoulos, V: Design, analysis, optimization, manufacturing, and testing of a 2U CubeSat, International Journal of Aerospace Engineering, 2018. https://doi.org/10.1155/2018/9724263*
86. *Nanosatellite & CubeSat Database. Available online: https://www.nanosats.eu/sat/estcube-1 accessed on 1 April 2020*
87. *Pajusalu, M., Ilbis, E., Ilves, T., Veske, M., Kalde, J., Lillmaa, H., Rantsus, R., Pelakauskas, M., Leitu, A., Voormansik, K., Allik, V., Lätt, S., Envall, J., & Noorma, M. (2014). Design and pre-flight testing of the electrical power system for the ESTCube-1 nanosatellite. Proceedings of the Estonian Academy of Sciences, 63(2S), 232–241. https://doi.org/10.3176/proc.2014.2S.04*
88. *Yamagata, M., Tanaka, K., Tsuruda, Y., Sone, Y., Fukuda, S., Nakasuka, S., Kono, M., & Ishikawa, M.: The first lithium-ion battery with ionic liquid electrolyte demonstrated in extreme environment of space. J. Electrochemistry, 83(10), 918–924, 2015. https://doi.org/10.5796/electrochemistry.83.918*
89. *Nanosatellite & CubeSat Database. Available online: https://www.nanosats.eu/sat/istsat-1 accessed on 12 March 2020.*
90. *Monteiro, J. P., Rocha, R. M., Silva, A., Afonso, R., & Ramos, N. (2019). Integration and verification approach of ISTSat-1 CubeSat. Aerospace, 6(12). https://doi.org/10.3390/aerospace6120131*
91. *Clark, C. S., & Simon, E. (2007). Evaluation of Lithium Polymer Technology for Small Satellite Applications. 21st Annual AIAA/USU Conference on Small Satellites, August, 1–11.*
92. *Clark, C. (2010). Huge Power Demand...Itsy-Bitsy Satellite: Solving the CubeSat Power Paradox. 24th Annual AIAA/USU Conference on Small Satellites, August, 1–8.*
93. *Garzón, A., & Villanueva, Y. A. (2018). Thermal analysis of satellite Libertad 2: A guide to CubeSat temperature prediction. Journal of Aerospace Technology and Management, 10. https://doi.org/10.5028/jatm.v10.1011*

94. *S. Asada, N. Abe, SSC03-II-4 Launching Small Satellites on the H-IIA Rocket, pp. 1–6, Small Satellite Conference, Utah State University, Logan, UT, article ID SSC03-II-4, 2003.*
95. *Mitsubishi Heavy Industries Ltd, H2A Rocket User's Manual Ver.4.0, February 2015.*
96. *Center on Nanosatellite Testing, Kyutech, https://kyutech-cent.net/activity_e.html, accessed on 24 August 2020.*
97. *H. Masui, T. Hatamura, M. Cho, Testing of Micro / Nano Satellites and Their On-orbit Performance, 27th Annual AIAA/USU Conference of Small Satellite, Logan, UT, paper ID: SSC13-WK-8, pp. 1-7, 2013.*
98. *Ryunosuke Shibaki, Development and Verification of Power System for High Voltage Technology Demonstration Satellite "Horyu 2", Master's Thesis, The Kyushu Institute of Technology, Kitakyushu, Japan, 2011.*
https://kitsat.net/documents/shibagaki_part5.pdf
99. *ECSS. (2002). Space engineering testing ECSS-E-10-03A (Issue February).*
https://eop-cfi.esa.int/Repo/PUBLIC/DOCUMENTATION/SYSTEM_SUPPORT_DOCS/ECSS Standards for Ground Segments/ECSS-E-10-03A Testing .pdf
100. *Thomé, L., Moll, S., Debelle, A., Garrido, F., Sattonnay, G., & Jagielski, J. (2012). Radiation effects in nuclear ceramics. Advances in Materials Science and Engineering, 2012(November 2015).*
https://doi.org/10.1155/2012/905474
101. *Linn W Hobbs, Frank W Clinard Jr, Steven J. Zinkle, Rodney C Ewing. (1994). Radiation effects in ceramics. Journal of Nuclear Materials - Elsevier, 216, 291–321.*
102. *Tan, C., Lyons, D. J., Pan, K., Leung, K. Y., Chuirazzi, W. C., Canova, M., Co, A. C., & Cao, L. R. (2016). Radiation effects on the electrode and electrolyte of a lithium-ion battery. Journal of Power Sources, 318, 242–250.*
https://doi.org/10.1016/j.jpowsour.2016.04.015
103. *Qiu, J., He, D., Sun, M., Li, S., Wen, C., Hattrick-Simpers, J., Zheng, Y. F., & Cao, L. (2015). Effects of neutron and gamma radiation on lithium-ion batteries. Nuclear Instruments and Methods in Physics Research, Section B: Beam Interactions with Materials and Atoms, 345, 27–32.*
https://doi.org/10.1016/j.nimb.2014.12.058
104. *Essien Ewang, Akira Miyahara, and Arifur R. Khan, Photoelectron Current Measurement in Low Earth Orbit Using a Lean Satellite, HORYU-IV, International Review of Aerospace Engineering (I.RE.AS.E), vol. 10, n. 3,2017.*
https://doi.org/10.15866/irease.v10i3.12394
105. *JAXA, JAXA' Technical Standards, Spacecraft general test standard Handbook JERG-2-130-HB007A, Tokyo, 2017*
106. *Yamagata, M., Tanaka, K., Tsuruda, Y., Sone, Y., Fukuda, S., Nakasuka, S., Kono, M., & Ishikawa, M. (2015). The first lithium-ion battery with ionic liquid electrolyte demonstrated in extreme environment of space. Electrochemistry, 83(10), 918–924.*
https://doi.org/10.5796/electrochemistry.83.918
107. *Xapsos, M. A. (2017). New Approach to Total Dose Specification for Spacecraft Electronics.*
https://ntrs.nasa.gov/search.jsp?R=20170004853
108. *Flemming, H. (2001). DTU Satellite Systems and Design Course Cubesat Thermal Design.*
http://www.space.aau.dk/cubesat/documents/Cubesat_Thermal_Design.pdf
109. *Ratnakumar, B. V., Smart, M. C., Whitcanack, L. D., Davies, E. D., Chin, K. B., Deligiannis, F., & Surampudi, S. (2005). Behavior of Li-Ion Cells in High-Intensity Radiation Environments. Journal of The Electrochemical Society, 152(2), A357.*
https://doi.org/10.1149/1.1848212
110. *8-bit Microcontroller with 16/32K bytes of ISP Flash and USB Controller, Data Sheet, pp. 1–438, 2015.*

https://ww1.microchip.com/downloads/en/DeviceDoc/Atmel-7766-8-bit-AVR-ATmega16U4-32U4_Datasheet.pdf
111. "TP4056 1A Standalone Linear Li-Ion Battery Charger with Thermal Regulation in SOP-8," Data Sheet, p. 3, 2015. https://www.mikrocontroller.net/attachment/273612/TP4056.pdf
112. One Cell Lithium-ion/Polymer Battery Protection IC, "DW01-P-DS-10_EN Rev. 1.0", Data Sheet, pp. 1–11, 2006. https://cdn.sparkfun.com/assets/learn_tutorials/2/5/1/DW01-P_DataSheet_V10.pdf
113. 1.5A Single Resistor Rugged Linear Regulator with Monitors, Linear Technology, "Lt3081," Data Sheet, pp. 1–32, 2014. https://www.analog.com/media/en/technical-documentation/data-sheets/3081fc.pdf
114. INA21x Voltage Output, Low- or High-Side Measurement, Bidirectional, Zero-Drift Series, Current-Shunt Monitors, "INA21x", Data Sheet, pp .1-45, 2014. https://www.ti.com/lit/ds/sbos437j/sbos437j.pdf?ts=1614611086933&ref_url=https%253A%252F%252Fwww.google.co.kr%252F
115. Low Signal Relay, OMRON Corporation "G6A", pp. 1–9. https://omronfs.omron.com/en_US/ecb/products/pdf/en-g6a.pdf
116. G. Pistoia, Lithium-Ion Batteries: Advances and Applications, First edit, Elsevier B.V, pp. 664, 2014. https://doi.org/10.1016/C2011-0-09658-8
117. Samuel Russell, David Delafuente, Eric Darcy, Karla Bradley, Edgar O. Castro, and Lauri Hansen, NASA's Technical Standards. Crewed Space Vehicle Battery Safety Requirements, Houston, Texas, pp. 124, 2017. https://standards.nasa.gov/standard/jsc/jsc-20793
118. Tarascon, J. M., and Armand, M.: Issues and challenges facing rechargeable lithium batteries, J. Nature, 414(6861), 2001, 359–367. https://doi.org/10.1038/35104644
119. Capovilla, G., Cestino, E., Reyneri, L. M., & Romeo, G.: Modular multifunctional composite structure for cubesat applications: Preliminary design and structural analysis, J. Aerospace (MDPI), 7(2), 1–15, 2020. https://doi.org/10.3390/aerospace7020017
120. Japan Aerospace Exploration Agency (JAXA). JEM Payload Accommodation Handbook Small Satellite Deployment Interface Control Document. 8(March 2013), 1–101. 2015. https://iss.jaxa.jp/en/kiboexp/jssod/
121. Brian Dunbar: CubeSats Overview, Last modified 2018, https://www.nasa.gov/mission_pages/cubesats/overview (accessed September 20, 2020).
122. Jaroslav Menčík (April 13th 2016). Reliability of Systems, Concise Reliability for Engineers, Jaroslav Mencik, IntechOpen, DOI: 10.5772/62358. Available from: https://www.intechopen.com/books/concise-reliability-for-engineers/reliability-of-systems
123. Miria M. Finckenor, Kim K. de Groh. (2009). Space Environmental Effects, This International Space Station (ISS) Researcher's Guide. https://doi.org/10.1201/9781420084320-c27
124. NASA Website, Estimating the Temperature of a Flat Plate in Low Earth Orbit, https://www.grc.nasa.gov/www/k-12/Numbers/Math/Mathematical_Thinking/estimating_the_temperature.htm (accessed Mai 24, 2021).
125. Von Lukowicz, M., Schmiel, T., Rosenfeld, M., Heisig, J., & Tajmar, M. (2015). Characterisation of TEGs Under Extreme Environments and Integration Efforts Onto Satellites. Journal of Electronic Materials, 44(1), 362–370. https://doi.org/10.1007/s11664-014-3206-2
126. Sieger L., Nentvich O., & Urban M. (2019). Satellite temperature measurement in LEO and improvement method of temperature sensors calibration based on the measured data. Astronomische Nachrichten, 340(7), 652–657. https://doi.org/10.1002/asna.201913671

127. *Yuta Kakimoto, Hirokasu Masui, Sangkyun Kim, Mengu Cho. (2019). The Thermal Design for 1U, 2U, 3U Cubesatellite. 32nd International Symposium on Space Technology and Science&9th Nano Satellite Symposium, 1–8.*
128. *S. Corpino, M. Caldera, M. Masoero, F. Nichele, N. Viola, Thermal design and analysis of a nanosatellite in low earth orbit, Acta Astronautica, 2015. http://dx.doi.org/10.1016/j.actaastro.2015.05.012*
129. *Griffin Michael D., & James R. French. (2004). Space Vehicle Design, Second Edition, Educative series. In Space Vehicle Design, Second Edition. American Institute of Aeronautics and Astronautics, Inc. https://doi.org/10.2514/4.862403*
130. *WEL Research Company, Ltd, Research and Engineering of the spacecraft, http://www.wel.co.jp/?page_id=1211&lang=en, accessed on 1st September 2020.*
131. *Targray Company, Official website. https://www.targray.com/li-ion-battery/packaging-materials/aluminum-laminate-pouch (accessed April 5, 2021)*
132. *Lakhdar. L., Kei-Ichi, O., Jesus, G-L., & Hind, M-E. (2020). One Step Away from The Reliable Batteries for Small Spacecrafts with Solid-State-Ceramic Batteries. Proceedings of the 71st International Astronautical Congress – The CyberSpace Edition, IAC, Paper ID 55598, 2020-October. https://dl.iafastro.directory/event/IAC-2020/paper/55598/*